

AFML-TR-68-281



AD 685773

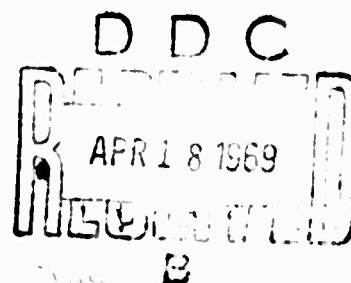
AN EXPERIMENTAL INVESTIGATION OF THE BUCKLING OF ANISOTROPIC FIBER REINFORCED PLASTIC PLATES

John F. Mandell

Case Western Reserve University

TECHNICAL REPORT AFML-TR-68-281

October 1968



This document has been approved for public
release and sale; its distribution is unlimited.

AIR FORCE MATERIALS LABORATORY
AIR FORCE SYSTEMS COMMAND
WRIGHT-PATTERSON AIR FORCE BASE, OHIO

CELLARIN HODGE
RESEARCH CENTER
WRIGHT-PATTERSON AIR FORCE BASE, OHIO

340

**BEST
AVAILABLE COPY**

NOTICE

When Government drawings, specifications, or other data are used for any purpose other than in connection with a definitely related Government procurement operation, the United States Government thereby incurs no responsibility nor any obligation whatsoever; and the fact that the Government may have formulated, furnished, or in any way supplied the said drawings, specifications, or other data, is not to be regarded by implication or otherwise as in any manner licensing the holder or any other person or corporation, or conveying any rights or permission to manufacture, use, or sell any patented invention that may in any way be related thereto.

| | |
|---------------------------------|---|
| ADDITIONAL | WHITE SECTION <input checked="" type="checkbox"/> |
| CFSTI | BUFF SECTION <input type="checkbox"/> |
| DDC | <input type="checkbox"/> |
| UNANNOUNCED | |
| JUSTIFICATION | |
| BY | |
| DISTRIBUTION AVAILABILITY CODES | |
| DDM. | AVAIL. and or SPECIAL |
| 1 | |

Copies of this report should not be returned unless return is required by security considerations, contractual obligations, or notice on a specific document.

AN EXPERIMENTAL INVESTIGATION OF THE
BUCKLING OF ANISOTROPIC FIBER REINFORCED PLASTIC PLATES

John F. Mandell

This document has been approved for public release and sale;
its distribution is unlimited.

BLANK PAGE

FOREWORD

The work reported herein was performed under the sponsorship of the Advanced Research Project Agency, Department of Defense, through a contract with the Air Force Materials Laboratory, MAN, Research and Technology Division, Wright-Patterson Air Force Base, Ohio, Contract No. AF 33(615)-3110, ARPA Order No. 719, Program Code No. 5950. Mr. H. S. Schwartz, MAN, is the Air Force Program Manager.

The prime contractor is Union Carbide Corporation, Carbon Products Division; the subcontractors are Case Western Reserve University and Bell Aerosystems Company, a Textron Company. The program is administered by a committee composed of: J. C. Bowman (Chairman) and G. B. Spence (Program Supervisor) from Union Carbide; R. H. Thomas and L. A. Schmit (Program Supervisor) from Case Western Reserve University; and W. H. Dukes and F. M. Anthony (Program Supervisor) from Bell Aerosystems Company.

This report is a reproduction of a thesis by J. F. Mandell submitted to Case Western Reserve University in partial fulfillment of the requirements for the degree of Master of Science. The study reported herein was carried out under the supervision of Professor Thomas P. Kicher.

The manuscript was released by the author October 1968 for publication.

This report covers work performed from June 1966 to June 1968.

This technical report has been reviewed and is approved.



A. M. Lovelace
Director
Air Force Materials Laboratory

ABSTRACT

Experimental buckling loads are determined for stiffened and unstiffened plates of the following materials: aluminum, steel, graphite fiber reinforced composite, glass fiber reinforced composite, and boron fiber reinforced composite. The plates are subjected to a uniformly distributed compressive edge load in one direction only. The boundary conditions are either simply supported on all four edges, or else simply supported on the loaded edges and free on the unloaded edges. The experimental buckling load is determined using the Southwell plot technique, and the results are compared to theoretical predictions obtained from a number of independent sources.

Correlation between theoretical and experimental results is generally acceptable. It is believed that problems connected with material fabrication and evaluation resulted in some discrepancies between theoretical and experimental results, while problems associated with the test fixture and test procedure can be blamed for other discrepancies. The effects of bending-torsion and bending-membrane coupling is clearly shown in both the theoretical and experimental results.

TABLE OF CONTENTS

| | | |
|-----------|---|----|
| CHAPTER 1 | INTRODUCTION | 1 |
| CHAPTER 2 | THEORETICAL PREDICTION OF BUCKLING LOADS | 4 |
| 2.1 | Elastic Stiffnesses | 4 |
| 2.2 | Classical Orthotropic Plate Formulation | 4 |
| 2.3 | Reduced Flexural Stiffness Method | 7 |
| 2.4 | Numerical Methods | 8 |
| 2.4.1 | Ritz Method | 9 |
| 2.4.2 | Galerkin Method | 9 |
| 2.4.3 | Geometrically Nonlinear Finite Element Method | 10 |
| CHAPTER 3 | EXPERIMENTAL DETERMINATION OF BUCKLING LOADS | 11 |
| 3.1 | Test Specimens | 11 |
| 3.2 | Southwell Plot | 11 |
| 3.3 | Test Fixture | 16 |
| 3.3.1 | Application of the Load | 23 |
| 3.3.2 | Side Supports | 25 |
| 3.3.3 | Deflection Measurement | 26 |
| 3.4 | Test Procedure | 28 |
| CHAPTER 4 | RESULTS | 30 |
| CHAPTER 5 | DISCUSSION | 44 |
| 5.1 | Discussion of the Test Fixture | 44 |
| 5.1.1 | Load Distribution | 44 |
| 5.1.2 | Friction, Edge Fixity, and Fixture Alignment | 49 |
| 5.1.3 | Deflection Measurement | 54 |
| 5.1.4 | Reliability of Test Fixture | 56 |

| | | |
|------------|--|----|
| 5.2 | Discussion of Test Specimens | 57 |
| 5.2.1 | Quality of Test Specimens | 57 |
| 5.2.2 | Added Problems with Very Thin Plates | 61 |
| 5.3 | Correlation of Theoretical and Experimental Results | 63 |
| 5.3.1 | General Comments | 63 |
| 5.3.2 | Effect of D_{16} and D_{26} Terms | 71 |
| 5.3.3 | Effect of Membrane-Bending Coupling Terms | 72 |
| 5.4 | Conclusions and Recommendations | 78 |
| REFERENCES | | 80 |
| APPENDIX A | MATERIAL CHARACTERISTICS OF TEST SPECIMENS | 82 |
| A.1 | Notation for Laminated, Anisotropic Plates | 82 |
| A.1.1 | Single Ply Notation | 82 |
| A.1.2 | Gross Plate Notation | 82 |
| A.2 | Fabrication Techniques | 86 |
| A.2.1 | Balanced "Thorne1" Plates | 86 |
| A.2.2 | Balanced Boron Plates | 86 |
| A.2.3 | Stiffened Fiberglass Plates | 86 |
| A.2.4 | Unbalanced Plates | 87 |
| APPENDIX B | DETERMINATION OF ELASTIC STIFFNESSES FOR LAMINATED, ANISOTROPIC PLATES | 88 |
| B.1 | Determination of Individual Ply Properties | 88 |
| B.2 | Determination of Elastic Stiffnesses for Unstiffened Plates | 91 |
| B.3 | Determination of Elastic Stiffnesses for Stiffened Plates | 92 |

| | | |
|------------|---|-----|
| B.4 | Constituent Properties and Resulting Elastic Stiffnesses | 94 |
| APPENDIX C | TEST DATA, LOAD-DEFLECTION CURVES, SOUTHWELL PLOTS, AND MODE SHAPES | 101 |
| APPENDIX D | PLANS AND ASSEMBLY DRAWINGS FOR THE TEST FIXTURE | 291 |

| Figure | LIST OF ILLUSTRATIONS | Page |
|--------|---|------|
| 1. | Schematic Diagram of a Typical Test Specimen with Assumed Load and Boundary Conditions. | 6 |
| 2. | Southwell Plot and Load Deflection Curve for Plate No. 404, 2 Sides Supported (Neutral Buckling). | 17 |
| 3. | Southwell Plot and Load Deflection Curve for Plate No. 201, 4 Sides Supported (Stable Symmetric). | 18 |
| 4. | Test Fixture with Deflection Measuring Device. | 19 |
| 5. | Test Fixture in Two Sides Supported Configuration. | 20 |
| 6. | Test Fixture in Four Sides Supported Configuration | 21 |
| 7. | Back View of Test Fixture with Perturbation Load Device in Place. | 22 |
| 8. | Test Plate with Metal Contacts, Teflon Strip, and Knife Edges. | 24 |
| 9. | Location of Points at Which Deflection is Measured. | 27 |
| 10. | Undeformed (solid line) and Deformed (broken line) Isotropic or Orthotropic Plate Specimen (exaggerated). | 45 |
| 11. | Location of Strain Gages on 0.063 Inch Thick Aluminum Plate (identical front and back) with Four Sides Simply Supported. | 47 |
| 12. | Possible Source of Error in Knife Edge Supports. | 52 |
| 13. | Typical Test Specimens: "Thornel" (upper left), Fiber-glass (upper right), Stiffened Fiberglass (lower right), and Aluminum (lower left). | 58 |
| 14. | Integrally Stiffened Fiberglass Plates. | 59 |
| 15. | Models for Eleven Inch Wide Unidirectional Plates. | 66 |
| 16. | Deviation of Experimental Buckling Load from Ritz Theory for Unidirectional and Interspersed Ply Orientations for Balanced Boron Plates. | 68 |
| 17. | Expected Trends in the Deviation of the Experimental Buckling Load from Theory Due to Various Factors. | 70 |

| | |
|---|-----|
| 18. Effect of Ply Orientation on Buckling of Boron Plates Normalized to a Thickness of 0.106 in. | 73 |
| 19. Theoretical and Experimental Load-Deflection Curves for Plate No. 209. | 76 |
| 20. Southwell Plot for Plate No. 209 Using Finite Element Load-Deflection Data. | 77 |
| 21. Single Ply Notation for Fibrous Composite. | 83 |
| 22. Southwell Plot and Load Deflection Curve for Plate No. 101, 2 Sides Supported. | 104 |
| 23. Southwell Plot and Load Deflection Curve for Plate No. 101, 4 Sides Supported. | 107 |
| 24. Southwell Plot and Load Deflection Curve for Plate No. 102, 2 Sides Supported. | 109 |
| 25. Southwell Plot and Load Deflection Curve for Plate No. 102, 4 Sides Supported. | 111 |
| 26. Southwell Plot and Load Deflection Curve for Plate No. 103, 2 Sides Supported. | 113 |
| 27. Southwell Plot and Load Deflection Curve for Plate No. 103, 4 Sides Supported. | 115 |
| 28. Southwell Plot and Load Deflection Curve for Plate No. 104, 2 Sides Supported. | 117 |
| 29. Southwell Plot and Load Deflection Curve for Plate No. 104, 4 Sides Supported. | 119 |
| 30. Southwell Plot and Load Deflection Curve for Plate No. 105, 2 Sides Supported. | 121 |
| 31. Southwell Plot and Load Deflection Curve for Plate No. 105, 4 Sides Supported. | 123 |
| 32. Southwell Plot and Load Deflection Curve for Plate No. 201, 2 Sides Supported. | 125 |
| 33. Southwell Plot and Load Deflection Curve for Plate No. 201, 4 Sides Supported. | 127 |
| 34. Southwell Plot and Load Deflection Curve for Plate No. 202, 2 Sides Supported. | 129 |

| | |
|---|-----|
| 35. Southwell Plot and Load Deflection Curve for Plate No. 202, 4 Sides Supported. | 132 |
| 36. Southwell Plot and Load Deflection Curve for Plate No. 203a, 2 Sides Supported. | 134 |
| 37. Southwell Plot and Load Deflection Curve for Plate No. 203b, 2 Sides Supported. | 137 |
| 38. Southwell Plot and Load Deflection Curve for Plate No. 203a, 4 Sides Supported. | 139 |
| 39. Southwell Plot and Load Deflection Curve for Plate No. 203b, 4 Sides Supported. | 142 |
| 40. Southwell Plot and Load Deflection Curve for Plate No. 204, 2 Sides Supported. | 144 |
| 41. Southwell Plot and Load Deflection Curve for Plate No. 204, 4 Sides Supported. | 146 |
| 42. Southwell Plot and Load Deflection Curve for Plate No. 205, 2 Sides Supported. | 148 |
| 43. Southwell Plot and Load Deflection Curve for Plate No. 205, 4 Sides Supported. | 150 |
| 44. Southwell Plot and Load Deflection Curve for Plate No. 206, 2 Sides Supported. | 152 |
| 45. Southwell Plot and Load Deflection Curve for Plate No. 206, 4 Sides Supported. | 154 |
| 46. Southwell Plot and Load Deflection Curve for Plate No. 207, 2 Sides Supported. | 156 |
| 47. Southwell Plot and Load Deflection Curve for Plate No. 207, 4 Sides Supported. | 158 |
| 48. Southwell Plot and Load Deflection Curve for Plate No. 208, 2 Sides Supported. | 160 |
| 49. Southwell Plot and Load Deflection Curve for Plate No. 208, 4 Sides Supported. | 162 |
| 50. Southwell Plot and Load Deflection Curve for Plate No. 209a, 2 Sides Supported. | 164 |
| 51. Southwell Plot and Load Deflection Curve for Plate No. 209b, 2 Sides Supported. | 167 |

| | | |
|-----|---|-----|
| 52. | Southwell Plot and Load Deflection Curve for Plate No. 209a, 4 Sides Supported, Unperturbed. | 169 |
| 53. | Southwell Plot and Load Deflection Curve for Plate No. 209a, 4 Sides Supported, with Reverse Perturbation Load. | 171 |
| 54. | Southwell Plot and Load Deflection Curve for Plate No. 209b, 4 Sides Supported, Unperturbed. | 174 |
| 55. | Southwell Plot and Load Deflection Curve for Plate No. 301, 2 Sides Supported. | 176 |
| 56. | Southwell Plot and Load Deflection Curve for Plate No. 301, 4 Sides Supported. | 178 |
| 57. | Southwell Plot and Load Deflection Curve for Plate No. 302, 2 Sides Supported. | 180 |
| 58. | Southwell Plot and Load Deflection Curve for Plate No. 302, 4 Sides Supported. | 182 |
| 59. | Southwell Plot and Load Deflection Curve for Plate No. 303, 2 Sides Supported. | 185 |
| 60. | Southwell Plot and Load Deflection Curve for Plate No. 303, 4 Sides Supported. | 188 |
| 61. | Southwell Plot and Load Deflection Curve for Plate No. 304, 2 Sides Supported. | 191 |
| 62. | Southwell Plot and Load Deflection Curve for Plate No. 304, 4 Sides Supported. | 194 |
| 63. | Southwell Plot and Load Deflection Curve for Plate No. 401, 2 Sides Supported. | 196 |
| 64. | Southwell Plot and Load Deflection Curve for Plate No. 401, 4 Sides Supported. | 199 |
| 65. | Southwell Plot and Load Deflection Curve for Plate No. 402, 2 Sides Supported. | 201 |
| 66. | Southwell Plot and Load Deflection Curve for Plate No. 402, 4 Sides Supported. | 204 |
| 67. | Southwell Plot and Load Deflection Curve for Plate No. 403a, 2 Sides Supported. | 206 |
| 68. | Southwell Plot and Load Deflection Curve for Plate No. 403b, 2 Sides Supported. | 208 |

| | |
|---|-----|
| 69. Southwell Plot and Load Deflection Curve for Plate No. 403a, 4 Sides Supported. | 210 |
| 70. Southwell Plot and Load Deflection Curve for Plate No. 403b, 4 Sides Supported. | 212 |
| 71. Southwell Plot and Load Deflection Curve for Plate No. 404, 2 Sides Supported. | 214 |
| 72. Southwell Plot and Load Deflection Curve for Plate No. 404, 4 Sides Supported. | 216 |
| 73. Southwell Plot and Load Deflection Curve for Plate No. 405, 2 Sides Supported. | 218 |
| 74. Southwell Plot and Load Deflection Curve for Plate No. 405, 4 Sides Supported. | 220 |
| 75. Southwell Plot and Load Deflection Curve for Plate No. 406, 2 Sides Supported. | 222 |
| 76. Southwell Plot and Load Deflection Curve for Plate No. 406, 4 Sides Supported. | 225 |
| 77. Southwell Plot and Load Deflection Curve for Plate No. 407, 2 Sides Supported. | 227 |
| 78. Southwell Plot and Load Deflection Curve for Plate No. 407, 4 Sides Supported. | 230 |
| 79. Southwell Plot and Load Deflection Curve for Plate No. 408a, 2 Sides Supported. | 232 |
| 80. Southwell Plot and Load Deflection Curve for Plate No. 408b, 2 Sides Supported. | 235 |
| 81. Southwell Plot and Load Deflection Curve for Plate No. 408a, 4 Sides Supported. | 238 |
| 82. Southwell Plot and Load Deflection Curve for Plate No. 408b, 4 Sides Supported. | 240 |
| 83. Southwell Plot and Load Deflection Curve for Plate No. 409a, 2 Sides Supported. | 242 |
| 84. Southwell Plot and Load Deflection Curve for Plate No. 409b, 2 Sides Supported. | 244 |
| 85. Southwell Plot and Load Deflection Curve for Plate No. 409a, 4 Sides Supported. | 247 |

| | |
|---|-----|
| 86. Southwell Plot and Load Deflection Curve for Plate No. 409b, 4 Sides Supported. | 249 |
| 87. Southwell Plot and Load Deflection Curve for Plate No. 501, 2 Sides Supported. | 251 |
| 88. Southwell Plot and Load Deflection Curve for Plate No. 501, 4 Sides Supported. | 253 |
| 89. Southwell Plot and Load Deflection Curve for Plate No. 502, 2 Sides Supported. | 255 |
| 90. Southwell Plot and Load Deflection Curve for Plate No. 502, 4 Sides Supported. | 257 |
| 91. Southwell Plot and Load Deflection Curve for Plate No. 503, 2 Sides Supported. | 259 |
| 92. Southwell Plot and Load Deflection Curve for Plate No. 503, 4 Sides Supported. | 261 |
| 93. Southwell Plot and Load Deflection Curve for Plate No. 504, 2 Sides Supported. | 263 |
| 94. Southwell Plot and Load Deflection Curve for Plate No. 504, 4 Sides Supported. | 265 |
| 95. Southwell Plot and Load Deflection Curve for Plate No. 505, 2 Sides Supported. | 267 |
| 96. Southwell Plot and Load Deflection Curve for Plate No. 505, 4 Sides Supported. | 269 |
| 97. Southwell Plot and Load Deflection Curve for Plate No. 506, 2 Sides Supported. | 271 |
| 98. Southwell Plot and Load Deflection Curve for Plate No. 506, 4 Sides Supported. | 273 |
| 99. Southwell Plot and Load Deflection Curve for Plate No. 507, 2 Sides Supported. | 275 |
| 100. Southwell Plot and Load Deflection Curve for Plate No. 507, 4 Sides Supported. | 277 |
| 101. Southwell Plot and Load Deflection Curve for Plate No. 508, 2 Sides Supported. | 279 |
| 102. Southwell Plot and Load Deflection Curve for Plate No. 508, 4 Sides Supported. | 281 |

| | | |
|------|---|-----|
| 103. | Southwell Plot and Load Deflection Curve for Plate No 509a, 2 Sides Supported. | 283 |
| 104. | Southwell Plot and Load Deflection Curve for Plate No 509b, 2 Sides Supported. | 285 |
| 105. | Southwell Plot and Load Deflection Curve for Plate No. 509a, 4 Sides Supported. | 287 |
| 106. | Southwell Plot and Load Deflection Curve for Plate No. 509b, 4 Sides Supported. | 289 |
| 107. | Front View of Test Fixture. | 291 |
| 108. | Horizontal Section Through Test Fixture. | 292 |
| 109. | Vertical Section Through Test Fixture. | 293 |
| 110. | Loading Bar. | 294 |
| 111. | Typical Middle Piston. | 295 |
| 112. | Restraining Bar. | 295 |
| 113. | Side Supports. | 296 |
| 114. | Typical End Piston. | 297 |
| 115. | Slotted Bar Roller Support. | 298 |
| 116. | Slotted Bar Connector. | 298 |
| 117. | Typical Knife Edge. | 299 |
| 118. | Ball Bushing Spacer. | 299 |
| 119. | Micrometer Bushing | 300 |
| 120. | Top Plate. | 301 |
| 121. | Side Channel. | 302 |
| 122. | Front Angle Guide for Loading Bar. | 303 |
| 123. | Back Angle Guide for Loading Bar. | 304 |
| 124. | Side Support Connector. | 305 |
| 125. | Top Channel Connector. | 305 |
| 126. | Bottom Channel Connector. | 306 |

| | |
|---|-----|
| 127. Base Plate. | 306 |
| 128. Perturbation Rod Support Bar Connector. | 307 |
| 129. Perturbation Rod Support Bar. | 307 |
| 130. Piston Filler Ring. | 308 |
| 131. Negator Spring Core. | 308 |
| 132. Micrometer Holder. | 309 |
| 133. Micrometer End Cap. | 309 |
| 134. Micrometer Guide Plate. | 310 |
| 135. Side Support for Guide Plate. | 311 |
| 136. Top and Bottom Supports for Guide Plate. | 311 |
| 137. Load Cell. | 312 |
| 138. Bearing Support. | 312 |
| 139. Load Cell Support. | 313 |
| 140. Load Cell Cover. | 313 |
| 141. Spacer. | 314 |
| 142. Negator Spring Core Support. | 314 |
| 143. Ball Bushing Housing. | 315 |
| 144. Perturbation Rod End Cover. | 315 |

| Table | LIST OF TABLES | Page |
|-------|--|------|
| 1. | PLATE MATERIALS, CONFIGURATIONS, AND DIMENSIONS | 32 |
| 2. | EXPERIMENTAL AND THEORETICAL BUCKLING LOADS | 36 |
| 3. | STRAIN DISTRIBUTION IN 0.063 INCH THICK ALUMINUM PLATE WITH FOUR SIDES SIMPLY SUPPORTED | 48 |
| 4. | EFFECT OF FRICTION ON THE BUCKLING LOADS FOR BORON PLATES | 51 |
| 5. | EFFECT OF SUPPORT MISALIGNMENT | 54 |
| 6. | EFFECT OF THE METHOD OF THICKNESS DETERMINATION ON THE THEORETICAL BUCKLING LOAD FOR THIN PLATES | 61 |
| 7. | TEST CASE USING IDENTICAL STIFFNESSES ^a | 74 |
| 8. | CONVENTIONS FOR EXPRESSING PLATE CONFIGURATIONS FOR BALANCED PLATES | 85 |
| 9. | CONVENTIONS FOR EXPRESSING PLATE CONFIGURATIONS FOR UNBALANCED PLATES | 85 |
| 10. | METHOD USED TO PREDICT SINGLE PLY PROPERTIES FOR EACH PLATE SERIES AND CORRESPONDING BUCKLING THEORY | 90 |
| 11. | CONSTITUENT PROPERTIES FOR "THORNEL" AND UNSTIFFENED FIBER-GLASS PLATES ^(4,13) (moduli $\times 10^6$ psi) | 94 |
| 12. | EXPERIMENTAL SINGLE PLY PROPERTIES FOR BORON ⁽¹⁴⁾ AND STIFFENED FIBERGLASS ⁽¹⁶⁾ PLATES | 95 |
| 13. | MEMBRANE STIFFNESSES (10^3 lb/in) ^a | 96 |
| 14. | FLEXURAL STIFFNESSES (in/lb) ^a | 98 |
| 15. | COUPLING STIFFNESSES FOR UNBALANCED PLATES (10^3 lb) ^a | 100 |
| 16. | DATA AND CALCULATIONS FOR PLATE NO. 101, 2 SIDES SUPPORTED | 102 |
| 17. | MODE SHAPE FOR PLATE NO. 101, 2 SIDES SUPPORTED, 10^{-4} in. | 103 |
| 18. | DATA AND CALCULATIONS FOR PLATE NO. 101, 4 SIDES SUPPORTED | 105 |
| 19. | MODE SHAPE FOR PLATE NO. 101, 4 SIDES SUPPORTED, 10^{-4} in. | 106 |
| 20. | DATA AND CALCULATIONS FOR PLATE NO. 102, 2 SIDES SUPPORTED | 108 |

| | |
|---|-----|
| 21. DATA AND CALCULATIONS FOR PLATE NO. 102, 4 SIDES SUPPORTED | 110 |
| 22. DATA AND CALCULATIONS FOR PLATE NO. 103, 2 SIDES SUPPORTED | 112 |
| 23. DATA AND CALCULATIONS FOR PLATE NO. 103, 4 SIDES SUPPORTED | 114 |
| 24. DATA AND CALCULATIONS FOR PLATE NO. 104, 2 SIDES SUPPORTED | 116 |
| 25. DATA AND CALCULATIONS FOR PLATE NO. 104, 4 SIDES SUPPORTED | 118 |
| 26. DATA AND CALCULATIONS FOR PLATE NO. 105, 2 SIDES SUPPORTED | 120 |
| 27. DATA AND CALCULATIONS FOR PLATE NO. 105, 4 SIDES SUPPORTED | 122 |
| 28. DATA AND CALCULATIONS FOR PLATE NO. 201, 2 SIDES SUPPORTED | 124 |
| 29. DATA AND CALCULATIONS FOR PLATE NO. 201, 4 SIDES SUPPORTED | 126 |
| 30. DATA AND CALCULATIONS FOR PLATE NO. 202, 2 SIDES SUPPORTED | 128 |
| 31. DATA AND CALCULATIONS FOR PLATE NO. 202, 4 SIDES SUPPORTED | 130 |
| 32. MODE SHAPE FOR PLATE NO. 202, 4 SIDES SUPPORTED, 10^{-4} in. | 131 |
| 33. DATA AND CALCULATIONS FOR PLATE NO. 203a, 2 SIDES SUPPORTED | 133 |
| 34. DATA AND CALCULATIONS FOR PLATE NO. 203b, 2 SIDES SUPPORTED | 135 |
| 35. MODE SHAPE FOR PLATE NO. 203b, 2 SIDES SUPPORTED, 10^{-4} in. | 136 |
| 36. DATA AND CALCULATIONS FOR PLATE NO. 203a, 4 SIDES SUPPORTED | 138 |
| 37. DATA AND CALCULATIONS FOR PLATE NO. 203b, 4 SIDES SUPPORTED | 140 |
| 38. MODE SHAPE FOR PLATE NO. 203b, 4 SIDES SUPPORTED, 10^{-4} in. | 141 |
| 39. DATA AND CALCULATIONS FOR PLATE NO. 204, 2 SIDES SUPPORTED | 143 |
| 40. DATA AND CALCULATIONS FOR PLATE NO. 204, 4 SIDES SUPPORTED | 145 |
| 41. DATA AND CALCULATIONS FOR PLATE NO. 205, 2 SIDES SUPPORTED | 147 |
| 42. DATA AND CALCULATIONS FOR PLATE NO. 205, 4 SIDES SUPPORTED | 149 |
| 43. DATA AND CALCULATIONS FOR PLATE NO. 206, 2 SIDES SUPPORTED | 151 |
| 44. DATA AND CALCULATIONS FOR PLATE NO. 206, 4 SIDES SUPPORTED | 153 |
| 45. DATA AND CALCULATIONS FOR PLATE NO. 207, 2 SIDES SUPPORTED | 155 |

| | | |
|-----|---|-----|
| 46. | DATA AND CALCULATIONS FOR PLATE NO. 207, 4 SIDES SUPPORTED | 157 |
| 47. | DATA AND CALCULATIONS FOR PLATE NO. 208, 2 SIDES SUPPORTED | 159 |
| 48. | DATA AND CALCULATIONS FOR PLATE NO. 208, 4 SIDES SUPPORTED | 161 |
| 49. | DATA AND CALCULATIONS FOR PLATE NO. 209a, 2 SIDES SUPPORTED | 163 |
| 50. | DATA AND CALCULATIONS FOR PLATE NO. 209b, 2 SIDES SUPPORTED | 165 |
| 51. | MODE SHAPE FOR PLATE NO. 209b, 2 SIDES SUPPORTED, 10^{-4} in. | 166 |
| 52. | DATA AND CALCULATIONS FOR PLATE NO. 209a, 4 SIDES SUPPORTED, UNPERTURBED | 168 |
| 53. | DATA AND CALCULATIONS FOR PLATE NO. 209a, 4 SIDES SUPPORTED, WITH REVERSE PERTURBATION | 170 |
| 54. | DATA AND CALCULATIONS FOR PLATE NO. 209b, 4 SIDES SUPPORTED | 172 |
| 55. | MODE SHAPE FOR PLATE NO. 209b, 4 SIDES SUPPORTED, 10^{-4} in. | 173 |
| 56. | DATA AND CALCULATIONS FOR PLATE NO. 301, 2 SIDES SUPPORTED | 175 |
| 57. | DATA AND CALCULATIONS FOR PLATE NO. 301, 4 SIDES SUPPORTED | 177 |
| 58. | DATA AND CALCULATIONS FOR PLATE NO. 302, 2 SIDES SUPPORTED | 179 |
| 59. | DATA AND CALCULATIONS FOR PLATE NO. 302, 4 SIDES SUPPORTED | 181 |
| 60. | DATA AND CALCULATIONS FOR PLATE NO. 303, 2 SIDES SUPPORTED | 183 |
| 61. | MODE SHAPE FOR PLATE NO. 303, 2 SIDES SUPPORTED, 10^{-4} in. | 184 |
| 62. | DATA AND CALCULATIONS FOR PLATE NO. 303, 4 SIDES SUPPORTED | 186 |
| 63. | MODE SHAPE FOR PLATE NO. 303, 4 SIDES SUPPORTED, 10^{-4} in. | 187 |
| 64. | DATA AND CALCULATIONS FOR PLATE NO. 304, 2 SIDES SUPPORTED | 189 |
| 65. | MODE SHAPE FOR PLATE NO. 304, 2 SIDES SUPPORTED, 10^{-4} in | 190 |
| 66. | DATA AND CALCULATIONS FOR PLATE NO. 304, 4 SIDES SUPPORTED | 192 |
| 67. | MODE SHAPE FOR PLATE NO. 304, 4 SIDES SUPPORTED, 10^{-4} in | 193 |
| 68. | DATA AND CALCULATIONS FOR PLATE NO. 401, 2 SIDES SUPPORTED | 195 |
| 69. | DATA AND CALCULATIONS FOR PLATE NO. 401, 4 SIDES SUPPORTED | 197 |

| | |
|---|-----|
| 70. MODE SHAPE FOR PLATE NO. 401, 4 SIDES SUPPORTED, 10^{-4} in | 198 |
| 71. DATA AND CALCULATIONS FOR PLATE NO. 402, 2 SIDES SUPPORTED | 200 |
| 72. DATA AND CALCULATIONS FOR PLATE NO. 402, 4 SIDES SUPPORTED | 202 |
| 73. MODE SHAPE FOR PLATE NO. 402, 4 SIDES SUPPORTED, 10^{-4} in. | 203 |
| 74. DATA AND CALCULATIONS FOR PLATE NO. 403a, 2 SIDES SUPPORTED | 205 |
| 75. DATA AND CALCULATIONS FOR PLATE NO. 403b, 2 SIDES SUPPORTED | 207 |
| 76. DATA AND CALCULATIONS FOR PLATE NO. 403a, 4 SIDES SUPPORTED | 209 |
| 77. DATA AND CALCULATIONS FOR PLATE NO. 403b, 4 SIDES SUPPORTED | 211 |
| 78. DATA AND CALCULATIONS FOR PLATE NO. 404, 2 SIDES SUPPORTED | 213 |
| 79. DATA AND CALCULATIONS FOR PLATE NO. 404, 4 SIDES SUPPORTED | 215 |
| 80. DATA AND CALCULATIONS FOR PLATE NO. 405, 2 SIDES SUPPORTED | 217 |
| 81. DATA AND CALCULATIONS FOR PLATE NO. 405, 4 SIDES SUPPORTED | 219 |
| 82. DATA AND CALCULATIONS FOR PLATE NO. 406, 2 SIDES SUPPORTED | 221 |
| 83. DATA AND CALCULATIONS FOR PLATE NO. 406, 4 SIDES SUPPORTED | 223 |
| 84. MODE SHAPE FOR PLATE NO. 406, 4 SIDES SUPPORTED, 10^{-4} in. | 224 |
| 85. DATA AND CALCULATIONS FOR PLATE NO. 407, 2 SIDES SUPPORTED | 226 |
| 86. DATA AND CALCULATIONS FOR PLATE NO. 407, 4 SIDES SUPPORTED | 228 |
| 87. MODE SHAPE FOR PLATE NO. 407, 4 SIDES SUPPORTED | 229 |
| 88. DATA AND CALCULATIONS FOR PLATE NO 408a, 2 SiDES SUPPORTED | 231 |
| 89. DATA AND CALCULATIONS FOR PLATE NO. 408b, 2 SIDES SUPPORTED | 233 |
| 90. MODE SHAPE FOR PLATE NO. 408b, 2 SIDES SUPPORTED, 10^{-4} in. | 234 |
| 91. DATA AND CALCULATIONS FOR PLATE NO 408a, 4 SIDES SUPPORTED | 236 |
| 92. MODE SHAPE FOR PLATE NO 408a, 4 SIDES SUPPORTED, 10^{-4} in | 237 |
| 93. DATA AND CALCULATIONS FOR PLATE NO. 408b, 4 SIDES SUPPORTED | 239 |
| 94. DATA AND CALCULATIONS FOR PLATE NO. 409a, 2 SIDES SUPPORTED | 241 |

| | | |
|------|---|-----|
| 95. | DATA AND CALCULATIONS FOR PLATE NO. 409b, 2 SIDES SUPPORTED | 243 |
| 96. | DATA AND CALCULATIONS FOR PLATE NO. 409a, 4 SIDES SUPPORTED | 245 |
| 97. | MODE SHAPE FOR PLATE NO. 409a, 4 SIDES SUPPORTED, 10^{-4} in. | 246 |
| 98. | DATA AND CALCULATIONS FOR PLATE NO. 409b, 4 SIDES SUPPORTED | 248 |
| 99. | DATA AND CALCULATIONS FOR PLATE NO. 501, 2 SIDES SUPPORTED | 250 |
| 100. | DATA AND CALCULATIONS FOR PLATE NO. 501, 4 SIDES SUPPORTED | 252 |
| 101. | DATA AND CALCULATIONS FOR PLATE NO. 502, 2 SIDES SUPPORTED | 254 |
| 102. | DATA AND CALCULATIONS FOR PLATE NO. 502, 4 SIDES SUPPORTED | 256 |
| 103. | DATA AND CALCULATIONS FOR PLATE NO. 503, 2 SIDES SUPPORTED | 258 |
| 104. | DATA AND CALCULATIONS FOR PLATE NO. 503, 4 SIDES SUPPORTED | 260 |
| 105. | DATA AND CALCULATIONS FOR PLATE NO. 504, 2 SIDES SUPPORTED | 262 |
| 106. | DATA AND CALCULATIONS FOR PLATE NO. 504, 4 SIDES SUPPORTED | 264 |
| 107. | DATA AND CALCULATIONS FOR PLATE NO. 505, 2 SIDES SUPPORTED | 266 |
| 108. | DATA AND CALCULATIONS FOR PLATE NO. 505, 4 SIDES SUPPORTED | 268 |
| 109. | DATA AND CALCULATIONS FOR PLATE NO. 506, 2 SIDES SUPPORTED | 270 |
| 110. | DATA AND CALCULATIONS FOR PLATE NO. 506, 4 SIDES SUPPORTED | 272 |
| 111. | DATA AND CALCULATIONS FOR PLATE NO. 507, 2 SIDES SUPPORTED | 274 |
| 112. | DATA AND CALCULATIONS FOR PLATE NO. 507, 4 SIDES SUPPORTED | 276 |
| 113. | DATA AND CALCULATIONS FOR PLATE NO. 508, 2 SIDES SUPPORTED | 278 |
| 114. | DATA AND CALCULATIONS FOR PLATE NO. 508, 4 SIDES SUPPORTED | 280 |
| 115. | DATA AND CALCULATIONS FOR PLATE NO. 509a, 2 SIDES SUPPORTED | 282 |
| 116. | DATA AND CALCULATIONS FOR PLATE NO. 509b, 2 SIDES SUPPORTED | 284 |
| 117. | DATA AND CALCULATIONS FOR PLATE NO. 509a, 4 SIDES SUPPORTED | 286 |
| 118. | DATA AND CALCULATIONS FOR PLATE NO. 509b, 4 SIDES SUPPORTED | 288 |

COMMON NOTATION

Symbols

| | |
|----------------------------|--|
| A | stiffener area |
| A_{ij} | membrane stiffness matrix |
| A_m, A_{mn}, a_1, a_{11} | maximum amplitude |
| a | x dimension of plate |
| B_{ij} | stiffness coupling matrix |
| b | y dimension of plate |
| C_{ij} | ply stiffness matrix |
| D_{ij} | flexural stiffness matrix |
| D_{ij}^* | reduced flexural stiffness matrix |
| D_3 | torsional stiffness |
| D | flexural stiffness of isotropic plate |
| d | stiffener spacing |
| E | modulus of elasticity |
| G | shear modulus |
| h | plate thickness |
| h_x | thickness of stiffeners in x direction |
| h_y | thickness of stiffeners in y direction |
| K, K^*, K_f | constants, Equation (B.4) |
| M_{ij} | moment matrix |
| m | number of half waves in x direction |

| | |
|------------------------------------|--|
| N_{ij} | membrane internal force matrix |
| N_x | applied force in x direction |
| n | number of half waves in y direction |
| P | total load |
| V_f | fiber volume ratio |
| w | total deflection of plate in z direction |
| w_0 | initial imperfection |
| w_1 | deflection due to load |
| x, y, z | structural coordinate axes |
| α | ratio of actual load to critical load |
| Δ | total deflection at any point |
| $\epsilon, \bar{\epsilon}, \gamma$ | strain |
| θ | single ply orientation |
| κ | curvature |
| μ, ν | Poisson's ratio |
| σ, τ | stress |

Subscripts

| | |
|--------|----------------------------------|
| f | fiber property |
| i | array index |
| j | array index |
| L | along the fiber direction |
| r | radial direction of fiber |
| T | perpendicular to fiber direction |
| x, y | structural coordinate axes |

BLANK PAGE

CHAPTER 1

INTRODUCTION

The study of anisotropic plate stability has recently come into focus in response to the development of fiber-reinforced composite materials whose stiffness to weight ratios are sufficiently high to make them competitive with popular isotropic materials. The purpose of this study was to provide sufficient experimental data to verify existing classical and numerical solutions, as well as to provide test cases for solutions which might be found in the future.

The tests were restricted to ten inch and eleven inch square plates subjected to an evenly distributed in-plane compressive edge load in one direction only. The following two types of boundary conditions were employed:

1. Loaded edges simply supported, unloaded edges free.
2. All four edges simply supported.

The supports along the loaded edges consisted of a series of short knife-edges, while the unloaded edges were supported by a roller on either side of the plate. The load was applied through a series of individually acting, spring loaded pistons to insure that the load remained evenly distributed.

Tests were run on thirty-six different plates encompassing the following materials: aluminum, steel, graphite fiber reinforced composite, glass fiber reinforced composite, and boron fiber reinforced composite. Both stiffened and unstiffened plates were tested.

Although most buckling theories assume that a plate remains flat

until the first critical load is reached, an actual plate always has some initial curvature and will deflect as the load is applied. If this deflection becomes appreciable before the buckling load is reached, then the actual buckling load cannot simply be observed, but must be determined from the load-deflection data. Since many of the test specimens were expensive, and further testing was planned, it was also desirable that the tests be nondestructive. To overcome these difficulties, the Southwell plot was used to determine the critical load. The use of the Southwell plot requires only that the deflections be large with respect to the initial imperfection and that the maximum deflection be within the small deflection plate theory requirement.

The isotropic plates were tested as a means of calibrating the test fixture, assuming the isotropic buckling theory to be accurate. In testing the remainder of the plates, an attempt was made to verify the following six theoretical methods of solution:

1. Classical orthotropic theory for unstiffened plates.^(1,2)
2. Classical orthotropic theory for stiffened plates using a smear technique to find the stiffnesses of an equivalent plate.⁽¹⁵⁾
3. Classical orthotropic theory using the reduced flexural stiffness method to account for bending-membrane coupling.^(3,4)
4. General Dynamics' anisotropic plate analysis based on the Ritz method.⁽⁵⁾
5. Chamis' anisotropic plate analysis based on the Galerkin method.⁽⁶⁾

6. Monforton's geometrically nonlinear finite element method.⁽⁷⁾

The third method was suggested originally by Chamis, and the results given for the fourth, fifth, and sixth methods were supplied by General Dynamics, Chamis, and Monforton respectively.

In an attempt to make this study more valuable to those who might wish to verify future theories, all pertinent plate properties and test data are included in Appendices B and C. Appendix A explains the notation and fabrication techniques for anisotropic plates, and Appendix D gives detailed plans for the test fixture.

CHAPTER 2

THEORETICAL PREDICTION OF BUCKLING LOADS

2.1 Elastic Stiffnesses

The theoretical determination of the buckling load for an anisotropic plate first requires the accurate prediction of the elastic stiffnesses of the plate. Three fundamental methods are employed in this study to determine the elastic constants of unstiffened and stiffened plates.

Unstiffened Plates:

1. A micromechanics theory is used to determine the properties of a single ply.
2. Experimental data are used as the properties of a single ply.

The individual ply properties are used in an expression of equilibrium along with the Love-Kirchhoff hypothesis to determine the gross properties of the laminated plate.

Stiffened Plates:

3. A decomposition of the stresses into a biaxial state in the skin and a uniaxial state in the stiffeners leads directly to the gross properties of the plate.

Appendix B gives a detailed formulation or explanation for each of the above methods, as well as the assumed constituent material properties and resulting stiffnesses for each test plate.

2.2 Classical Orthotropic Plate Formulation

The differential equation^(1,2) describing the bending of an orthotropic plate subjected to an in-plane edge loading and neglecting any bending-membrane coupling terms is

$$\begin{aligned}
& D_{11} \frac{\partial^4 w}{\partial x^4} + 4 D_{16} \frac{\partial^4 w}{\partial x^3 \partial y} + 2 D_3 \frac{\partial^4 w}{\partial x^2 \partial y^2} + 4 D_{26} \frac{\partial^4 w}{\partial x \partial y^3} \\
& + D_{22} \frac{\partial^4 w}{\partial y^4} + N_x \frac{\partial^2 w}{\partial x^2} + 2 N_{xy} \frac{\partial^2 w}{\partial x \partial y} + N_y \frac{\partial^2 w}{\partial y^2} = 0
\end{aligned} \quad (2.1)$$

For the orthotropic case with the principal axes parallel to the sides of the plate, and with $N_{xy} = N_y = 0$, Equation (2.1) becomes

$$D_{11} \frac{\partial^4 w}{\partial x^4} + 2 D_3 \frac{\partial^4 w}{\partial x^2 \partial y^2} + D_{22} \frac{\partial^4 w}{\partial y^4} + N_x \frac{\partial^2 w}{\partial x^2} = 0 \quad (2.2)$$

where $D_3 = D_{12} + 2 D_{66}$.

The discussion will now be restricted to a rectangular orthotropic plate as described in Figure 1. The plate will be subjected to the following boundary conditions:

- 1) Two loaded edges simply supported, other two edges free (simple-free).
- 2) All four edges simply supported (simple-simple).

For the simple-free case, the following approximate assumed mode shape will satisfy the boundary conditions along the loaded edges but will introduce artificial moments along the free edges.

$$w = A_m \sin \frac{m\pi x}{a} \quad (2.3)$$

In this case all derivatives with respect to y are zero, and the differential equation reduces to

$$D_{11} \frac{\partial^4 w}{\partial x^4} + N_x \frac{\partial^2 w}{\partial x^2} = 0 \quad (2.4)$$

Substituting (2.3) into (2.4) yields the first critical load ($m = 1$)

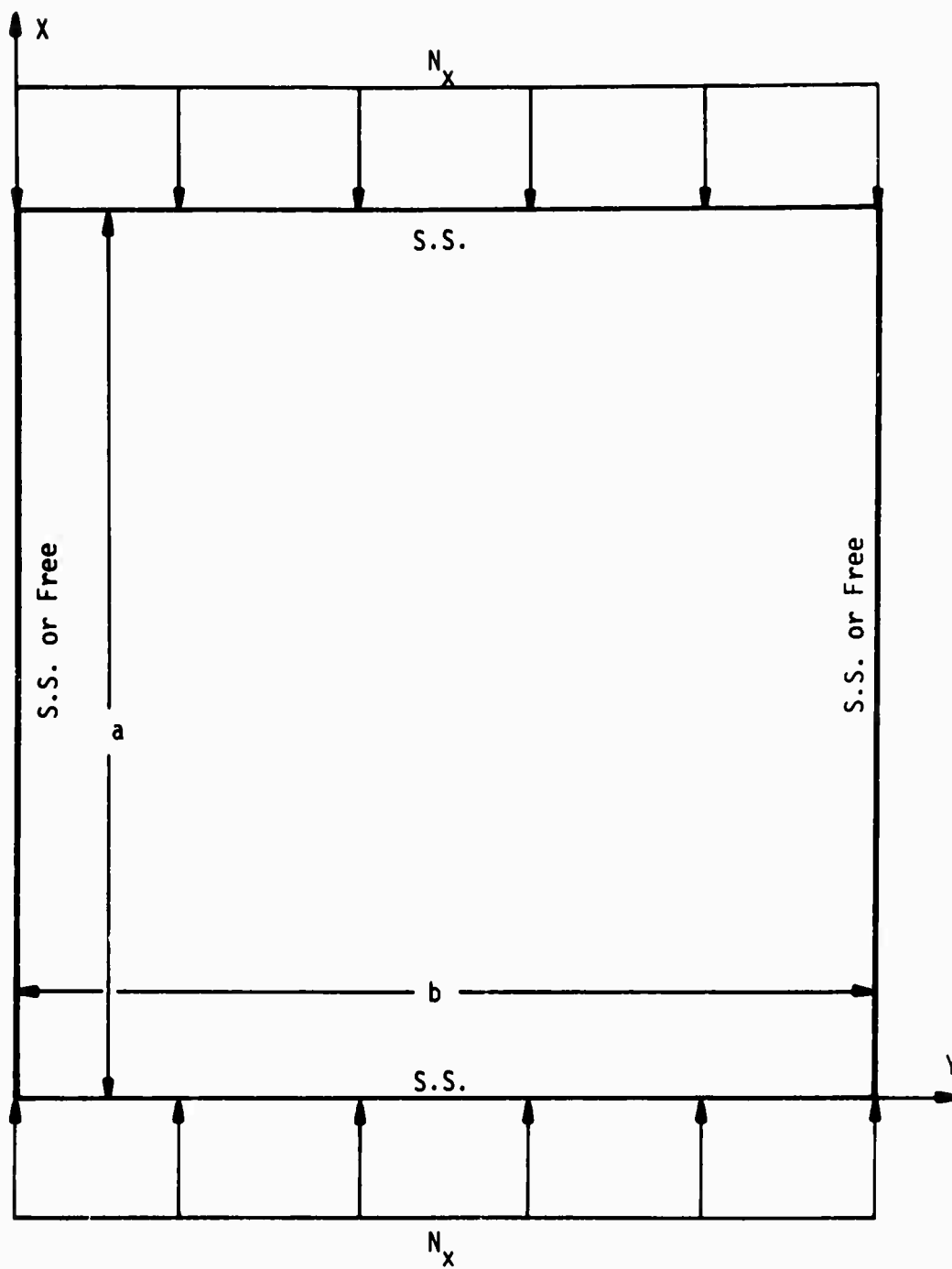


Figure 1. Schematic Diagram of a Typical Test Specimen with Assumed Load and Boundary Conditions.

$$(N_x)_{cr} = D_{11} \pi^2/a^2 \quad (2.5)$$

For the simple-simple case the mode shape is assumed to be

$$w = A_{mn} \sin \frac{m\pi x}{a} \sin \frac{n\pi y}{b} \quad (2.6)$$

Substituting (2.6) into (2.2), we find the critical load to be

$$(N_x)_{cr} = \frac{\pi^2}{b^2} \left[D_{11} \frac{m^2 b^2}{a^2} + 2 D_3 n^2 + D_{22} \frac{a^2 n^2}{m^2 b^2} \right] \quad (2.7)$$

where m and n are chosen to make $(N_x)_{cr}$ a minimum. Since n appears only in the numerator, the minimum occurs at $n = 1$.

$$\text{For an isotropic plate } D_{11} = D_{22} = D_3 = D = \frac{Eh^3}{12(1-\nu^2)},$$

and Equation (2.5) becomes

$$(N_x)_{cr} = \frac{\pi^2}{a^2} D \quad (2.8)$$

while Equation (2.7) becomes

$$(N_x)_{cr} = \frac{\pi^2 D}{b^2} \left[\frac{mb}{a} + \frac{a}{mb} \right]^2 \quad (2.9)$$

$$\text{and, for a square isotropic plate, } (N_x)_{cr} = \frac{4\pi^2 D}{b^2} \quad (2.10)$$

2.3 Reduced Flexural Stiffness Method

The stiffness coupling matrix, $[B]$, will be non-zero if the plate configuration is unbalanced (see Appendix A). If the coupling matrix does have non-zero terms, the preceding eigenvalue formulation can be used only if the effect of the coupling terms can be approximated by

adjusting the flexural stiffnesses.⁽³⁾ This can be accomplished by first considering the force-deformation equations given in Appendix A:

$$\begin{Bmatrix} N \\ M \end{Bmatrix} = \begin{bmatrix} A & B \\ B & D \end{bmatrix} \begin{Bmatrix} \epsilon \\ -\kappa \end{Bmatrix}$$

These equations can be solved for $[M]$ by solving the first equation for $\{\epsilon\}$ and then substituting its value into the second equation as follows:⁽⁴⁾

$$\{N\} = [A] \{\epsilon\} - [B] \{\kappa\}$$

$$\{\epsilon\} = [A]^{-1} \{N\} + [A]^{-1} [B] \{\kappa\}$$

$$[M] = [B] \{\epsilon\} - [D] \{\kappa\}$$

$$[M] = [B] [A]^{-1} \{N\} + [B] [A]^{-1} [B] \{\kappa\} - [D] \{\kappa\}$$

$$[M] = ([B] [A]^{-1} [B] - [D]) \{\kappa\} + [B] [A]^{-1} \{N\}$$

$$[M] = (D - [B] [A]^{-1} [B]) \{-\kappa\} + [B] [A]^{-1} \{N\} \quad (2.11)$$

$$[M] = [D^*] \{-\kappa\} + [B] [A]^{-1} \{N\} \quad (2.12)$$

$$\text{where } [D^*] = [D] - [B] [A]^{-1} [B]$$

The reduced stiffness matrix, $[D^*]$, can easily be calculated and used in place of $[D]$ in the buckling predictions. The term $[B] [A]^{-1} \{N\}$ is neglected here and will be discussed in Chapter 5.

2.4 Numerical Methods

Buckling loads for plates for which the D_{16} and D_{26} terms are of the same order of magnitude as the other flexural stiffness terms cannot be found by classical orthotropic theory. A number of

numerical methods are available which can be applied to plates of this type. Results from Ritz,⁽⁵⁾ Galerkin,⁽⁶⁾ or finite element⁽⁷⁾ methods are presented in Table 2, Chapter 4 for any plates which display relatively strong D_{16} and D_{26} terms. This section will give a very brief description of each of these methods.

2.4.1 Ritz Method

For a solution based on the Ritz Method, functions which satisfy the boundary conditions are multiplied by unknown coefficients. The total potential energy is minimized with respect to the unknown coefficients. General Dynamics, Fort Worth Division has developed a computer capability based on the Ritz Method using beam functions for the approximate deflected surface. A total of forty-nine unknowns are used in the expansion to determine the buckling loads. The method was developed to treat only those plates which are elastically symmetric about the midsurface. The buckling loads for all the symmetric boron plates were predicted by this method, the predictions having been supplied by General Dynamics, Fort Worth Division.

2.4.2 Galerkin Method

For a solution based on the Galerkin Method, functions which satisfy the boundary conditions are used in an expansion for the displacements. The displacement expansions will in general not satisfy the governing differential equation of the field so it is required that the work done by the unbalanced forces over the field should be zero, namely

$$\iint [L(c_i \phi_i(x,y))] \phi_j(x,y) dx dy = 0$$

where L represents the governing differential equation. This type of formulation was developed at Case Western Reserve University, by C. C. Chamis for anisotropic plates using the following expansion for W :

$$W = \sum_{m=1}^M \sum_{n=1}^N A_{mn} \sin \frac{m\pi x}{a} \sin \frac{n\pi y}{b}$$

where M and N are large enough to guarantee convergence of the buckling.

Frequently, as in this situation, it is difficult to select approximate functions which satisfy both the natural and imposed boundary conditions. If expansions which satisfy the imposed boundary conditions are selected, the natural boundary conditions can be treated in the large by adding the work done on the boundaries to the work done in the field and equating the sum to zero. The Jacobi method was then used to determine the eigenvalues which represent the buckling loads.

2.4.3 Geometrically Nonlinear Finite Element Method

The geometrically nonlinear finite element method can also be applied to a generally anisotropic plate. This method uses rectangular elements based on first order Hermite interpolation polynomials which satisfy the admissibility condition of the theorem of minimum potential energy. The method of solution is a direct energy minimization using load increments to obtain a load-deflection curve.

In the case of a plate with no membrane-bending coupling, the buckling load can be determined by finding the intersection of the load-deflection curve for a flat plate with the load axis. If membrane-bending coupling is present, the buckling load must, in some cases, be determined from the load-deflection curve by some method such as the Southwell plot described in Chapter 3.

CHAPTER 3

EXPERIMENTAL DETERMINATION OF BUCKLING LOADS

The general purpose of the experimental portion of the program was to verify the various theoretical buckling predictions. In order to achieve this purpose it was necessary to meet the following requirements:

- (1) Suitable test specimens had to be acquired or fabricated so that a wide range of material characteristics could be included.
- (2) A method had to be found to determine when the critical load was reached in a plate.
- (3) A test fixture capable of imposing the desired boundary and load conditions had to be designed and built.

3.1 Test Specimens

The plate specimens listed in Chapter 4, Table 1, were tested with both simple-simple and simple-free support conditions. These test specimens are also discussed in Appendix A with regard to notation and fabrication techniques. Since many of these plates were to be used in other tests, requirements number two and three above were further restricted to be non-destructive.

3.2 Southwell Plot

Classical plate buckling theory assumes that a plate remains flat as it is loaded until the critical load is reached, at which time the plate assumes some deflected shape. All real plates, however, have some initial curvature or are loaded eccentrically and will deflect as they are loaded. The experimental verification of most buckling theories, then, will require some criteria for determining when the

actual plate would have reached its critical load had it remained flat during loading.

In 1932, Southwell⁽⁸⁾ presented a method for determining the critical load for a column with an initial imperfection. He first showed that the actual load-deflection curve for such a column would be a rectangular hyperbola with asymptotes at zero deflection and at $P = P_{cr}$, where P_{cr} is the critical load for a perfectly straight column. Southwell then showed that, by a change in coordinates from P versus Δ to Δ/P versus Δ , the hyperbola could be transformed into a straight line with a slope of $1/P_{cr}$.

The buckling of plates, particularly those with only the loaded edges supported, is very similar to the buckling of columns. Southwell, in his original paper, suggested that his method could be applied to plates just as it has been applied to columns. In this section the applicability of the Southwell plot to plates will be verified by a formulation which closely parallels Southwell's original formulation.

A plate with simple-free boundary conditions can be considered to be a column. Timoshenko and Gere⁽⁹⁾ have investigated the case of a slender column with an initial imperfection of the form

$$w_0 = a_1 \sin \pi x/a \quad (3.1)$$

subjected to a longitudinal compressive force P .

By substituting Equation (3.1) into the differential equation and applying the boundary conditions to the general solution, the

deflection resulting from the load will be

$$w_1 = \frac{\alpha}{1-\alpha} a_1 \sin \pi x/a = \Delta$$

where $\alpha = \frac{P}{P_{cr}}$

and the total deflection will be

$$\begin{aligned} w &= w_0 + w_1 = a_1 \sin \frac{\pi x}{a} + \frac{\alpha}{1-\alpha} a_1 \sin \frac{\pi x}{a} \\ &= \frac{a_1}{1-\alpha} \sin \frac{\pi x}{a} \end{aligned}$$

at $x = a/2$, $\sin \frac{\pi x}{a} = 1$, and

$$\Delta = \frac{\alpha a_1}{1-\alpha}$$

Rearranging,

$$\Delta - \Delta \alpha - \alpha a_1 = 0$$

which is the equation of a hyperbola. Dividing by P , we find that

$$\Delta/P - \frac{\Delta}{P_{cr}} - \frac{a_1}{P_{cr}} = 0$$

$$\Delta/P = \frac{1}{P_{cr}} (\Delta + a_1) \quad (3.2)$$

This technique can be extended to a plate with all four edges simply supported, subjected to a compressive edge load in the x direction. If the plate is orthotropic or isotropic, the deflection pattern for the first mode, as determined by Timoshenko and Gere,⁽⁹⁾

will be

$$w = w_0 + w_1 = \frac{a_{11}}{1-\alpha} \sin \frac{\pi x}{a} \sin \frac{\pi y}{b}$$

where $\alpha = \frac{N_x}{(N_x)_{cr}}$

and $w_1 = a_{11} \left[\frac{1}{1-\alpha} - 1 \right] \sin \frac{\pi x}{a} \sin \frac{\pi y}{b}$

as before, at $x = a/2, y = b/2$

$$\frac{\Delta}{N_x} = \frac{1}{(N_x)_{cr}} (\Delta + a_{11}) \quad (3.3)$$

This obviously can be generalized to any point on the plate and to any mode, providing $\sin \frac{m\pi x}{a} \sin \frac{n\pi y}{b}$ remains non-zero.

As long as the deflection due to the load overshadows the initial imperfection, and the deflection still remains small, the Southwell plot can be applied to any portion of the load-deflection curve.

This feature of the Southwell plot is particularly important for the following reasons:

1. The critical load can be found experimentally without actually buckling the plate. Thus, as long as the deflections can be made large enough to overshadow the initial imperfection without damaging the plate, the test will be nondestructive.
2. The experimental data can be taken at relatively low load levels, and there is less danger of the predicted experimental behavior being influenced by a deviation of the material from Hooke's Law.
3. A test fixture need not be capable of imposing high loads on a very stiff or flat plate. Instead, the plate can be perturbed by a lateral load, and, by

the principle of superposition, the deflection caused by this perturbation can be considered to be the same as an initial imperfection. Thus, the load can be increased up to the limit of the test fixture, and the critical load can be predicted for very stiff plates if a sufficient amount of deflection is achieved.

The nature of buckling of the generally anisotropic plate is similar to that of the orthotropic plate, although the plate may show more deflection due to an unbalanced configuration or it may have a twisted deflection pattern rather than the symmetric sine-sine pattern of the orthotropic plate. These differences, however, should not restrict the use of the Southwell plot, since the basic nature of the buckling phenomena used in the preceding derivations is preserved, as was witnessed in the actual tests.

Horton, et. al.,⁽¹⁰⁾ give a very detailed review of the applicability of the Southwell plot to linear buckling problems. Their conclusions tend to reinforce the arguments presented thus far.

During the actual testing of a plate, the deflections must be large enough so that any initial misalignment in the test fixture, as well as any initial imperfection, is overshadowed by the deflection due to the load. This may require that the deflections be larger than those acceptable for the small deflection theory on which the Southwell plot is based. It is desirable, therefore, to consider the effects of large deflections on the Southwell plot.

The problem of nonlinear elastic stability as it relates to the Southwell plot has been investigated by Roorda,⁽¹¹⁾ and his findings provide some insight into the case of plate buckling. With the support conditions previously described, there are two types of post-

buckling behavior possible, the neutral and the stable-symmetric. These two types are illustrated for two of the test plates in Figures 2 and 3, where the dotted lines depict the load-deflection curves for the actual plates. The neutral case is the one assumed by Southwell, and the stable-symmetric case considers the nonlinearities associated with large deflections. The plate with simple-free support conditions is not exactly the neutral case, but approximates it in the deflection region under consideration. For further explanation, see Reference 10.

The Southwell plots associated with each of the buckling types, as suggested by Roorda, are given in Figures 2 and 3 for two of the test plates. He further suggests that the critical load is overestimated by the Southwell plot in the case of stable-symmetric buckling, while the neutral case estimates the critical load correctly. The amount of discrepancy in the stable-symmetric case will depend on the curvature of the post-buckling curve for an ideal (flat) plate at $\Delta = 0$.

3.3 Test Fixture

The test fixture (see Figures 4, 5, 6, and 7, and Appendix D) features roller supports (if required) on the sides of the test plate and nine individual knife-edge support points top and bottom through which the load is transmitted to the plate. The load is either read out through a load cell or else read directly off of the testing machine. Deflections are measured by closing an electrical circuit with a micrometer and a metal contact on the plate.

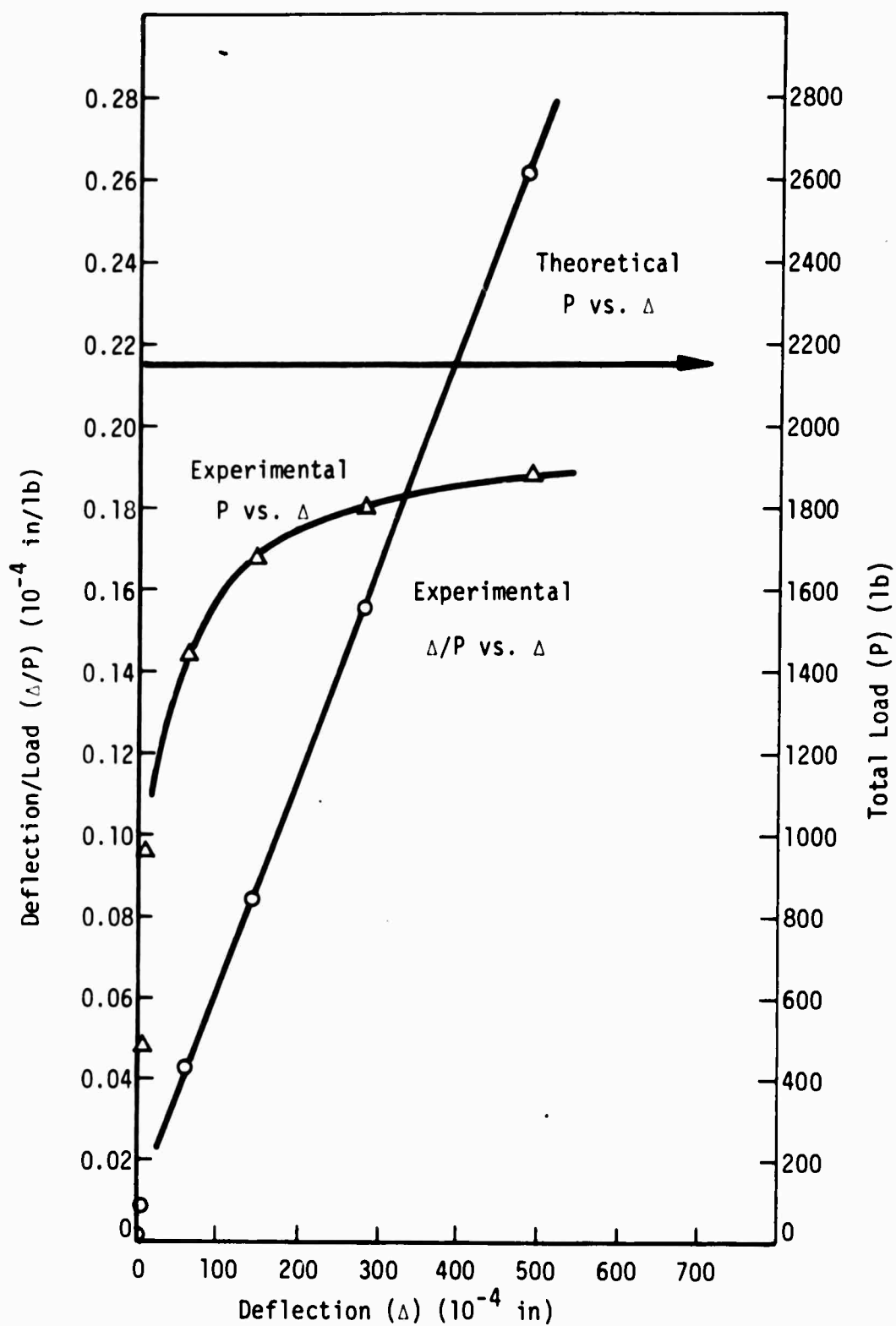


Figure 2. Southwell Plot and Load Deflection Curve for Plate No. 404, 2 Sides Supported. (Neutral Buckling)

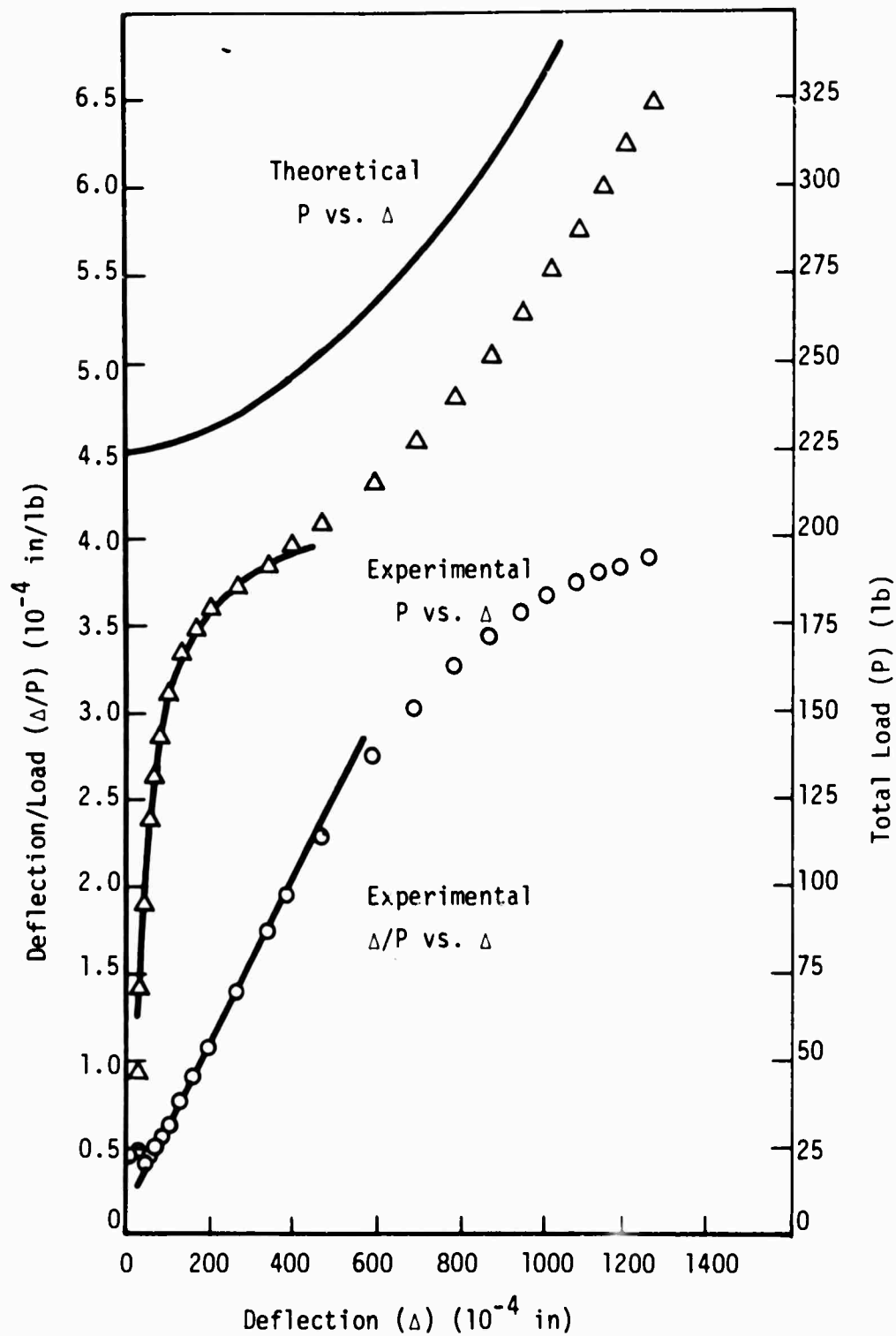


Figure 3. Southwell Plot and Load Deflection Curve for Plate No. 201, 4 Sides Supported (Stable Symmetric)

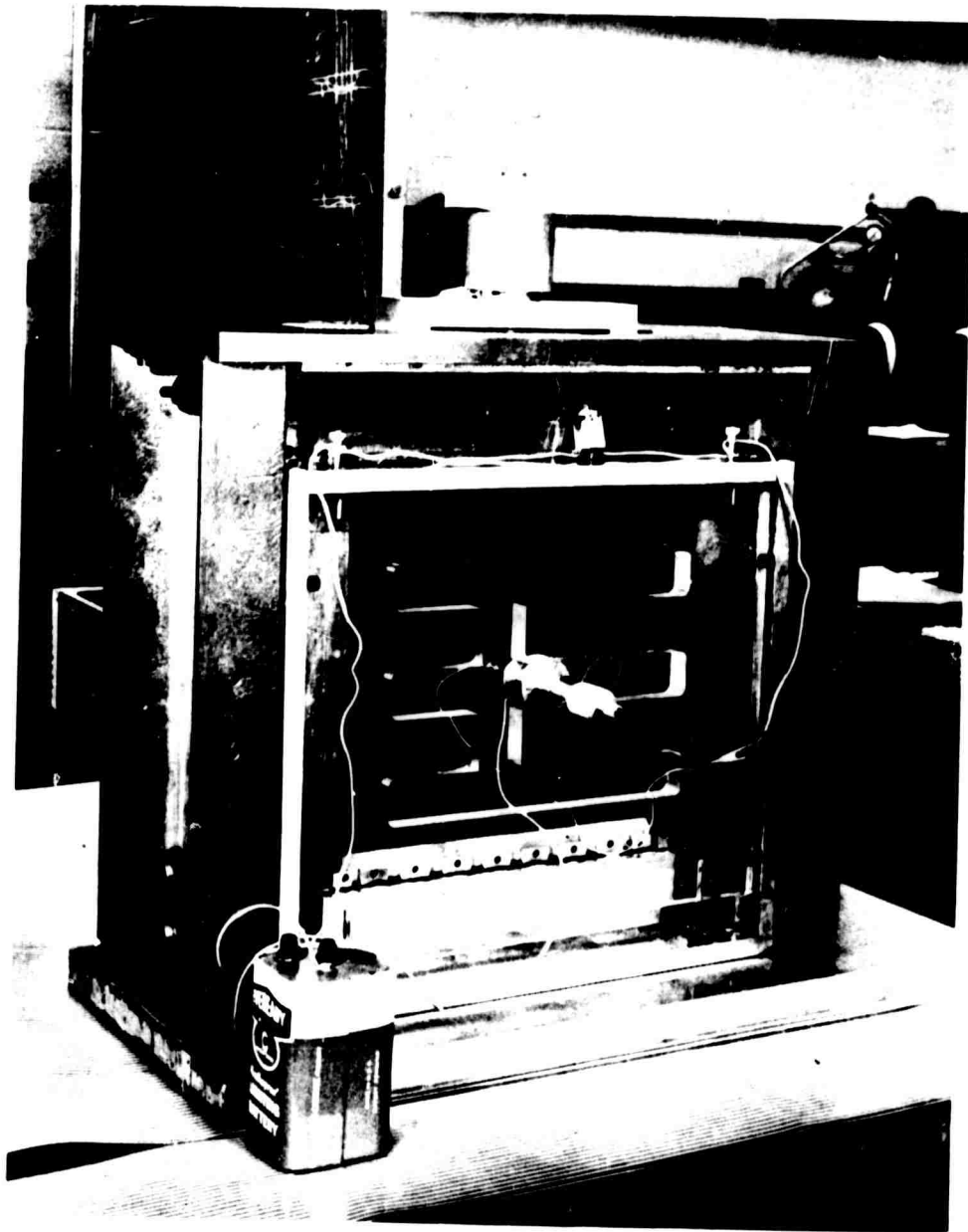


Figure 4. Test Fixture with Deflection
Measuring Device.

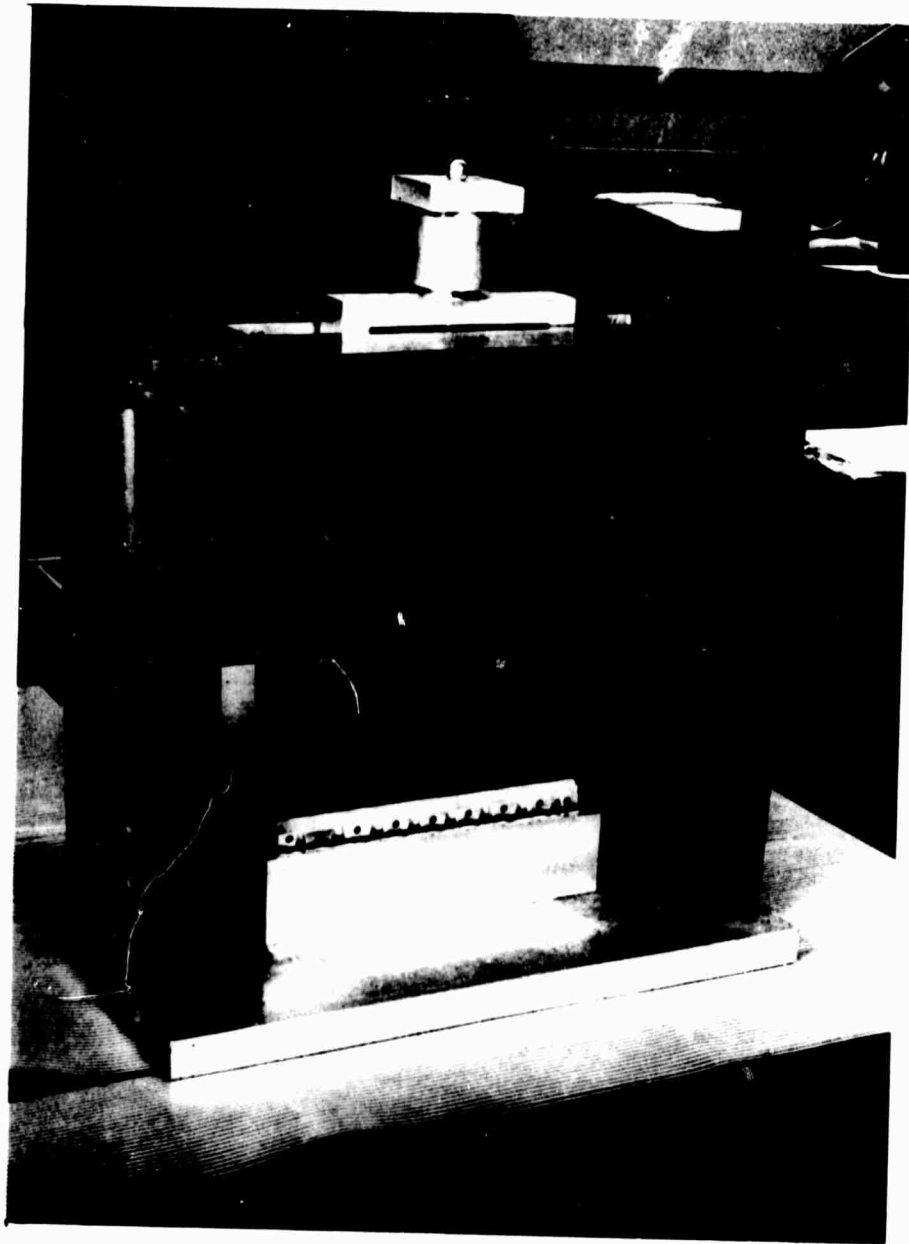


Figure 5. Test Fixture in Two Sides
Supported Configuration.

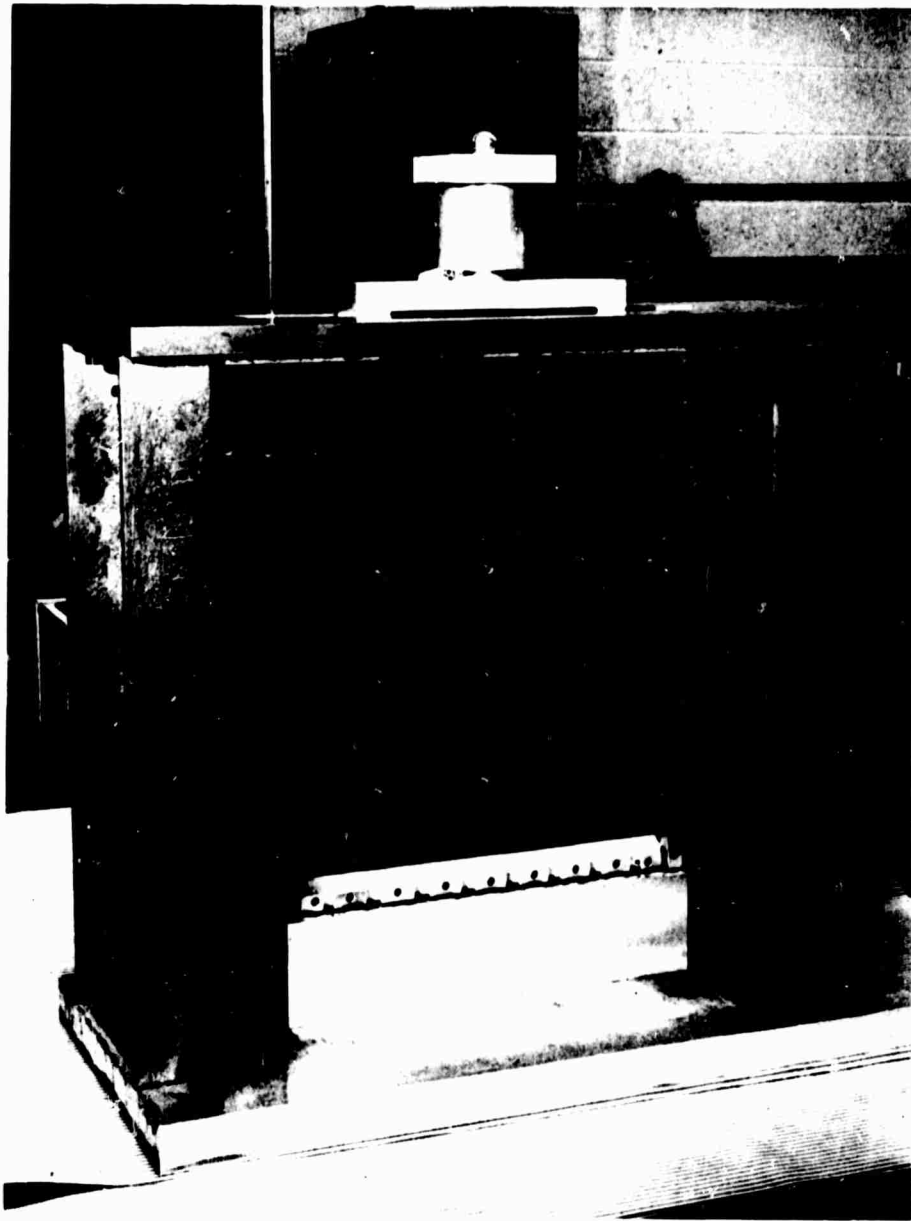


Figure 6. Test Fixture in Four Sides Supported Configuration.

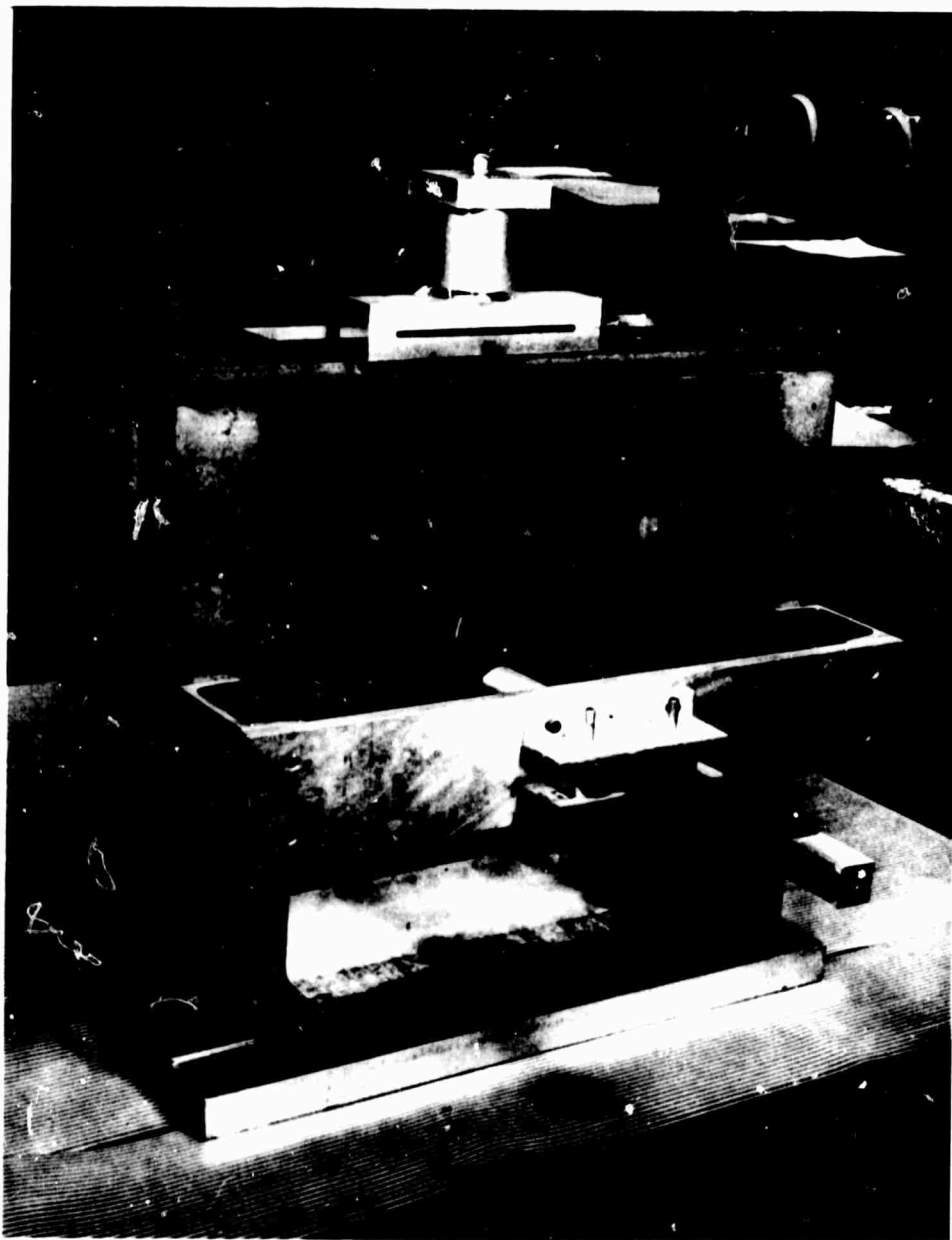


Figure 7. Back View of Test Fixture With
Perturbation Load Device in Place.

3.3.1 Application of the Load

The load is applied through a ball bearing and load cell to a rigid loading bar. The ball bearing permits only vertical force to be applied to the loading bar and eliminates any moments which could result from a misalignment between the testing machine and the loading bar. The loading bar distributes the load along the edge of the plate by means of nine individual spring-position-knife-edge combinations as illustrated in Appendix D. This arrangement keeps the load evenly distributed despite the possible presence of large deflections in the plate. A small variation in compressed length from one spring to the next will not cause a large difference in the force exerted by the springs if the springs are near the middle of their deflection range.

The knife-edges (see Figure 8) are attached to and centered on the plate by means of a set screw on either side. The screws butt up against either a metal or a Teflon strip which protects the plate. Each knife edge fits into a V-groove in one of the pistons, and is free to rotate independently of the other knife-edges. Since there is a matching spring-piston combination at the bottom, as well as at the top, the plate translates vertically downward as a rigid body by the amount that the springs at the bottom compress. The load bar at the top must be free to move vertically downward by the total amount of the deflection in the springs top and bottom, plus any vertical deflection in the plate itself. This movement amounts to a maximum of about one inch and is accomplished by allowing the loading bar to

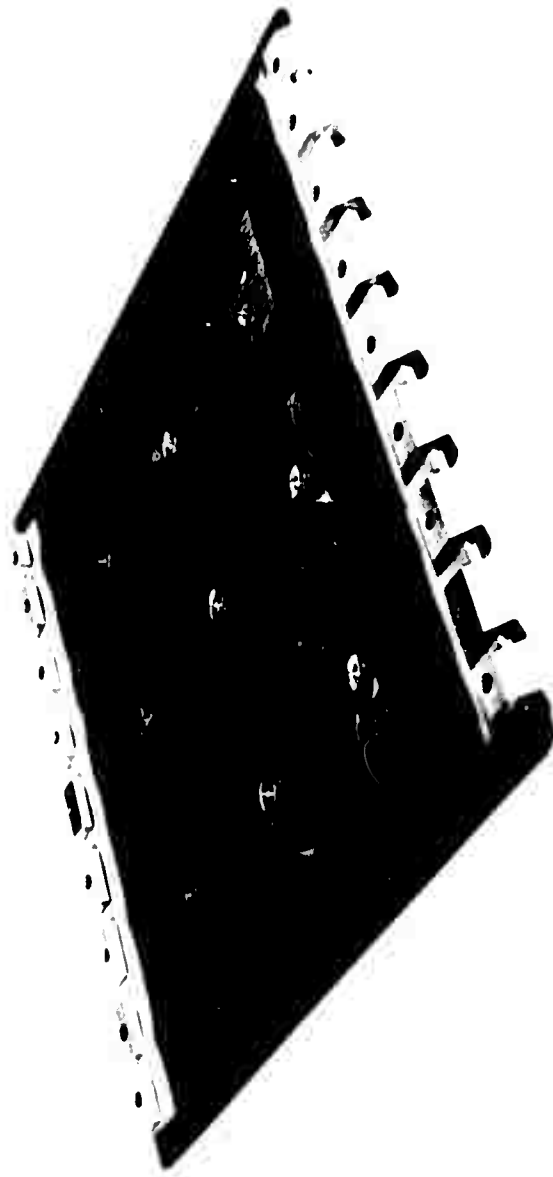


Figure 8. Test Plate with Metal Contacts,
Teflon Strip, and Knife Edges.

slide between two rigid angles.

3.3.2 Side Supports

The vertical movement of the plate complicates the side supports. The plate must either slide between the side supports or else the side supports must move with the plate. The latter was found to be more feasible, and the rollers are encased in a slotted bar which is forced to slide along with the plate. In some cases the plates were eleven inches square rather than the usual ten inches square, and in this case larger rollers were used which were not encased in a slotted bar. The plate was then free to either slide between the rollers or to drag the rollers along by friction developed between the roller and the plate. The latter case usually prevailed.

The test fixture can be adjusted to accommodate plates of thicknesses up to one-eighth of an inch. Setscrews in the side supports and in the knife-edges accomplish the necessary spacing of the rollers and centering of the side supports and knife-edges. Plates which are larger than ten inches square present some problems. In the case of the eleven inch square boron plates, the side supports were altered as described above, but the rollers remained 9.75 inches apart, leaving an overhang on either side. Larger rollers were used so that they could be extended beyond the usual ten inches supported by the slotted bars. This left about one inch at the top end of the rollers unsupported, but it is believed that the rollers were sufficiently stiff to support the plate over this distance.

3.3.3 Deflection Measurement

One of the most crucial parts of a test which relies on the Southwell plot to predict the critical load is the measurement of the deflections. It is desirable to measure the deflections at the point on the plate which experiences the greatest displacement. The two principal reasons for this are:

1. There is often a limit to the amount of displacement which may be imposed on the plate without causing some damage to the plate. If displacements are not measured at the maximum point, this limit may be exceeded without realizing it.
2. Measurements of deflection are more accurate if the deflections are large, and, therefore, the critical load prediction will be more accurate.

Since the maximum deflection is not always at the center of the plate, and since the definition of the mode shape, if desired, requires the deflection at numerous points on the plate, a deflection measuring system which can measure deflections at numerous points on the plate was used. In order to measure the deflection at any point on the plate, a metal contact is attached to the plate at the desired point with double-sided cellophane tape. This contact is a large thumbtack on which the point has been rounded and the back has been ground flat. One contact is placed wherever the deflection is to be measured. These contacts are then connected in a series circuit which includes a small light bulb, a battery, and a micrometer. The micrometer is mounted in front of the test plate on a plexiglass holder (see Figure 4), and can be moved along three horizontal slots in order to find the mode shape of the plate. Locations of the con-

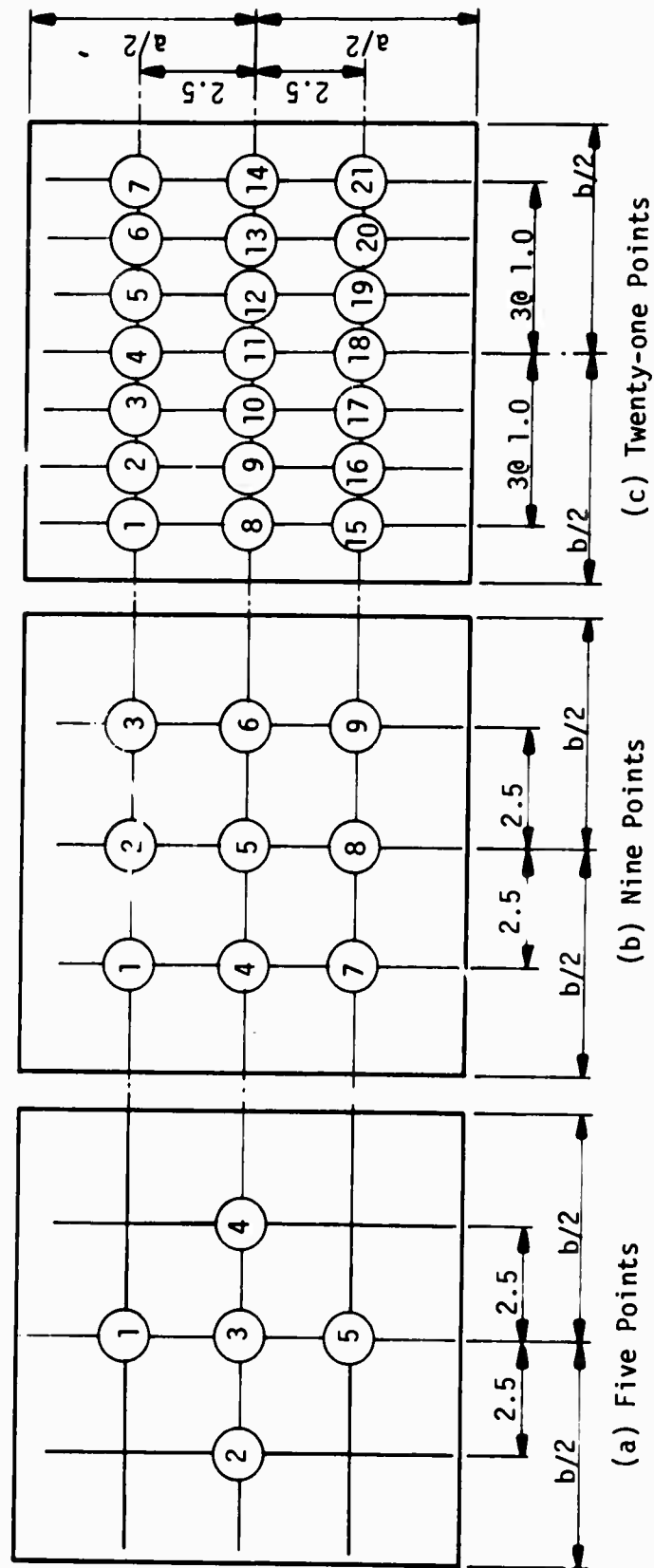


Figure 9. Location of Points at Which Deflection is Measured

tacts for the three arrangements used (5, 9, or 21 contacts) are given in Figure 9.

Readings are taken by bringing the micrometer up to the contact until the circuit is closed and the light bulb illuminates. Successive readings at two loads can be subtracted to find the deflection caused by that particular load increment. Since the plate is constantly moving downward while the micrometer remains stationary, the end of the micrometer is fitted with a wide, flat tip which has a larger diameter than the possible translation of the plate. Thus, assuming that the plate moves perpendicular to the micrometer, deflections can be measured at the same point on the plate throughout the test. The curvature of the plate causes the contact to tilt somewhat, but this effect has been calculated to be very small in comparison to the usual deflection. Although this arrangement for measuring deflections is rather simple in nature, it accomplishes two major goals: it measures deflections to an accuracy of one ten-thousandths of an inch for a small load increment, and it exerts no appreciable lateral force on the plate.

3.4 Test Procedure

A plate is prepared for testing (see Figure 8) by first attaching the contacts at the desired locations. The knife-edges are then attached along the edges to be loaded, with a strip of thin metal or, in the case of plates with a high Poisson's ratio, a strip of Teflon between the knife-edge and the plate. This strip protects the edge of the plate and, in the case of the Teflon, cuts down on the

friction between the plate and the knife-edge. The plate is then ready to be inserted into the fixture for testing.

Before the test is actually run, a load is applied to the plate and then released repeatedly until the micrometer readings at zero load remain the same within one or two-thousandths of an inch. This takes out much of the misalignment in the fixture and gives some indication of the load levels to be expected during the test. Usually only one load application is necessary to achieve this initial shake down. The test is then run, and deflections are normally taken up to at least one-half the plate thickness, and often higher in the case of very thin plates.

The test yields a deflection reading for each load increment, and a load-deflection curve can then be plotted. Deflections are normally taken at the middle of the plate for a first mode deflection or at the maximum deflection point for a higher or twisted mode shape.

Once the loads and deflections are known, Δ/P can be calculated at each load, and the Southwell plot can be drawn. If the ends of the plot do not fall on the straight line portion of the curve, they are truncated, and the remaining points are used in calculating the critical load. This calculation is done by a computer program which finds the best straight line through the points by a least-squares curve fit. The program then determines the critical load of the plate by calculating the inverse of the slope of the straight line.

CHAPTER 4

RESULTS

Numerical results are listed in this chapter for all of the plates which were tested. Table 1 lists the materials, configurations, and dimensions for each plate, and Table 2 lists the experimental buckling loads for each support condition as well as any theoretical buckling loads available.

Plate dimensions as given are for the actual size of the plate, not for the distance between supports. The actual distance between the knife edges at the top and bottom is one-half inch longer than the second dimension given for the plate. The actual distance between the roller supports is 9.75 inches for the eleven inch square plates and the ten inch by eleven inch plate, while for all other plates it is slightly under ten inches. The load is considered to be distributed over ten inches for all plates except those for which the distance between side supports is 9.75 inches, in which case the load is considered to be distributed over 9.75 inches. Dimensions used in the theoretical prediction are ten inches by ten inches except for those plates for which the roller supports are 9.75 inches apart, in which case the dimensions are considered to be $a = 11$ inches and $b = 9.75$ inches (see Figure 1). Appendix A explains the notation used for the plate configurations as well as the fabrication technique for the unbalanced and stiffened plates.

The following remarks pertain to the results listed in Table 2:

1. Plates No. 102, 103, and 104 are basically the same plate but have different dimensions as given in Table 2.
2. Plate No. 202 may have been damaged.
3. All plates buckled in the first mode (as predicted by the theories) except the following:
 - a. Plates No. 207, 401, 405, and 407 buckled in the second mode with simple-simple supports as predicted by the theories.
 - b. Plate No. 508 buckled in the second mode with simple-simple supports although both theories predicted first mode.
 - c. Plates No. 406, 407, and 408 displayed twisted mode shapes with simple-simple supports.
4. There is no theory readily available for Plates No. 303 and 304.
5. Plate No. 209 and all of the 500 series plates varied considerably in thickness, and an average thickness was used in the buckling calculations.

TABLE 1
PLATE MATERIALS, CONFIGURATIONS, AND DIMENSIONS

| Plate No. ^c | Material | Plate Configuration | Stiffener Configuration | Stiffener Direction | Dimensions (in.) |
|------------------------|---------------------------|---------------------|-------------------------|---------------------|------------------|
| 101 | Aluminum | ----- | ----- | ----- | 10 x 10 x .063 |
| 102 | Aluminum | ----- | ----- | ----- | 10 x 10 x .090 |
| 103 | Aluminum | ----- | ----- | ----- | 11 x 11 x .090 |
| 104 | Aluminum | ----- | ----- | ----- | 10 x 11 x .090 |
| 105 | Steel | ----- | ----- | ----- | 10 x 10 x .078 |
| 201 | "Thorne1"-25 ^d | (0,90,90,0) | ----- | ----- | 10 x 10 x .055 |
| 202 | "Thorne1"-25 | 9(0,90) | ----- | ----- | 10 x 10 x .121 |
| 203a | "Thorne1"-25 | 9(+45) | ----- | ----- | 10 x 10 x .116 |
| 203b | "Thorne1"-25 | 9(+45) | ----- | ----- | 10 x 10 x .116 |
| 204 | "Thorne1"-40 | 5(0,90) | ----- | ----- | 10 x 10 x .043 |
| 205 | "Thorne1"-40 | 5(90,0) | ----- | ----- | 10 x 10 x .043 |
| 206 | "Thorne1"-40 | (0,90,90,0) | ----- | ----- | 10 x 10 x .034 |
| 207 | "Thorne1"-40 | (90,0,0,90) | ----- | ----- | 10 x 10 x .034 |

TABLE 1, CONTINUED

| Plate No. ^c | Material | Plate Configuration | Stiffener Configuration | Stiffener Direction | Dimensions (in.) |
|------------------------|--------------|--------------------------|-------------------------|---------------------|-----------------------------------|
| 208 | "Thornel"-40 | (0,45,45,45,0) | ----- | ----- | 10 x 10 x .038 |
| 209a | "Thornel"-40 | (0,0,90,90) ^b | ----- | ----- | 10 x 10 x .091 |
| 209b | "Thornel"-40 | (90,90,0,0) ^b | ----- | ----- | 10 x 10 x .091 |
| 301 | Fiberglass | (0,90,0,90) | 8(0) | (0,90) | 10 x 10 x .033(.115) ^a |
| 302 | Fiberglass | (0,90,0,90,0,90) | 8(0) | (0,90) | 10 x 10 x .057(.133) |
| 303 | Fiberglass | (0,90,0,90) | 7(0) | (+45) | 10 x 10 x .031(.112) |
| 304 | Fiberglass | (0,90,0,90) | 7(0) | (-30,60) | 10 x 10 x .033(.118) |
| 401 | Boron | 20(+60) | ----- | ----- | 11 x 11 x .110 |
| 402 | Boron | 20(+30) | ----- | ----- | 14 x 11 x .110 |
| 403a | Boron | 20(+45) | ----- | ----- | 11 x 11 x .101 |
| 403b | Boron | 20(+45) | ----- | ----- | 11 x 11 x .101 |
| 404 | Boron | 20(0) | ----- | ----- | 11 x 11 x .096 |
| 405 | Boron | 20(90) | ----- | ----- | 11 x 11 x .096 |
| 406 | Boron | 20(30) | ----- | ----- | 11 x 11 x .106 |

TABLE 1, CONTINUED

| Plate No. ^c | Material | Plate Configuration | Stiffener Configuration | Stiffener Direction | Dimensions (in.) |
|------------------------|------------|------------------------------|-------------------------|---------------------|------------------|
| 407 | Boron | 20(60) | ----- | ----- | 11 x 11 x .106 |
| 408a | Boron | 20(45) | ----- | ----- | 11 x 11 x .095 |
| 408b | Boron | 20(-45) | ----- | ----- | 11 x 11 x .095 |
| 409a | Boron | 10(45), 10(-45) ^b | ----- | ----- | 11 x 11 x .109 |
| 409b | Boron | 10(-45), 10(45) ^b | ----- | ----- | 11 x 11 x .109 |
| 501 | Fiberglass | (90,+45,-45,90) ^b | ----- | ----- | 10 x 10 x .103 |
| 502 | Fiberglass | (0,-45,+45,0) ^b | ----- | ----- | 10 x 10 x .103 |
| 503 | Fiberglass | (45,90,90,-45) ^b | ----- | ----- | 10 x 10 x .108 |
| 504 | Fiberglass | (-45,0,0,45) ^b | ----- | ----- | 10 x 10 x .108 |
| 505 | Fiberglass | (90,25,-25,90) ^b | ----- | ----- | 10 x 10 x .103 |
| 506 | Fiberglass | (0,-25,25,0) ^b | ----- | ----- | 10 x 10 x .103 |
| 507 | Fiberglass | (25,90,90,-25) ^b | ----- | ----- | 10 x 10 x .085 |
| 508 | Fiberglass | (-65,0,0,65) ^b | ----- | ----- | 10 x 10 x .085 |
| 509a | Fiberglass | 4(0), 4(90) ^b | ----- | ----- | 10 x 10 x .090 |

TABLE 1, CONTINUED

| Plate No. ^c | Material | Plate Configuration | Stiffener Configuration | Stiffener Direction | Dimensions (in.) |
|------------------------|------------|--------------------------|-------------------------|---------------------|------------------|
| 509b | Fiberglass | 4(90), 4(0) ^b | ----- | ----- | 10 x 10 x .090 |

^aThe first thickness given represents the plate thickness while the second thickness (in parenthesis) represents the total thickness including stiffeners.

^bSee Appendix A, Section 2, for a more complete description of these configurations.

^cWhere an a and b are included after a plate number, this indicates that the plate was tested in two perpendicular directions represented by a and b.

^d"Thorne1" is a registered trademark.

TABLE 2
EXPERIMENTAL AND THEORETICAL BUCKLING LOADS

| Plate No. | Assumed Dimensions (in.) | | $(N_x)_{cr}$ (lb/in) | | | |
|--------------|-----------------------------|------|----------------------|--------------------------|------------------------|--------------------------|
| | | | Simple-Free Supports | | Simple-Simple Supports | |
| | | | Experimental | Theoretical ^a | Experimental | Theoretical ^a |
| 101 | 10 | 10 | 22.3 | 22.9 | 89.3 | 91.6 |
| 102 | 10 | 10 | 64.3 | 66.7 | 255 | 267 |
| 103 | 11 | 9.75 | 56.4 | 55.6 | 270 | 273 |
| 104 | 11 | 9.75 | 53.2 | 55.6 | 282 | 273 |
| 105 | 10 | 10 | 121 | 125 | 516 | 520 |
| 201 | 10 | 10 | 11.3 | 12.5 | 21.7 | 19.1 |
| 202 | 10 | 10 | 84.9 | 105 | 189 | 204 |
| 203a | 10 | 10 | 33.8 | 44.9 | 313 | 292 |
| 203b | 10 | 10 | 34.7 | 44.9 | 283 | 292 |
| 204 | 10 | 10 | 10.8 | 12.7 | 15.5 | 18.7 |

TABLE 2, CONTINUED

| Plate No. | Assumed Dimensions (in.) | | $(N_x)_{cr}$ (lb/in) | | | |
|-----------|--------------------------|----|----------------------|--------------------------|------------------------|--------------------------|
| | a | b | Simple-Free Supports | | Simple-Simple Supports | |
| | | | Experimental | Theoretical ^a | Experimental | Theoretical ^a |
| 205 | 10 | 10 | 2.74 | 3.83 | 16.3 | 18.7 |
| 206 | 10 | 10 | 5.26 | 6.92 | 6.69 | 8.72 |
| 207 | 10 | 10 | 0.848 | 1.29 | 6.65 | 7.44 |
| 208 | 10 | 10 | 8.27 | 9.30 | 13.8 | 12.7 |
| 209a | 10 | 10 | 20.7 | 62.3 | 72.1 | 142 |
| | | | | 23.7 ^d | | 71.5 ^b |
| | | | | | | 74.2 ^d |
| | | | | | | 77.0 ^e |
| 209b | 10 | 10 | 19.7 | 62.3 | 73.7 | 142 |
| | | | | 23.7 ^c | | 71.5 ^b |
| | | | | | | 74.2 ^d |
| | | | | | | 77.0 ^e |

TABLE 2, CONTINUED

| Plate No. | Assumed | | $(N_x)_{cr}$ (lb/in) | | | |
|-----------|------------------|------|----------------------|---------------------------|------------------------|---|
| | Dimensions (in.) | | Simple-Free Supports | | Simple-Simple Supports | |
| | a | b | Experimental | Theoretical ^a | Experimental | Theoretical ^a |
| 301 | 10 | 10 | 21.4 | 35.2 | 66.3 | 73.0 |
| 302 | 10 | 10 | 32.0 | 48.9 | 99.3 | 106 |
| 303 | 10 | 10 | 13.6 | ----- | 70.6 | ----- |
| 304 | 10 | 10 | 15.5 | ----- | 68.4 | ----- |
| 401 | 11 | 9.75 | 30.3 | 37.8 34.3 ^c | 661 | 636 600 ^b 666 ^c |
| 402 | 11 | 9.75 | 137 | 161 150 ^c | 642 | 648 616 ^b 665 ^c |
| 403a | 11 | 9.75 | 53 | 70.6 60.8 ^c | 582 | 642 682 ^b 664 ^c |

TABLE 2, CONTINUED

| Plate No. | Assumed Dimensions (in.) | | $(N_x)_{cr}$ (lb/in) | | | |
|-----------|--------------------------|------|----------------------|---------------------------|------------------------|---|
| | a | b | Simple-Free Supports | | Simple-Simple Supports | |
| | | | Experimental | Theoretical ^a | Experimental | Theoretical ^a |
| 403b | 11 | 9.75 | 45 | 70.6 60.8 ^c | 602 | 642 682 ^b 664 ^c |
| 404 | 11 | 9.75 | 199 | 215 216 ^c | 271 | 292 285 ^b 299 ^c |
| 405 | 11 | 9.75 | 23.3 | 23.7 23.6 ^c | 251 | 223 210 ^b 226 ^c |
| 406 | 11 | 9.75 | 89 | 150 132 ^c | 399 | 595 425 ^b 449 ^c |
| 407 | 11 | 9.75 | 30.1 | 35.1 30.0 ^c | 433 | 589 381 ^b 417 ^c |

TABLE 2, CONTINUED

| Plate No. | Assumed Dimensions (in.) | | $(N_x)_{cr}$ (lb/in) | | | |
|-----------|--------------------------|------|----------------------|---------------------------|------------------------|---|
| | a | b | Simple-Free Supports | | Simple-Simple Supports | |
| | | | Experimental | Theoretical ^a | Experimental | Theoretical ^a |
| 408a | 11 | 9.75 | 41.6 | 70.6 51.8 ^c | 356 | 566 405 ^b 412 ^c |
| 408b | 11 | 9.75 | 34.2 | 70.6 51.8 ^c | 372 | 566 406 ^b 412 ^c |
| 409a | 11 | 9.75 | 38.5 | 70.6 42.7 ^d | 347 | 745 376 ^b 357 ^d 391 ^e |
| 409b | 11 | 9.75 | 36.1 | 70.6 42.7 ^d | 394 | 745 376 ^b 357 ^d 391 ^e |

TABLE 2, CONTINUED

| Plate No. | Assumed Dimensions (in.) | | $(N_x)_{cr}$ (lb/in) | | | |
|-----------|--------------------------|----|----------------------|---------------------------|------------------------|---|
| | | | Simple-Free Supports | | Simple-Simple Supports | |
| | a | b | Experimental | Theoretical ^a | Experimental | Theoretical ^a |
| 501 | 10 | 10 | 13.7 | 15.4 | 120 | 90.2 100 ^b |
| 502 | 10 | 10 | 36.6 | 43.4 | 102 | 90.2 100 ^b |
| 503 | 10 | 10 | 18.3 | 22.5 18.9 ^d | 113 | 126 111 ^b 102 ^d |
| 504 | 10 | 10 | 23.0 | 26.8 23.2 ^d | 108 | 126 111 ^b 102 ^d |
| 505 | 10 | 10 | 12.5 | 15.4 | 101 | 88.4 99.0 ^b |
| 506 | 10 | 10 | 39.1 | 42.6 | 88 | 88.4 99.0 ^b |

TABLE 2, CONTINUED

| Plate No. | Assumed | | $(N_x)_{cr}$ (lb/in) | | | |
|--------------|------------------|----|----------------------|---------------------------|------------------------|--|
| | Dimensions (in.) | | Simple-Free Supports | | Simple-Simple Supports | |
| | a | b | Experimental | Theoretical ^a | Experimental | Theoretical ^a |
| 507 | 10 | 10 | 12.8 | 20.5 16.6 ^d | 57.3 | 64 53 ^b 52.9 ^d |
| 508 | 10 | 10 | 9.51 | 11.2 10.9 ^d | 68.8 | 64 53 ^b 52.9 ^d |
| 509a | 10 | 10 | 15.4 | 23.9 17.6 ^d | 63.7 | 69.5 53 ^b 55.4 ^d |
| 509b | 10 | 10 | 15.3 | 23.9 17.6 ^d | 72.7 | 69.5 53 ^b 55.4 ^d |

TABLE 2, CONTINUED

^aAll theoretical predictions use standard orthotropic theory unless otherwise noted.

^bGalerkin method

^cRitz method

^dOrthotropic theory with reduced flexural stiffness matrix

^eGeometrically nonlinear finite element method

CHAPTER 5

DISCUSSION

5.1 Discussion of the Test Fixture

The test fixture is designed to serve the following functions: (1) to distribute the imposed load uniformly along the loaded edges of the plate, and (2) to support the edges of the plate in the desired manner. During the course of the study, it was found that the care with which both of these functions were executed largely determined whether the test results gave an accurate representation of the buckling load of the plate under the assumed load and boundary conditions.

5.1.1 Load Distribution

Uniform loads have traditionally been applied to plates by means of a rigid bar. This method, however, actually imposes only a uniform end-shortening on the plate, and the load distribution may, in fact, be very non-uniform. In the early stages of this study, a rigid bar was used to load the plate, and it was found that the load was not evenly distributed when there were large deflections in the plate.

Figure 10 illustrates what is believed to be the reason for this poor load distribution. As a square plate with four sides supported and an initial imperfection is loaded with a flat bar, the line $y = b/2$ deflects into a half sine wave, while the lines $y = 0$ and $y = b$ remain essentially straight. Since the length of the arc of the half sine wave must be equal to the length of the straight lines

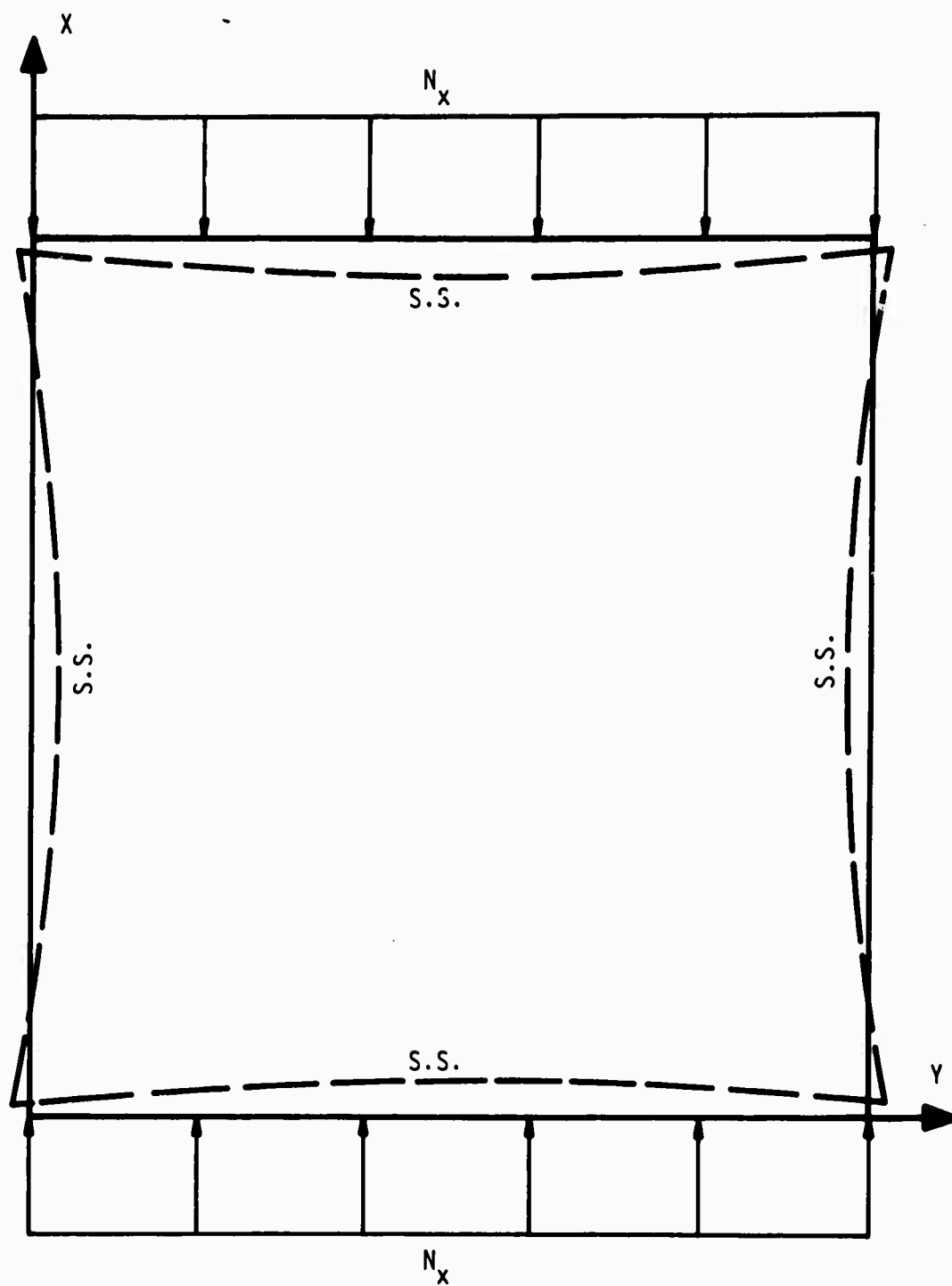


Figure 10. Undeformed (solid line) and Deformed (broken line) Isotropic or Orthotropic Plate Specimen (exaggerated).

$y = 0$ and $y = b$, the length of chord of the half sine wave must be less than the lengths of the lines $y = 0$ and $y = b$. Thus, as the deflections become larger, the flat bar will only contact the plate at the corners, and a uniform load will not be achieved. This effect will, of course, hold along the unloaded edges as well.

The curvature of the edges was plainly observable when the deflections in a plate became large. The knife edges in the central portion of an edge could be seen to pull out of the V-groove slightly, while those at the corners remained in full contact.

In order to achieve the desired load distribution, the combination of spring loaded pistons and individual knife edge supports described in Chapter 3 was substituted for the flat loading bar. The springs were selected to have about one-half inch of deflection at the maximum load for a particular plate specimen. It was found that five sets of springs (see Appendix D) were necessary to accommodate the whole spectrum of plates to be tested. Since the edges of the plate curve only a very small amount due to large deflections in the plate, the difference in the deflected length of the springs is not sufficiently large to affect the load exerted on the plate by each spring.

The actual load distribution for an aluminum plate was found by placing strain gages along one edge at five different points. At each point, one gage was placed parallel to the load direction and one perpendicular to it on each side of the plate. Figure 11 gives the location of the points at which the strains were measured. The

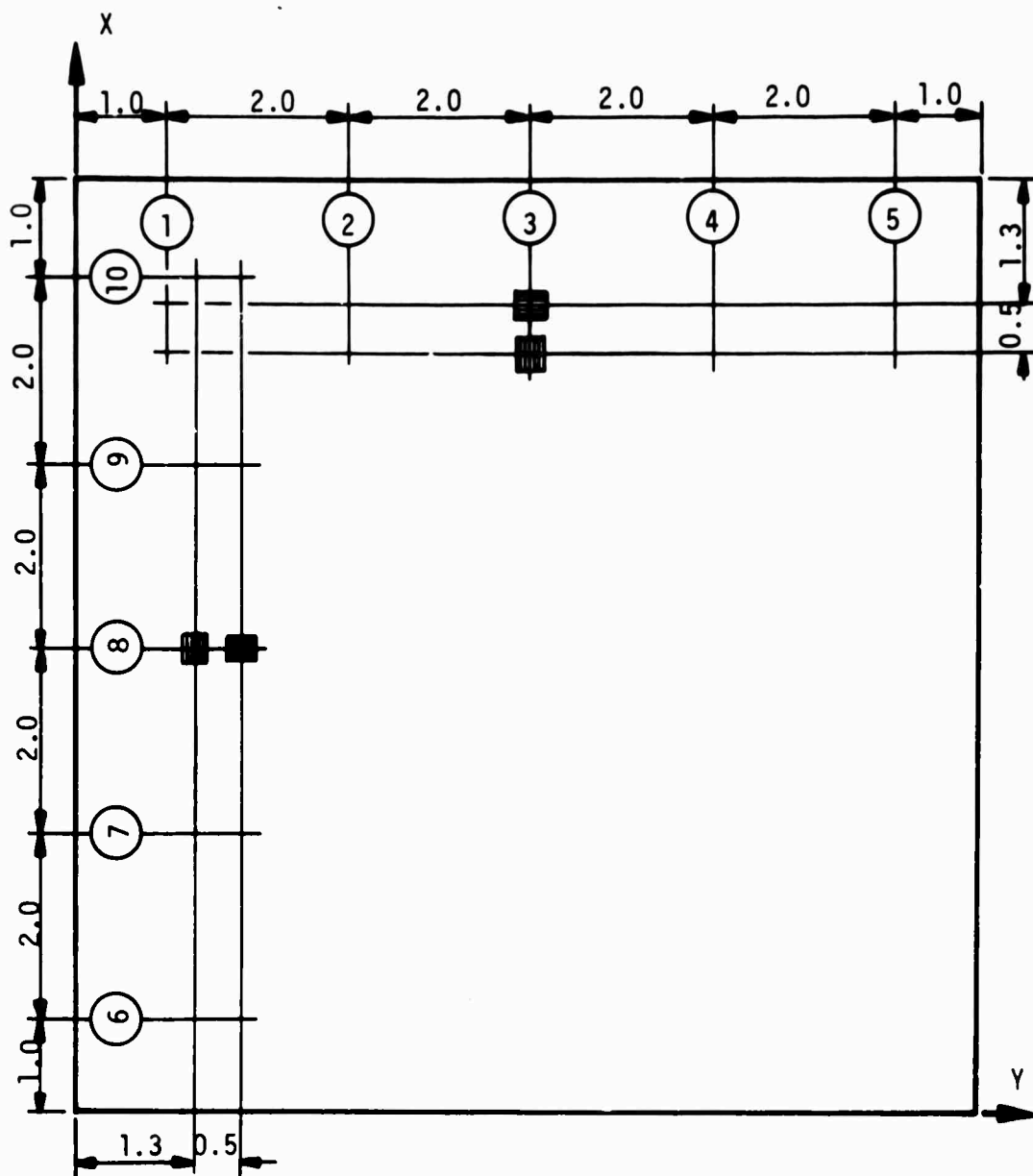


Figure 11. Location of Strain Gages on 0.063 inch Thick Aluminum Plate (identical front and back) with Four Sides Simply Supported

gages were actually placed along only one edge, but the plate was tested in two perpendicular directions to get the strain distribution along the top and left side. The strain measured in both directions at each point is given in Table 3. The strains listed in the table are actually the average of the measured strains on each side of the plate, and, therefore, do not include the effect of the moment at that point.

TABLE 3
STRAIN DISTRIBUTION IN 0.063 INCH THICK ALUMINUM
PLATE WITH FOUR SIDES SIMPLY SUPPORTED

| Point on Plate (See Figure 11) | Average of Strain at Front and Back of Plate (10^{-6} in/in) Between $N_x = 10$ lb/in and $N_x = 50$ lb/in | |
|-----------------------------------|--|-------------|
| | X direction | Y direction |
| 1 | -116 | 40 |
| 2 | -119 | 41 |
| 3 | -117 | 35 |
| 4 | -116 | 48 |
| 5 | -117 | 51 |
| 6 | -109 | 37 |
| 7 | -116 | 40 |
| 8 | -112 | 38 |
| 9 | -113 | 38 |
| 10 | -113 | 42 |

Table 3 indicates that the load distribution is very nearly

uniform. The average stress in the x direction for points 1 through 5 is 38.2 pounds, which is close to the 40.0 pounds indicated on the testing machine. The difference may be attributed to the small number of points considered and to friction in the test fixture. The average strain of points 6 through 10 in the x direction is -113, while the average strain in the y direction is 39. This yields an experimental Poisson's ratio of 0.345, as compared to the accepted value of 0.33 for this material. This indicates that there is probably very little compressive load in the y direction due to restraint at the side supports. If there were a compressive load, the experimental Poisson's ratio would be less than 0.33. The small difference from 0.33 can be attributed to the small amount of data taken.

5.1.2 Friction, Edge Fixity and Fixture Alignment

The fixture has three possible sources of sliding friction:

1. The pistons must slide within the loading bar.
2. The loading bar must slide between the two guide angles at the top.
3. The slotted bars which contain the rollers at the sides must slide in the side supports as the plate moves vertically downward due to the compression of the springs.

All of the sliding surfaces are lubricated with a silicon spray to reduce friction, and the pistons and side supports are made of brass to further reduce the friction. Because the pistons only contact the loading bar, any friction resulting from their sliding surface will affect only the load distribution and not the total load

imposed on the plate. The loading bar slides quite freely between the guide angles, and it is not believed that any substantial friction is produced there. The roller support bars produce the only friction which is believed to be in any way important. This friction can be partially controlled by adjusting the distance between the side supports which hold the bars (see Figure 109). This friction is believed to have a noticeable effect only in the most flexible of the test specimens.

The most troublesome friction occurs at the knife edge supports. The importance of friction along the loaded edges was suggested by Dr. James E. Ashton of General Dynamics, Fort Worth Division, in a series of private conversations during the Fall and Winter of 1967. Reference 14 describes similar problems encountered in plate buckling tests at General Dynamics. Friction along the top edge of the plate will inhibit the free expansion of the plate in the y direction. If the screws which hold the knife edges to the plate are tightened firmly against the metal protective strip along the edge of the plate, the free expansion of the plate will be further inhibited. This will cause a biaxial state of compression in the plate if the Poisson's ratio of the plate is appreciable. To overcome this problem, a Teflon strip can be substituted for the metal strip, and the screws in the knife edges can be tightened less firmly. The difference that these simple steps can make in the buckling load is rather astounding, and is well illustrated in the case of the boron plates.

The boron plates which displayed large Poisson's ratios were

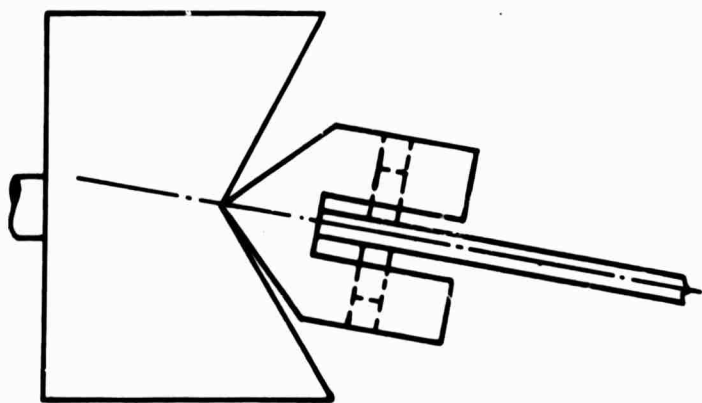
tested first using a metal strip to protect the plates, and then using a Teflon strip. The results for both cases are given in Table 4. The amount of friction induced by using the metal strip will vary

TABLE 4
EFFECT OF FRICTION ON THE BUCKLING LOADS FOR BORON PLATES

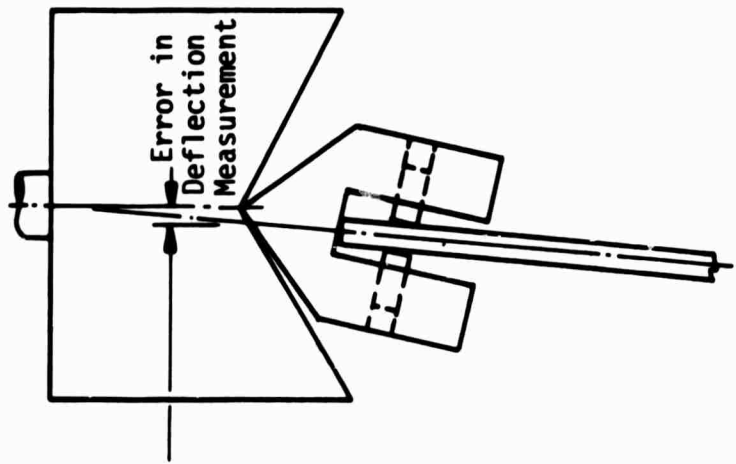
| Plate No. | Buckling Load with Simple-Simple Supports (lb/in) | |
|-----------|---|--------------|
| | Metal Strip | Teflon Strip |
| 501 | 583 | 661 |
| 502 | 533 | 662 |
| 503 | 477 | 602 |
| 506 | 379 | 394 |
| 507 | 327 | 433 |
| 508 | 316 | 372 |

with the firmness with which the screws in the knife edges are tightened down and with the roughness of the surface of the plate. It is, therefore, not surprising to find a considerable variation in the change observed in the buckling load when the metal strip is replaced by a Teflon strip. It is quite possible that some friction still exists even with the Teflon, but it is thought that most of the friction has been eliminated

Another possible source of error at the top and bottom supports is illustrated in Figure 12. It is possible for the plate to rotate within the knife edge supports, causing inaccurate deflection measurement as well as possible moments. This phenomena was in no



(a) Correct Support



(b) Incorrect Support

Figure 12. Possible Source of Error in Knife-Edge Supports

way observable, but it is felt that it may have occurred when the thinner plates were tested, particularly with the simple-free boundary conditions. It is doubtful that a wide plate would have rotated within the supports, particularly at the higher load levels present with the simple-simple boundary conditions. If the plate did rotate within the supports, the deflection measurements would indicate a deflection in the plate greater than that which actually occurred. The critical load predicted by the Southwell plot would, therefore, be lower than the actual critical load of the plate if the error in the deflection measurement was appreciable compared to the actual deflection in the plate.

Misalignment between the V-grooves in the loading bar and the roller supports on the sides of the plate can cause both large discrepancies in the load distribution and large moments in the y direction along the loaded edges of the plate. The alignment of these supports is accomplished by means of set screws, and checked by scale measurement or else by observation. It was found that a minor misalignment caused no appreciable trouble, but that a large and easily observable misalignment could cause the critical load of the plate to be lowered significantly.

To illustrate the effect of a very poor alignment, the load distribution was determined exactly as described in Section 4.1.1, but this time a misalignment was purposely imposed on the plate. The stress distribution in the x direction at five points along the top of the plate was found both with the supports aligned and with the

supports misaligned (see Figure 11). A comparison of the results is given in Table 5.

TABLE 5
EFFECT OF SUPPORT MISALIGNMENT

| Point on Plate (See Figure 11) | Average of Strain at Front and Back of Test Plate (10^{-6} in/in) ^a | |
|-----------------------------------|--|------------|
| | Aligned | Misaligned |
| 1 | -116 | -116 |
| 2 | -119 | -148 |
| 3 | -117 | -136 |
| 4 | -116 | -166 |
| 5 | -117 | -147 |

^aAligned strains based on a load of 40.0 lb/in, misaligned strains based on a load of 50.0 lb/in.

5.1.3 Deflection Measurement

The apparatus employed to measure deflections of the plate specimens had two separate functions:

1. To measure deflections at one point on the plate for the purpose of defining a load-deflection curve.
2. To measure deflections at a number of points on the plate for the purpose of defining the deflection pattern of the plate.

The first function is of greatest concern since the prediction of the critical load is based on the load-deflection curve. When deflections are measured at one point on the plate, the micrometer can be fastened permanently at one spot on the plexiglass holder.

As the plate moves vertically downward with an increase in load, the point of concern on the plate may not move exactly perpendicular to the micrometer, thus causing an error in the deflection reading. Since this is the only important source of error in this case, the maximum expected error in the deflection readings can be found by sliding a typical plate between the supports without loading the plate. This was done repeatedly, readjusting the supports each time, and the maximum change in the deflection readings for a one-half inch translation of the plate was less than two thousandths of an inch. The usual translation of the plate during the portion of the test which is used to predict the critical load is only a small fraction of the one-half inch used in the determination of the maximum error. Assuming the error to be the same when the plate is under load as it was when the plate was unloaded, the maximum error in the predicted buckling load due to an error in the deflection measurement is very small.

The measurement of deflections at a number of points on the plate in order to determine the mode shape involves an additional error resulting from sliding the micrometer along the slots in the plexiglass holder. Repeated measurements at the same point on the plate, removing and replacing the micrometer between each of the readings, reveals the maximum difference in readings to be about two thousandths of an inch. Since the mode shape is found by measuring the deflection at two different values of load which are relatively close together, the maximum error due to the phenomena described in

the previous paragraph is some fraction of two thousandths of an inch. These two sources of error, when added together, yield a maximum possible error in the mode shape readings of between two and four thousandths of an inch. Since the usual mode shape involves deflections of twenty-five thousandths of an inch or more, the average error will not significantly affect the shape.

5.1.4 Reliability of Test Fixture

In the previous sections of this chapter, four possible sources of error which could lead to large discrepancies in the predicted buckling loads have been discussed. These are:

1. Use of improper springs in the loading bar.
2. Failure to use a Teflon strip along the edge of a plate which has a large Poisson's ratio.
3. Poor alignment between knife edges and roller supports.
4. Rotation of plate within knife-edge supports.

It has been found that any of the first three of these sources of error can cause large enough discrepancies in the predicted buckling loads to render the tests useless. All of these sources are easily avoidable, however, if reasonable care is taken in the testing procedure. The fourth source, on the other hand, is not easily avoided nor easily detected, and the extent to which it can influence the results is not known. It is believed that this source of error will occur, if at all, only with thin plates at low load levels.

Other sources of error, such as friction, small deviations in load distribution, or inaccurate deflection or load measurement, are usually present to some extent, but their combined effect is not

believed to be greater than a few percent of the buckling load. It was found that a number of independent tests on the same plate yields predicted buckling loads within one or two percent of each other. This fact attests to the general accuracy of the test results. Even in cases where a large discrepancy existed between the theoretical and experimental buckling load, the tests were very repeatable. In a number of cases tests were repeated on the same plate several months apart, and the results were virtually the same.

5.2 Discussion of Test Specimens

The testing program included test specimens made from five different materials (see Figures 13 and 14): aluminum, steel, fiberglass, graphite fiber reinforced epoxy, and boron fiber reinforced epoxy. The variety of plate materials, configurations, thicknesses, and fabrication techniques provide insight into the problems which can occur with both quality control of the plates and evaluation of the actual properties of the plates once they are fabricated.

5.2.1 Quality of Test Specimens

The fabrication of laminated, fiber reinforced composite plates is a relatively new field in which many problems still exist. The principal problem which affects the plates tested in this study involves the fabrication of unbalanced plates. If an unbalanced plate is layed up in a press and cured as a balanced plate would be, it warps sufficiently in most cases to render it useless.

As described in detail in Section A.4.2, the fabrication procedure used for unbalanced plates was to make up a number of

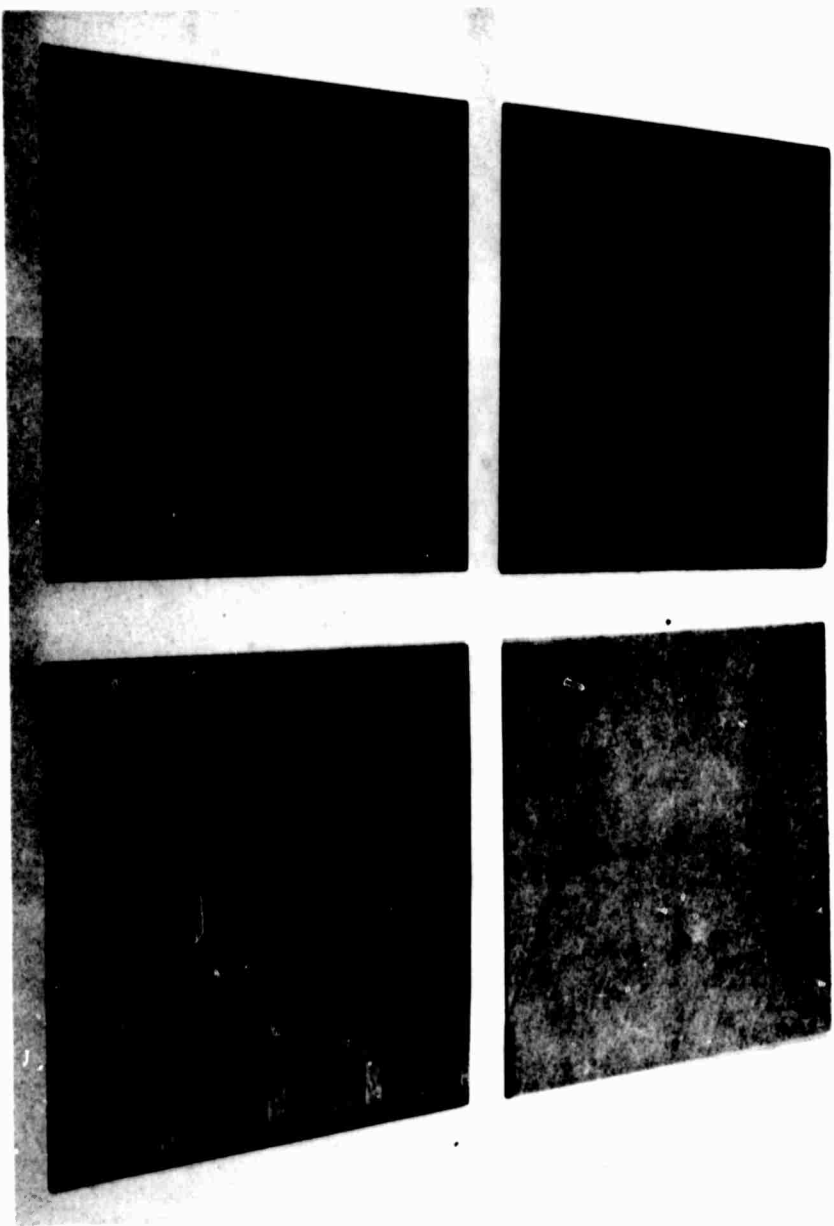


Figure 13. Typical Test Specimens: "Thorne1" (upper left), Unstiffened Fiberglass (upper right), Stiffened Fiberglass (lower right), and Aluminum (lower left).

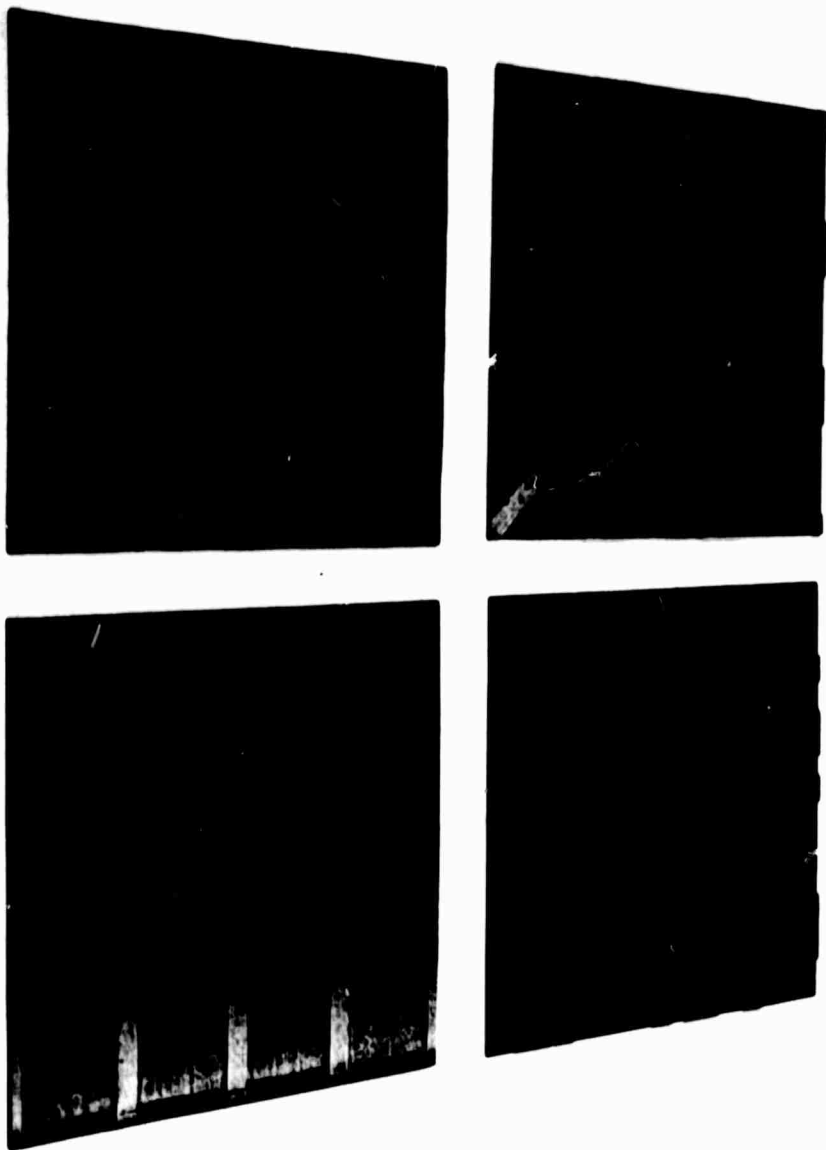


Figure 14. Integrally Stiffened Fiberglass Plates.

balanced sub-plates, and then to bond these sub-plates together with a room-temperature curing adhesive. This process is acceptable as long as the bond layers adhere well to the sub-plates and are both thin and uniform. In any event, the fiber content of the gross plate is lowered by the amount of glue used in adhering the sub-plates together.

The desirability of having the bond layer thin, and, at the same time, having the plate remain flat presents a further problem. The only feasible way of achieving a thin bond layer is to apply pressure to the plate while the glue is curing. If enough pressure is applied to achieve a thin and uniform bond layer, the resulting plate usually warps to some degree. This problem was not completely resolved, and all of the plates fabricated in this manner display either some warpage or else a relatively thick, non-uniform bond layer. Plates 409, 507, and 508 were somewhat warped, while plates 209, 501, 502, 503, 504, 505, 506, and 509 had thicker bond layers (about 4 mils on the average), and varied as much as ten percent in thickness.

There were a number of other, less significant problems with the quality of the test specimens. Most of the thin "Thornel" plates were warped to some degree, and plate 202 appeared to have resin-poor areas on the surface. In a number of the plates, the fibers were not oriented as specified, but were off by a couple of degrees at most. The stiffened fiberglass plates were of general poor quality with resin-poor areas and warpage. Some of the plates were not cut

exactly to the specified size, but varied by a sixteenth of an inch or less in length or width.

5.2.2 Added Problems with Very Thin Plates

Given constant single ply properties, the flexural stiffnesses of a plate vary with the thickness cubed. If the plate is very thin, then a small variation in the thickness measurement will cause a large percentage difference in the stiffness calculations. If a plate has only four or five plies, then the uniformity of the ply thickness becomes important. It is very difficult to determine the thickness of each ply once the plate has been fabricated.

Plates 204, 205, 206, and 207 were all very thin, and their surfaces were dimpled due to the release cloth used during the curing of the plates. The thickness of each plate was determined to be 0.003 inches less using a point micrometer than it was using a standard flat micrometer. The effect of this difference on the buckling load is illustrated in Table 6. The theoretical buckling

TABLE 6

EFFECT OF THE METHOD OF THICKNESS DETERMINATION ON THE
THEORETICAL BUCKLING LOAD FOR THIN PLATES

| Plate No. | Theoretical $(N_x)_{cr}$ (lb/in) simple-simple supports | | % Difference |
|-----------|---|--|--------------|
| | Thickness Determined by Point Micrometer | Thickness Determined by Standard Flat Micrometer | |
| 204 | 23.6 | 18.7 | 26.2 |
| 205 | 23.6 | 18.7 | 26.2 |
| 206 | 11.9 | 8.72 | 36.4 |
| 207 | 10.2 | 7.44 | 37.1 |

loads given in Chapter 4 were calculated using the smaller thickness determined by the point micrometer. The reason for using the lesser of the two thicknesses is that the lesser thickness describes the structural plate, while the greater thickness results from ridges of the matrix material which cover the surface of the plate. These ridges are very narrow and cover only a very small fraction of the surface area of the plate, but are close enough together to support the flat micrometer.

The sensitivity of the theoretical buckling load to a small change in the estimated thickness indicates that the determination of the actual characteristics of a thin plate are of utmost importance. One can speculate on the effects of other variations in the assumed characteristics. If the surface of the plate underneath the ridges were covered with a thickness of 0.001 inches of matrix material, which is not improbable, the theoretical buckling load would be reduced even further. If the plies were of slightly unequal thickness, then the stiffnesses would change, and the plate would probably have non-zero bending-membrane coupling terms. The fact that the thin plates are usually somewhat warped adds credence to the latter argument. Plates of greater thickness would be subject to these same problems, but their effect would be much less noticeable.

Another problem which is peculiar to thin plates is caused by the weight of the loading bar and load cell assembly. This weight (about 6.4 pounds) is a significant percentage of the buckling load of the plate in some cases, and was included in the load-deflection

data if the expected total critical load was less than 200 pounds. In all cases, the deflection caused by this weight was neglected, but this is not expected to have a significant effect on the results.

5.3 Correlation of Theoretical and Experimental Results

The questionable nature of many of the test specimens greatly complicates attempts to correlate theoretical and experimental buckling load predictions. On the other hand, the wide range of material properties included in the test program provides for a good overall examination of both the dependability of the theoretical methods and the reliability of the test fixture.

5.3.1 General Comments

All of the experimental buckling loads for isotropic plates showed excellent agreement with theory. The maximum difference was less than five percent, and the average difference was much less than five percent. The ten inch square isotropic plates (101, 102, and 105) showed experimental results consistently a few percent lower than theory predicted. This can probably be attributed to the assumption that the plate is ten inches long in the x direction, while, for the actual plate, the knife edges add one-half inch to the total length. This extra one-half inch was neglected because the plate itself is only ten inches long, and the effect of the added length due to the knife edges was not known.

While the test fixture was designed primarily to determine the buckling load of a plate, the post-buckling behavior can also be studied. Because the plate is loaded by a uniform load rather than

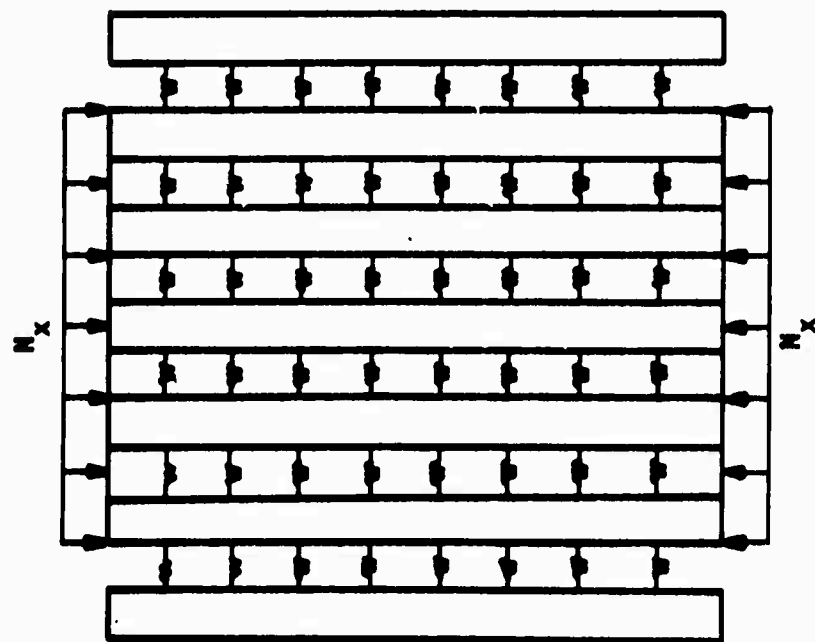
by a uniform displacement, large deflections in the plate cause little redistribution of the load. An example of post-buckling behavior is given in Figure 3 for a (0,90,90,0) "Thornel"-25 plate. The theoretical load-deflection curve was determined by Monforton's geometrically nonlinear finite element method using four elements to model one-quarter of the plate. Most of the thin "Thornel" plates were taken into the post-buckling region, and the load-deflection curves are given in Appendix C. The curves shown in Figures 2 and 3 agree well with the predictions by Roorda⁽¹¹⁾ for both the load-deflection curves and the Southwell plots.

All of the 400 series plates were eleven inches square. As explained previously, the larger dimensions necessitated some changes in the buckling fixture, and the resulting support conditions were somewhat different than for the ten inch square plates. The roller supports at the sides of the eleven inch square plates were placed only 9.75 inches apart, which left five-eighths of an inch of overhang on each side. The question immediately arose as to which portion of the plate carried the imposed load. To give some insight into this question, an aluminum plate was tested first as an eleven inch square plate, and then the width was reduced to ten inches while the height remained eleven inches. As might be expected, the total buckling load for the simple-free support condition dropped by about six percent when the width was reduced. The total buckling load for the simple-simple support condition increased slightly, however, as the width was reduced. It is believed that this slight increase was due

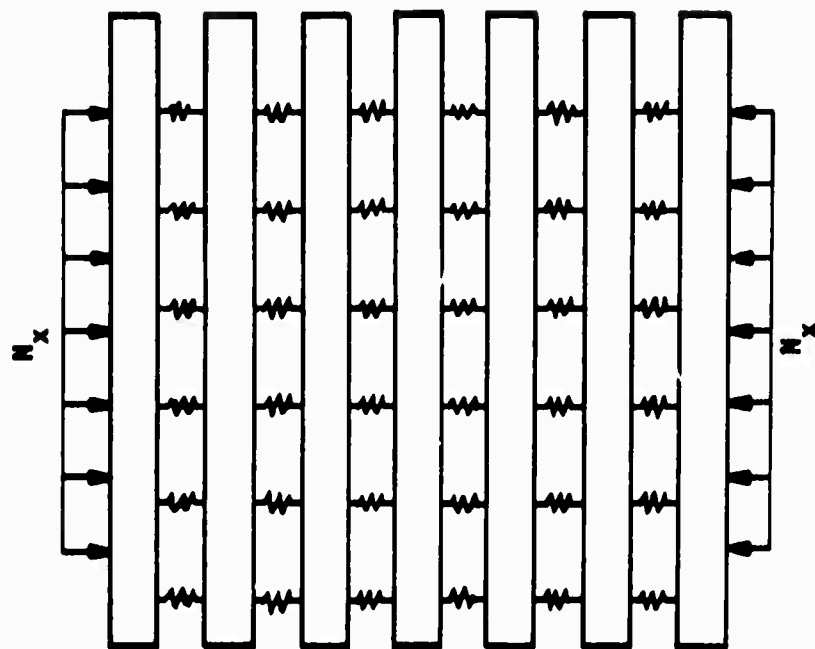
to the reduction in overhang at the sides. It can be conjectured that the overhang has the effect of lowering the aspect ratio (a/b), which, in turn, lowers the buckling load since the minimum buckling load will occur when the aspect ratio is 1.0,⁽⁹⁾ as is evidenced by Equation (2.19). The results for the isotropic plate indicate, then, that, in the case of the simple-free support conditions, the effect of the added width is almost offset by the added length due to the knife edges, while, in the case of the simple-simple support condition, there is only a small effect from the added width. In both cases, the error involved is quite acceptable.

The effect of the overhang on the buckling of the boron plates can be expected to vary considerably from its effect on the isotropic plates. One might anticipate that the effect of the overhang will vary with the orientation of the fibers within the particular plate. This argument is further enhanced by considering the models illustrated in Figure 15. The overhang could be expected to have little effect in the case of the 0° plate, while, in the case of the 90° plate, the overhang might carry a portion of the load consistent with that carried by the rest of the plate. For plates of other orientations, one would expect the amount of the load carried by the overhang to vary between these extremes.

Unidirectional anisotropic plates tend to twist as they are loaded. It is likely that this twist contributes to the friction problems along the loaded edges because the imposed load will be inclined to the edge of the plate. Figure 16 illustrates the devia-



(a) Unidirectional 0°



(b) Unidirectional 90°

Figure 15. Models for Eleven Inch Wide Unidirectional Plates

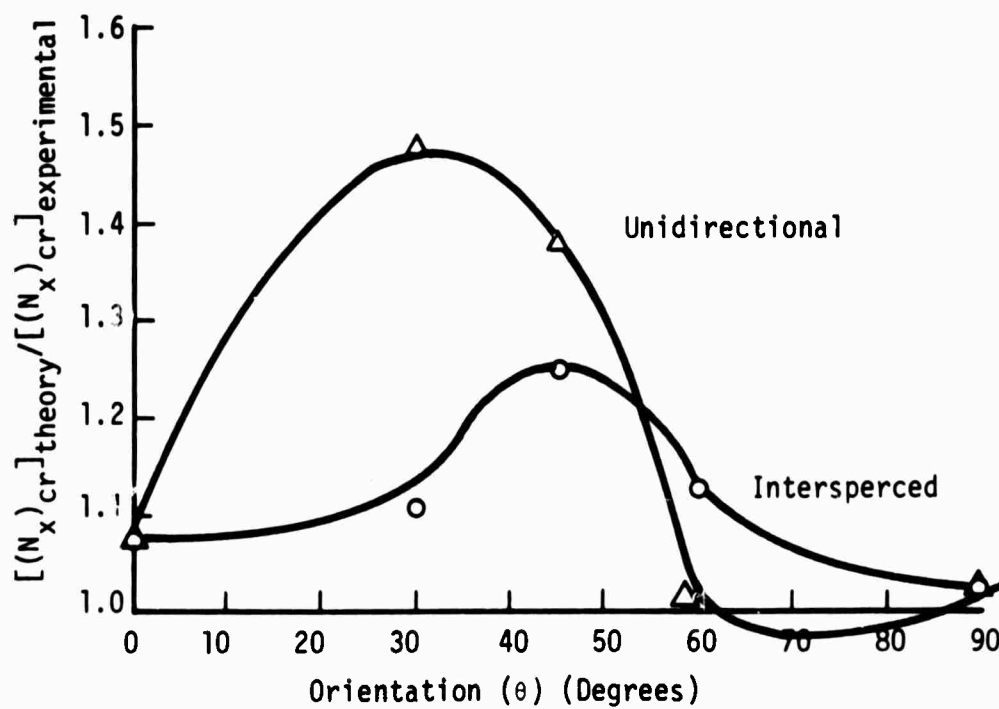
tion of the experimental buckling load from that predicted by the Ritz method for both the unidirectional and interspersed ply configurations for the balanced boron plates. Since the Poisson's ratio is larger in the interspersed case, it would seem that the overhang, twist due to anisotropy, and additional length due to the knife edges are the dominating influences for this support condition. If the effect of friction due to Poisson's ratio were the dominating factor, then a greater deviation would be expected for the interspersed curve in Figure 16(a), but much more deviation is seen in the unidirectional case.

Two additional factors could account for the particularly large errors in the case of the plates with a fiber orientation of thirty or forty-five degrees:

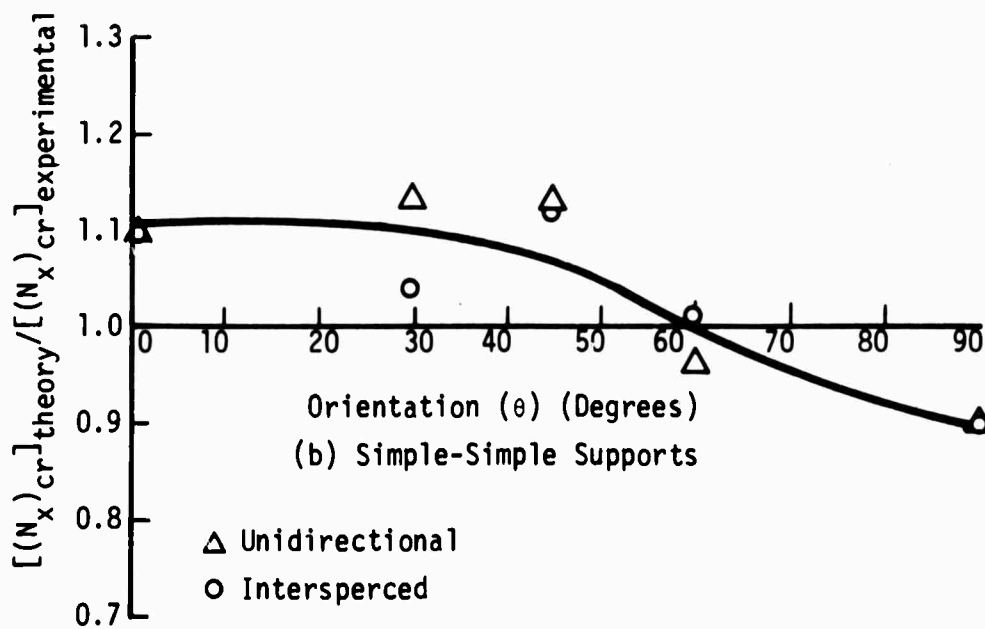
- 1) The actual fiber orientations for the forty-five degree plates were not exactly forty-five degrees, but were about one or two degrees in error for both the unidirectional and interspersed plates.
- 2) If there were a small difference between the actual and the assumed Poisson's ratios, the predicted buckling load could be greatly in error.

The influence of the first factor is considered to be minor, but the second factor could have a profound effect in some cases. For example, the Poisson's ratios for the unidirectional forty-five degree plate were calculated to be about 0.66. If these calculated Poisson's ratios were a mere five percent higher than the actual ones, the formula for the first flexural stiffness,

$$D_{11} = \frac{E_1 h^3}{12(1 - \nu_{12}\nu_{21})}$$



(a) Simple-Free Supports



(b) Simple-Simple Supports

Figure 16. Deviation of Experimental Buckling Load from Ritz Theory for Unidirectional and Interspersed Ply Orientations for Balanced Boron Plates.

indicates that the calculated stiffness would be eight percent higher than the actual stiffness. The effect on the other flexural stiffnesses would be similar, and the overall effect on the buckling load could be expected to be about eight percent. Experimental data taken from a plate similar to those tested, however, indicated only a very small error in the prediction of Poisson's ratio.

All of the factors which have been discussed can be separated into two groups: those which affect the material characteristics, and those which affect the testing of a given material. It is difficult to make any general comments about the effect of a variation in a material characteristic such as Poisson's ratio, because the effect will depend upon whether the predicted value is higher or lower than the actual value. Most of those factors which affect the testing of a given plate, however, can be described as a function of the fiber orientation. Figure 17 shows the expected effect of friction, overhang, and added length due to the knife edges. While these factors cannot be evaluated quantitatively, their general influence on the buckling load is illustrated in Figure 17. The general trends shown by these curves, combined with the previous discussions of material characteristics, can easily be used to explain the disagreement between theory and experiment illustrated in Figure 16 for the boron plates.

The errors encountered with most of the plates not already mentioned can be attributed to a variation in material characteristics. The "Thorne1" plates were mostly very thin, and, as discussed in

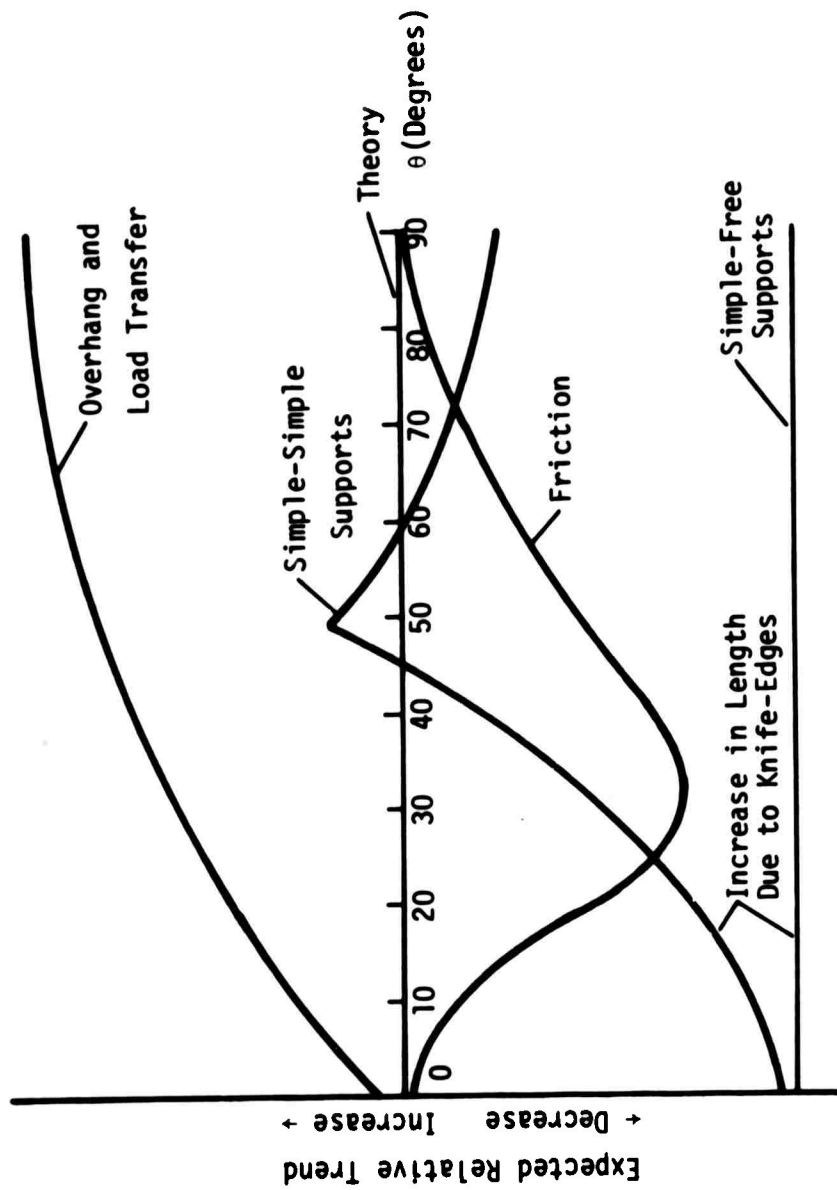


Figure 17. Expected Trends in the Deviation of the Experimental Buckling Load from Theory Due to Various Factors.

Section 5.2.2, the buckling load is very sensitive to a number of factors for very thin plates. Plate No. 202 was possibly damaged, and Plate No. 203 would have shown much less error if an anisotropic theory had been used. Also, Plate No. 203 has a $\pm 45^\circ$ configuration, and fits into the argument presented in the previous paragraphs.

The 300 series plates showed a great deal of variation from theory. These plates were of rather poor quality, however, and the theory was based on a plate with a large number of stiffeners. The technique used to smear out the effect of the stiffeners is of questionable value when there are only a few stiffeners.

Plates in the 500 series, as discussed previously, had a considerable amount of thickness variation. In calculating the theoretical buckling loads, an average thickness was used. It is evident from the results in Chapter 4 that the use of an average thickness tended to result in high predictions for the simple-free support conditions, but low predictions for the simple-simple support conditions. It should be emphasized that the thickness was measured only around the outside of the plates, and was assumed to vary similarly in the interior.

5.3.2 Effect of D_{16} and D_{26} Terms

Any plate which has at least one ply with fibers oriented at some angle other than zero or ninety degrees must have either D_{16} and D_{26} terms, bending-membrane coupling terms, or else both. This section considers the effects of D_{16} and D_{26} terms, and Section 5.3.3 considers the effects of stiffness coupling terms

As a plate with D_{16} and D_{26} terms deflects, the mode shape will be twisted rather than being symmetric or antisymmetric about the lines $x = a/2$ and $y = b/2$. This twisting is displayed in the mode shapes given in Appendix C for the boron plates (400 series).

When these terms are present, the standard orthotropic theory for buckling cannot be applied. General Dynamics' Ritz method and Chamis' Galerkin method were used to find theoretical buckling loads for these plates. The principal reason for the differences between the results for these two methods lies in the determination of the stiffnesses for the plates. The two methods were tested with identical stiffness inputs (see Table 7), and the maximum difference was three percent.

The effect of the D_{16} and D_{26} terms is to lower the buckling load below that of an otherwise identical plate. The magnitude of this effect is clearly illustrated in the case of the boron plates. Figure 18 shows the results for the boron plates with unidirectional (high D_{16} and D_{26}) and interspersed (low D_{16} and D_{26}) configurations. All plates are normalized to a thickness of 0.106 inches for the purpose of clarity. They are normalized by the following relationship:

$$(N_x)_{cr} \Big|_{t = .106} = (N_x)_{cr} \Big|_{t = t_{act}} \cdot (.106/t_{act})^2$$

5.3.3 Effect of Membrane-Bending Coupling Terms

The effect of the membrane-bending coupling terms on the buckling load has largely been neglected in the past. While it is quite

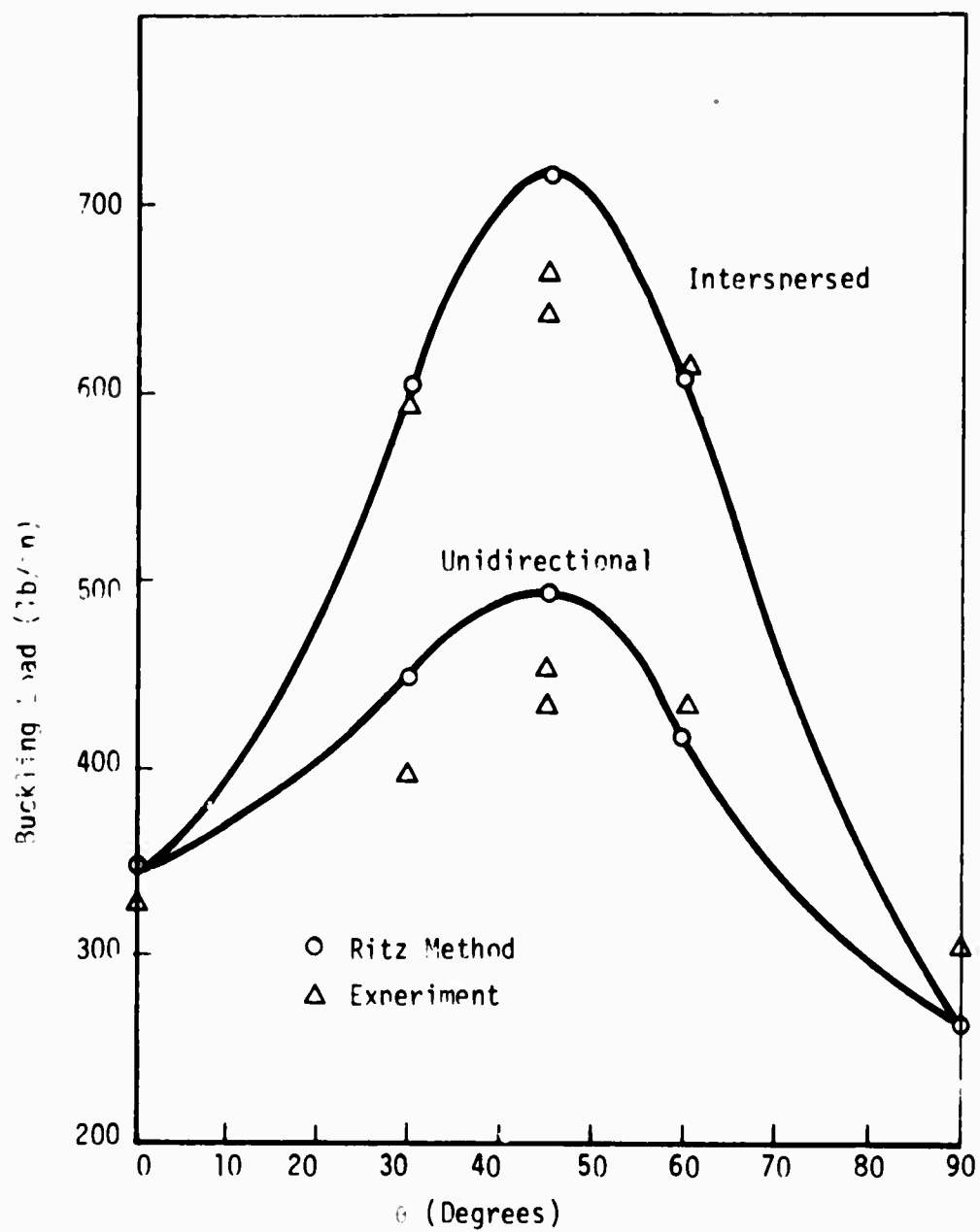


Figure 18. Effect of Ply Orientation on Buckling of Boron Plates Normalized to a Thickness of 0.106 in.

TABLE 7
TEST CASE USING IDENTICAL STIFFNESSES^a

| θ (Degrees) | $(N_x)_{cr}$ (lb/in) | | Galerkin Ritz |
|-----------------------|----------------------|-----------------|------------------|
| | Ritz Method | Galerkin Method | |
| +45 | 661 | 663 | 1.00 |
| +30 | 590 | 591 | 1.00 |
| +60 | 580 | 581 | 1.00 |
| 90 | 195 | 195 | 1.00 |
| 0 | 320 | 320 | 1.00 |
| +30 | 411 | 420 | 1.02 |
| +45 | 429 | 425 | 0.99 |
| +60 | 377 | 387 | 1.03 |

^aTest case was run for a ten inch square plate with four sides simply supported. Assumed properties were slightly different than those given for boron in Appendix B.

clear from Equation (2.20) that coupling will have very little effect in most cases because of the relative magnitudes of the $[A]^{-1}$ and $[B]$ matrices, it has been found that, in some cases, the coupling terms cannot be ignored. Plates No. 209 and 409 are extreme cases of coupling and provide good test cases for the theories which consider coupling. Plates in the 500 series all display coupling to a much lesser degree, but the buckling loads are still reduced noticeably in a few cases.

The theory discussed in Section 2.3 was found to be very

effective in predicting the buckling loads for plates with coupling. The second term in Equation (2.20), $[B] [A]^{-1} \{N\}$, has been neglected. Though this term was not included in Chamis' Galerkin method either, it was included in Monforton's nonlinear finite element method and had little effect on the buckling load at the load levels considered in this study.

Plate No. 209 displayed very strong membrane-bending coupling, but, unfortunately, the plate was rather non-uniform in thickness. Figure 19 gives the experimental load-deflection curves and the load-deflection curve for the nonlinear finite element method. A Southwell plot was constructed from the initial portion of the load-deflection curve for the nonlinear finite element method. This plot, along with the predicted buckling load, is given in Figure 20. When the plate was tested in the "a" direction, the resulting Southwell plot was not linear. A lateral force of three pounds was placed on the plate so as to restrict the deflection, and the resulting Southwell plot did have a linear region. When the plate was tested in the "b" direction, the plate behaved much differently, and the Southwell plot was linear for the unperturbed plate. It was found that the shape of the load-deflection curve depended upon how the plate was placed in the test fixture. It is believed that a small moment imposed on the edge of the plate caused an unusually large amount of deflection. The mode shape for this plate (see Appendix C) was very symmetric for both support conditions.

Plate No. 509 displayed strong B_{16} and B_{26} terms. Though this

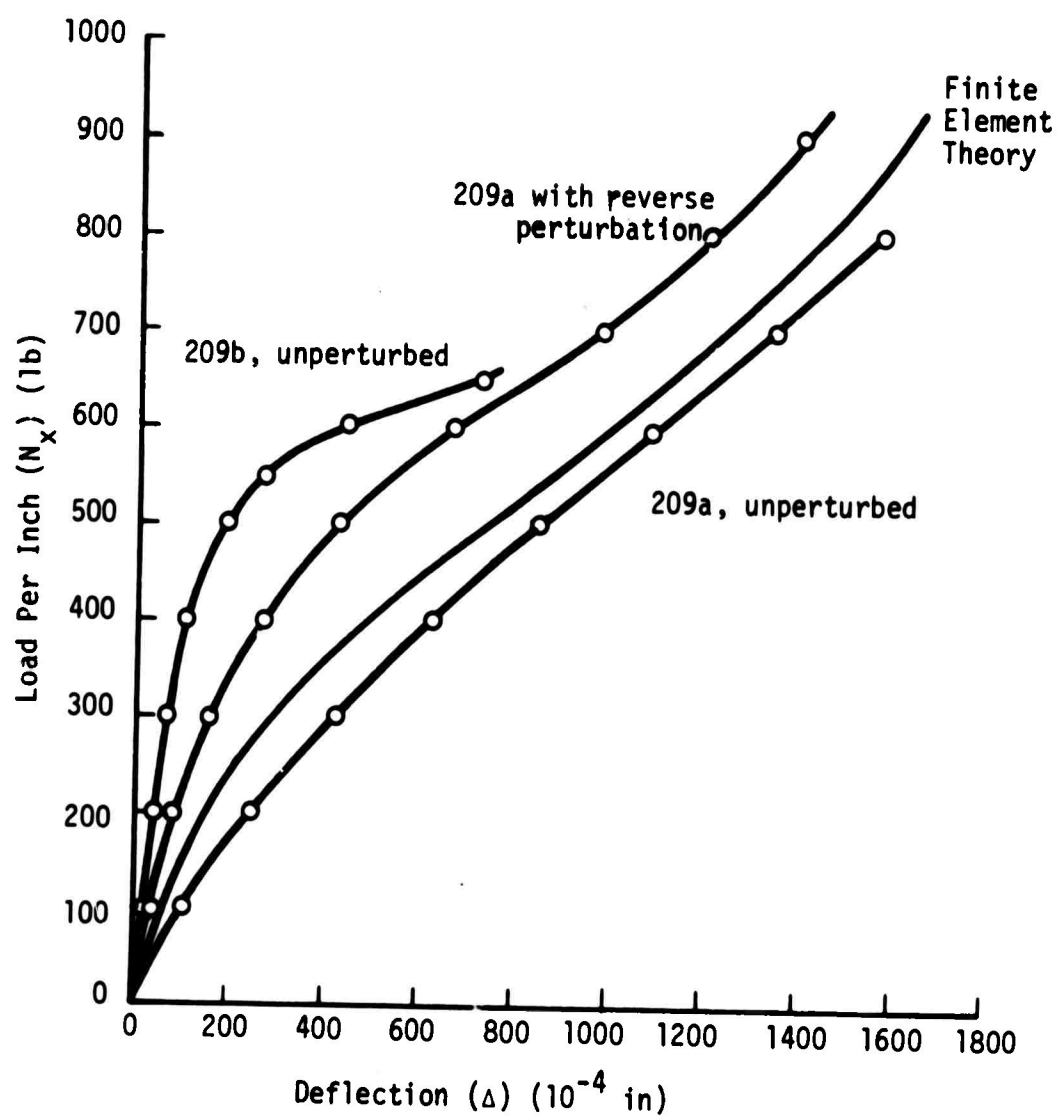


Figure 19. Theoretical and Experimental Load-Deflection Curves for Plate No. 209.

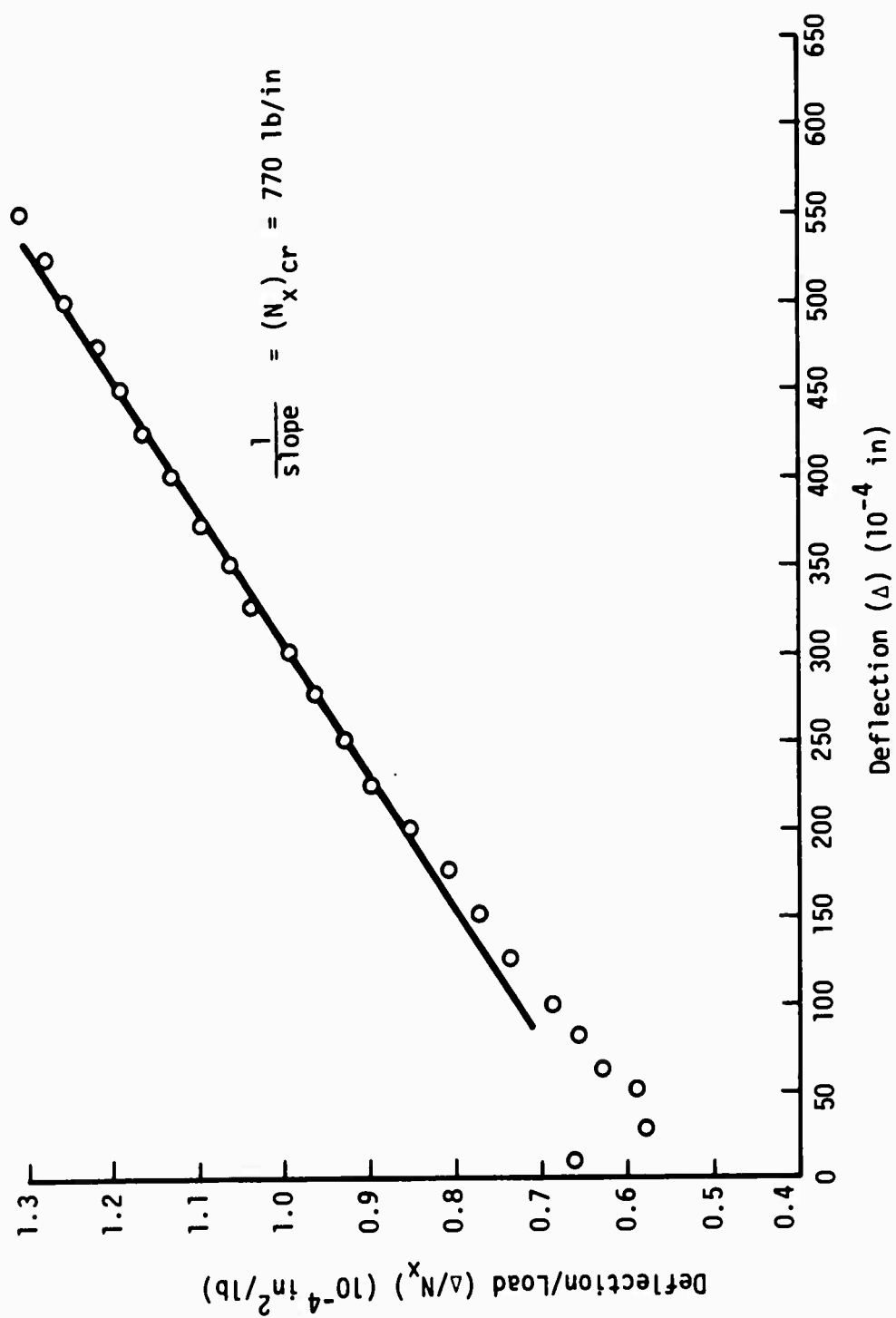


Figure 20. Southwell Plot for Plate No. 209 using Finite Element Load-Deflection Data.

plate behaved very much like an uncoupled plate, its buckling load was strongly affected by the coupling terms. The theoretical load-deflection curve found by the nonlinear finite element method was very well behaved, and the flat plate assumed by the theory remained flat until buckling occurred.

Results for the 500 series plates show little effect from the coupling terms. The theoretical and experimental results agree reasonably well considering the variation in thickness present in most of the plates. Results for all of the coupled plates are given in Chapter 4.

5.4 Conclusions and Recommendations

Conclusions:

On the basis of the results of the testing program, the following conclusions can be made:

- 1) It can be concluded that the test fixture used in this study, when combined with the Southwell plot, can be used to predict the buckling load of ten inch square anisotropic plates within reasonable engineering accuracy. The use of eleven inch square plates introduces some additional error, but the results are still generally acceptable.
- 2) It can be concluded that the classical orthotropic theory, Ritz method, and Galerkin method all give an accurate representation of the buckling load of plates to which they were meant to apply. It can be tentatively concluded from the results of Plates No. 209 and 409 that the reduced flexural stiffness and nonlinear finite element methods also predict the buckling load of appropriate plates accurately.
- 3) The results from Plates No. 209, 406, 407, 408, and 409 indicate that classical orthotropic theory cannot be used to predict the buckling load for any plate which is strongly anisotropic. Results of Plates No. 203, 401, 402, 403, and all of the plates in the 500

series indicate that classical orthotropic theory can be used for plates which are only weakly anisotropic.

- 4) It is extremely difficult to predict the buckling load for a very thin plate.

Recommendations:

The problems encountered in this study indicate that the following recommendations are in order:

- 1) A complete series of unbalanced plates should be tested in order to further study the accuracy of the reduced flexural stiffness method.
- 2) Techniques for fabricating unbalanced plates should be refined.
- 3) If thin plates are to be used in practice, then a method for more accurately determining the actual properties and dimensions should be found.
- 4) A test program should be initiated to investigate the buckling of anisotropic plates under combined loadings.

REFERENCES

1. Hearmon, R.F.S., A Introduction to Applied Anisotropic Elasticity, Oxford University Press, London (1961).
2. Lekhnitski, S.G., "Anisotropic Plates," Contributions to the Metallurgy of Steel No. 5, Am. Iron and Steel Inst. (1956)
3. Chamis, C. C., Private Communication (1967)
4. Chamis, C. C., "Micro and Structural Mechanics and Structural Synthesis of Multilayered Filamentary Composite Panels," Ph D. Thesis, Case Western Reserve University (1967).
5. Ashton, J. E., "Anisotropic Plate Analysis," General Dynamics Research and Engineering Report, FZM-4899 (1967)
6. Chamis, C. C., "Thermal Structural Response, Structural Synthesis and Material Optimization of Particulate Composite Plates," Case Western Reserve University Report, (in preparation).
7. Monforton, G. R., "Discrete Element Finite Displacement Analysis of Anisotropic Sandwich Shells," Ph.D. Thesis, Case Western Reserve University, (in preparation).
8. Southwell, R.V., "On the Analysis of Experimental Observations in Problems of Elastic Stability," Proceedings of the Royal Society, A, Vol. 135, 601-616 (1932).
9. Timoshenko, S. P., and Gere, J.M., Theory of Elastic Stability, McGraw-Hill Book Company, Inc., Second Edition (1961).
10. Horton, W. H., Cundari, F.L., Johnson, R.W., "A Review of the Applicability of the 'Southwell' plot to the Interpretation of Test Data Obtained from Stability Studies of Elastic Column and Plate Structures," Stanford University, SUDAAR 296 (1966).
11. Roorda, J. "Some Thoughts on the Southwell Plot," J of the Engineering Mechanics Division, ASCE, Vol. 93, No. EM6, 37-48 (1967).
12. Whitney, J. M., "Elastic Moduli of Composite Materials Reinforced with Orthotropic Filaments," Wright-Patterson Air Force Base, AFML-TR-65-411, also AD-630251 (1966).
13. Chao, T. L., "A Study of Elastic Properties of Filamentary Composites. Part I - Two Dimensional Mechanical Properties," Case Institute of Technology, SMSMD R-3 (1967).

14. Ashton, J.E., and Love, T.S., "Stability of Anisotropic Plates," General Dynamics Research and Engineering Report, FZM-4992 (1968).
15. Kicher, T.P., "Structural Synthesis of Integrally Stiffened Cylinders," AIAA/ASME 8th Structures, Structural Dynamics, and Materials Conference, Palm Springs, California, 217-229 (1967).
16. MMM Brochure on Type 1400 "Scotchply" Properties (1966)

APPENDIX A

MATERIAL CHARACTERISTICS OF THE TEST SPECIMENS

A.1 Notation for Laminated, Anisotropic Plates

A.1.1 Single Ply Notation

A single ply of one of the laminated plate test specimens is made up of fibers oriented in one direction only, along with some matrix material, usually an epoxy, surrounding each fiber. In the case of the "Thornel" and fiberglass plates, each ply contains many fibers through the thickness, whereas, in the case of the boron plate, each ply contains only one fiber through the thickness.

The notation used to describe each ply is given in Figure 21. Since a plate is usually made up of a number of plies, considered to be equal in thickness, percent fiber content by volume, and constituent properties, the only information actually needed for each individual ply is the fiber orientation, θ . In some cases the plies are different in one or more of these categories, and then more than just the orientation must be specified.

A.1.2 Gross Plate Notation

Each ply in a laminated plate is considered to be orthotropic, i.e., it has two perpendicular axes of elastic symmetry in the plane of the ply. These two perpendicular axes are along the fibers (L) and perpendicular to the fiber (T). Through the thickness, the fibers are considered to be arranged symmetrically about the central plane. If the fiber orientation happens to be along the structural axes of the ply ($\theta = 0^\circ$ or 90°), then the ply is often called specially

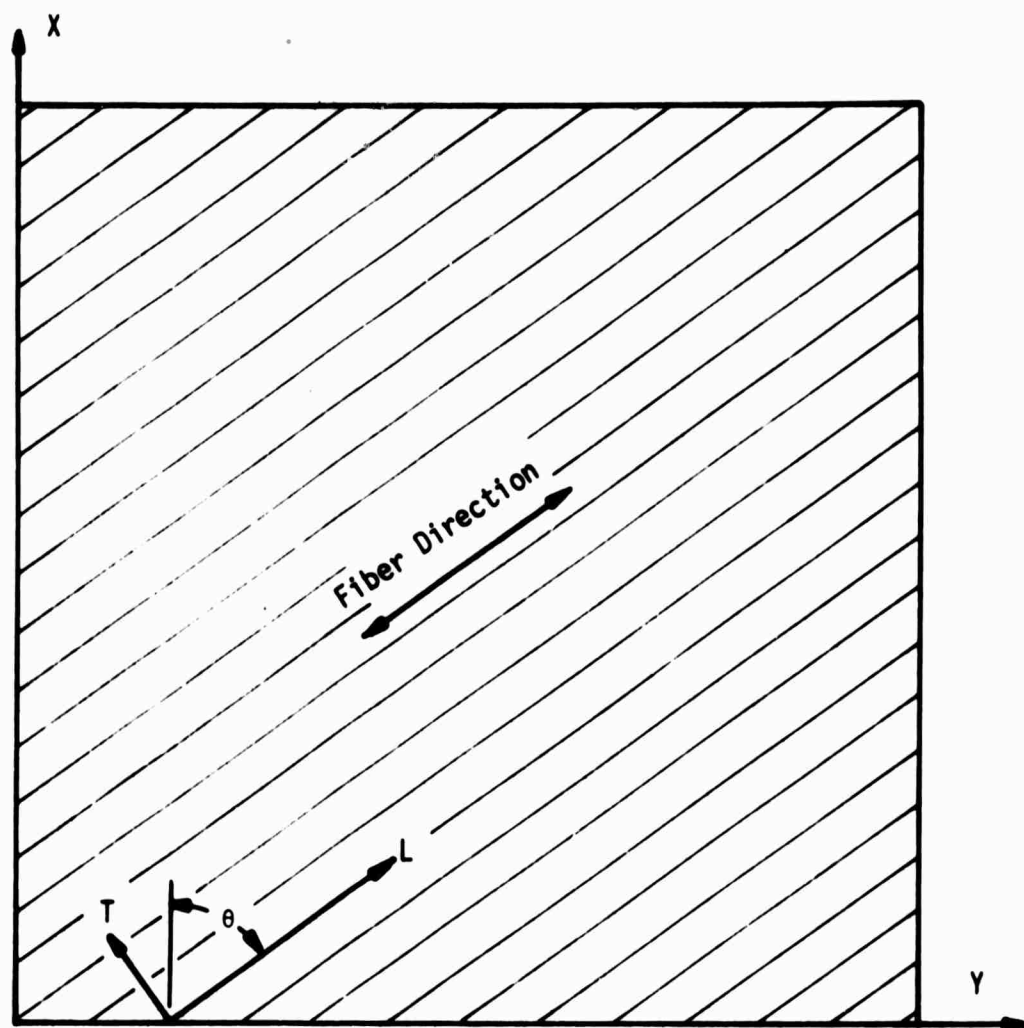


Figure 21. Single Ply Notation for Fibrous Composite.

orthotropic, and, in Equation (B.5), $C_{16} = C_{26} = 0$. If the fiber orientation is not along the structural axes, the ply is called generally orthotropic, and the C matrix is filled.

If a number of plies are combined with random orientations to form a laminated plate, then the plate is called anisotropic. If the plate is anisotropic in the most general sense, then all of the elements in the membrane, coupling, and flexural stiffness matrices (A_{ij} , B_{ij} , and D_{ij}) will be non-zero. Depending upon the manner in which the individual plies are oriented with respect to each other about the central plane of the plate, the degree of anisotropy may be affected in any, or all, of the following ways:

1. If the plate has two perpendicular axes of elastic symmetry in the plane of the plate and these axes are aligned with the structural axes of the plate, then the flexural stiffness matrix elements $D_{16} = D_{26} = 0$.
2. If the plies are oriented symmetrically about the central plane of the plate ($\theta_3, \theta_2, \theta_1, \theta_1, \theta_2, \theta_3$), then all of the elements in the stiffness coupling matrix, B_{ij} , are zero.
 - a. If the ply orientations on one side of the central plane are symmetric with respect to, or are the mirror image of those on the other side ($+\theta_3, +\theta_2, +\theta_1, -\theta_2, -\theta_3$), then all of the stiffness coupling terms except B_{16} and B_{26} are zero.
 - b. If the orientations of plies on one side of the central plane are equal to the orientation of their counterpart plies on the other side, except for plies which are oriented at 0° or 90° , then the B_{16} and B_{26} terms are zero ($90, \theta_2, \theta_1, \theta_1, \theta_2, 0^\circ$).

For the purpose of this study, a plate is considered to be

orthotropic only if both conditions (1) and (2) hold. In this case the plate has two perpendicular axes of elastic symmetry in its plane, and these axes are aligned with the structural axes of the plate. In addition to this, the orientations of the plies on either side of the central plane must be symmetric (balanced).

The following tables give examples of the usual conventions for expressing the orientations of the plies within the plate.

TABLE 8
CONVENTIONS FOR EXPRESSING PLATE CONFIGURATIONS
FOR BALANCED PLATES

| Notation | Actual Plate Configuration |
|-------------|--|
| (0,90,90,0) | $0^\circ, 90^\circ, 90^\circ, 0^\circ$ |
| 5(0,90) | $0^\circ, 90^\circ, 0^\circ, 90^\circ, 0^\circ$ |
| 4(0) | $0^\circ, 0^\circ, 0^\circ, 0^\circ$ |
| 4(+45) | $45^\circ, -45^\circ, -45^\circ, 45^\circ$ |
| 5(+45) | $45^\circ, -45^\circ, 45^\circ, -45^\circ, 45^\circ$ |

TABLE 9
CONVENTIONS FOR EXPRESSING PLATE CONFIGURATIONS
FOR UNBALANCED PLATES

| Notation | Actual Plate Configuration ^a |
|-------------|---|
| (0,0,90,90) | $0^\circ, 0^\circ, G, 0^\circ, 0^\circ, G, 90^\circ, 90^\circ, G, 90^\circ, 90^\circ$ |
| (90,+25,90) | $90^\circ, 90^\circ, G, 25^\circ, 25^\circ, G, -25^\circ, -25^\circ, G, 90^\circ, 90^\circ$ |
| 4(90), 4(0) | $90^\circ, 90^\circ, 90^\circ, 90^\circ, G, 0^\circ, 0^\circ, 0^\circ, 0^\circ$ |

^a"G" stands for glue layer.

A.2 Fabrication Techniques

A.2.1 Balanced "Thornel" Plates

All balanced "Thornel" plates were fabricated by Union Carbide Corporation, Parma Technical Center, Parma Ohio. The fibers were wound into individual plies which were partially cured. The plies were then stacked in a press in the desired configuration, and curing was completed under pressure.

A.2.2 Balanced Boron Plates

All boron plates were fabricated by General Dynamics, Fort Worth Division. Individual plies were made from prepreg tape, and were arranged in the plate with a fiberglass scrim cloth between each ply. The curing cycle was then completed with the plate in a press under pressure. A more detailed explanation of the fabrication procedure for the boron plates can be found in Reference 14.

A.2.3 Stiffened Fiberglass Plates

Individual plies of the plate and the stiffeners were made of prepreg tape. The plate plies and the stiffener plies were then placed in a form which was slotted for the stiffeners, and curing was completed in an oven. At the intersection of the stiffeners a build-up of stiffener plies was avoided by first continuing a ply from one stiffener through the intersection while cutting the corresponding ply from the other intersecting stiffener on either side of the continuous one. In the next lamina that was added, the process was repeated in reverse, letting the ply from the other stiffener be continuous.

A.2.4 Unbalanced Plates

Unbalanced plates tend to warp rather severely if fabricated in the same manner as were those plates described above. The reason for this warpage is that, as the plate is curing, the matrix material tends to shrink much more severely than do the fibers. This differential shrinkage results in residual stresses while the plate is in the press, and, when the plate is removed from the press, these residual stresses cause the plate to warp.

To avoid the problem of differential shrinkage, the plates can be fabricated by first curing a number of balanced sub-plates, and then bonding these sub-plates together with a room temperature curing adhesive. In order to achieve a uniformly thick bond layer, or layers, the plate should be placed in a press under pressure while the glue is curing. It was found that the plate tended to warp if the bond layer was made too thin by applying too much pressure to the plate. The best results were achieved when a pressure of about twenty pounds per square inch was applied initially, then released completely as soon as the glue became tacky.

In all cases, the unbalanced plates were fabricated by first making up a set of unidirectional sub-plates at some desired fiber orientation. In the case of the "Thorne1" and boron unbalanced plates, a fiberglass scrim cloth was placed between each ply of the unidirectional sub-plate to avoid the possibility of damaging the sub-plate before fabrication was completed. The sub-plates were then bonded together with a room temperature curing adhesive.

APPENDIX B
DETERMINATION OF THE ELASTIC STIFFNESSES FOR
LAMINATED, ANISOTROPIC PLATES

B.1 Determination of the Individual Ply Properties

A single ply of an anisotropic plate as described in Section A.1.1 can be completely defined by four elastic constants: E_L , E_T , G_{LT} , and ν_{LT} . These properties can be determined either theoretically, experimentally, or by some combination of theory and experiment.

Since there are no purely theoretical methods available which predict these constants accurately for a plate with orthotropic fibers, and since it is not feasible to test experimentally each ply which is to be used in a plate, a method which combines theory and experiment was used in all cases.

Whitney's⁽¹²⁾ micromechanic theory can be applied to a composite having isotropic or orthotropic fibers. This method is purely theoretical, but must be adjusted slightly if good agreement with experimental data is to be achieved. The following formulas are used to predict the elastic constants for a single ply:

$$E_L = \nu_f E_{fL} + (1 - \nu_f) E_m \quad (B.1)$$

$$\nu_{LT} = \nu_f \nu_{fLT} + (1 - \nu_f) \nu_m \quad (B.2)$$

$$G_{LT} = \frac{[(G_f + G_m) + (G_f - G_m) \nu_f]}{(G_f + G_m) - (G_f - G_m) \nu_f} \quad (B.3)$$

$$E_T = \frac{2 K^* [1 - \nu_{r\theta} \nu_f - \nu_m (1 - \nu_f)] E_L}{E_L + 4 K^* \nu_{LT}^2} \quad (B.4)$$

where

$$K^* = \frac{(K_f + G_m) K + (K_f - K) G_m v_f}{(K_f + G_m) - (K_f - K) v_f}$$

$$K_f = \frac{E_{fL} E_{fT}}{2[(1 - \nu_{r\theta}) E_{fL} - 2 E_{fT} \nu_{fLT}^2]}$$

$$K = \frac{E_m}{2(1 - \nu_m - 2\nu_m^2)}$$

The above elastic constants agree well with experimental data if G_{LT} is multiplied by a factor of 1.4.⁽¹³⁾ This factor was used in finding the single ply properties whenever Whitney's method was employed.

Another micromechanic theory which relies more heavily on experimental data is Chamis' semi-empirical method.⁽⁴⁾ As applied in this study, Chamis' method uses experimental single ply properties of a representative ply as a starting point. The method then uses either experimental or theoretical relationships for the particular material to determine the elastic constants for a ply of any thickness. This method shows good agreement with Whitney's method if G_{LT} in Whitney's method is adjusted to agree with experimental data

A third method employed to determine individual ply properties was used by General Dynamics,⁽¹⁴⁾ and is almost totally experimental. This method uses the experimental properties of a representative ply, and assumes that the final buckling load calculated for a plate of nominal thickness can be corrected by the following relationship:

$$[(N_x)_{cr}]_{actual} = [(N_x)_{cr}]_{nominal} \times [t_{actual}/t_{nominal}]^2$$

The critical loads calculated using this method showed more sensitivity to a variation in the thickness from the nominal than did Chamis' method.

Table 10 shows which of the preceding three methods were used in conjunction with the buckling theories given in Chapter 2.

TABLE 10
METHOD USED TO PREDICT SINGLE PLY PROPERTIES FOR EACH PLATE
SERIES AND CORRESPONDING BUCKLING THEORY

| Method | Plate Series | Buckling Theory |
|--------------------------------------|--------------|--|
| Whitney's Micromechanic Method | 200 | Classical Orthotropic, Finite Element, Reduced Flexural Stiffness |
| | 500 | Classical Orthotropic, Reduced Flexural Stiffness |
| Chamis' Semi-Empirical Method | 200 | Galerkin |
| | 400 | Galerkin |
| | 500 | Galerkin |
| General Dynamics' Method | 400 | Ritz, Classical Orthotropic, Finite Element, Reduced Flexural Stiffness |
| | | |

In the case of the stiffened fiberglass plates, the ply properties employed were as suggested by the manufacturer⁽¹⁶⁾ of the prepreg tape

used to fabricate the plates. Any variations of the actual thickness from the nominal thickness assumed by the manufacturer were not considered in the single ply property predictions.

The elastic constants determined by any of the preceding methods are referenced parallel with and perpendicular to the fiber direction. These constants are then transformed to comply with the orientation assumed by the ply relative to the principal axes of the plate. Once this transformation is completed, the elastic stiffnesses for the gross plate can be determined.

B.2 Determination of the Elastic Stiffnesses for Unstiffened Plates

Once the single ply properties have been determined and transformed to account for some fiber orientation, the following stress-strain relations are known for the k^{th} ply. (13)

$$\begin{Bmatrix} \sigma_x \\ \sigma_y \\ \tau_{xy} \end{Bmatrix}_k = [C]_k \begin{Bmatrix} \bar{\epsilon}_x \\ \bar{\epsilon}_y \\ \bar{\gamma}_{xy} \end{Bmatrix}_k \quad (\text{B.5})$$

where $[C]$ is the stiffness matrix.

Combining the individual ply properties and neglecting transverse shear and stretching due to bending, the following force deformation equations are found for the laminated plate

$$\begin{Bmatrix} N \\ M \end{Bmatrix} = \begin{bmatrix} A & B \\ B & D \end{bmatrix} \begin{Bmatrix} \epsilon \\ -\kappa \end{Bmatrix} \quad (\text{B.6})$$

where

A is the in-plane membrane stiffness matrix, lb/in.

B is the stiffness coupling matrix, lb.

D is the flexural stiffness matrix, in. lb.

and

$$A_{ij} = \int_{-h/2}^{h/2} C_{ij} dz \quad i, j = 1, 2, 3$$

$$B_{ij} = \int_{-h/2}^{h/2} z C_{ij} dz$$

$$D_{ij} = \int_{-h/2}^{h/2} z^2 C_{ij} dz$$

B.3 Determination of the Elastic Stiffnesses for Stiffened Plates

Theoretical buckling loads for stiffened orthotropic (300 series) plates have been determined by finding the stiffnesses of an equivalent orthotropic plate, then using the standard formulas to find the critical loads. Equivalent stiffnesses for a stiffened orthotropic plate can be determined by a technique which smears out the effect of the stiffeners. To use this method we start with the stress-strain relations given by Lekhnitski.⁽²⁾ A typical plate is shown in Figure 13, and here we assume that the stiffeners are parallel to the edges of the plate. For the plate:

$$\sigma_{11} = \frac{1}{1 - \nu_{12}\nu_{21}} [E_{11} \epsilon_{11} + \nu_{12} E_{22} \epsilon_{22}]$$

$$\begin{aligned}\sigma_{22} &= \frac{1}{1-\nu_{12}\nu_{21}} [E_{22} \epsilon_{22} + \nu_{21} E_{11} \epsilon_{11}] \\ \sigma_{12} &= \frac{1}{1-\nu_{12}\nu_{21}} [(1-\nu_{12}\nu_{21}) E_{12} \epsilon_{12}]\end{aligned}\quad (B.7)$$

For the stiffeners:

$$\begin{aligned}\sigma_x &= E_x \epsilon_1 \\ \sigma_y &= E_y \epsilon_2\end{aligned}\quad (B.8)$$

Then

$$\begin{aligned}M_{11} &= \int_{-h/2}^{h/2} z \sigma_{11} + \frac{1}{d} \int_{h/2}^{h/2 + h_x} z \sigma_x \\ M_{22} &= \int_{-h/2}^{h/2} z \sigma_{22} + \frac{1}{d} \int_{h/2}^{h/2 + h_y} z \sigma_y \\ M_{12} &= - \int_{-h/2}^{h/2} z \sigma_{12}\end{aligned}\quad (B.9)$$

and, after integrating and simplifying, we find that

$$\begin{aligned}D_{11} &= \frac{E_{11} h^3}{12(1-\nu_{12}\nu_{21})} + \frac{A_x E_x}{d} \left[\left(\frac{h}{2}\right)^2 + \frac{hh_x}{2} + \frac{h_x^2}{3} \right] \\ D_{22} &= \frac{E_{22} h^3}{12(1-\nu_{12}\nu_{21})} + \frac{A_y E_y}{d} \left[\left(\frac{h}{2}\right)^2 + \frac{hh_y}{2} + \frac{h_y^2}{3} \right] \\ D_{66} &= \frac{1}{6} h^3 E_{12}\end{aligned}\quad (B.10)$$

where h = thickness of plate

$h_x = h_y$ = thickness of the stiffeners

d = stiffener spacing

A = area of stiffener

Subscripts x and y refer to the x and y directions, respectively.

B.4 Constituent Properties and Resulting Elastic Stiffnesses

The single ply properties for plates in the 200 and 500 series were determined by either Whitney's or Chamis' micromechanic methods or else by both. The constituent material properties for these plates are listed in Table 11. Any glue layers were assumed to have the same properties as the matrix material. These glue layers were included as separate plies if Whitney's method was used, but were averaged into the other plies equally if Chamis' method or General Dynamics' method was used.

TABLE 11
CONSTITUENT PROPERTIES FOR "THORNE1" AND UNSTIFFENED
FIBERGLASS PLATES^(4,13) (moduli $\times 10^6$ psi)

| Material | E_{fL} | E_{fT} | E_m | G_f | G_m | ν_{fLT} | ν_{fTP} |
|--------------|----------|----------|-------|-------|-------|-------------|-------------|
| "Throne1"-25 | 24.7 | 1.0 | 0.57 | 1.0 | 0.207 | 0.20 | 0.15 |
| "Thorne1"-40 | 40.0 | 1.0 | 0.57 | 1.0 | 0.207 | 0.20 | 0.15 |
| Fiberglass | 12.4 | 12.4 | 0.50 | 0.508 | 0.185 | 0.22 | 0.22 |

Single ply properties for the 300 and 400 series plates were based on experimental data. These properties are given in Table 12.

TABLE 12
EXPERIMENTAL SINGLE PLY PROPERTIES FOR BORON⁽¹⁴⁾
AND STIFFENED FIBERGLASS⁽¹⁶⁾ PLATES

| Material | E_L (10^6 psi) | E_T (10^6 psi) | G_{LT} (10^6 psi) | ν_{LT} | Nominal Thickness (in.) |
|------------|------------------------|------------------------|---------------------------|------------|----------------------------|
| Boron | 31.0 | 3.4 | 0.75 | 0.28 | 0.0053 |
| Fiberglass | 6.2 | 1.8 | 0.50 | 0.29 | 0.009 |

The elastic stiffnesses calculated for each plate, using the preceding constituent or single ply properties, are given in Tables 13, 14, and 15. The stiffnesses are based on single ply properties predicted by one of the methods in Section B.1, and, in general, stiffnesses calculated by any of the other methods would be in reasonably good agreement with those given.

TABLE 13

MEMBRANE STIFFNESSES (10^3 lb/in)^a

| Plate No. | % Fiber by Volume ^b | A ₁₁ | A ₁₂ | A ₁₃ | A ₂₂ | A ₂₆ | A ₆₆ |
|-----------|-----------------------------------|-----------------|-----------------|-----------------|-----------------|-----------------|-----------------|
| 201 | 40.0 | 311.8 | 17.68 | 0 | 311.8 | 0 | 27.30 |
| 202 | 40.0 | 748.9 | 38.91 | 0 | 623.7 | 0 | 60.09 |
| 203 | 40.0 | 405.4 | 290.1 | -30.02 | 405.4 | -30.02 | 310.4 |
| 204 | 60.0 | 644.7 | 12.34 | 0 | 444.4 | 0 | 28.68 |
| 205 | 60.0 | 444.4 | 12.34 | 0 | 644.7 | 0 | 28.68 |
| 206 | 60.0 | 430.6 | 9.76 | 0 | 430.6 | 0 | 22.68 |
| 207 | 60.0 | 430.6 | 9.76 | 0 | 430.6 | 0 | 22.68 |
| 208 | 60.0 | 532.3 | 136.8 | -132.8 | 178.3 | -132.8 | 151.2 |
| 209 | 50.0 | 863.3 | 27.46 | 0 | 863.3 | 0 | 48.15 |
| 401 | 48.2 | 476 | 649 | 0 | 1926 | 0 | 661 |
| 402 | 48.2 | 1296 | 649 | 0 | 476 | 0 | 661 |
| 403 | 57.0 | 1141 | 921 | 0 | 1141 | 0 | 940 |
| 404 | 57.2 | 3335 | 88.0 | 0 | 427 | 0 | 106 |
| 405 | 57.2 | 427 | 88.0 | 0 | 3335 | 0 | 106 |
| 406 | 51.7 | 1996 | 673 | 986 | 513 | 299 | 688 |
| 407 | 51.7 | 513 | 673 | 299 | 1996 | 986 | 688 |
| 408 | 58.6 | 1115 | 893 | 732 | 1115 | 732 | 912 |

TABLE 13, CONTINUED

| Plate No. | % Fiber by Volume ^b | A ₁₁ | A ₁₂ | A ₁₃ | A ₂₂ | A ₂₆ | A ₆₆ |
|-----------|-----------------------------------|-----------------|-----------------|-----------------|-----------------|-----------------|-----------------|
| 409 | 49.1 | 1021 | 850 | 0 | 1021 | 0 | 862 |
| 501 | 44.0 | 195.8 | 88.23 | 0 | 385.2 | 0 | 101.1 |
| 502 | 44.0 | 385.2 | 88.23 | 0 | 195.8 | 0 | 101.1 |
| 503 | 44.0 | 198.0 | 88.98 | 0 | 387.4 | 0 | 101.8 |
| 504 | 44.0 | 387.4 | 88.98 | 0 | 198.0 | 0 | 101.8 |
| 505 | 44.0 | 275.0 | 69.87 | 0 | 342.7 | 0 | 82.78 |
| 506 | 44.0 | 342.7 | 69.87 | 0 | 275.0 | 0 | 82.78 |
| 507 | 44.0 | 246.3 | 62.22 | 0 | 307.8 | 0 | 74.06 |
| 508 | 44.0 | 330.0 | 42.05 | 0 | 330.0 | 0 | 55.09 |
| 509 | 44.0 | 330.0 | 42.05 | 0 | 330.0 | 0 | 55.09 |

^aStiffnesses for the 200 and 500 series plates were based on Whitney's micromechanic method corrected to agree with experimental data, while the 400 series plates were based on Chamis' semi-empirical method.

^bAll fiber volumes were estimated by empirical methods. Glue layers, when present, were not included in the fiber volumes.

TABLE 14
FLEXURAL STIFFNESSES (in/lb)^a

| Plate No. | % Fiber by Volume ^b | D ₁₁ | D ₁₂ | D ₁₆ | D ₂₂ | D ₂₆ | D ₆₆ |
|-----------|-----------------------------------|-----------------|-----------------|-----------------|-----------------|-----------------|-----------------|
| 201 | 40 | 127 | 4.45 | 0 | 30.2 | 0 | 6.88 |
| 202 | 40 | 1065 | 47.5 | 0 | 611 | 0 | 73.4 |
| 203 | 40 | 455 | 326 | -100 | 455 | -100 | 349 |
| 204 | 60 | 129 | 1.90 | 0 | 38.8 | 0 | 4.42 |
| 205 | 60 | 38.8 | 1.90 | 0 | 129 | 0 | 4.42 |
| 206 | 60 | 70.1 | 0.94 | 0 | 12.9 | 0 | 2.18 |
| 207 | 60 | 12.9 | 0.94 | 0 | 70.1 | 0 | 2.18 |
| 208 | 60 | 10.7 | 6.77 | -5.75 | 94.2 | -5.75 | 8.50 |
| 209 | 50 | 631 | 19.1 | 0 | 631 | 0 | 34.5 |
| 401 | 48.2 | 480 | 655 | 44.6 | 1943 | 145 | 666 |
| 402 | 48.2 | 1943 | 655 | 145 | 480 | 44.6 | 666 |
| 403 | 57.0 | 970 | 782 | 97.3 | 970 | 97.3 | 799 |
| 404 | 57.2 | 2562 | 67.3 | 0 | 328 | 0 | 81.2 |
| 405 | 57.2 | 328 | 67.3 | 0 | 2562 | 0 | 81.2 |
| 406 | 51.7 | 1870 | 631 | 923 | 481 | 298 | 644 |
| 407 | 51.7 | 481 | 631 | 298 | 1870 | 923 | 644 |
| 408 | 58.6 | 839 | 671 | 551 | 839 | 551 | 686 |

TABLE 14, CONTINUED

| Plate No. | % Fiber by Volume ^b | D ₁₁ | D ₁₂ | D ₁₆ | D ₂₂ | D ₂₆ | D ₆₆ |
|-----------|-----------------------------------|-----------------|-----------------|-----------------|-----------------|-----------------|-----------------|
| 409 | 49.1 | 1011 | 842 | 0 | 1011 | 0 | 854 |
| 501 | 44.0 | 139 | 47.8 | 0 | 440 | 0 | 59.5 |
| 502 | 44.0 | 440 | 47.8 | 0 | 139 | 0 | 59.5 |
| 503 | 44.0 | 229 | 120 | 0 | 272 | 0 | 133 |
| 504 | 44.0 | 272 | 120 | 0 | 229 | 0 | 133 |
| 505 | 44.0 | 156 | 43.9 | 0 | 431 | 0 | 55.6 |
| 506 | 44.0 | 431 | 43.9 | 0 | 156 | 0 | 55.6 |
| 507 | 44.0 | 208 | 49.5 | 0 | 113 | 0 | 56.9 |
| 508 | 44.0 | 113 | 49.5 | 0 | 208 | 0 | 56.9 |
| 509 | 44.0 | 242 | 30.4 | 0 | 242 | 0 | 40.1 |

^aStiffnesses for the 200 and 500 series plates were based on Whitney's micromechanic method corrected to agree with experimental data, while the 400 series plates were based on Chamis' semi-empirical method.

^bAll fiber volumes were estimated by empirical methods. Glue layers, when present, were not included in the fiber volumes.

TABLE 15
COUPLING STIFFNESSES FOR UNBALANCED PLATES (10^3 lb)^a

| Plate No. | % Fiber by Volume ^b | B ₁₁ | B ₁₂ | B ₁₆ | B ₂₂ | B ₂₆ | B ₆₆ |
|-----------|-----------------------------------|-----------------|-----------------|-----------------|-----------------|-----------------|-----------------|
| 209 | 50.0 | -18.33 | 0 | 0 | 18.33 | 0 | 0 |
| 409 | 49.1 | 0 | 0 | 19.9 | 0 | 19.9 | 0 |
| 501 | 44.0 | 0 | 0 | 0.6215 | 0 | 0.6215 | 0 |
| 502 | 44.0 | 0 | 0 | -0.6215 | 0 | -0.6215 | 0 |
| 503 | 44.0 | 0 | 0 | 1.953 | 0 | 1.953 | 0 |
| 504 | 44.0 | 0 | 0 | -1.953 | 0 | -1.953 | 0 |
| 505 | 44.0 | 0 | 0 | 0.7632 | 0 | 0.1889 | 0 |
| 506 | 44.0 | 0 | 0 | -0.1889 | 0 | -0.7632 | 0 |
| 507 | 44.0 | 0 | 0 | 1.721 | 0 | 0.4259 | 0 |
| 508 | 44.0 | 0 | 0 | -0.4259 | 0 | -1.721 | 0 |
| 509 | 44.0 | -4.546 | 0 | 0 | 4.546 | 0 | 0 |

^aStiffnesses for the 200 and 500 series plates were based on Whitney's micromechanic method corrected to agree with experimental data, while the 400 series plates were based on Chamis' semi-empirical method.

^bAll fiber volumes were estimated by empirical methods. Glue layers, when present, were not included in the fiber volumes.

APPENDIX C
TEST DATA, LOAD-DEFLECTION CURVES,
SOUTHWELL PLOTS, AND MODE SHAPES

The tables and figures in this appendix represent all of the test data taken for each plate. The Appendix is arranged according to plate number, and all of the tables and figures for each plate are grouped together. The mode shape, if recorded, is included after the load-deflection data. Location of the points at which the mode shape was taken are given in Figure 9.

The load given in the data tables is the total load on the plate. To find the critical buckling load given in Table 2, the total load must be divided by the effective width, b , of the plate. Deflections were recorded at the center of the plate in most cases, but if the maximum deflection did not occur at the center, then the deflection was recorded as close to the maximum deflection point as possible.

TABLE 16
DATA AND CALCULATIONS FOR PLATE NO. 101,
2 SIDES SUPPORTED

| Total Load (P) (lb.) | Deflection (Δ) (10^{-4} in.) | Total Load/Deflection (Δ/P) (10^{-4} in./lb.) |
|-------------------------|---|--|
| 6.4 | 0 | 0 |
| 30.4 | 19 | .625 |
| 48.4 | 35 | .722 |
| 66.4 | 48 | .722 |
| 84.4 | 81 | .959 |
| 102.4 | 111 | 1.082 |
| 114.4 | 136 | 1.188 |
| 120.4 | 149 | 1.236 |
| 126.4 | 166 | 1.313 |
| 132.4 | 195 | 1.472 |
| 138.4 | 201 | 1.452 |
| 144.4 | 227 | 1.571 |
| 150.4 | 254 | 1.686 |
| 156.4 | 302 | 1.930 |
| 162.4 | 340 | 2.09 |
| 168.4 | 381 | 2.26 |

TABLE 17
MODE SHAPE FOR PLATE NO. 101,
2 SIDES SUPPORTED, 10^{-4} in.

| | | |
|-----|-----|-----|
| 339 | 324 | 341 |
| 499 | 478 | 506 |
| 359 | 322 | 371 |

Note: See Figure 9.

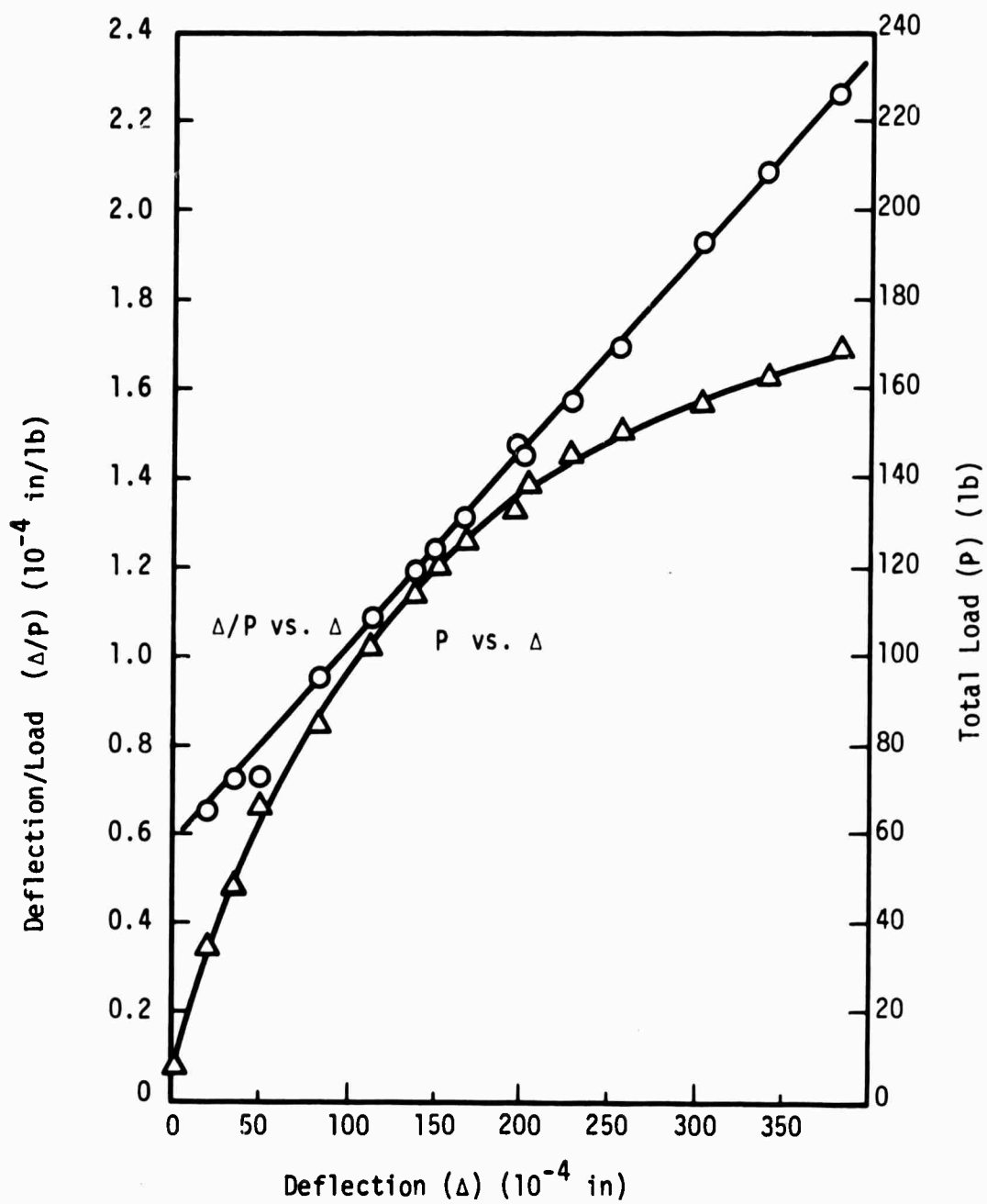


Figure 22. Southwell Plot and Load Deflection Curve
for Plate No. 101, 2 Sides Supported

TABLE 18
DATA AND CALCULATIONS FOR PLATE NO. 101,
4 SIDES SUPPORTED

| Total Load (P) (lb.) | Deflection (Δ) (10^{-4} in.) | Total Load/Deflection (Δ/P) (10^{-4} in./lb.) |
|-------------------------|---|--|
| 0 | 0 | 0 |
| 60 | --- | --- |
| 120 | --- | --- |
| 180 | --- | --- |
| 240 | 1 | .00417 |
| 300 | 6 | .0200 |
| 360 | 10 | .0288 |
| 420 | 16 | .0381 |
| 480 | 28 | .0583 |
| 510 | 36 | .0706 |
| 540 | 44 | .0815 |
| 570 | 50 | .0877 |
| 600 | 58 | .0967 |
| 630 | 67 | .1063 |
| 660 | 77 | .1166 |
| 690 | 95 | .1377 |
| 720 | 118 | .1639 |
| 732 | 129 | .1760 |
| 750 | 152 | .203 |
| 762 | 164 | .215 |
| 774 | 184 | .238 |
| 786 | 202 | .257 |

TABLE 19
MODE SHAPE FOR PLATE NO. 101,
4 SIDES SUPPORTED, 10^{-4} in.

| | | |
|-----|-----|-----|
| 126 | 175 | 119 |
| 204 | 282 | 207 |
| 159 | 210 | 140 |

Note: See Figure 9.

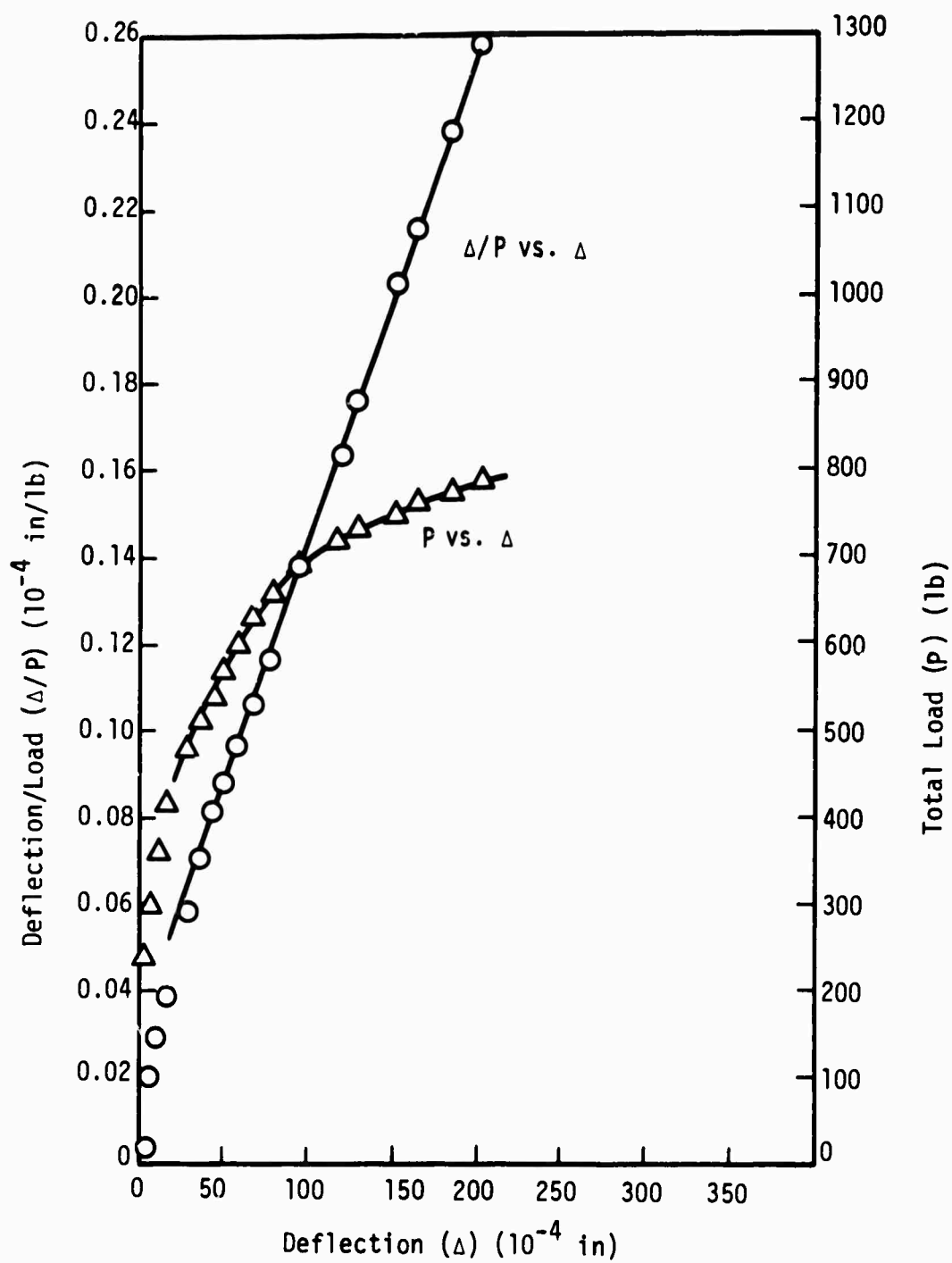


Figure 23. Southwell Plot and Load Deflection Curve
for Plate No. 101, 4 Sides Supported

TABLE 20
DATA AND CALCULATIONS FOR PLATE NO. 102,
2 SIDES SUPPORTED

| Total Load (P) (lb.) | Deflection (Δ) (10^{-4} in.) | Total Load/Deflection (Δ/P) (10^{-4} in./lb.) |
|-------------------------|---|--|
| 0 | 0 | 0 |
| 60 | 26 | .433 |
| 120 | 38 | .317 |
| 180 | 47 | .261 |
| 240 | 61 | .254 |
| 300 | 77 | .257 |
| 360 | 94 | .261 |
| 420 | 123 | .293 |
| 444 | 136 | .306 |
| 468 | 154 | .329 |
| 492 | 181 | .368 |
| 516 | 230 | .446 |
| 540 | 294 | .545 |
| 564 | 408 | .723 |

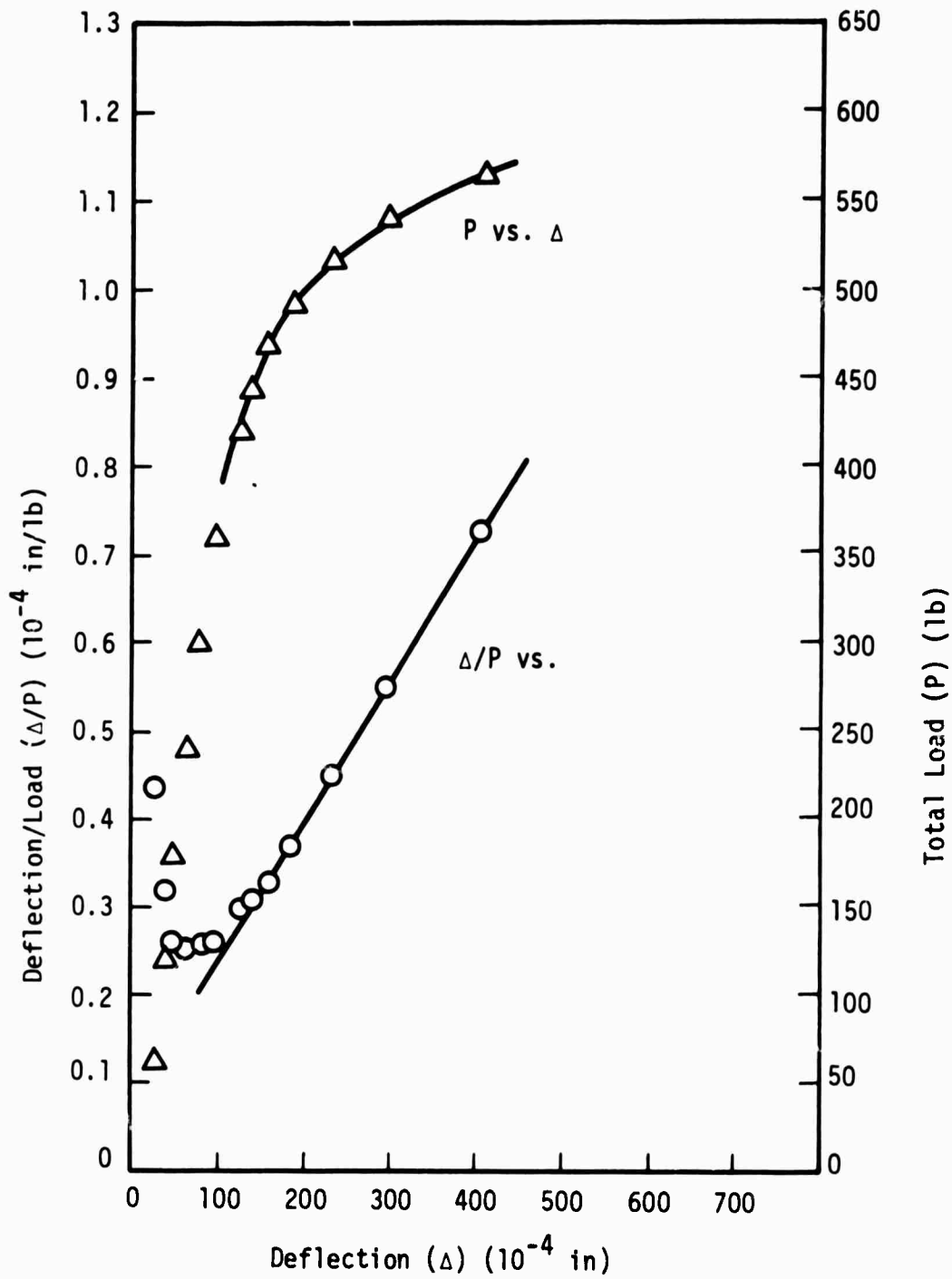


Figure 24. Southwell Plot and Load Deflection Curve
for Plate No. 102, 2 Sides Supported

TABLE 21
DATA AND CALCULATIONS FOR PLATE NO. 102,
4 SIDES SUPPORTED

| Total Load (P) (lb.) | Deflection (Δ) (10^{-4} in.) | Total Load/Deflection (Δ/P) (10^{-4} in./lb.) |
|-------------------------|---|--|
| 0 | 0 | 0 |
| 120 | 7 | .0583 |
| 240 | 11 | .0458 |
| 360 | 13 | .0361 |
| 480 | 20 | .0417 |
| 600 | 26 | .0433 |
| 720 | 38 | .0528 |
| 840 | 46 | .0547 |
| 960 | 60 | .0625 |
| 1080 | 73 | .0676 |
| 1200 | 88 | .0733 |
| 1320 | 107 | .0810 |
| 1440 | 127 | .0882 |
| 1560 | 152 | .0974 |
| 1620 | 165 | .1019 |
| 1680 | 186 | .1106 |
| 1740 | 210 | .1207 |
| 1800 | 236 | .1310 |
| 1860 | 273 | .1468 |

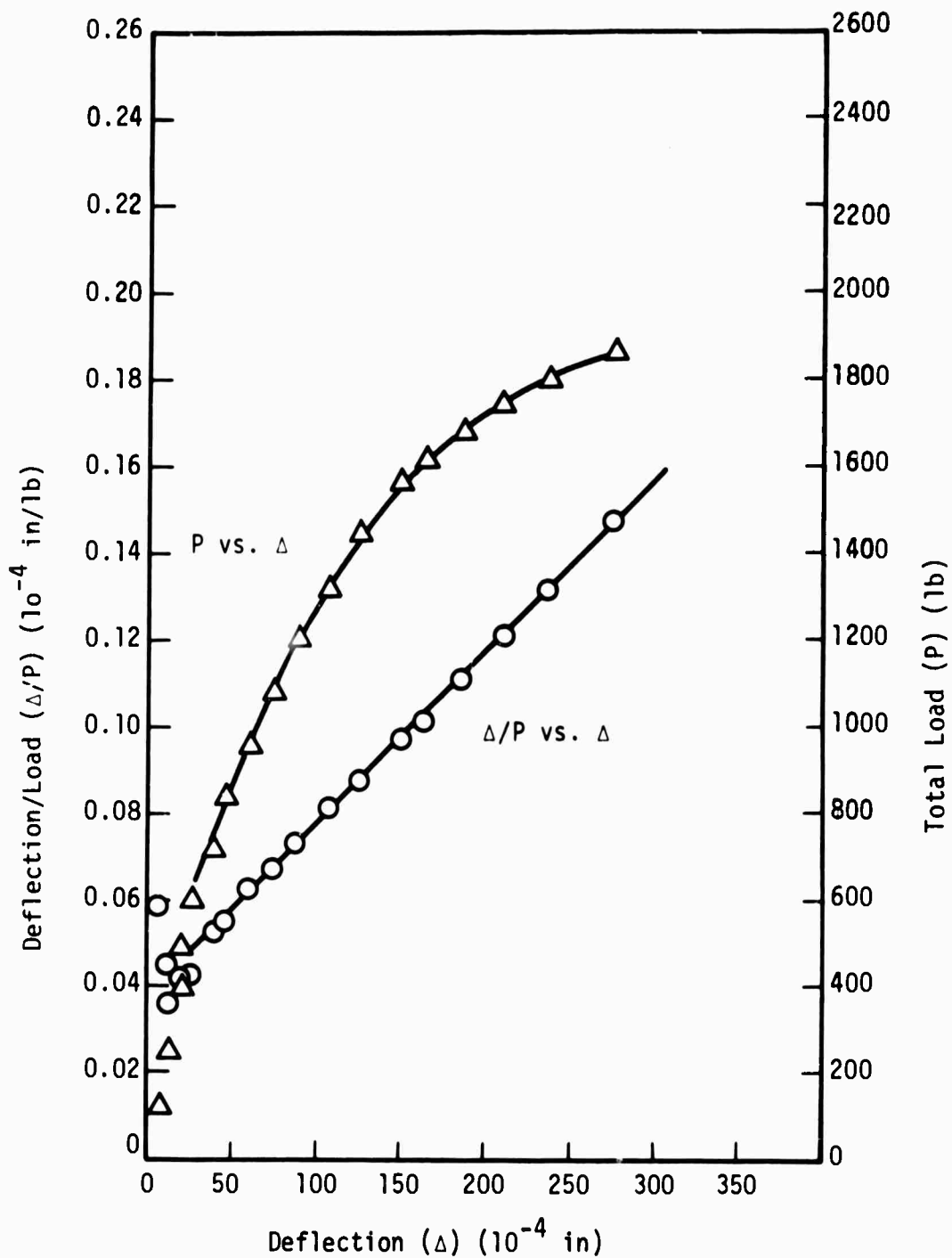


Figure 25. Southwell Plot and Load Deflection Curve
for Plate No. 102, 4 Sides Supported

TABLE 22
DATA AND CALCULATIONS FOR PLATE NO. 103,
2 SIDES SUPPORTED

| Total Load (P) (lb.) | Deflection (Δ) (10^{-4} in.) | Total Load/Deflection (Δ/P) (10^{-4} in./lb.) |
|-------------------------|---|--|
| 0 | 0 | 0 |
| 60 | 8 | .133 |
| 120 | 15 | .125 |
| 180 | 27 | .150 |
| 240 | 45 | .188 |
| 270 | 54 | .200 |
| 300 | 65 | .217 |
| 330 | 88 | .267 |
| 360 | 119 | .331 |
| 390 | 149 | .382 |
| 420 | 194 | .462 |
| 450 | 267 | .593 |

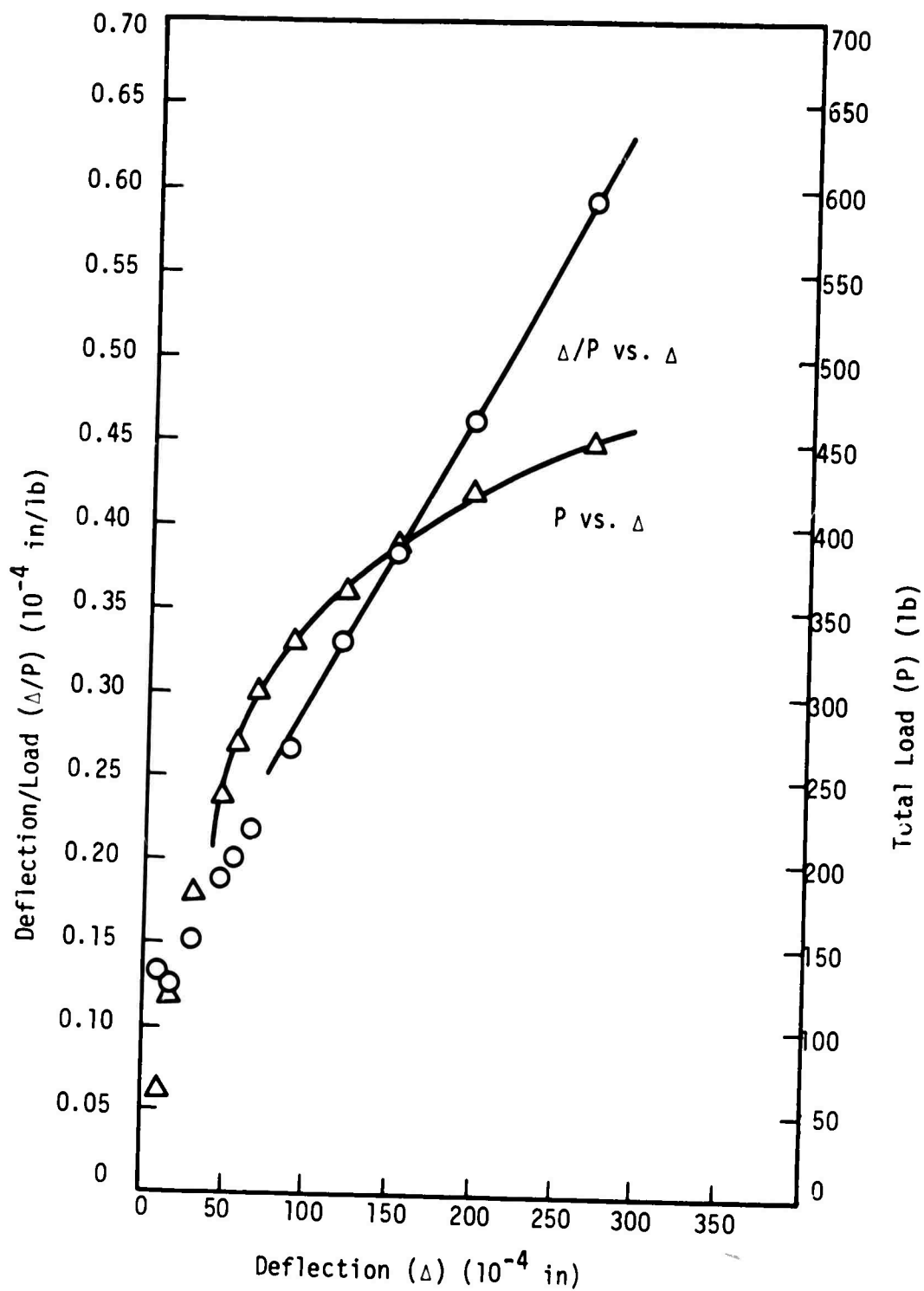


Figure 26. Southwell Plot and Load Deflection Curve
for Plate No. 103, 2 Sides Supported

TABLE 23
DATA AND CALCULATIONS FOR PLATE NO. 103,
4 SIDES SUPPORTED

| Total Load (P) (lb.) | Deflection (Δ) (10 ⁻⁴ in.) | Total Load/Deflection (Δ/P) (10 ⁻⁴ in./lb.) |
|-------------------------|--|---|
| 0 | 0 | 0 |
| 240 | 20 | .0833 |
| 480 | 33 | .0687 |
| 720 | 50 | .0693 |
| 960 | 74 | .0771 |
| 1140 | 98 | .0860 |
| 1260 | 116 | .0920 |
| 1350 | 134 | .0993 |
| 1410 | 146 | .1036 |
| 1470 | 160 | .1088 |
| 1530 | 176 | .1150 |
| 1590 | 191 | .1201 |
| 1650 | 206 | .1248 |
| 1710 | 221 | .1293 |
| 1770 | 239 | .1350 |

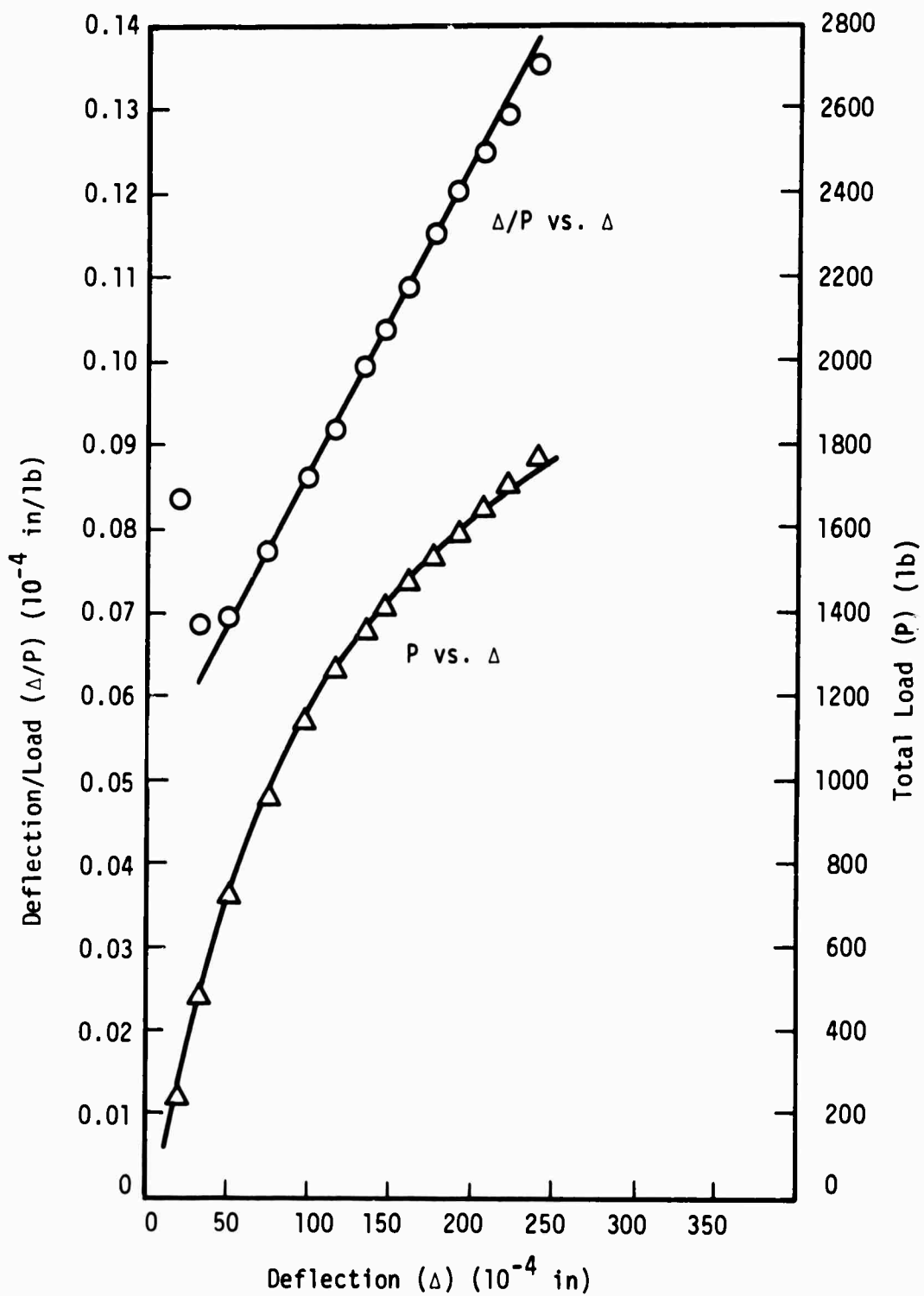


Figure 27. Southwell Plot and Load Deflection Curve
for Plate No. 103, 4 Sides Supported

TABLE 24
DATA AND CALCULATIONS FOR PLATE NO. 104,
2 SIDES SUPPORTED

| Total Load (P) (lb.) | Deflection (Δ) (10^{-4} in.) | Total Load/Deflection (Δ/P) (10^{-4} in./lb.) |
|-------------------------|---|--|
| 0 | 0 | 0 |
| 25 | 10 | .400 |
| 50 | 22 | .440 |
| 75 | 38 | .507 |
| 100 | 54 | .540 |
| 125 | 70 | .560 |
| 150 | 86 | .573 |
| 175 | 108 | .617 |
| 200 | 136 | .679 |
| 225 | 165 | .733 |
| 250 | 198 | .792 |
| 275 | 242 | .880 |
| 300 | 290 | .966 |

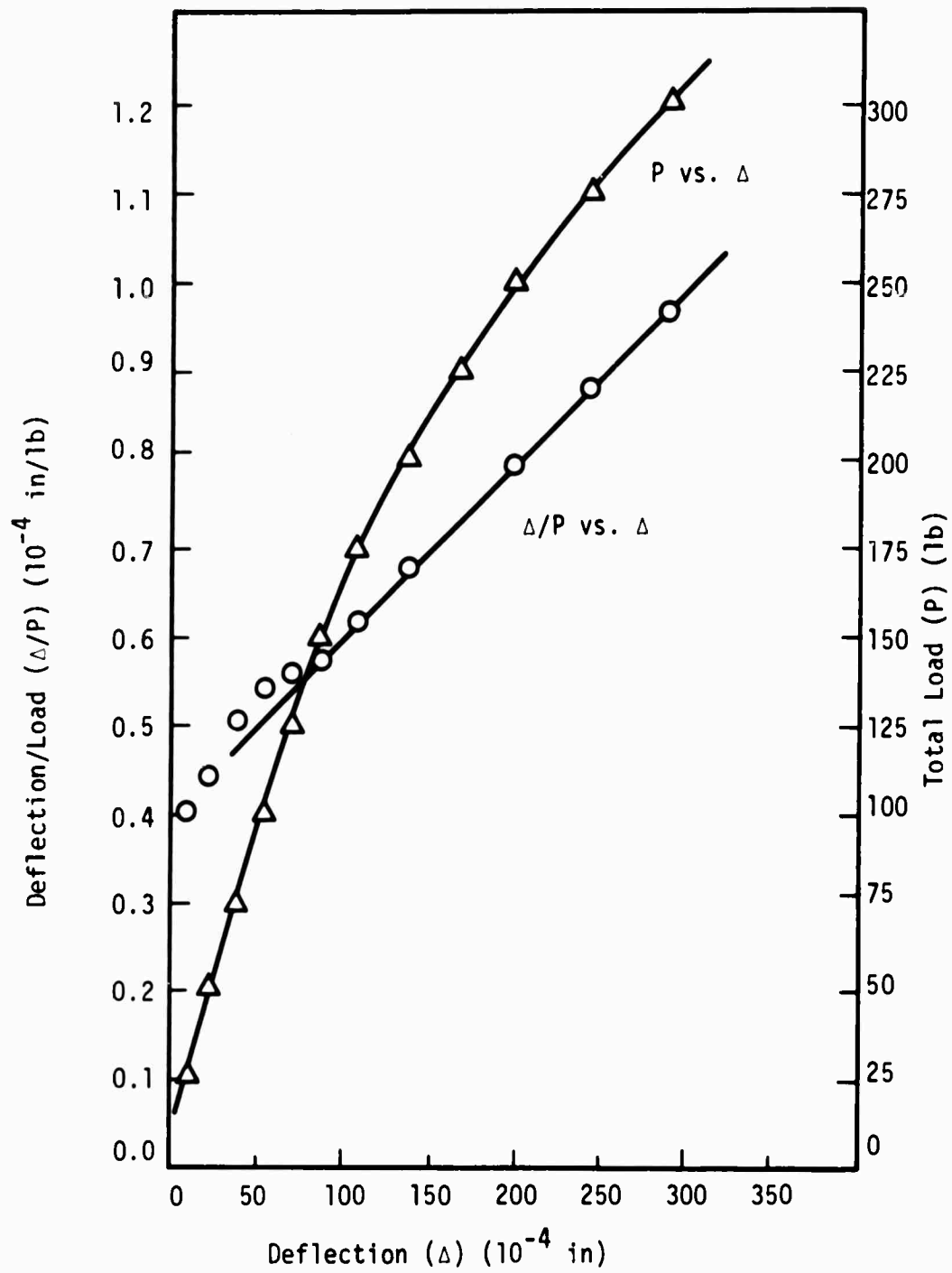


Figure 28. Southwell Plot and Load Deflection Curve
for Plate No. 104, 2 Sides Supported

TABLE 25
DATA AND CALCULATIONS FOR PLATE NO. 104,
4 SIDES SUPPORTED

| Total Load (P) (lb.) | Deflection (Δ) (10^{-4} in.) | Total Load/Deflection (Δ/P) (10^{-4} in./lb.) |
|-------------------------|---|--|
| 0 | 0 | 0 |
| 200 | 17 | .0850 |
| 400 | 35 | .0875 |
| 600 | 61 | .1016 |
| 800 | 84 | .1050 |
| 900 | 95 | .1055 |
| 1000 | 114 | .1140 |
| 1100 | 136 | .1236 |
| 1200 | 157 | .1310 |
| 1300 | 180 | .1385 |
| 1400 | 210 | .1500 |
| 1500 | 236 | .1572 |
| 1600 | 273 | .1705 |
| 1700 | 316 | .1860 |

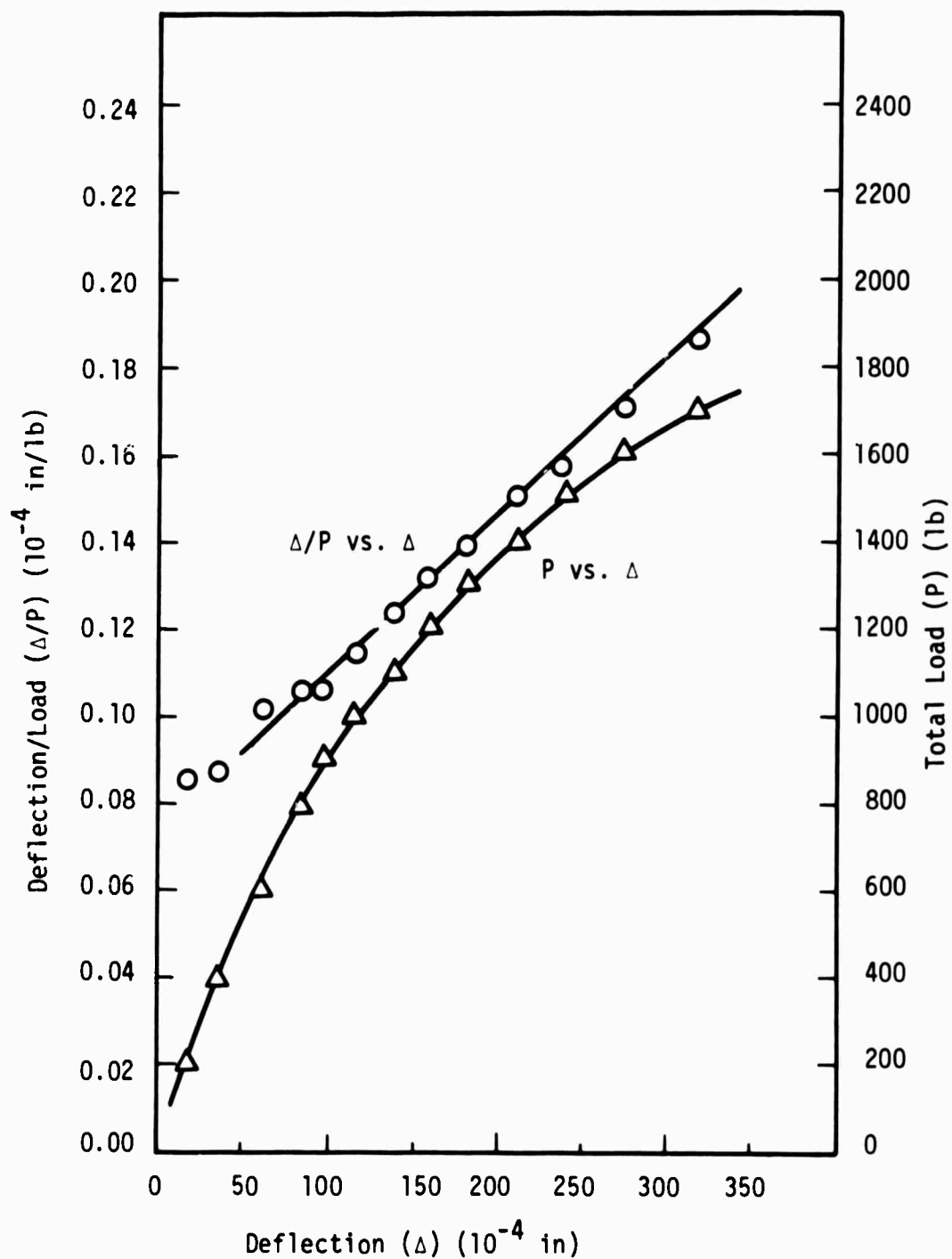


Figure 29. Southwell Plot and Load Deflection Curve
for Plate No. 104, 4 Sides Supported

TABLE 26
DATA AND CALCULATIONS FOR PLATE NO. 105,
2 SIDES SUPPORTED

| Total Load (P) (lb.) | Deflection (Δ) (10^{-4} in.) | Total Load/Deflection (Δ/P) (10^{-4} in./lb.) |
|-------------------------|---|--|
| 0 | 0 | 0 |
| 100 | 31 | .310 |
| 200 | 63 | .315 |
| 300 | 100 | .333 |
| 400 | 141 | .353 |
| 500 | 191 | .382 |
| 600 | 261 | .435 |
| 650 | 306 | .471 |
| 700 | 363 | .518 |
| 750 | 429 | .572 |
| 800 | 516 | .645 |
| 825 | 566 | .687 |
| 850 | 676 | .795 |

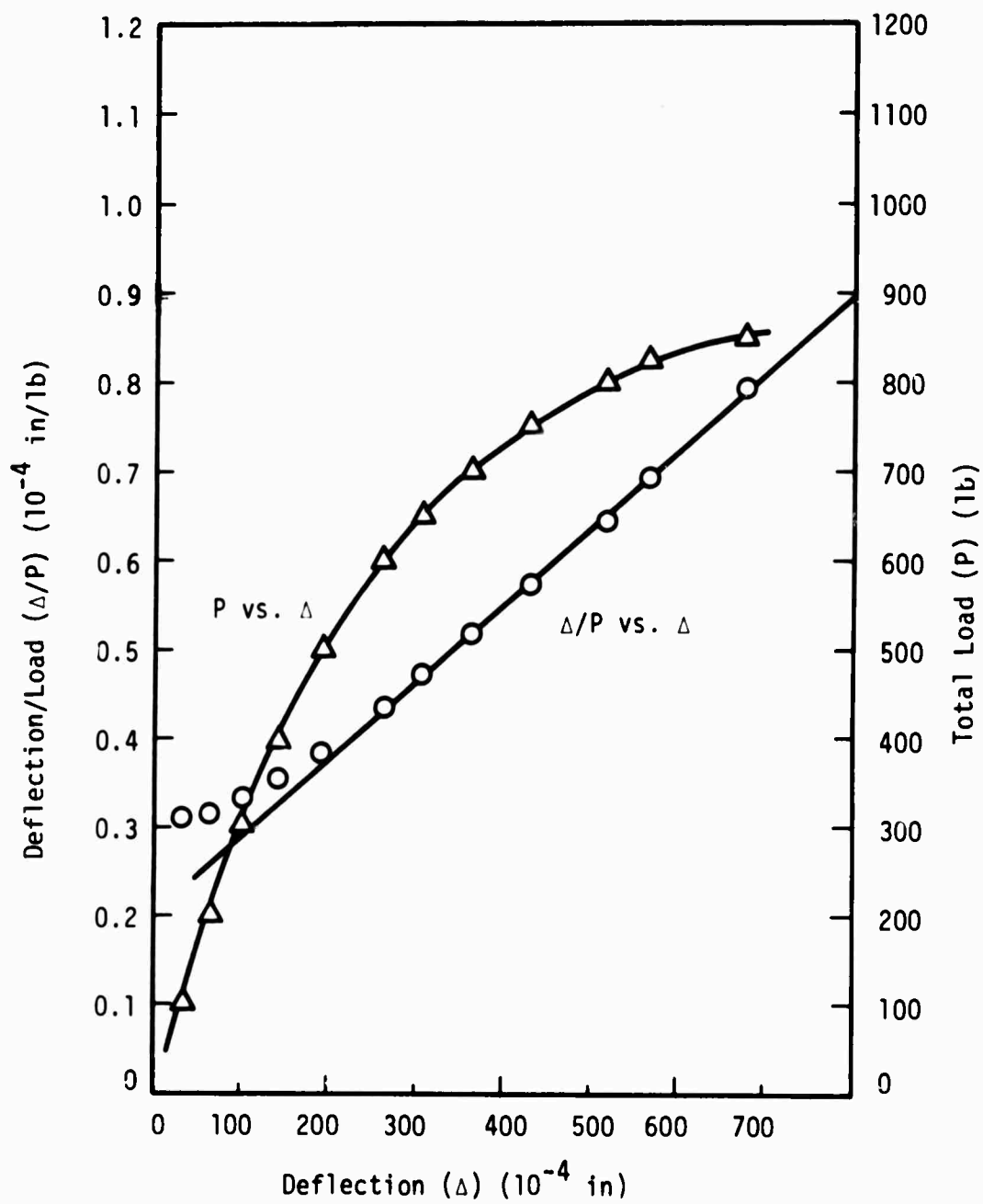


Figure 30. Southwell Plot and Load Deflection Curve
for Plate No. 105, 2 Sides Supported

TABLE 27
DATA AND CALCULATIONS FOR PLATE NO. 105,
4 SIDES SUPPORTED

| Total Load (P) (lb.) | Deflection (Δ) (10^{-4} in.) | Total Load/Deflection (Δ/P) (10^{-4} in./lb.) |
|-------------------------|---|--|
| 0 | 0 | 0 |
| 500 | --- | --- |
| 1000 | --- | --- |
| 1500 | --- | --- |
| 2000 | --- | --- |
| 2500 | --- | --- |
| 3000 | 6 | .00200 |
| 3500 | 33 | .00943 |
| 3750 | 50 | .01333 |
| 4000 | 68 | .01700 |
| 4250 | 117 | .0275 |
| 4400 | 150 | .0341 |
| 4600 | 213 | .0463 |
| 4700 | 270 | .0574 |
| 4750 | 304 | .0640 |
| 4800 | 330 | .0687 |
| 4850 | 355 | .0731 |
| 4900 | 380 | .0775 |

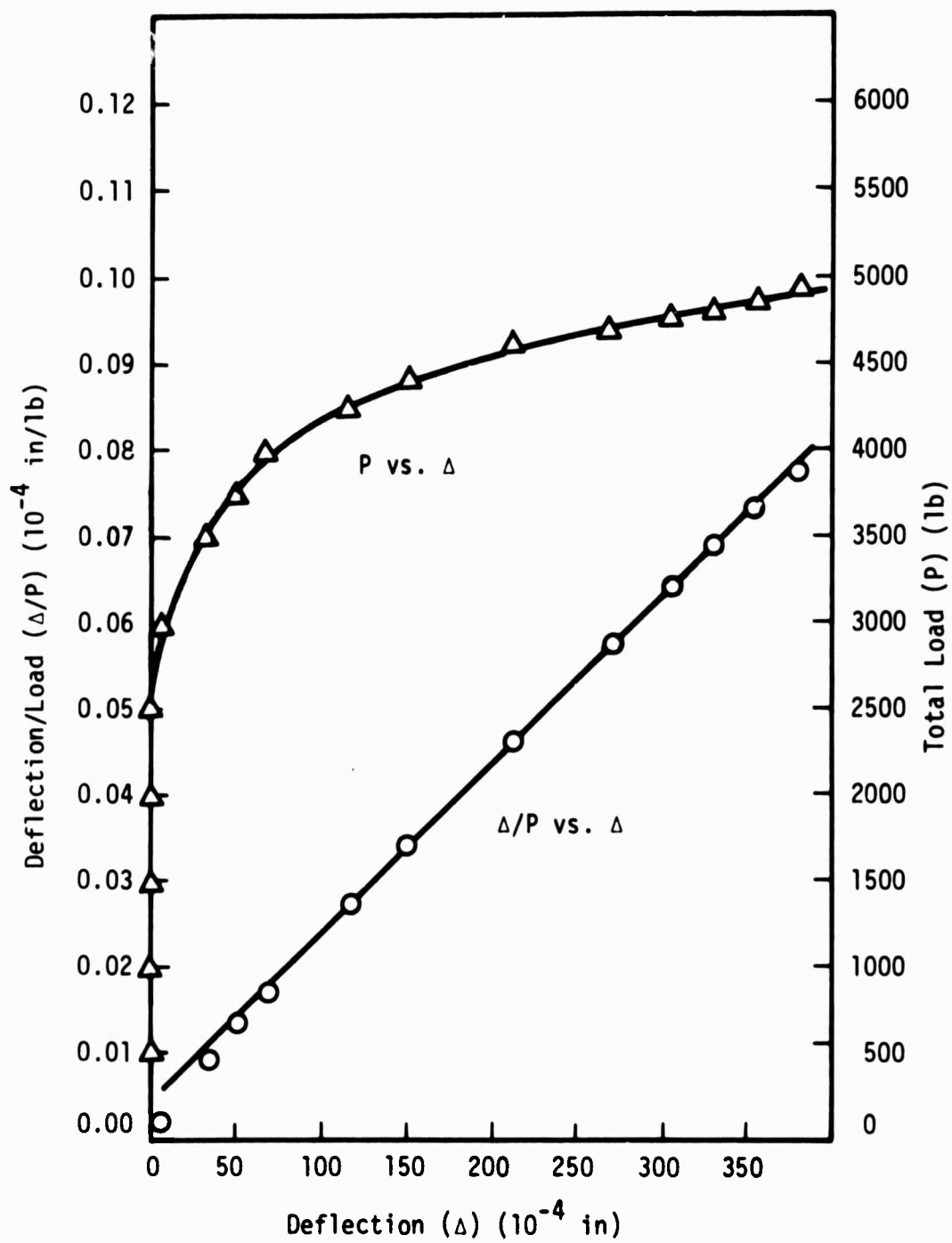


Figure 31. Southwell Plot and Load Deflection Curve
for Plate No. 105, 4 Sides Supported

TABLE 28
DATA AND CALCULATIONS FOR PLATE NO. 201,
2 SIDES SUPPORTED

| Total Load (P) (lb.) | Deflection (Δ) (10^{-4} in.) | Total Load/Deflection (Δ/P) (10^{-4} in./lb.) |
|-------------------------|---|--|
| 6.4 | 0 | 0 |
| 16.4 | 18 | 1.097 |
| 26.4 | 43 | 1.630 |
| 36.4 | 75 | 2.06 |
| 46.4 | 109 | 2.35 |
| 56.4 | 157 | 2.78 |
| 66.4 | 223 | 3.36 |
| 71.4 | 270 | 3.78 |
| 76.4 | 334 | 4.37 |
| 81.4 | 396 | 4.87 |
| 86.4 | 515 | 5.96 |

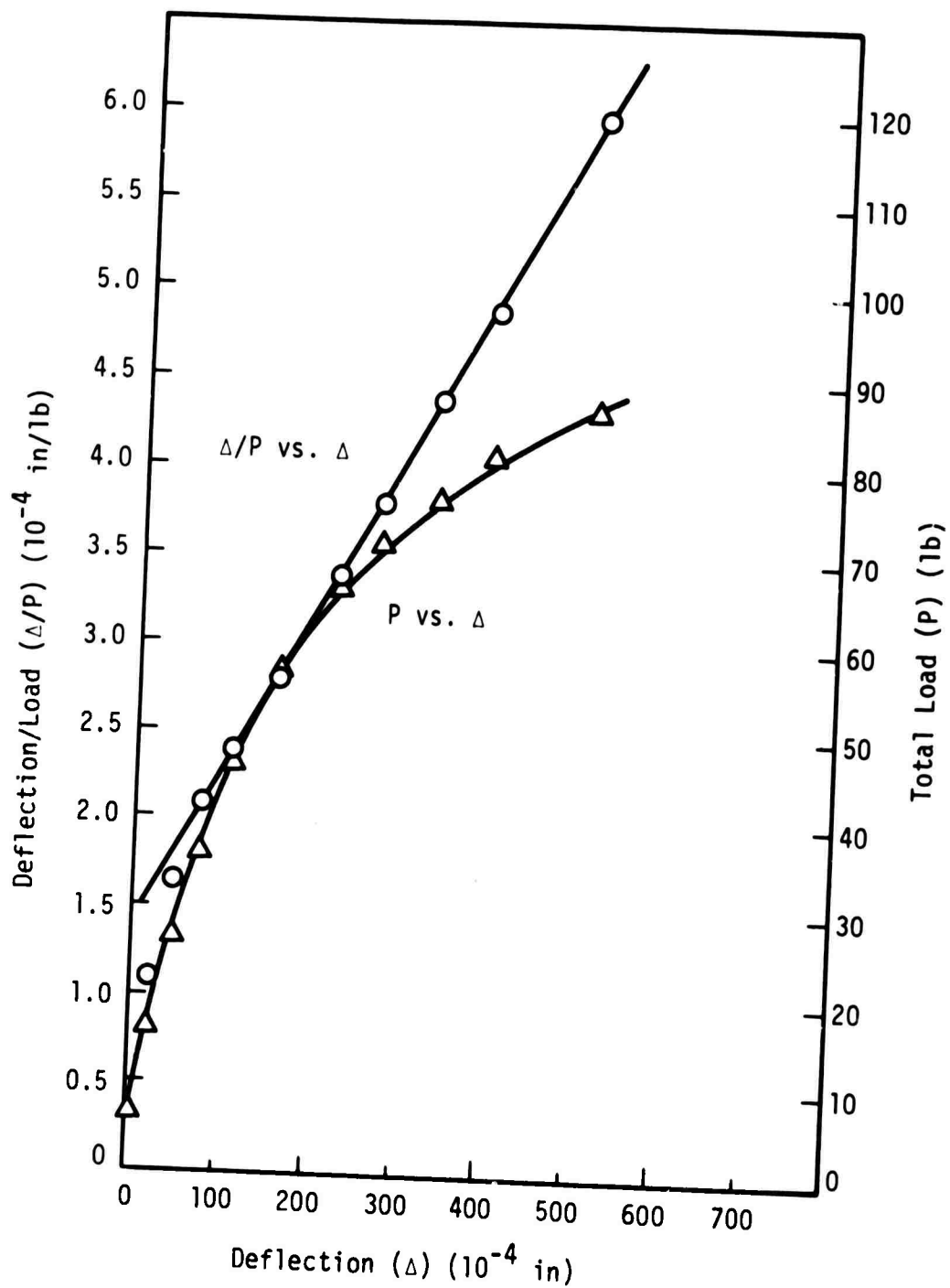


Figure 32. Southwell Plot and Load Deflection Curve
for Plate No. 201, 2 Sides Supported

TABLE 29
DATA AND CALCULATIONS FOR PLATE NO. 201,
4 SIDES SUPPORTED

| Total Load (P) (lb.) | Deflection (Δ) (10^{-4} in.) | Total Load/Deflection (Δ/P) (10^{-4} in./lb.) |
|-------------------------|---|--|
| 0 | 0 | 0 |
| 24 | 11 | .458 |
| 48 | 26 | .541 |
| 72 | 34 | .472 |
| 96 | 41 | .427 |
| 120 | 58 | .483 |
| 132 | 71 | .538 |
| 144 | 84 | .583 |
| 156 | 102 | .654 |
| 168 | 133 | .793 |
| 174 | 161 | .925 |
| 180 | 195 | 1.08 |
| 186 | 263 | 1.41 |
| 192 | 339 | 1.76 |
| 198 | 389 | 1.96 |
| 204 | 468 | 2.29 |
| 216 | 593 | 2.75 |
| 228 | 691 | 3.03 |
| 240 | 786 | 3.27 |
| 252 | 868 | 3.45 |
| 264 | 941 | 3.57 |
| 276 | 1011 | 3.67 |
| 288 | 1080 | 3.75 |
| 300 | 1143 | 3.81 |
| 312 | 1197 | 3.84 |
| 324 | 1268 | 3.91 |

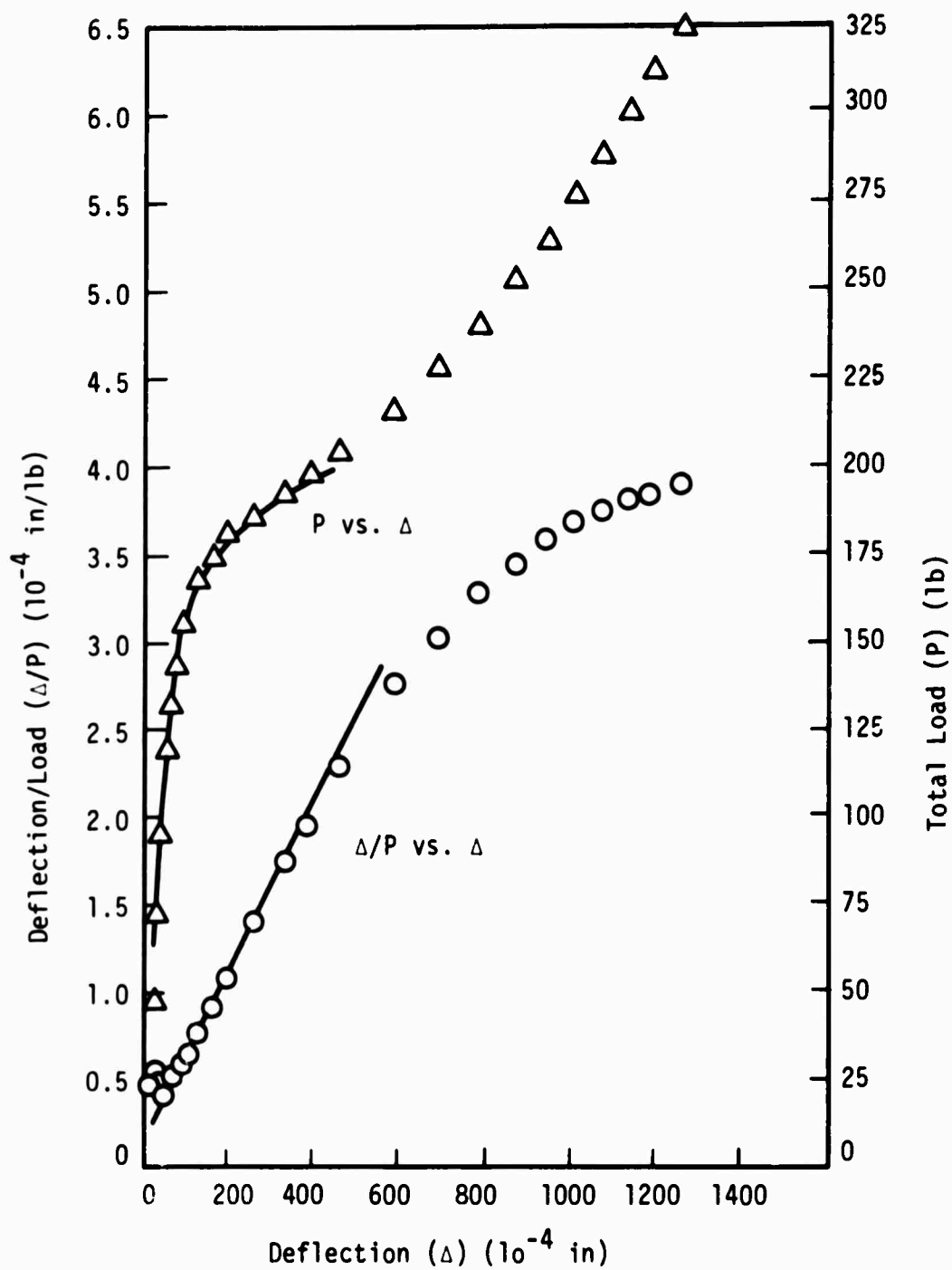


Figure 33. Southwell Plot and Load Deflection Curve
for Plate No. 201, 4 Sides Supported

TABLE 30
DATA AND CALCULATIONS FOR PLATE NO. 202,
2 SIDES SUPPORTED

| Total Load (P) (lb.) | Deflection (Δ) (10^{-4} in.) | Total Load/Deflection (Δ/P) (10^{-4} in./lb.) |
|-------------------------|---|--|
| 0 | 0 | 0 |
| 120 | 34 | .283 |
| 240 | 61 | .256 |
| 330 | 96 | .291 |
| 390 | 127 | .326 |
| 450 | 179 | .398 |
| 510 | 236 | .463 |
| 570 | 310 | .544 |
| 630 | 438 | .695 |
| 690 | 669 | .970 |

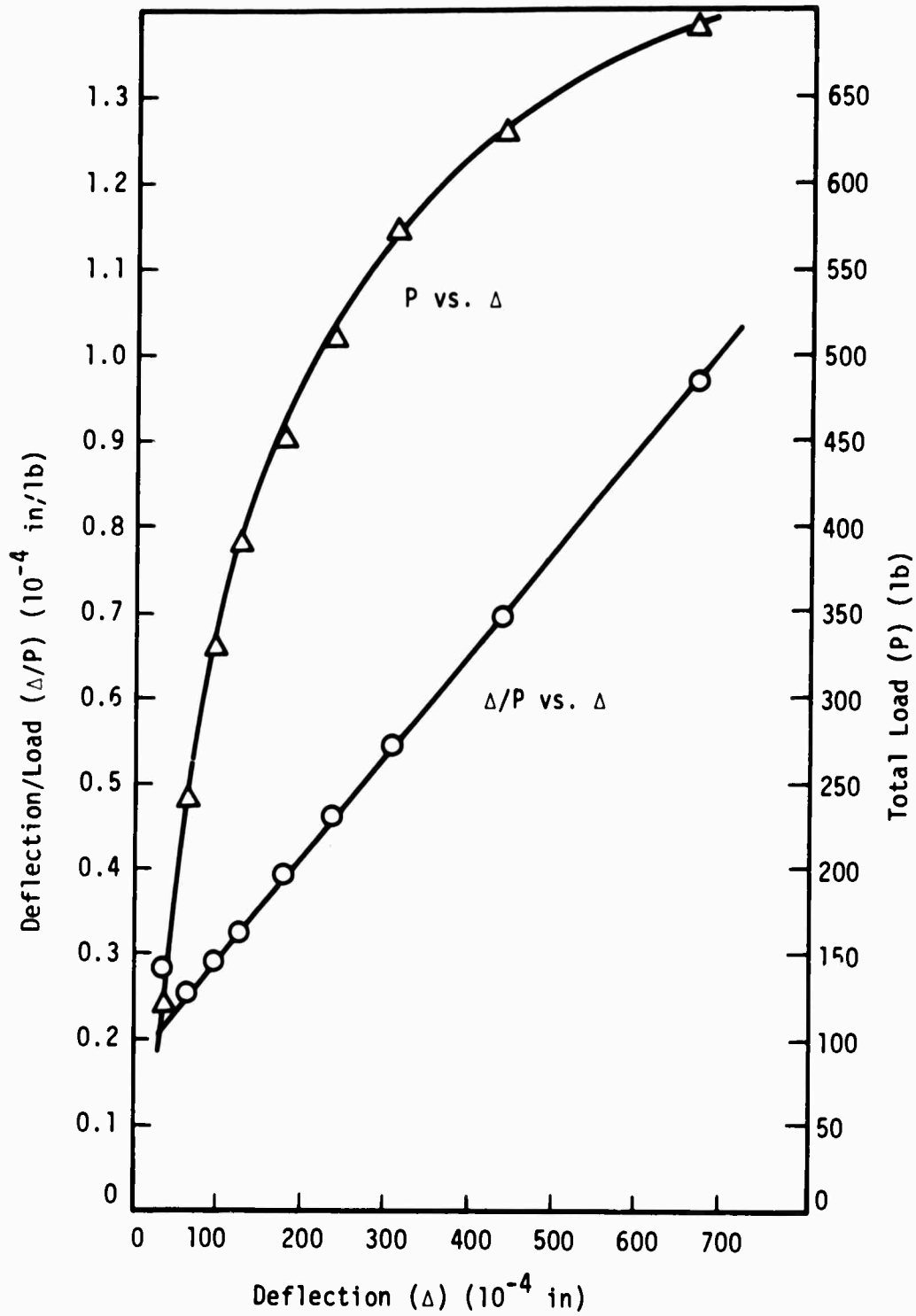


Figure 34. Southwell Plot and Load Deflection Curve
for Plate No. 202, 2 Sides Supported

TABLE 31
DATA AND CALCULATIONS FOR PLATE NO. 202,
4 SIDES SUPPORTED

| Total Load (P) (lb.) | Deflection (Δ) (10^{-4} in.) | Total Load/Deflection (Δ/P) (10^{-4} in./lb.) |
|-------------------------|---|--|
| 0 | 0 | 0 |
| 60 | 1 | .0167 |
| 120 | 7 | .0583 |
| 180 | 4 | .0222 |
| 240 | 8 | .0333 |
| 300 | 15 | .0500 |
| 360 | 22 | .0611 |
| 420 | 34 | .0809 |
| 480 | 41 | .0855 |
| 540 | 49 | .0908 |
| 600 | 59 | .0983 |
| 660 | 71 | .107 |
| 720 | 81 | .112 |
| 780 | 97 | .126 |
| 840 | 109 | .130 |
| 900 | 127 | .141 |
| 960 | 152 | .158 |
| 1020 | 178 | .174 |
| 1080 | 206 | .191 |
| 1140 | 231 | .203 |
| 1200 | 269 | .224 |
| 1260 | 313 | .248 |
| 1320 | 360 | .273 |
| 1380 | 432 | .313 |
| 1440 | 510 | .354 |
| 1500 | 605 | .403 |
| 1560 | 698 | .448 |
| 1620 | 808 | .498 |
| 1680 | 905 | .538 |
| 1740 | 1048 | .603 |

TABLE 32
MODE SHAPE FOR PLATE NO. 202,
4 SIDES SUPPORTED, 10^{-4} in.

| | | |
|-----|-----|-----|
| 247 | 336 | 222 |
| 307 | 438 | 298 |
| 215 | 317 | 243 |

Note: See Figure 9.

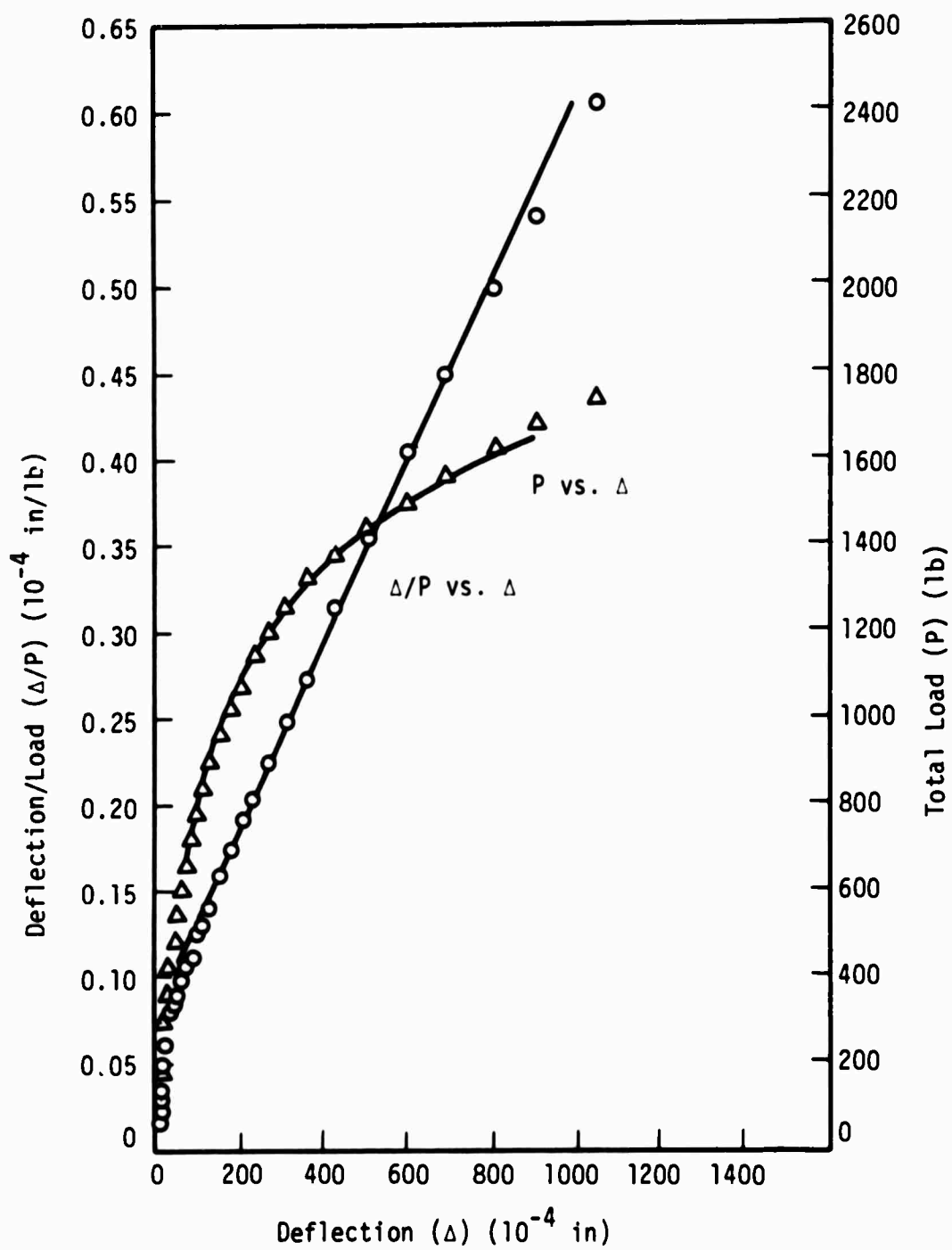


Figure 35. Southwell Plot and Load Deflection Curve
for Plate No. 202, 4 Sides Supported

TABLE 33
DATA AND CALCULATIONS FOR PLATE NO. 203a,
2 SIDES SUPPORTED

| Total Load (P) (lb.) | Deflection (Δ) (10^{-4} in.) | Total Load/Deflection (Δ/P) (10^{-4} in./lb.) |
|-------------------------|---|--|
| 0 | 0 | 0 |
| 50 | 42 | .839 |
| 100 | 61 | .610 |
| 150 | 70 | .467 |
| 200 | 114 | .570 |
| 225 | 134 | .595 |
| 250 | 169 | .676 |
| 270 | 205 | .758 |
| 280 | 235 | .838 |
| 290 | 280 | .965 |
| 300 | 380 | 1.266 |
| 310 | 730 | 2.35 |

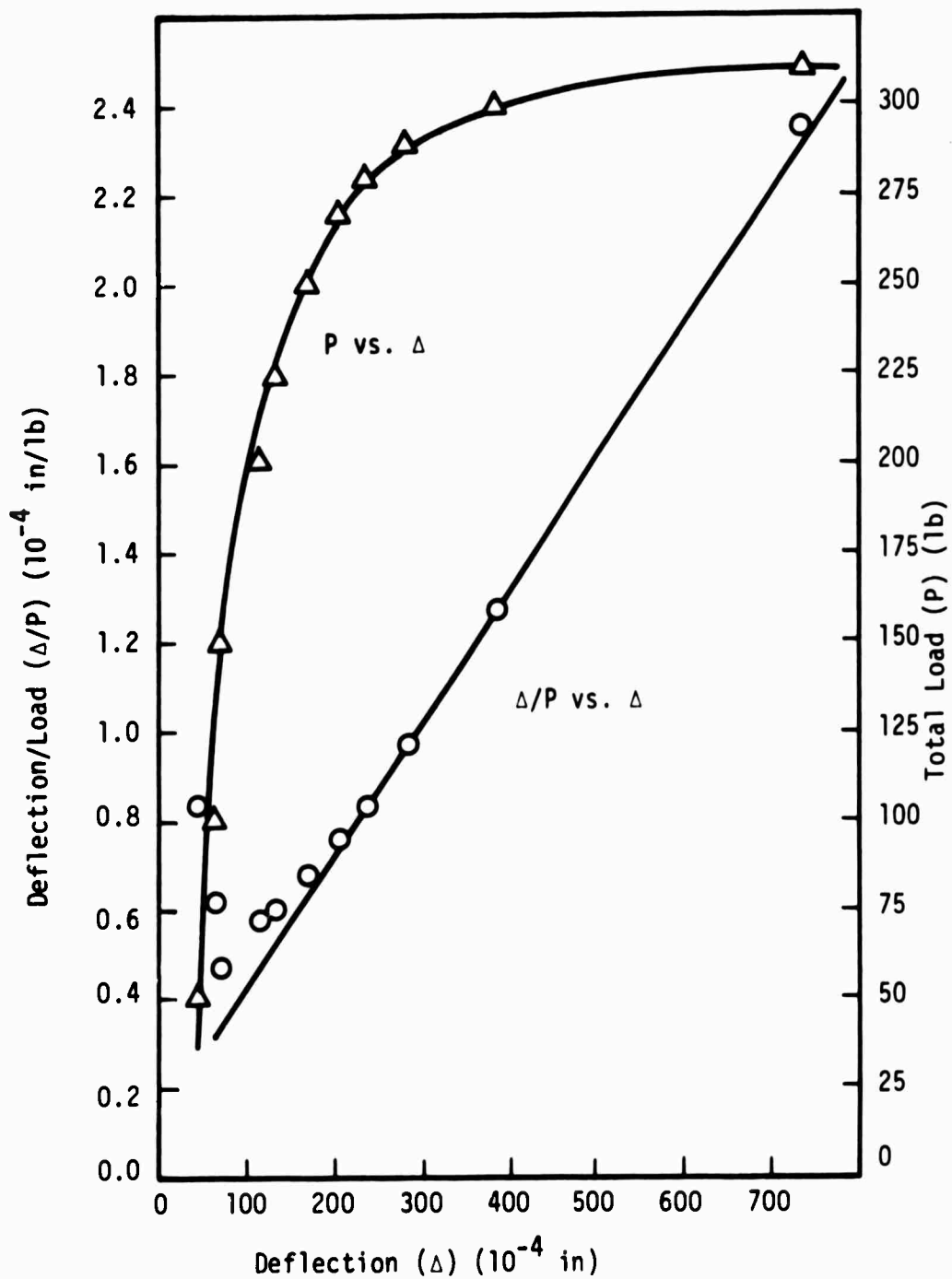


Figure 36. Southwell Plot and Load Deflection Curve
for Plate No. 203a, 2 Sides Supported

TABLE 34
DATA AND CALCULATIONS FOR PLATE NO. 203b,
2 SIDES SUPPORTED

| Total Load (P) (lb.) | Deflection (Δ) (10^{-4} in.) | Total Load/Deflection (Δ/P) (10^{-4} in./lb.) |
|-------------------------|---|--|
| 0 | 0 | 0 |
| 25 | 28 | 1.120 |
| 50 | 63 | 1.260 |
| 75 | 110 | 1.467 |
| 100 | 162 | 1.620 |
| 125 | 230 | 1.840 |
| 150 | 301 | 2.01 |
| 175 | 400 | 2.28 |
| 200 | 550 | 2.75 |
| 225 | 784 | 3.48 |

TABLE 35
MODE SHAPE FOR PLATE NO. 203b,
2 SIDES SUPPORTED, 10^{-4} in.

| | | |
|-----|-----|-----|
| 566 | 610 | 673 |
| 829 | 826 | 901 |
| 602 | 578 | 633 |

Note: See Figure 9.

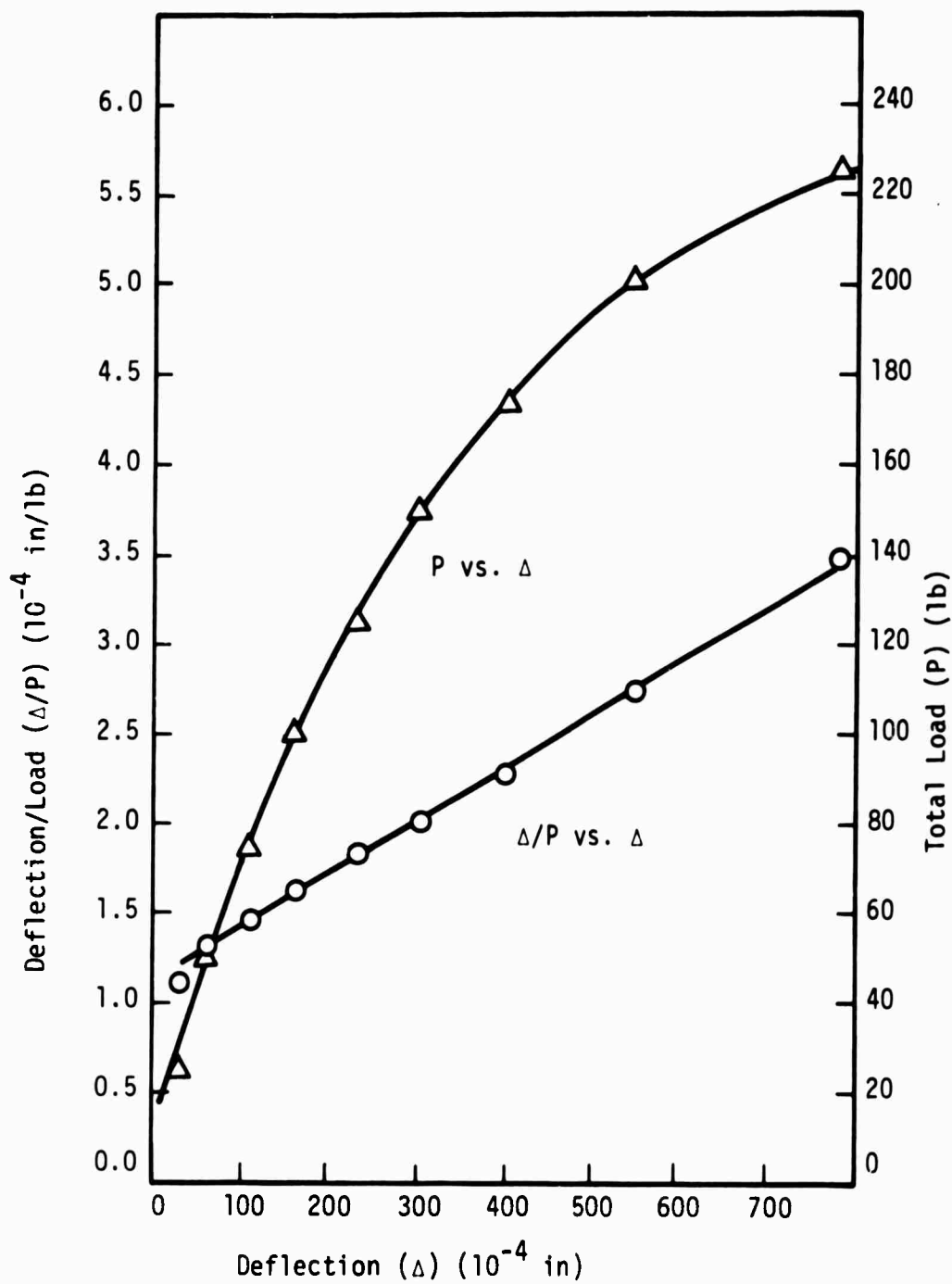


Figure 37. Southwell Plot and Load Deflection Curve
for Plate No. 203b, 2 Sides Supported

TABLE 36
DATA AND CALCULATIONS FOR PLATE NO. 203a,
4 SIDES SUPPORTED

| Total Load (P) (lb.) | Deflection (Δ) (10^{-4} in.) | Total Load/Deflection (Δ/P) (10^{-4} in./lb.) |
|-------------------------|---|--|
| 0 | 0 | 0 |
| 250 | 88 | .352 |
| 500 | 134 | .268 |
| 750 | 181 | .241 |
| 1000 | 232 | .232 |
| 1250 | 303 | .242 |
| 1400 | 363 | .259 |
| 1500 | 409 | .273 |
| 1600 | 469 | .293 |
| 1700 | 533 | .314 |
| 1800 | 612 | .340 |

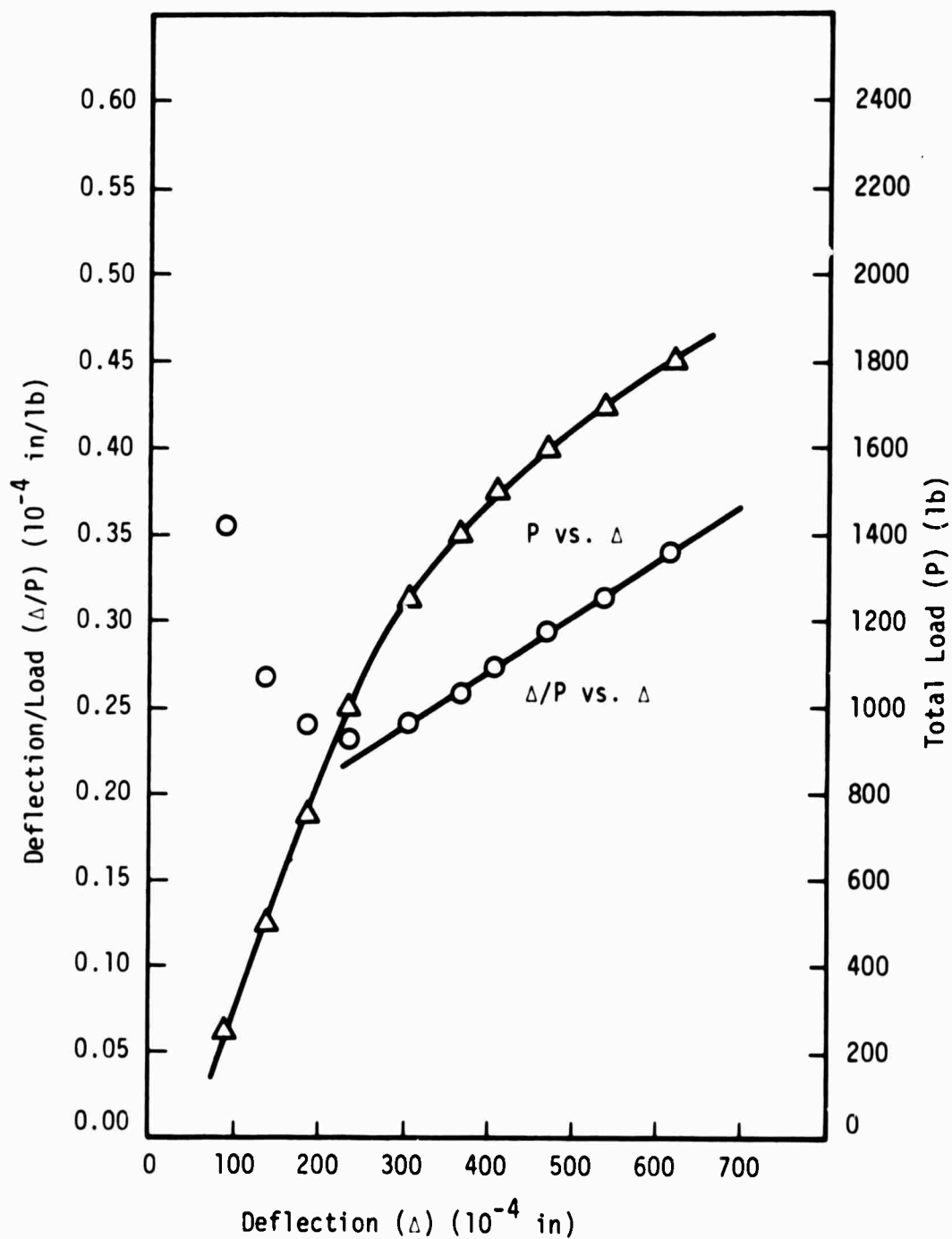


Figure 38. Southwell Plot and Load Deflection Curve
for Plate 203a, 4 Sides Supported

TABLE 37
DATA AND CALCULATIONS FOR PLATE NO. 203b,
4 SIDES SUPPORTED

| Total Load (P) (lb.) | Deflection (Δ) (10^{-4} in.) | Total Load/Deflection (Δ/P) (10^{-4} in./lb.) |
|-------------------------|---|--|
| 0 | 0 | 0 |
| 500 | 39 | .0780 |
| 1000 | 108 | .1080 |
| 1200 | 145 | .1208 |
| 1400 | 192 | .1372 |
| 1600 | 254 | .1587 |
| 1700 | 294 | .1730 |
| 1800 | 342 | .1900 |
| 1900 | 400 | .210 |
| 2000 | 475 | .237 |
| 2100 | 568 | .270 |
| 2200 | 683 | .310 |

TABLE 38
MODE SHAPE FOR PLATE NO. 203b,
4 SIDES SUPPORTED, 10^{-4} in.

| | | |
|-----|-----|-----|
| 221 | 239 | 151 |
| 257 | 349 | 262 |
| 101 | 152 | 147 |

Note: See Figure 9.

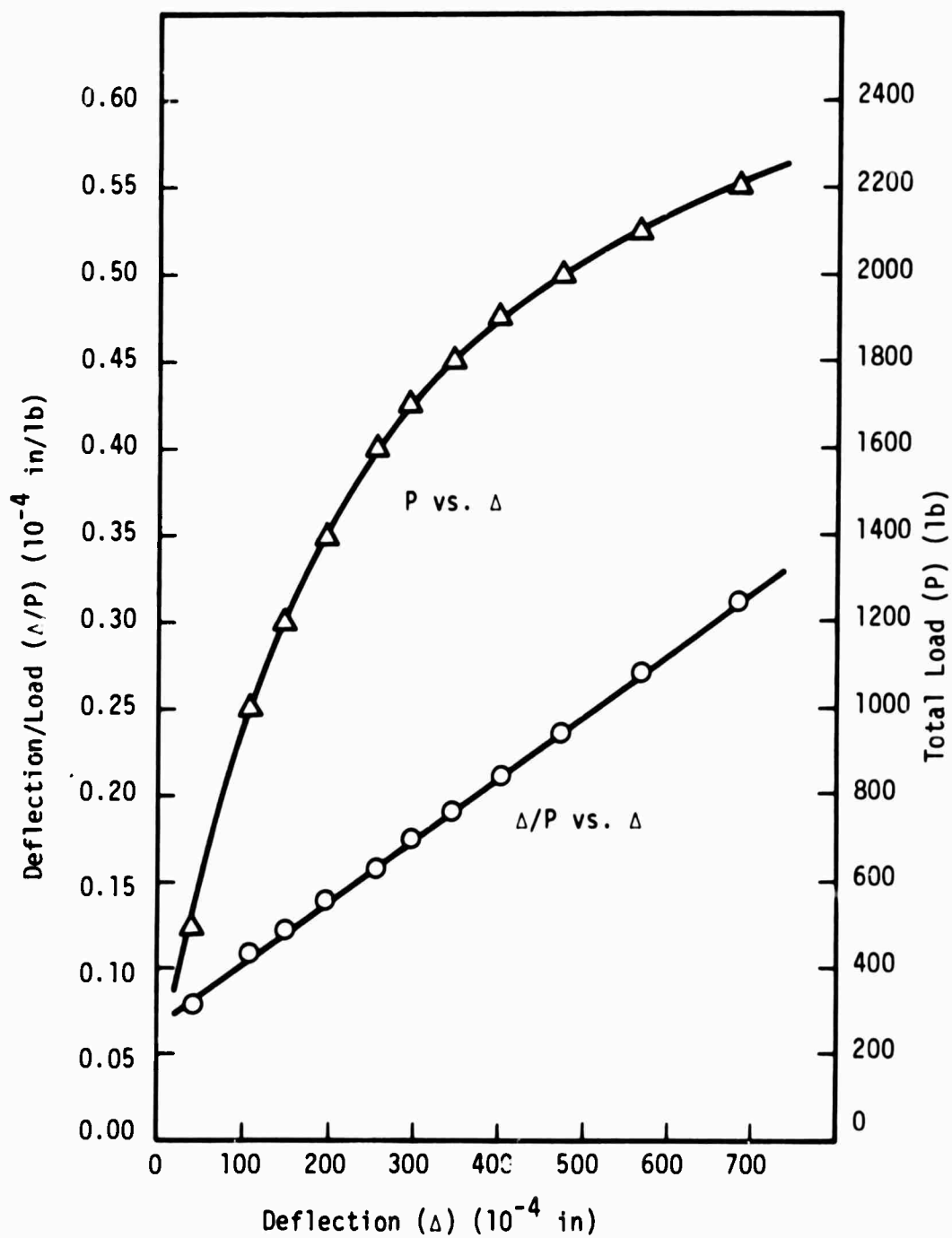


Figure 39. Southwell Plot and Load Deflection Curve
for Plate No. 203b, 4 Sides Supported

TABLE 39
DATA AND CALCULATIONS FOR PLATE NO. 204,
2 SIDES SUPPORTED

| Total Load (P) (lb.) | Deflection (Δ) (10^{-4} in.) | Total Load/Deflection (Δ/P) (10^{-4} in./lb.) |
|-------------------------|---|--|
| 6.4 | 0 | 0.00 |
| 16.4 | 14 | .853 |
| 26.4 | 34 | 1.288 |
| 36.4 | 56 | 1.539 |
| 46.4 | 77 | 1.657 |
| 56.4 | 111 | 1.967 |
| 61.4 | 137 | 2.23 |
| 66.4 | 164 | 2.47 |
| 71.4 | 193 | 2.70 |
| 76.4 | 243 | 3.18 |
| 81.4 | 296 | 2.64 |
| 86.4 | 400 | 4.63 |
| 91.4 | 574 | 6.28 |

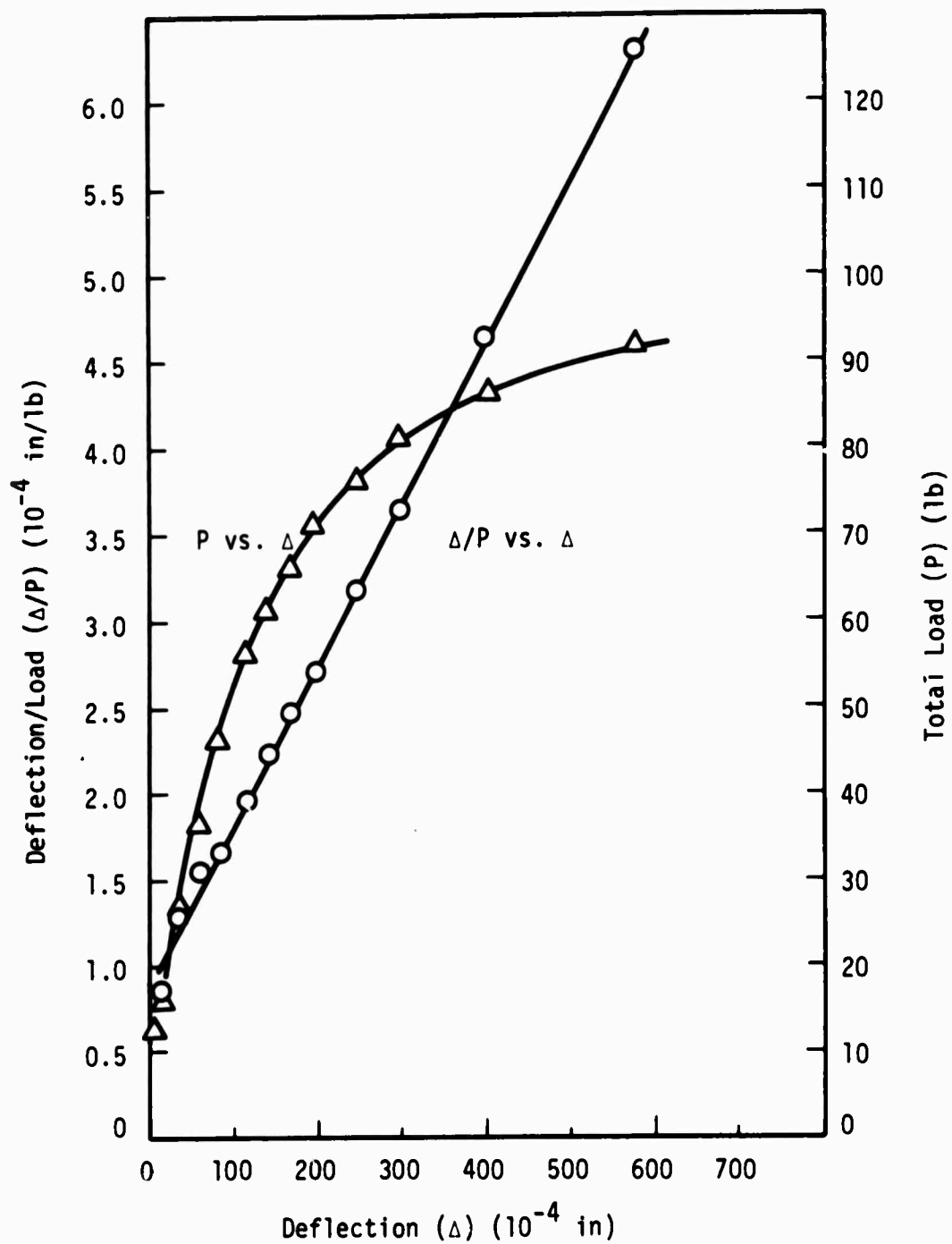


Figure 40. Southwell Plot and Load Deflection Curve
for Plate No. 204, 2 Sides Supported

TABLE 40
DATA AND CALCULATIONS FOR PLATE NO. 204,
4 SIDES SUPPORTED

| Total Load (P) (lb.) | Deflection (Δ) (10^{-4} in.) | Total Load/Deflection (Δ/P) (10^{-4} in./lb.) |
|-------------------------|---|--|
| 6.4 | 0 | 0 |
| 20 | 0 | --- |
| 40 | --- | --- |
| 60 | --- | --- |
| 80 | 9 | .112 |
| 85 | 13 | .153 |
| 90 | 17 | .189 |
| 95 | 18 | .190 |
| 100 | 20 | .200 |
| 105 | 27 | .257 |
| 110 | 34 | .309 |
| 115 | 43 | .374 |
| 120 | 56 | .466 |
| 125 | 69 | .552 |
| 130 | 101 | .778 |
| 133 | 118 | .888 |
| 136 | 142 | 1.045 |
| 139 | 173 | 1.245 |
| 142 | 212 | 1.493 |
| 145 | 248 | 1.710 |
| 150 | 321 | 2.14 |
| 155 | 401 | 2.59 |
| 160 | 449 | 2.81 |
| 170 | 536 | 3.15 |
| 180 | 632 | 3.50 |

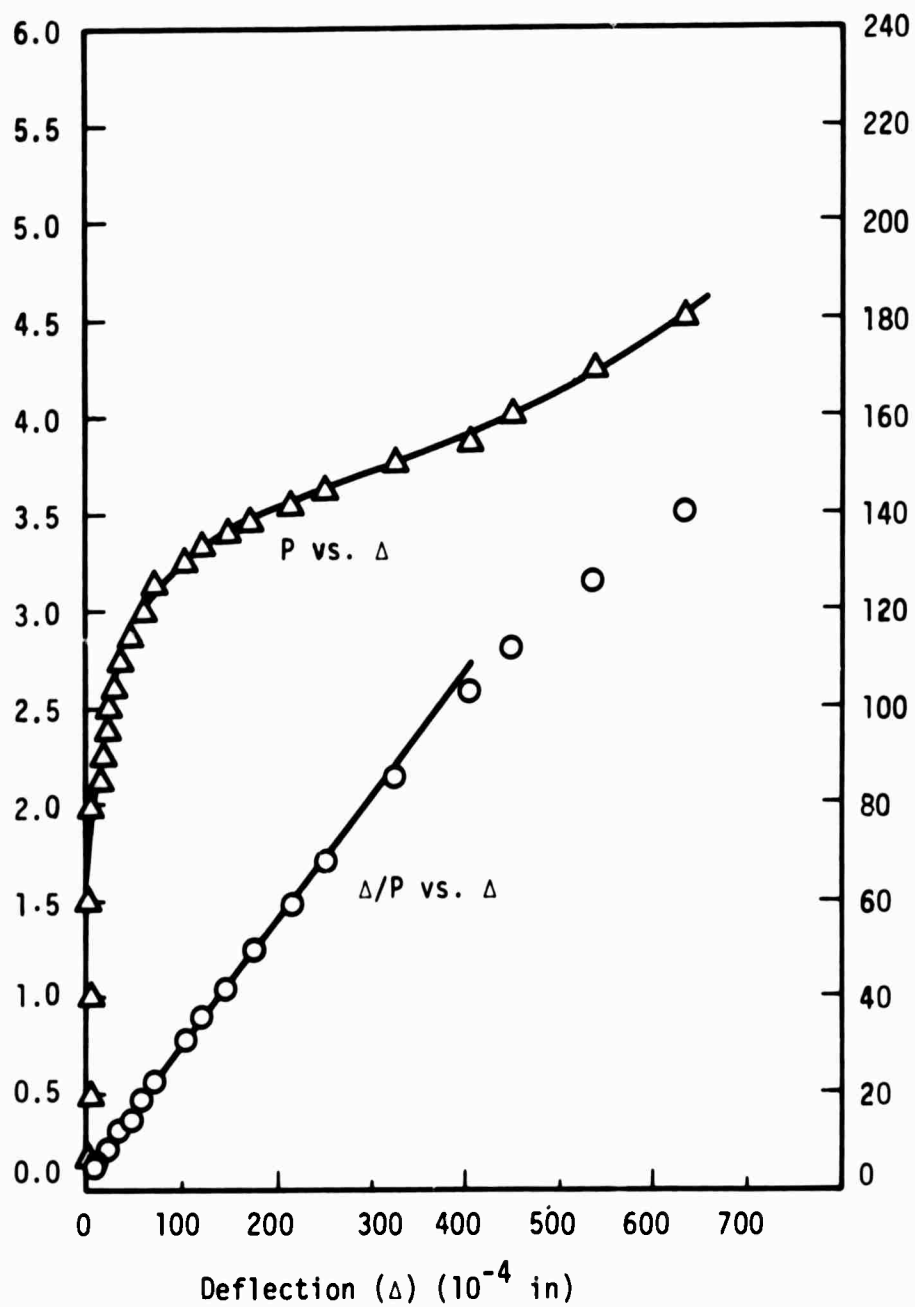


Figure 41. Southwell Plot and Load Deflection Curve
for Plate No. 204, 4 Sides Supported

TABLE 41
DATA AND CALCULATIONS FOR PLATE NO. 205,
2 SIDES SUPPORTED

| Total Load (P) (lb.) | Deflection (Δ) (10^{-4} in.) | Total Load/Deflection (Δ/P) (10^{-4} in./lb.) |
|-------------------------|---|--|
| 6.4 | 0 | 0 |
| 10.4 | 28 | 2.69 |
| 12.4 | 47 | 3.79 |
| 14.4 | 68 | 4.72 |
| 16.4 | 106 | 6.46 |
| 18.4 | 139 | 7.55 |
| 20.4 | 206 | 10.10 |
| 22.4 | 331 | 14.8 |
| 24.4 | 554 | 22.7 |

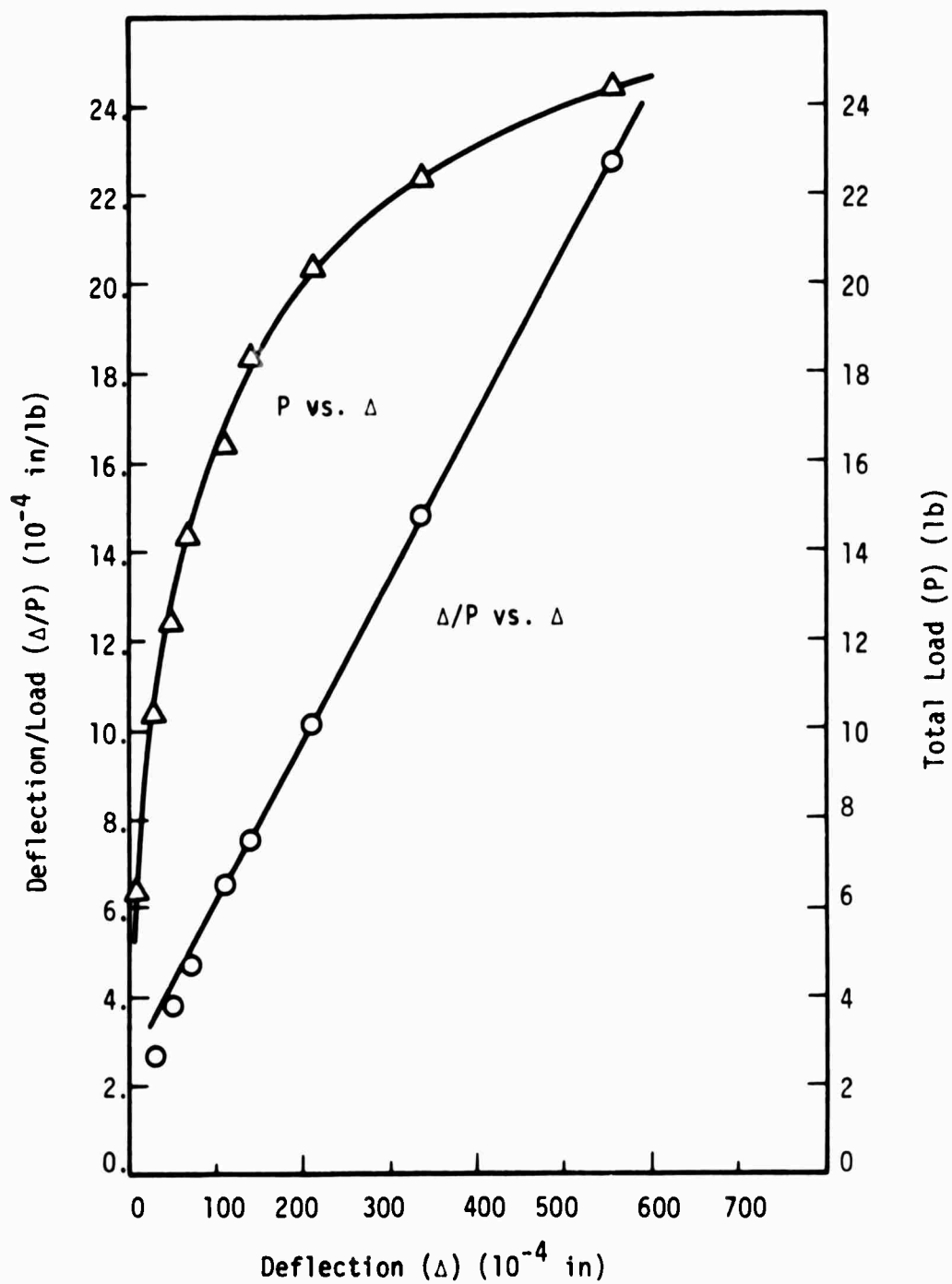


Figure 42. Southwell Plot and Load Deflection Curve for Plate No. 205, 2 Sides Supported

TABLE 42
DATA AND CALCULATIONS FOR PLATE NO. 205,
4 SIDES SUPPORTED

| Total Load (P) (lb.) | Deflection (Δ) (10^{-4} in.) | Total Load/Deflection (Δ/P) (10^{-4} in./lb.) |
|-------------------------|---|--|
| 6.4 | 0 | 0 |
| 10 | --- | --- |
| 20 | --- | --- |
| 30 | 24 | .800 |
| 40 | 39 | .975 |
| 50 | 55 | 1.100 |
| 60 | 72 | 1.200 |
| 70 | 94 | 1.342 |
| 80 | 122 | 1.525 |
| 90 | 155 | 1.722 |
| 100 | 195 | 1.950 |
| 110 | 245 | 2.23 |
| 120 | 286 | 2.39 |
| 130 | 327 | 2.52 |
| 140 | 369 | 2.64 |
| 150 | 423 | 2.82 |
| 160 | 491 | 3.07 |
| 170 | 538 | 3.17 |
| 180 | 580 | 3.22 |

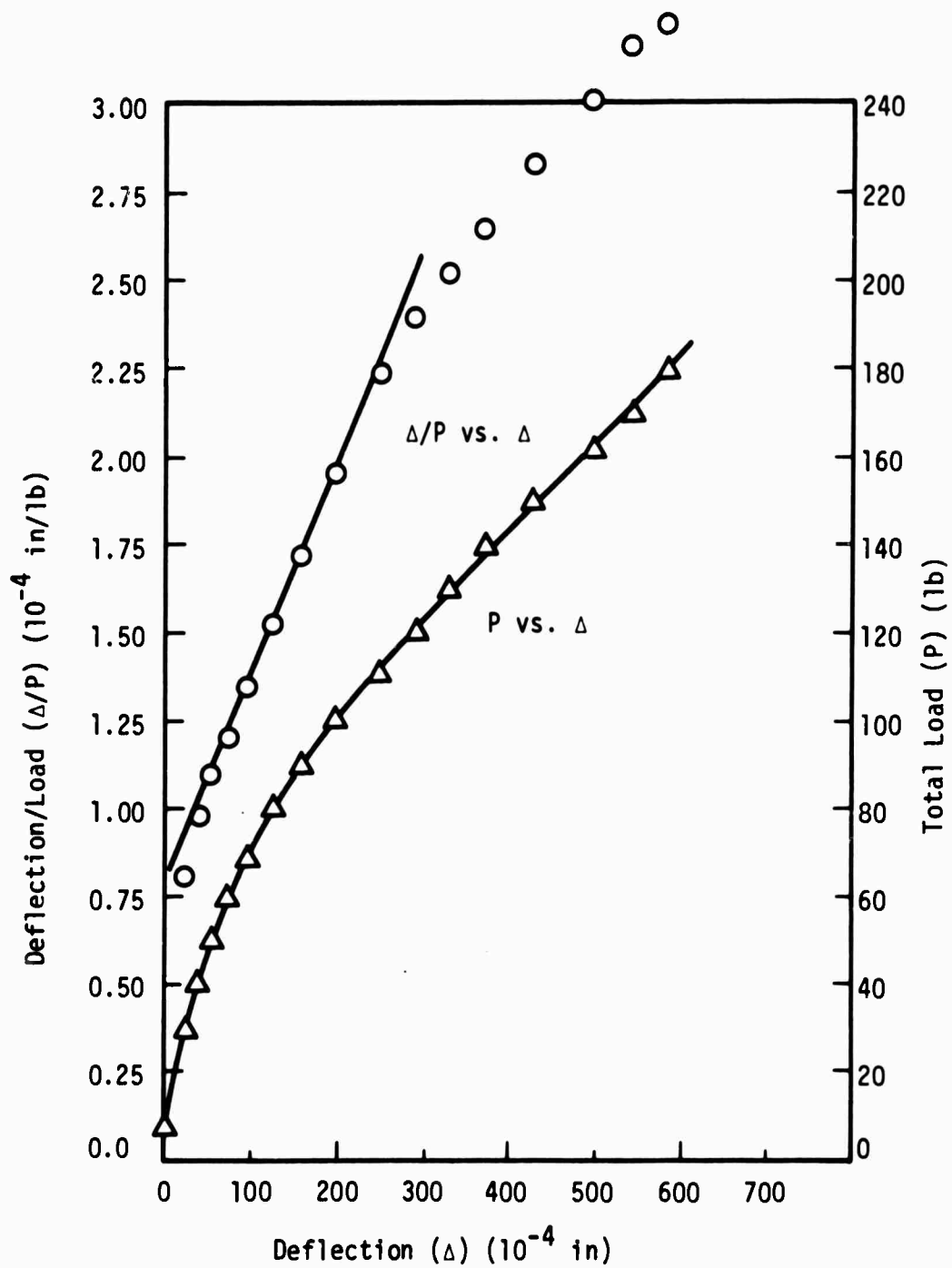


Figure 43. Southwell Plot and Load Deflection Curve
for Plate No. 205, 4 Sides Supported

TABLE 43
DATA AND CALCULATIONS FOR PLATE NO. 206,
2 SIDES SUPPORTED

| Total Load (P) (lb.) | Deflection (Δ) (10^{-4} in.) | Total Load/Deflection (Δ/P) (10^{-4} in./lb.) |
|-------------------------|---|--|
| 6.4 | 0 | 0 |
| 11.4 | 30 | 2.63 |
| 16.4 | 59 | 3.60 |
| 21.4 | 106 | 4.95 |
| 26.4 | 166 | 6.28 |
| 28.4 | 184 | 6.48 |
| 30.4 | 217 | 7.14 |
| 32.4 | 260 | 8.03 |
| 34.4 | 299 | 8.69 |
| 36.4 | 372 | 10.22 |
| 38.4 | 436 | 11.35 |
| 40.4 | 540 | 13.35 |
| 42.4 | 644 | 15.17 |

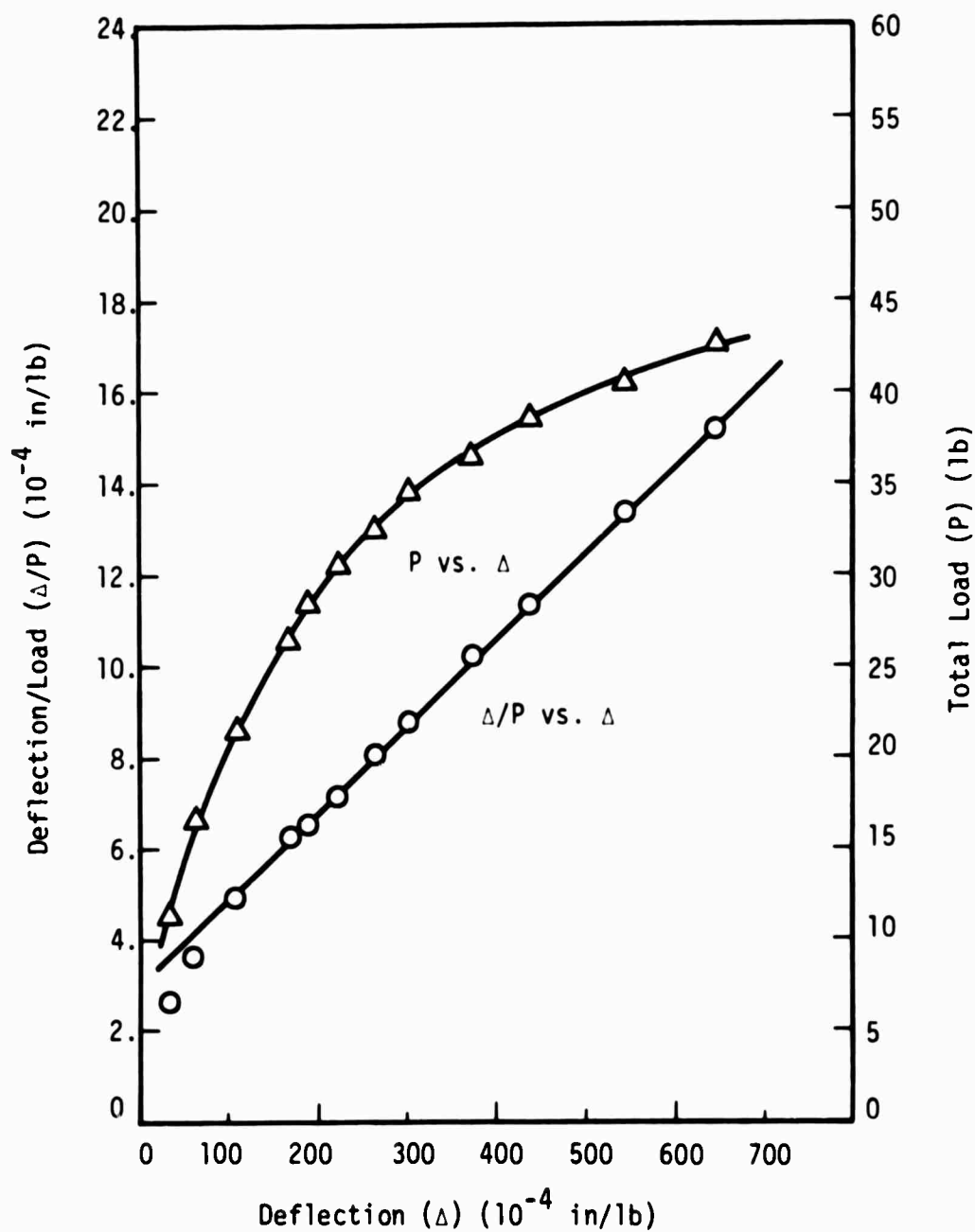


Figure 44. Southwell Plot and Load Deflection Curve
for Plate No. 206, 2 Sides Supported

TABLE 44
DATA AND CALCULATIONS FOR PLATE NO. 206,
4 SIDES SUPPORTED

| Total Load (P) (lb.) | Deflection (Δ) (10^{-4} in.) | Total Load/Deflection (Δ/P) (10^{-4} in./lb.) |
|-------------------------|---|--|
| 6.4 | 0 | 0 |
| 10 | 3 | .300 |
| 15 | 9 | .600 |
| 20 | 15 | .750 |
| 25 | 25 | 1.000 |
| 30 | 41 | 1.365 |
| 35 | 63 | 1.800 |
| 40 | 91 | 2.27 |
| 45 | 126 | 2.80 |
| 50 | 171 | 3.42 |
| 52 | 198 | 3.81 |
| 54 | 223 | 4.13 |
| 56 | 257 | 4.59 |
| 58 | 284 | 4.90 |
| 60 | 313 | 5.22 |
| 62 | 348 | 5.62 |
| 64 | 374 | 5.84 |
| 66 | 399 | 6.05 |
| 68 | 441 | 6.48 |
| 70 | 458 | 6.55 |
| 74 | 507 | 6.85 |
| 78 | 549 | 7.04 |
| 84 | 625 | 7.44 |
| 90 | 690 | 7.68 |
| 95 | 751 | 7.92 |
| 100 | 798 | 7.98 |
| 105 | 835 | 7.94 |
| 110 | 883 | 8.03 |
| 115 | 929 | 8.08 |
| 120 | 975 | 8.12 |
| 125 | 1019 | 8.15 |
| 130 | 1056 | 8.14 |

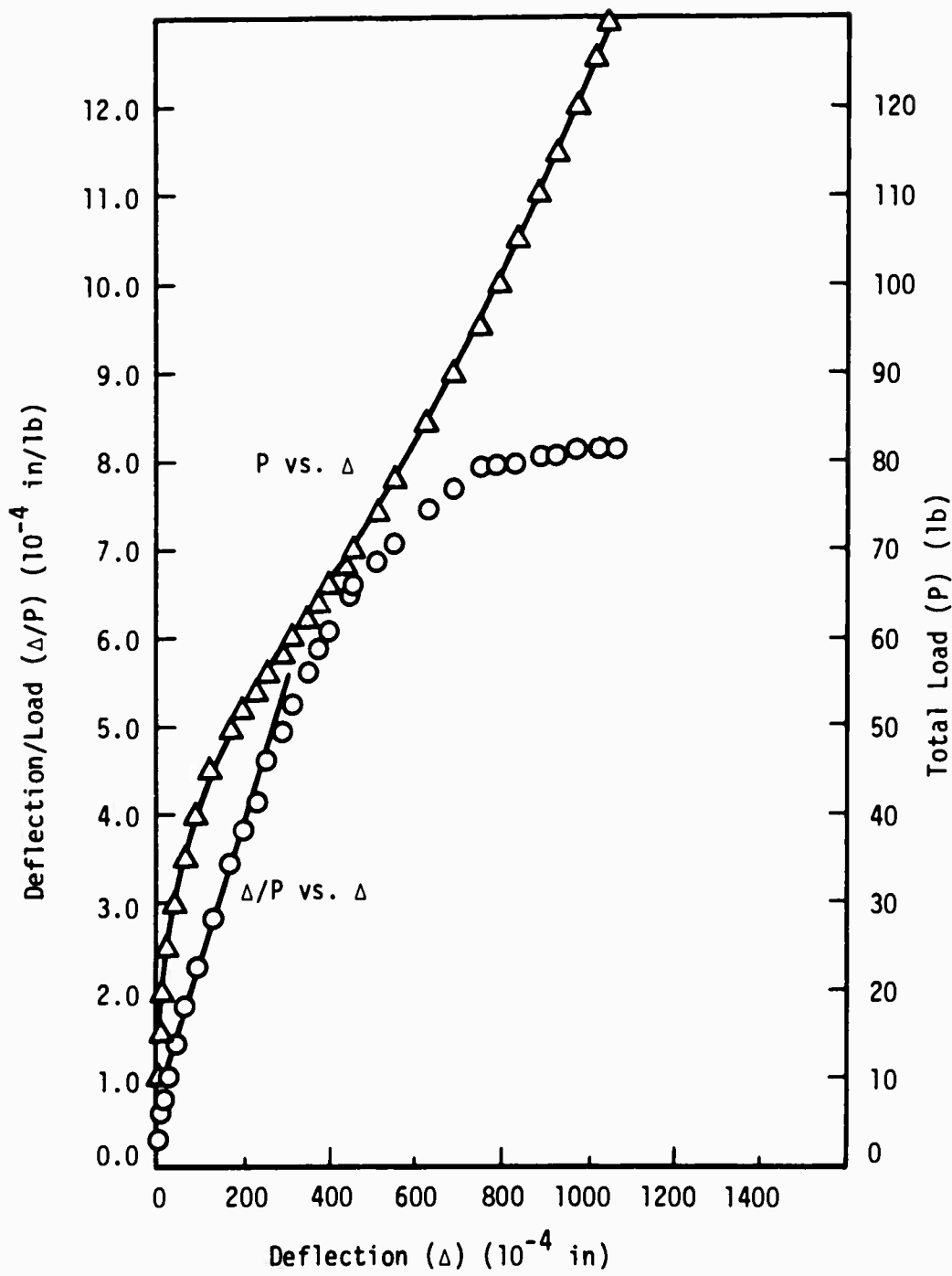


Figure 45. Southwell Plot and Load Deflection Curve
for Plate No. 206, 4 Sides Supported

TABLE 45
DATA AND CALCULATIONS FOR PLATE NO. 207,
2 SIDES SUPPORTED

| Total Load (P) (lb.) | Deflection (Δ) (10^{-4} in.) | Total Load/Deflection (Δ/P) (10^{-4} in./lb.) |
|-------------------------|---|--|
| 6.4 | 0 | 0 |
| 6.6 | 13 | 1.97 |
| 7.0 | 33 | 4.72 |
| 7.2 | 43 | 5.97 |
| 7.4 | 64 | 8.64 |
| 7.6 | 82 | 10.80 |
| 7.8 | 128 | 16.40 |
| 7.9 | 166 | 21.0 |
| 8.0 | 221 | 27.6 |
| 8.1 | 311 | 38.4 |
| 8.2 | 419 | 51.1 |
| 8.3 | 538 | 64.8 |
| 8.4 | 705 | 83.9 |

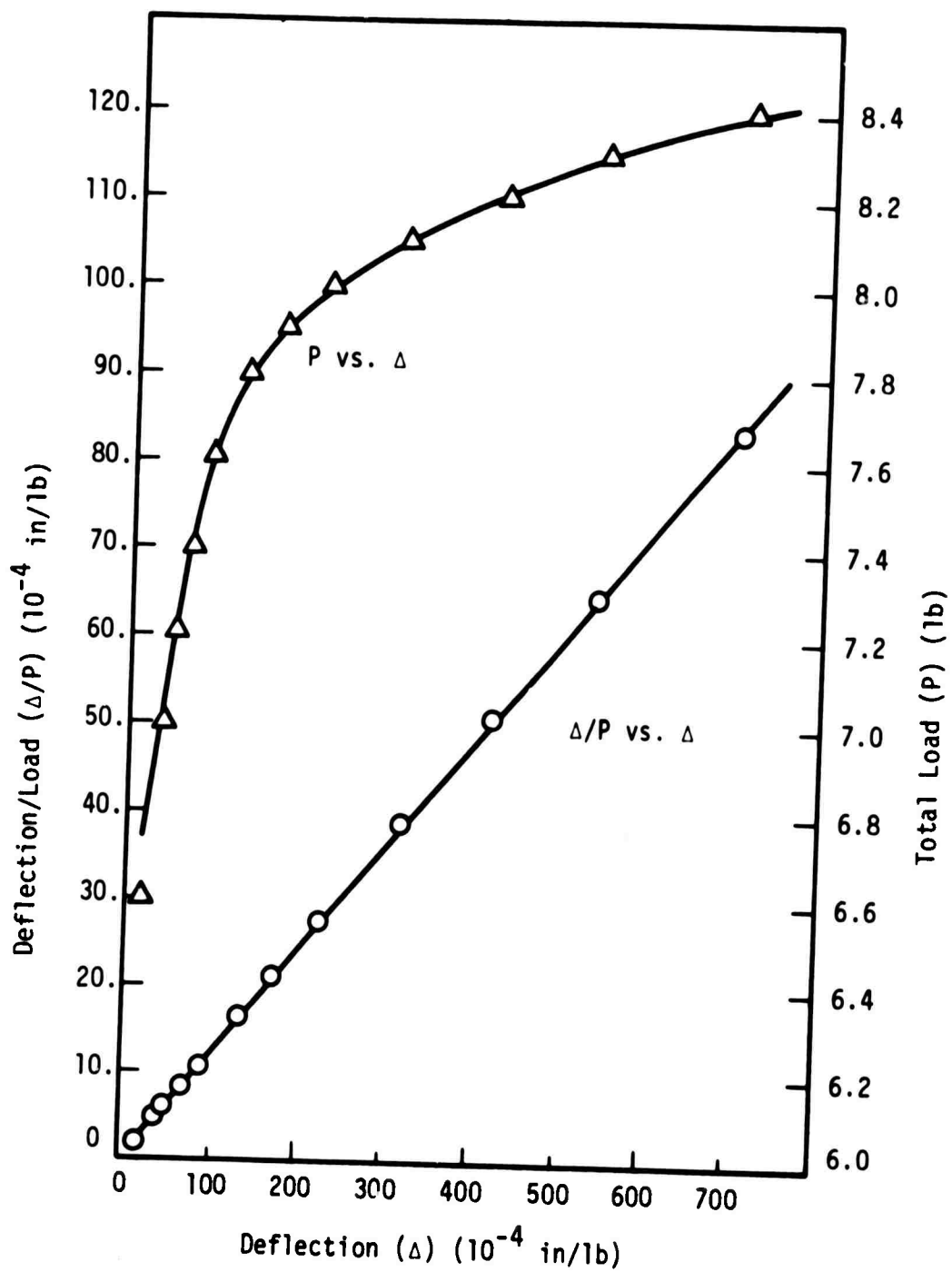


Figure 46. Southwell Plot and Load Deflection Curve
for Plate No. 207, 2 Sides Supported

TABLE 46
DATA AND CALCULATIONS FOR PLATE NO. 207,
4 SIDES SUPPORTED

| Total Load (P) (lb.) | Deflection (Δ) (10^{-4} in.) | Total Load/Deflection (Δ/P) (10^{-4} in./lb.) |
|-------------------------|---|--|
| 6.4 | 0 | 0 |
| 10 | 2 | .200 |
| 15 | 5 | .333 |
| 20 | 22 | 1.10 |
| 25 | 38 | 1.52 |
| 30 | 64 | 2.13 |
| 35 | 85 | 2.43 |
| 40 | 127 | 3.17 |
| 42 | 137 | 3.26 |
| 44 | 144 | 3.27 |
| 46 | 174 | 3.78 |
| 48 | 185 | 3.85 |
| 50 | 200 | 4.01 |
| 52 | 217 | 4.17 |
| 56 | 242 | 4.32 |
| 60 | 277 | 4.62 |
| 65 | 312 | 4.80 |
| 70 | 353 | 5.04 |
| 80 | 427 | 5.33 |
| 90 | 504 | 5.60 |
| 100 | 583 | 5.83 |
| 110 | 657 | 5.97 |
| 120 | 732 | 6.10 |
| 130 | 803 | 6.18 |

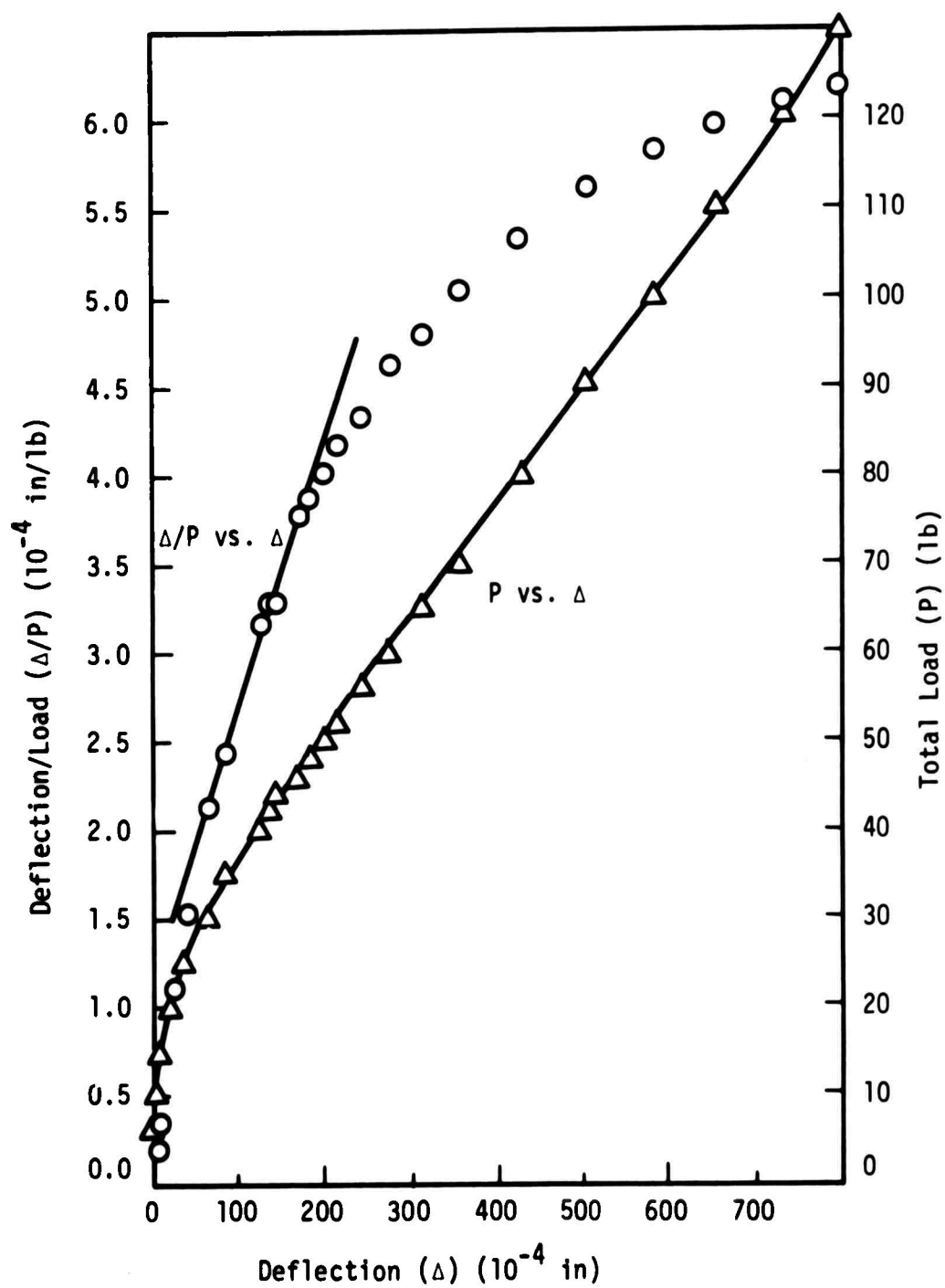


Figure 47. Southwell Plot and Load Deflection Curve
for Plate No. 207, 4 Sides Supported

TABLE 47
DATA AND CALCULATIONS FOR PLATE NO. 208,
2 SIDES SUPPORTED

| Total Load (P) (lb.) | Deflection (Δ) (10^{-4} in.) | Total Load/Deflection (Δ/P) (10^{-4} in./lb.) |
|-------------------------|---|--|
| 6.4 | 0 | 0 |
| 20 | 33 | 1.65 |
| 30 | 81 | 2.70 |
| 35 | 102 | 2.91 |
| 40 | 133 | 3.33 |
| 45 | 167 | 3.71 |
| 50 | 216 | 4.32 |
| 55 | 278 | 5.05 |
| 60 | 389 | 6.48 |
| 65 | 619 | 9.52 |

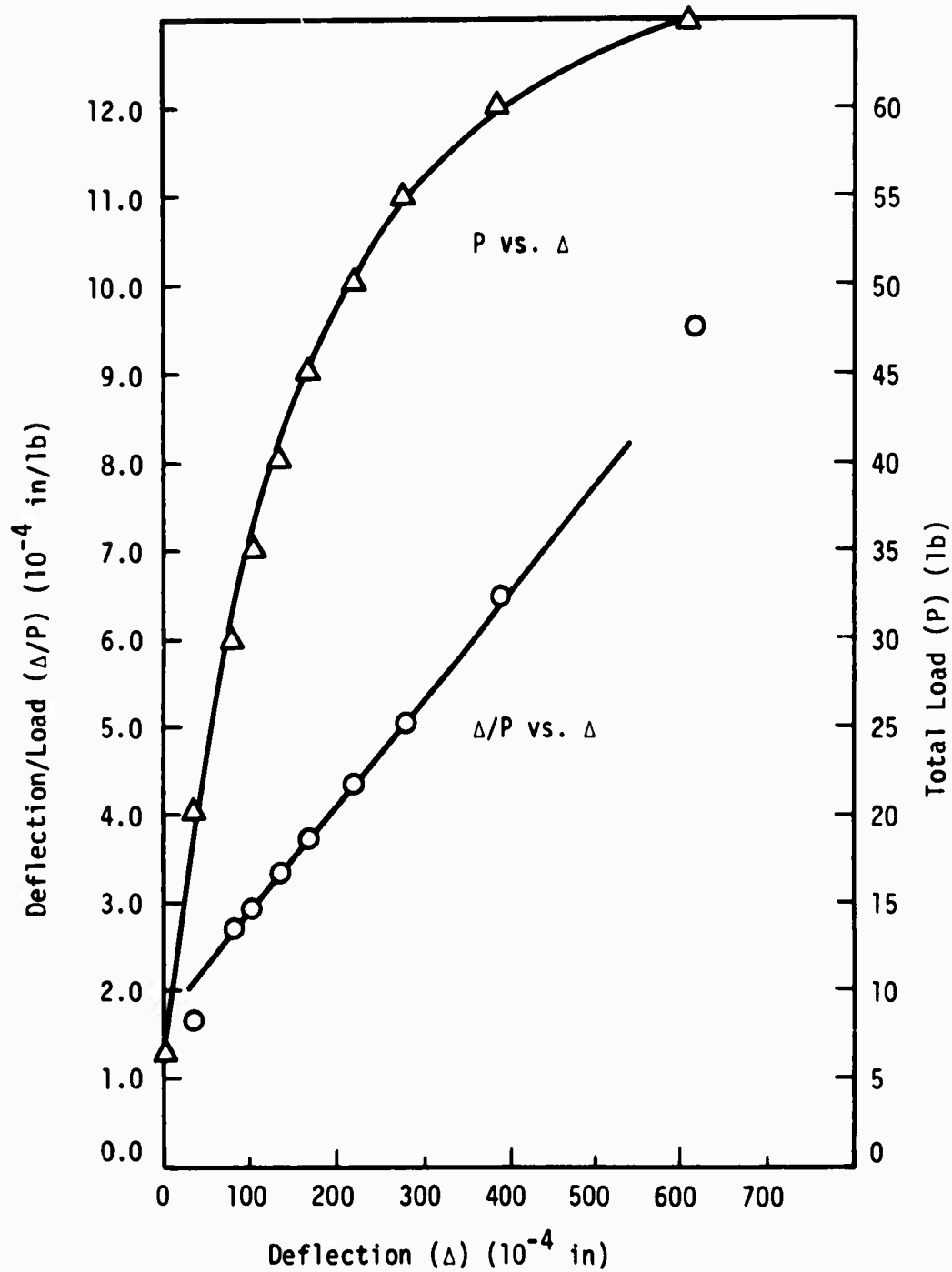


Figure 48. Southwell Plot and Load Deflection Curve
for Plate No. 208, 2 Sides Supported

TABLE 48
DATA AND CALCULATIONS FOR PLATE NO. 208,
4 SIDES SUPPORTED

| Total Load (P) (lb.) | Deflection (Δ) (10^{-4} in.) | Total Load/Deflection (Δ/P) (10^{-4} in./lb.) |
|-------------------------|---|--|
| 6.4 | 0 | 0 |
| 20 | 15 | .750 |
| 30 | 28 | .933 |
| 40 | 45 | 1.125 |
| 50 | 72 | 1.438 |
| 60 | 110 | 1.835 |
| 65 | 131 | 2.02 |
| 70 | 157 | 2.24 |
| 75 | 183 | 2.44 |
| 80 | 214 | 2.62 |
| 85 | 246 | 2.89 |
| 90 | 286 | 3.18 |
| 95 | 315 | 3.32 |
| 100 | 352 | 3.52 |
| 105 | 393 | 3.74 |
| 110 | 438 | 3.99 |
| 120 | 510 | 4.25 |
| 130 | 582 | 4.48 |
| 140 | 657 | 4.69 |
| 150 | 729 | 4.87 |

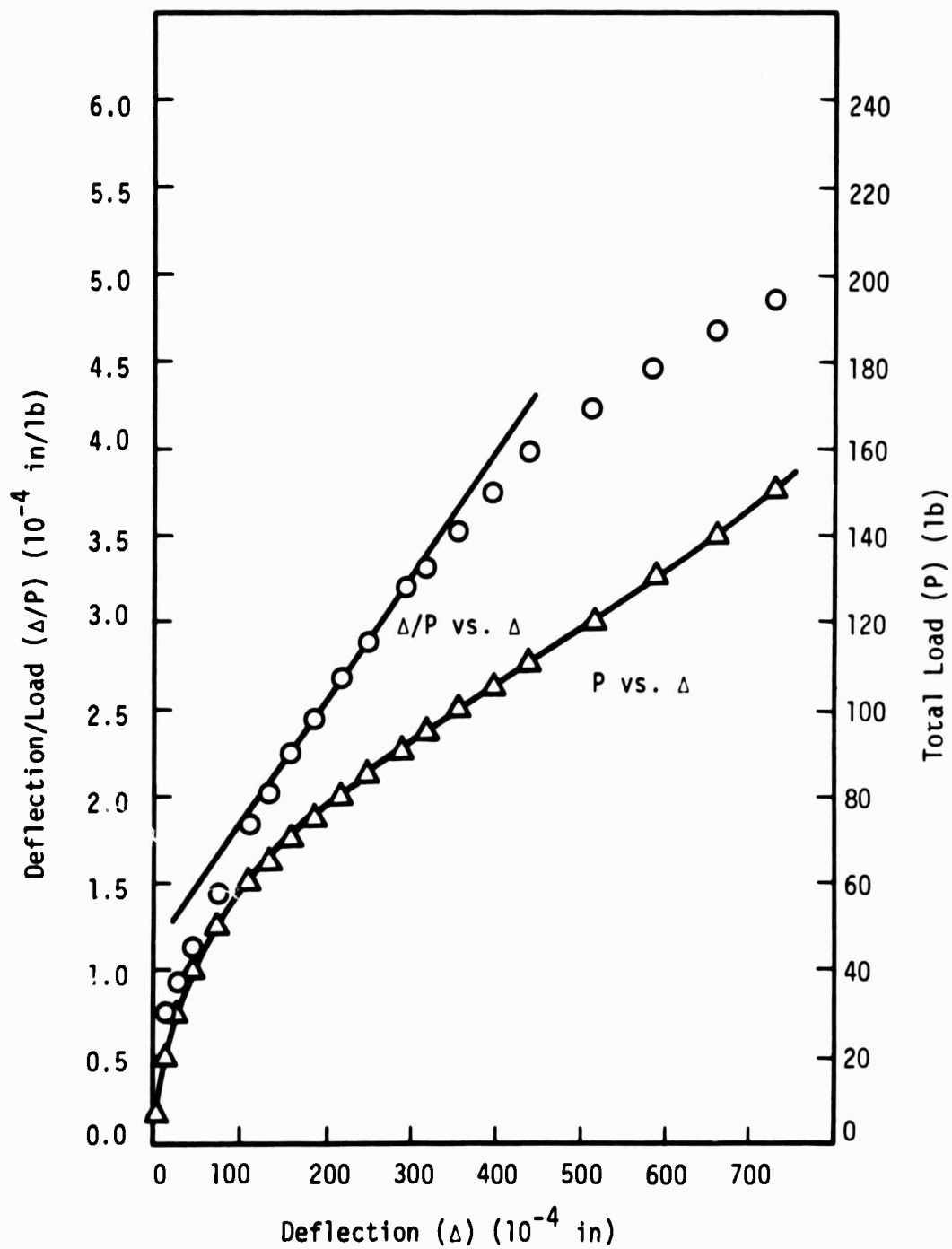


Figure 49. Southwell Plot and Load Deflection Curve
for Plate No. 208, 4 Sides Supported

TABLE 49
DATA AND CALCULATIONS FOR PLATE NO. 209a,
2 SIDES SUPPORTED

| Total Load (P) (lb.) | Deflection (Δ) (10^{-4} in.) | Total Load/Deflection (Δ/P) (10^{-4} in./lb.) |
|-------------------------|---|--|
| 6.4 | 0 | 0 |
| 20 | 16 | .800 |
| 40 | 47 | 1.175 |
| 60 | 91 | 1.516 |
| 70 | 118 | 1.685 |
| 80 | 144 | 1.800 |
| 90 | 180 | 2.00 |
| 100 | 219 | 2.19 |
| 110 | 269 | 2.44 |
| 120 | 338 | 2.82 |
| 130 | 405 | 3.12 |
| 140 | 488 | 3.48 |
| 150 | 638 | 4.25 |
| 160 | 799 | 4.99 |

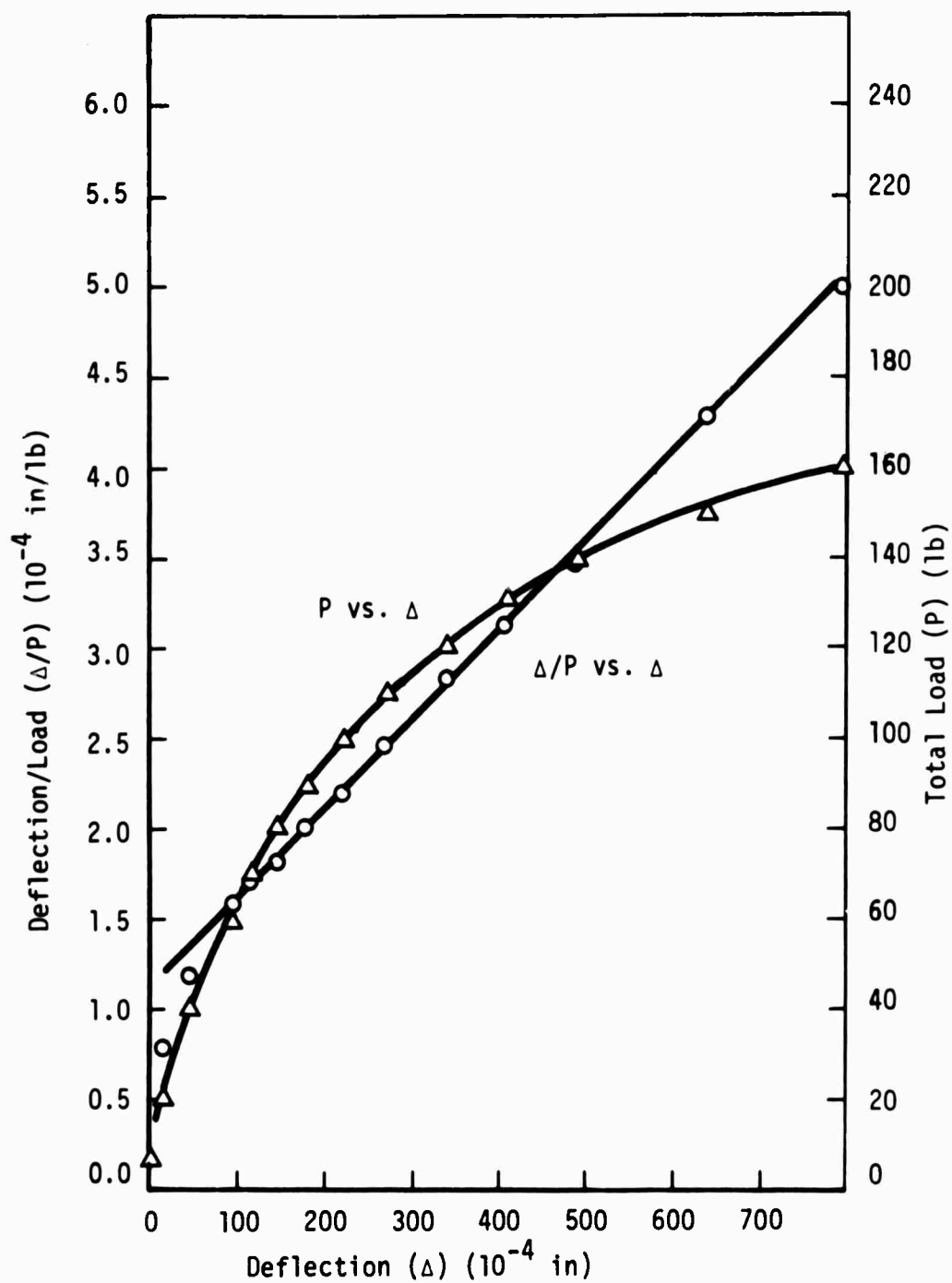


Figure 50. Southwell Plot and Load Deflection Curve
for Plate No. 209a, 2 Sides Supported

TABLE 50
DATA AND CALCULATIONS FOR PLATE NO. 209b,
2 SIDES SUPPORTED

| Total Load (P) (lb.) | Deflection (Δ) (10^{-4} in.) | Total Load/Deflection (Δ/P) (10^{-4} in./lb.) |
|-------------------------|---|--|
| 6.4 | 0 | 0 |
| 20 | 7 | .350 |
| 40 | 27 | .674 |
| 60 | 45 | .749 |
| 70 | 60 | .858 |
| 80 | 72 | .901 |
| 90 | 92 | 1.022 |
| 100 | 113 | 1.130 |
| 110 | 142 | 1.291 |
| 120 | 182 | 1.516 |
| 130 | 232 | 1.785 |
| 140 | 292 | 2.08 |
| 150 | 373 | 2.49 |
| 160 | 487 | 3.04 |
| 170 | 742 | 4.37 |

TABLE 51
MODE SHAPE FOR PLATE NO. 209b,
2 SIDES SUPPORTED, 10^{-4} in.

| | | |
|-----|-----|-----|
| 281 | 280 | 284 |
| 363 | 360 | 378 |
| 279 | 282 | 288 |

Note: See Figure 9.

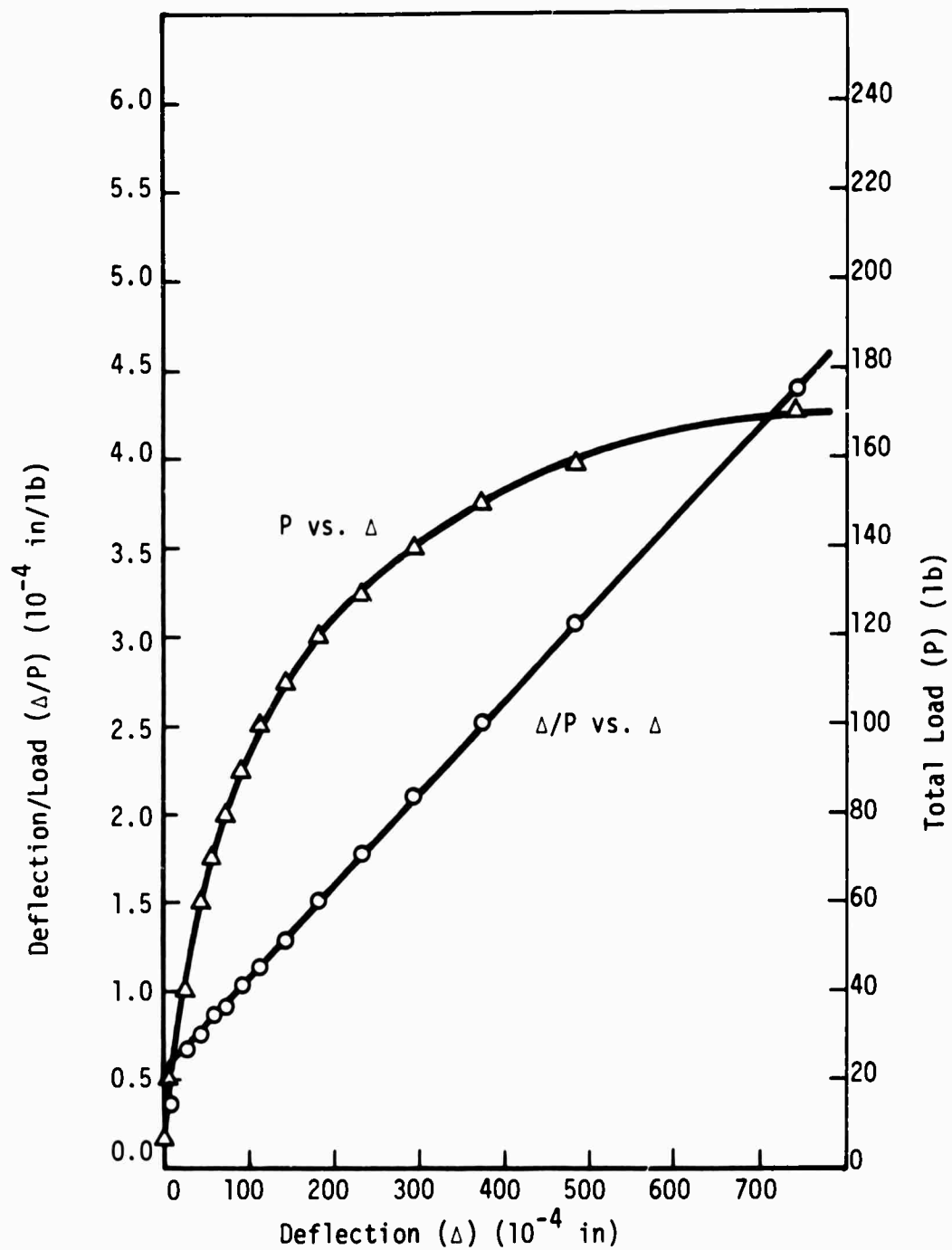


Figure 51. Southwell Plot and Load Deflection Curve
for Plate No. 209b, 2 Sides Supported

TABLE 52
DATA AND CALCULATIONS FOR PLATE NO. 209a,
4 SIDES SUPPORTED, UNPERTURBED

| Total Load (P) (lb.) | Deflection (Δ) (10^{-4} in.) | Total Load/Deflection (Δ/P) (10^{-4} in./lb.) |
|-------------------------|---|--|
| 0 | 0 | 0 |
| 50 | 37 | .738 |
| 100 | 103 | 1.030 |
| 150 | 173 | 1.153 |
| 200 | 247 | 1.235 |
| 225 | 278 | 1.235 |
| 250 | 328 | 1.312 |
| 275 | 375 | 1.364 |
| 300 | 425 | 1.417 |
| 325 | 475 | 1.463 |
| 350 | 529 | 1.513 |
| 375 | 577 | 1.540 |
| 400 | 634 | 1.586 |
| 450 | 741 | 1.647 |
| 500 | 850 | 1.700 |
| 550 | 958 | 1.743 |
| 600 | 1088 | 1.814 |
| 650 | 1219 | 1.876 |
| 700 | 1347 | 1.925 |
| 750 | 1468 | 1.958 |
| 800 | 1579 | 1.975 |

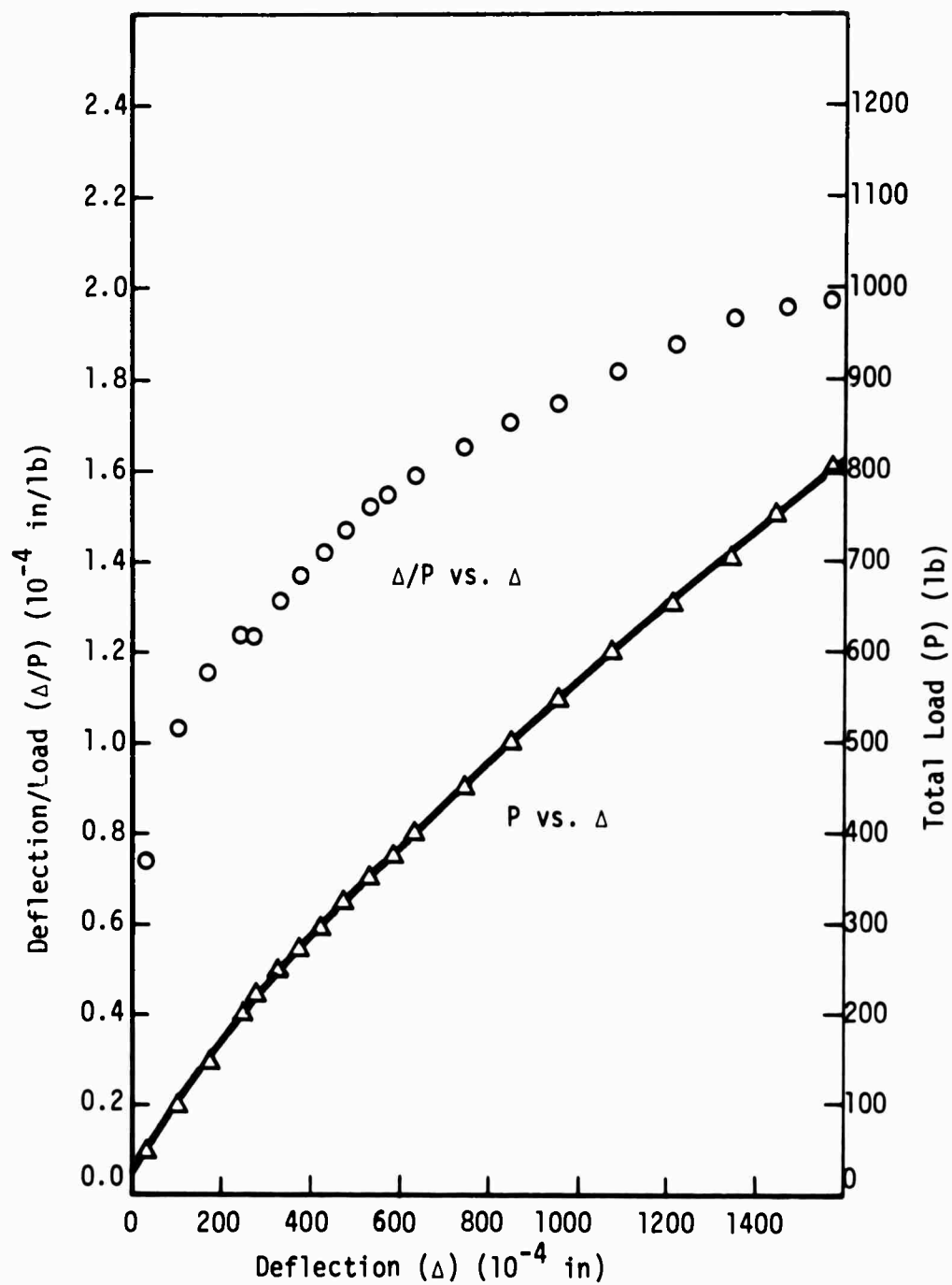


Figure 52. Southwell Plot and Load Deflection Curve
for Plate No. 209a, 4 Sides Supported, Unperturbed

TABLE 53
DATA AND CALCULATIONS FOR PLATE NO. 209a,
4 SIDES SUPPORTED, WITH REVERSE PERTURBATION

| Total Load (P) (lb.) | Deflection (Δ) (10^{-4} in.) | Total Load/Deflection (Δ/P) (10^{-4} in./lb.) |
|-------------------------|---|--|
| 0 | 0 | 0 |
| 50 | 23 | .460 |
| 100 | 42 | .420 |
| 150 | 64 | .427 |
| 200 | 84 | .420 |
| 250 | 111 | .443 |
| 300 | 156 | .519 |
| 350 | 208 | .594 |
| 400 | 272 | .680 |
| 425 | 306 | .719 |
| 450 | 342 | .760 |
| 475 | 394 | .828 |
| 500 | 436 | .872 |
| 550 | 542 | .985 |
| 600 | 662 | 1.104 |
| 650 | 802 | 1.235 |
| 700 | 982 | 1.405 |
| 750 | 1114 | 1.485 |
| 800 | 1212 | 1.515 |
| 850 | 1307 | 1.536 |
| 900 | 1409 | 1.565 |

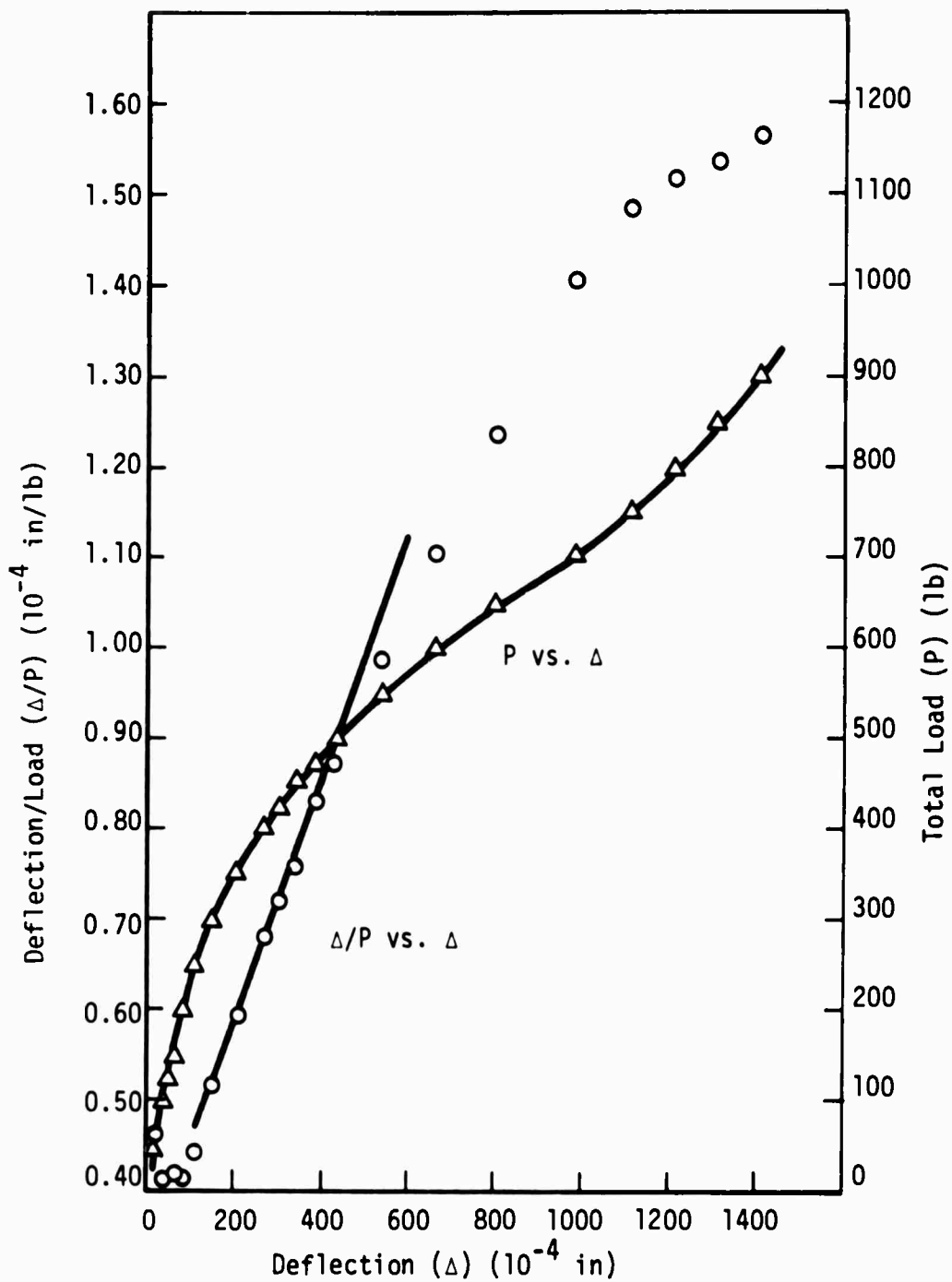


Figure 53. Southwell Plot and Load Deflection Curve for Plate No. 209a, 4 Sides Supported, with Reverse Perturbation Load.

TABLE 54
DATA AND CALCULATIONS FOR PLATE NO. 209b,
4 SIDES SUPPORTED

| Total Load (P) (lb.) | Deflection (Δ) (10^{-4} in.) | Total Load/Deflection (Δ/P) (10^{-4} in./lb.) |
|-------------------------|---|--|
| 0 | 0 | 0 |
| 100 | 19 | .190 |
| 200 | 38 | .190 |
| 300 | 68 | .227 |
| 400 | 106 | .265 |
| 450 | 148 | .329 |
| 500 | 199 | .398 |
| 525 | 231 | .440 |
| 550 | 273 | .496 |
| 575 | 339 | .589 |
| 600 | 448 | .747 |
| 610 | 499 | .819 |
| 620 | 548 | .883 |
| 630 | 604 | .958 |
| 640 | 669 | 1.045 |
| 650 | 728 | 1.120 |

TABLE 55
MODE SHAPE FOR PLATE NO. 209b,
4 SIDES SUPPORTED, 10^{-4} in.

| | | |
|-----|-----|-----|
| 220 | 309 | 216 |
| 285 | 404 | 293 |
| 223 | 330 | 223 |

Note: See Figure 9.

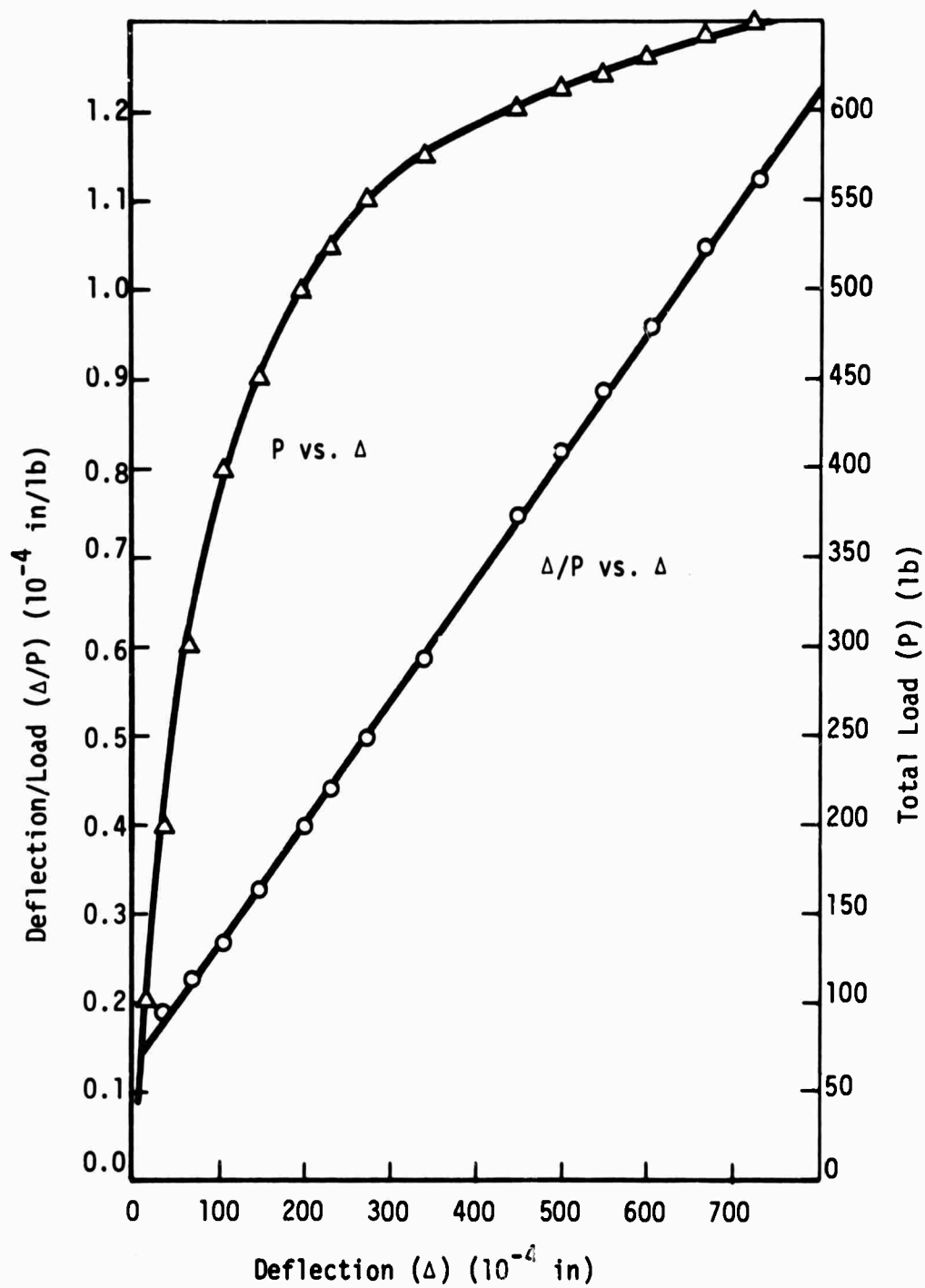


Figure 54. Southwell Plot and Load Deflection Curve for Plate No. 209b, 4 Sides Supported, Unperturbed

TABLE 56
DATA AND CALCULATIONS FOR PLATE NO. 301,
2 SIDES SUPPORTED

| Total Load (P) (lb.) | Deflection (Δ) (10^{-4} in.) | Total Load/Deflection (Δ/P) (10^{-4} in./lb.) |
|-------------------------|---|--|
| 6.4 | 0 | 0.0 |
| 18.4 | 33 | 1.795 |
| 30.4 | 56 | 1.841 |
| 42.4 | 80 | 1.885 |
| 54.4 | 108 | 1.970 |
| 66.4 | 152 | 2.27 |
| 78.4 | 192 | 2.45 |
| 90.4 | 226 | 2.50 |
| 102.4 | 265 | 2.59 |
| 114.4 | 343 | 3.00 |
| 126.4 | 442 | 3.49 |
| 138.4 | 556 | 4.02 |
| 150.4 | 746 | 4.96 |
| 162.4 | 964 | 5.93 |
| 174.4 | 1330 | 7.63 |

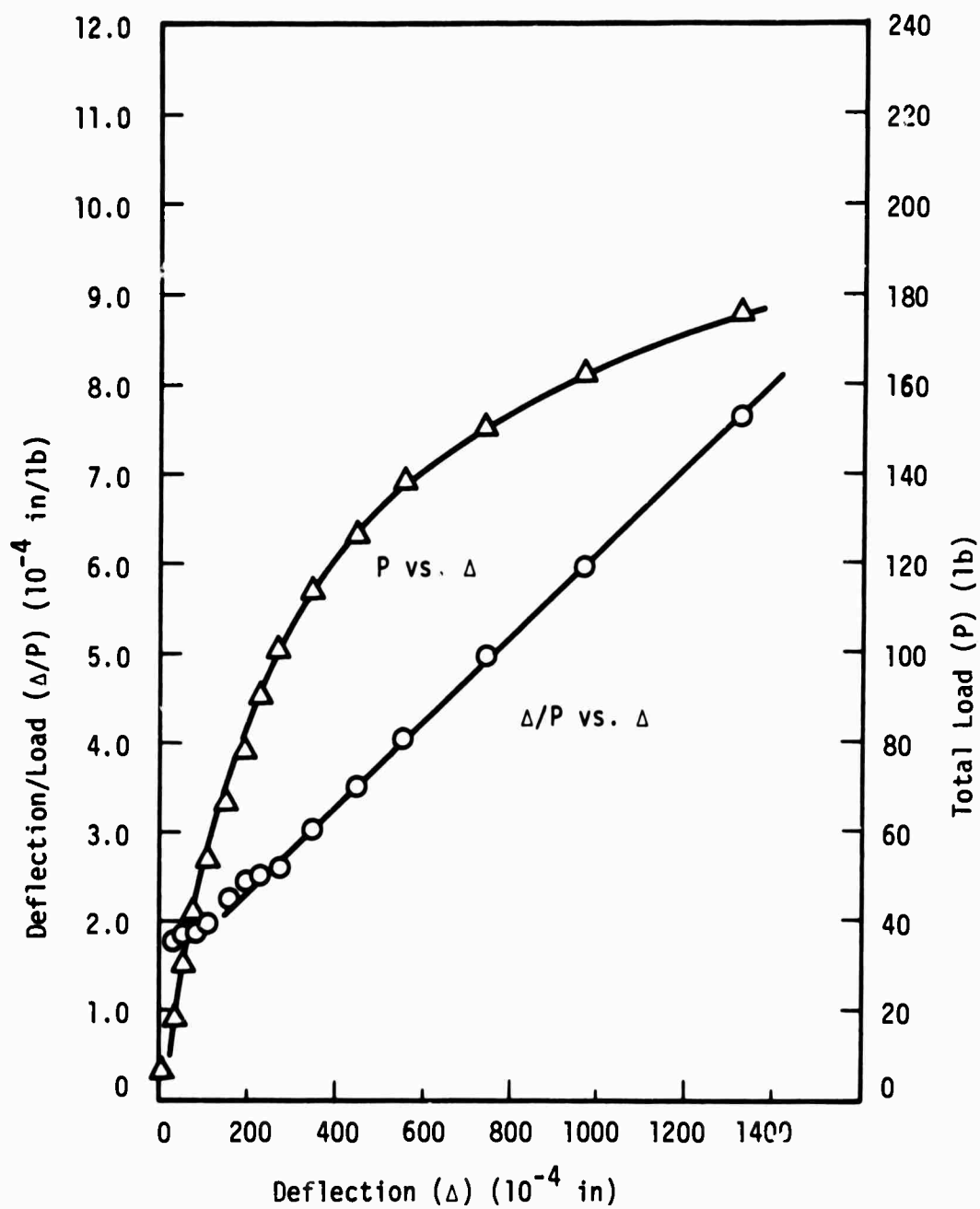


Figure 55. Southwell Plot and Load Deflection Curve
for Plate No. 301, 2 Sides Supported

TABLE 57
DATA AND CALCULATIONS FOR PLATE NO. 301,
4 SIDES SUPPORTED

| Total Load (P) (lb.) | Deflection (Δ) (10^{-4} in.) | Total Load/Deflection (Δ/P) (10^{-4} in./lb.) |
|-------------------------|---|--|
| 0.0 | 0.0 | 0.00 |
| 24.0 | 12.0 | 0.50 |
| 48.0 | 21.0 | 0.44 |
| 72.0 | 28.0 | 0.39 |
| 96.0 | 26.0 | 0.27 |
| 120.0 | 34.0 | 0.28 |
| 144.0 | 44.0 | 0.31 |
| 168.0 | 54.0 | 0.32 |
| 192.0 | 66.0 | 0.34 |
| 216.0 | 81.0 | 0.38 |
| 240.0 | 98.0 | 0.41 |
| 264.0 | 114.0 | 0.43 |
| 288.0 | 137.0 | 0.48 |
| 312.0 | 156.0 | 0.50 |
| 336.0 | 181.0 | 0.54 |
| 360.0 | 208.0 | 0.58 |
| 384.0 | 237.0 | 0.62 |
| 408.0 | 282.0 | 0.69 |
| 432.0 | 336.0 | 0.78 |
| 456.0 | 393.0 | 0.86 |
| 480.0 | 466.0 | 0.97 |
| 504.0 | 570.0 | 1.13 |
| 528.0 | 676.0 | 1.28 |

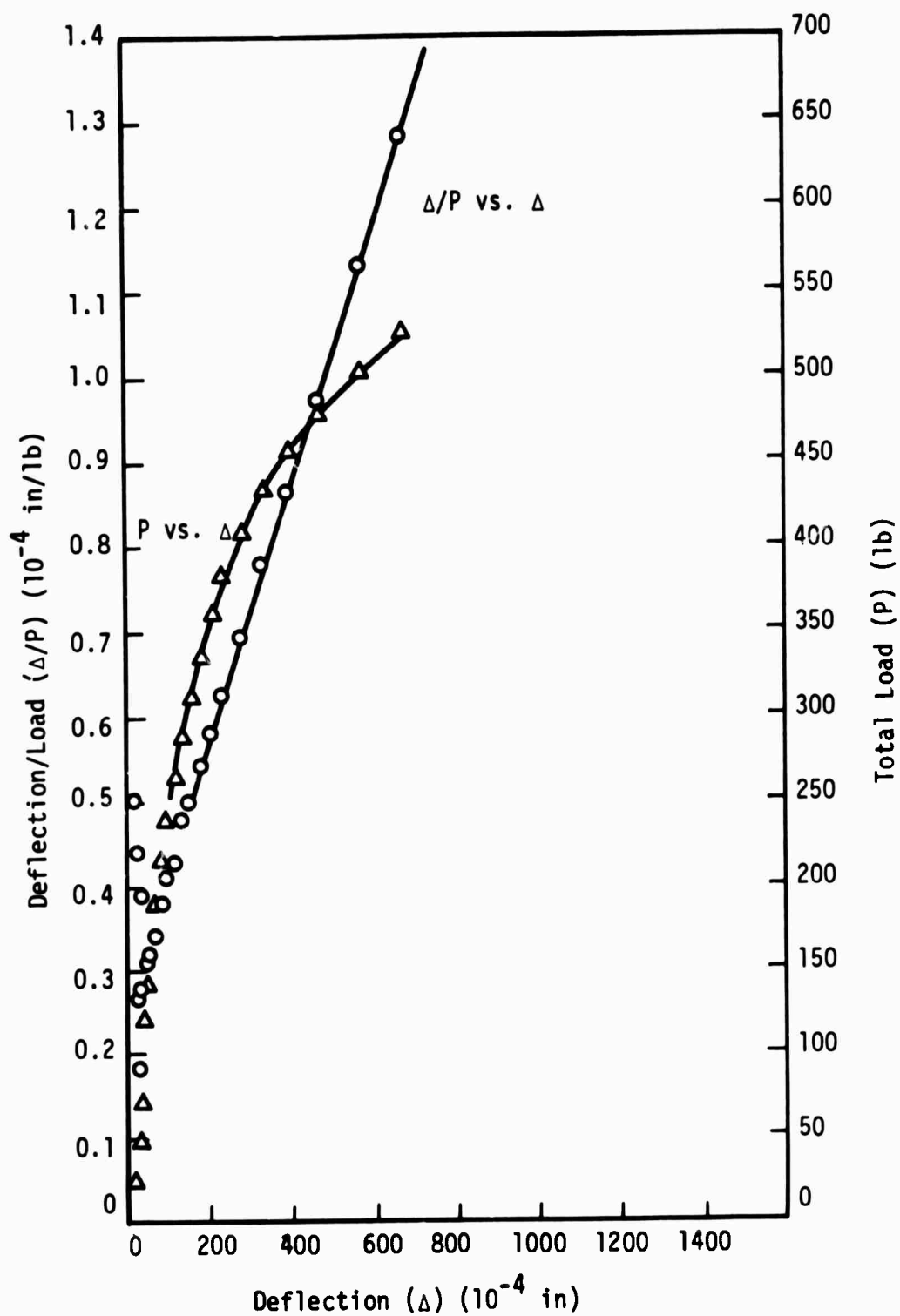


Figure 56. Southwell Plot and Load Deflection Curve for Plate No. 301, 4 Sides Supported

TABLE 58
DATA AND CALCULATIONS FOR PLATE NO. 302,
2 SIDES SUPPORTED

| Total Load (P) (lb.) | Deflection (Δ) (10^{-4} in.) | Total Load/Deflection (Δ/P) (10^{-4} in./lb.) |
|-------------------------|---|--|
| 0.0 | 0.0 | 0.00 |
| 12.0 | 8.0 | 0.67 |
| 24.0 | 16.0 | 0.67 |
| 36.0 | 21.0 | 0.58 |
| 48.0 | 27.0 | 0.56 |
| 60.0 | 35.0 | 0.58 |
| 72.0 | 43.0 | 0.60 |
| 84.0 | 51.0 | 0.61 |
| 96.0 | 66.0 | 0.69 |
| 108.0 | 77.0 | 0.71 |
| 120.0 | 90.0 | 0.75 |
| 132.0 | 107.0 | 0.81 |
| 144.0 | 127.0 | 0.88 |
| 156.0 | 148.0 | 0.85 |
| 168.0 | 175.0 | 1.04 |
| 180.0 | 201.0 | 1.12 |
| 192.0 | 234.0 | 1.22 |
| 204.0 | 272.0 | 1.33 |
| 216.0 | 319.0 | 1.48 |
| 228.0 | 391.0 | 1.71 |
| 240.0 | 479.0 | 2.00 |
| 252.0 | 585.0 | 2.32 |
| 264.0 | 729.0 | 2.76 |

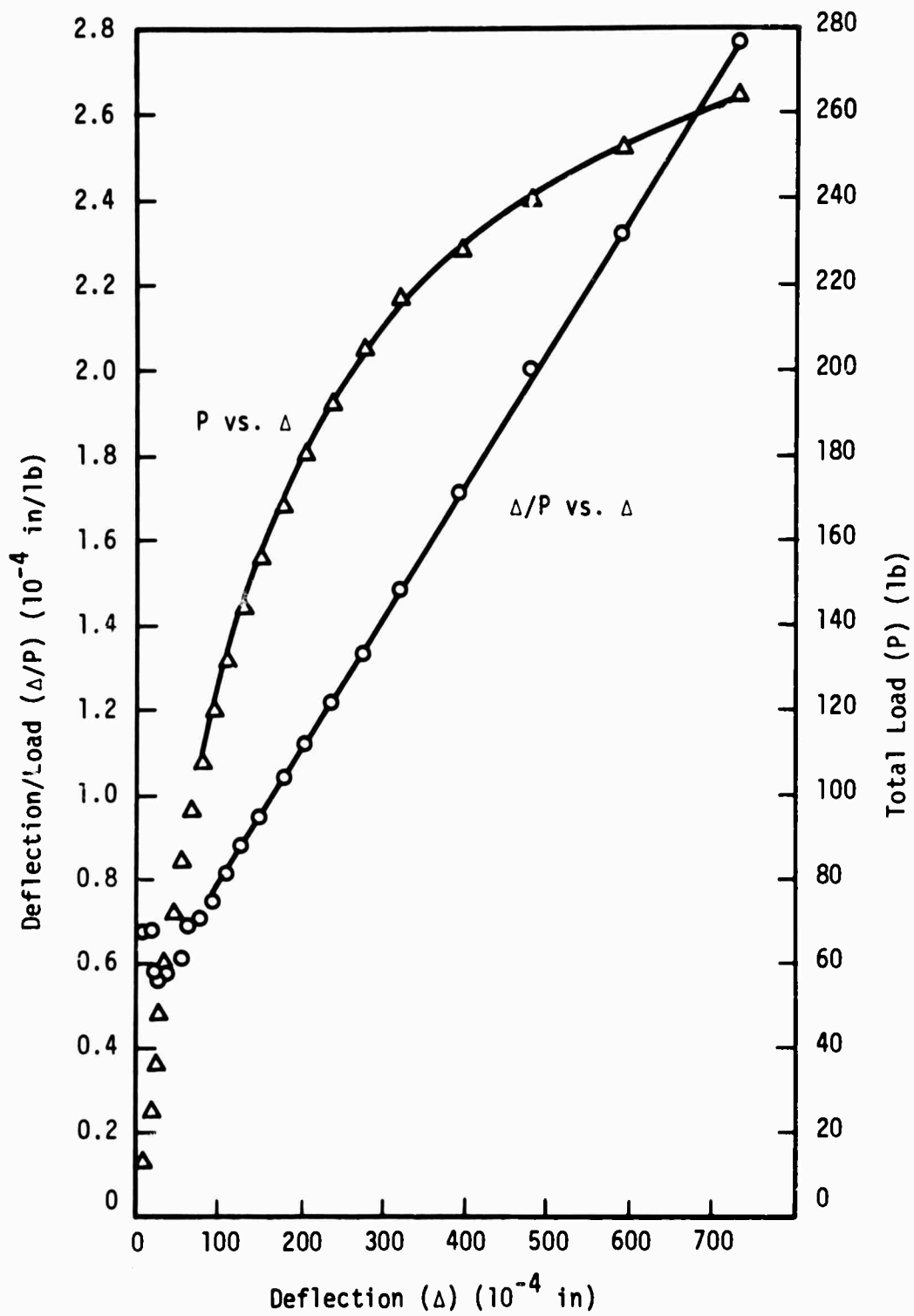


Figure 57. Southwell Plot and Load Deflection Curve for Plate No. 302, 2 Sides Supported

TABLE 59

DATA AND CALCULATIONS FOR PLATE NO. 302,

4 SIDES SUPPORTED

| Total Load (P) (lb.) | Deflection (Δ) (10^{-4} in.) | Total Load/Deflection (Δ/P) (10^{-4} in./lb.) |
|-------------------------|---|--|
| 0 | 0 | 0 |
| 120 | 15 | 0.13 |
| 240 | 33 | 0.14 |
| 360 | 55 | 0.15 |
| 480 | 91 | 0.19 |
| 576 | 133 | 0.23 |
| 624 | 166 | 0.27 |
| 672 | 203 | 0.30 |
| 720 | 259 | 0.36 |
| 768 | 328 | 0.43 |
| 816 | 457 | 0.56 |
| 864 | 696 | 0.78 |
| 912 | 1025 | 1.12 |
| 960 | 1342 | 1.40 |
| 1008 | 1663 | 1.65 |
| 1056 | 1928 | 1.83 |
| 1104 | 2168 | 1.96 |
| 1152 | 2383 | 2.07 |

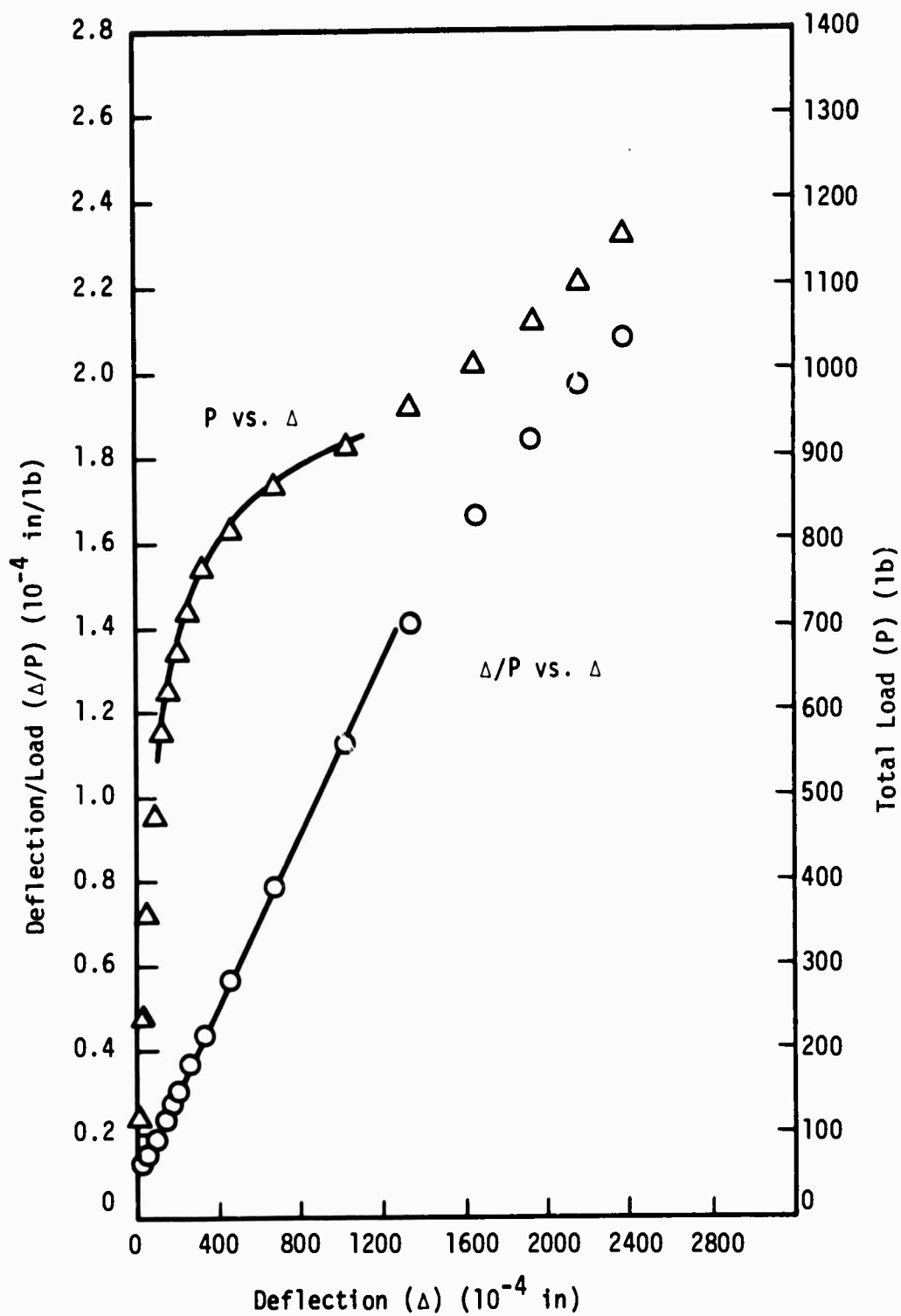


Figure 58. Southwell Plot and Load Deflection Curve
for Plate No. 302, 4 Sides Supported

TABLE 60
DATA AND CALCULATIONS FOR PLATE NO. 303,
2 SIDES SUPPORTED

| Total Load (P) (lb.) | Deflection (Δ) (10^{-4} in.) | Total Load/Deflection (Δ/P) (10^{-4} in./lb.) |
|-------------------------|---|--|
| 6.4 | 0 | 0 |
| 18.4 | 39 | 2.12 |
| 30.4 | 79 | 2.60 |
| 36.4 | 114 | 3.13 |
| 42.4 | 140 | 3.30 |
| 48.4 | 185 | 3.83 |
| 54.4 | 230 | 4.23 |
| 60.4 | 274 | 4.53 |
| 66.4 | 338 | 5.09 |
| 72.4 | 393 | 5.43 |
| 78.4 | 459 | 5.85 |
| 84.4 | 575 | 6.82 |
| 90.4 | 665 | 7.36 |

TABLE 61
MODE SHAPE FOR PLATE NO. 303,
2 SIDES SUPPORTED, 10^{-4} in.

| | | |
|-----|-----|-----|
| 191 | 205 | 196 |
| 314 | 333 | 310 |
| 198 | 242 | 222 |

Note: See Figure 9.

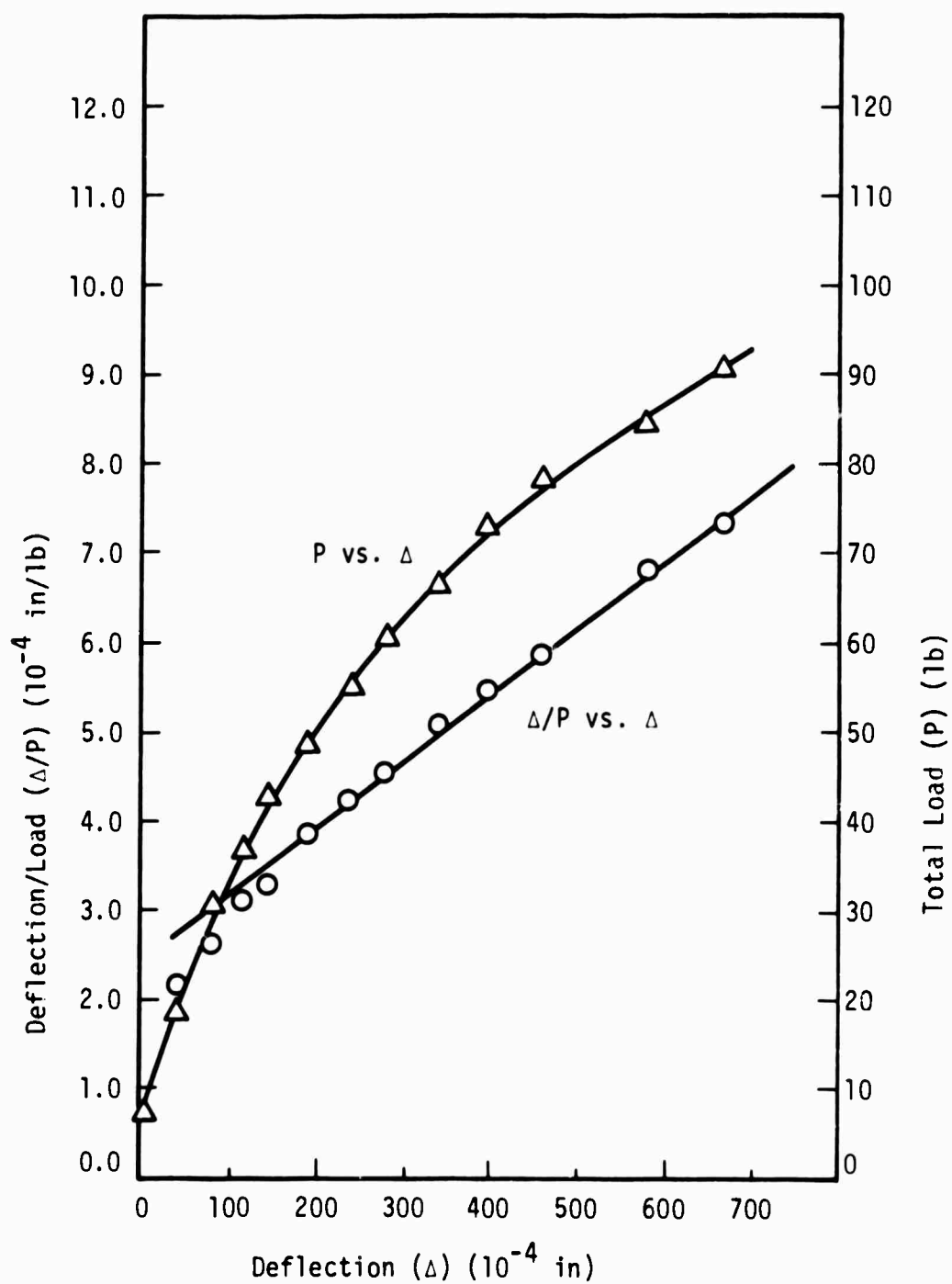


Figure 59. Southwell Plot and Load Deflection Curve
for Plate No. 303, 2 Sides Supported

TABLE 62
DATA AND CALCULATIONS FOR PLATE NO. 303,
4 SIDES SUPPORTED

| Total Load (P) (lb.) | Deflection (Δ) (10^{-4} in.) | Total Load/Deflection (Δ/P) (10^{-4} in./lb.) |
|-------------------------|---|--|
| 0 | 0 | 0 |
| 48 | 19 | .396 |
| 86 | 26 | .271 |
| 144 | 39 | .271 |
| 192 | 45 | .234 |
| 240 | 56 | .233 |
| 288 | 65 | .226 |
| 336 | 81 | .241 |
| 384 | 100 | .260 |
| 408 | 113 | .277 |
| 432 | 125 | .289 |
| 456 | 142 | .311 |
| 480 | 164 | .342 |
| 504 | 197 | .391 |
| 528 | 224 | .424 |
| 552 | 277 | .502 |
| 576 | 345 | .599 |
| 588 | 396 | .673 |
| 600 | 450 | .750 |
| 612 | 501 | .819 |
| 624 | 590 | .946 |
| 636 | 692 | 1.088 |

TABLE 63
MODE SHAPE FOR PLATE NO. 303,
4 SIDES SUPPORTED, 10^{-4} in.

| | | |
|-----|-----|-----|
| 257 | 360 | 241 |
| 327 | 537 | 376 |
| 373 | 516 | 318 |

Note: See Figure 9.

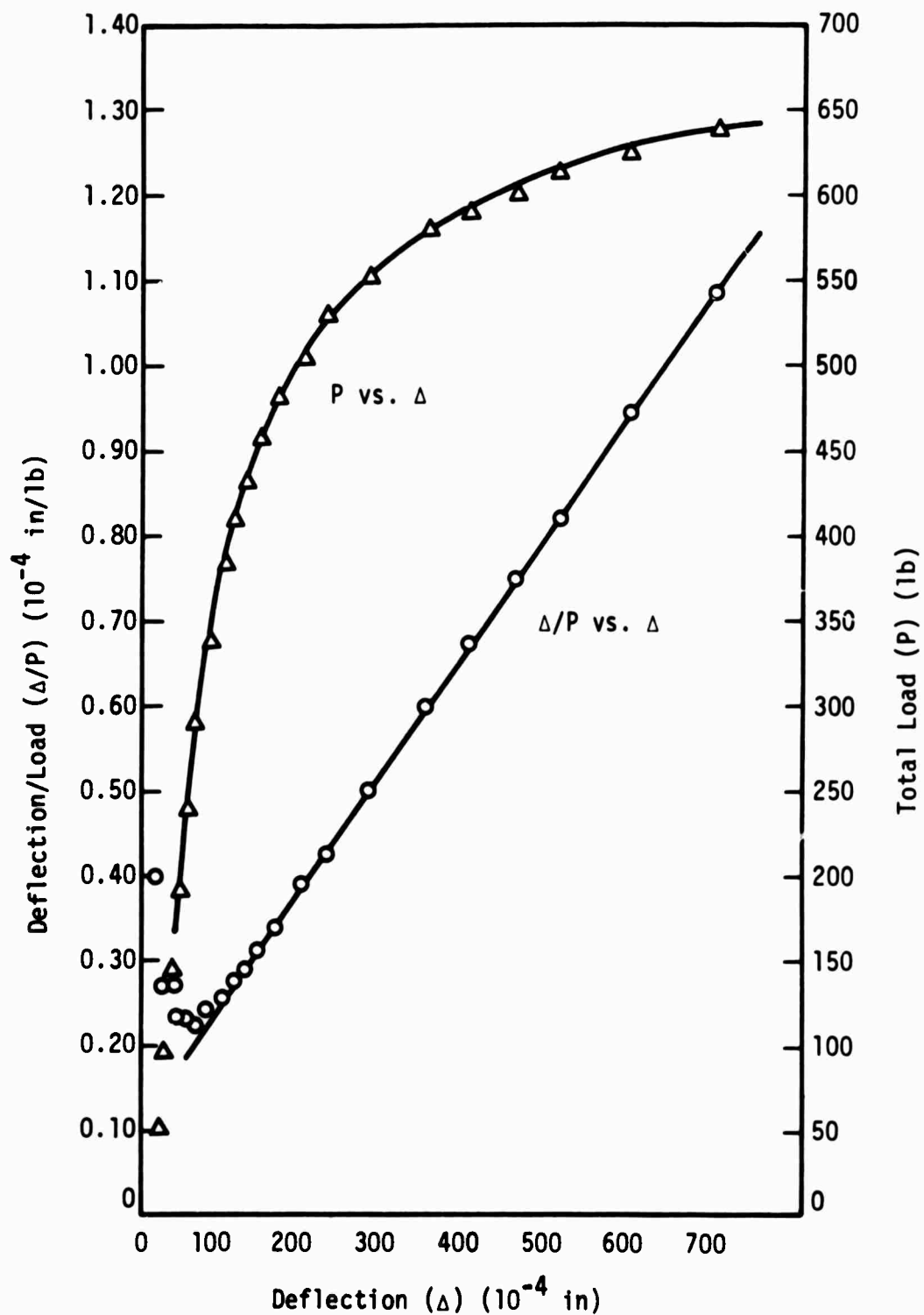


Figure 60. Southwell Plot and Load Deflection Curve for Plate No. 303, 4 Sides Supported

TABLE 64
DATA AND CALCULATIONS FOR PLATE NO. 304,
2 SIDES SUPPORTED

| Total Load (P) (lb.) | Deflection (Δ) (10^{-4} in.) | Total Load/Deflection (Δ/P) (10^{-4} in./lb.) |
|-------------------------|---|--|
| 6.4 | 0 | 0 |
| 18.4 | 12 | .652 |
| 30.4 | 47 | 1.546 |
| 42.4 | 94 | 2.22 |
| 48.4 | 117 | 2.41 |
| 54.4 | 135 | 2.48 |
| 60.4 | 177 | 2.93 |
| 66.4 | 214 | 3.22 |
| 72.4 | 253 | 3.49 |
| 78.4 | 294 | 3.75 |
| 84.4 | 344 | 4.08 |
| 90.4 | 399 | 4.42 |
| 96.4 | 469 | 4.87 |
| 102.4 | 535 | 5.22 |
| 108.4 | 660 | 6.08 |
| 114.4 | 794 | 6.97 |

TABLE 65
MODE SHAPE FOR PLATE NO. 304,
2 SIDES SUPPORTED, 10^{-4} in.

| | | |
|-----|-----|-----|
| 364 | 402 | 371 |
| 381 | 483 | 374 |
| 296 | 306 | 307 |

Note: See Figure 9.

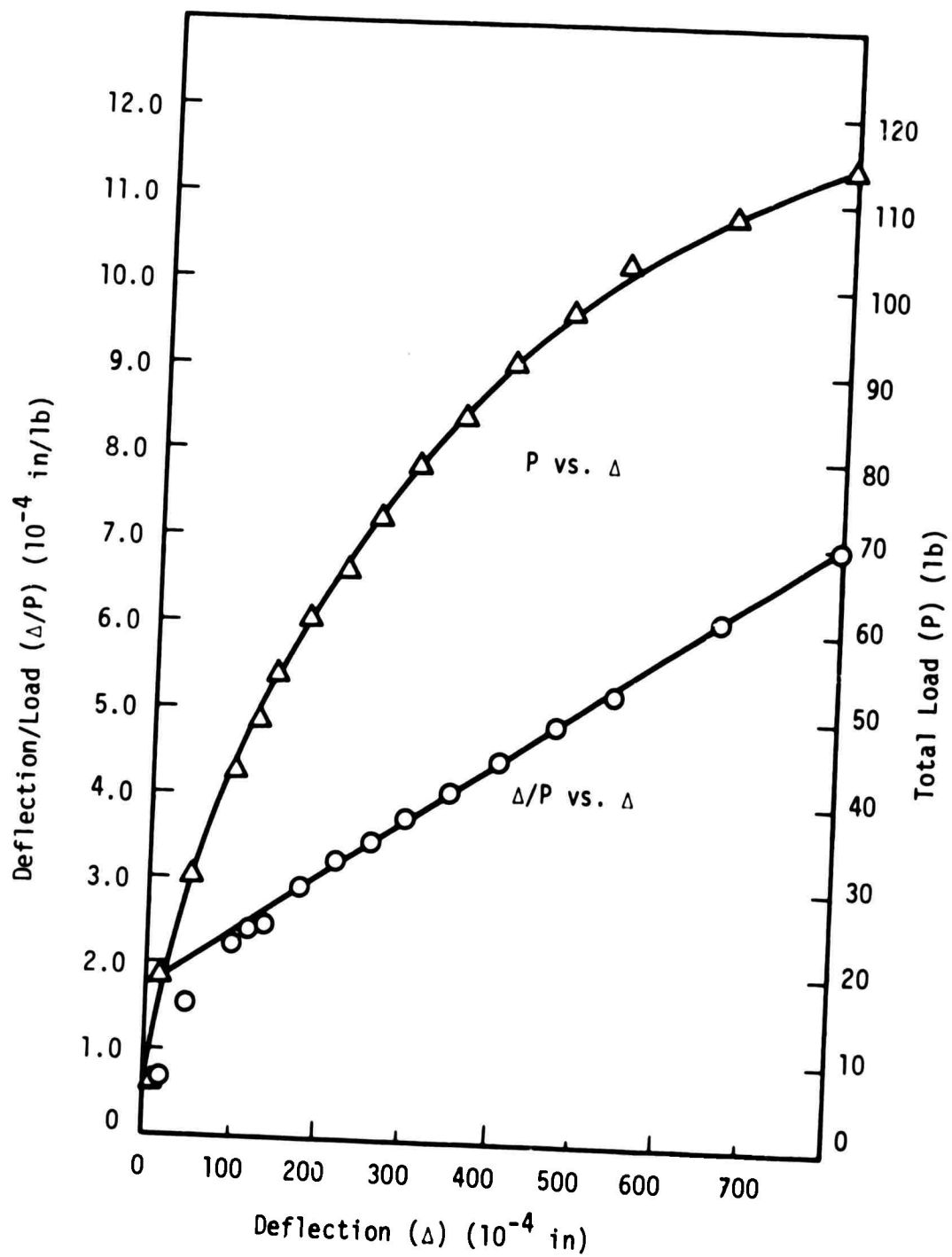


Figure 61. Southwell Plot and Load Deflection Curve
for Plate No. 304, 2 Sides Supported

TABLE 66
DATA AND CALCULATIONS FOR PLATE NO. 304,
4 SIDES SUPPORTED

| Total Load (P) (lb.) | Deflection (Δ) (10^{-4} in.) | Total Load/Deflection (Δ/P) (10^{-4} in./lb.) |
|-------------------------|---|--|
| 0 | 0 | 0 |
| 48 | 14 | .292 |
| 96 | 35 | .365 |
| 144 | 50 | .347 |
| 192 | 68 | .354 |
| 240 | 94 | .392 |
| 264 | 106 | .402 |
| 288 | 121 | .420 |
| 312 | 140 | .449 |
| 336 | 164 | .488 |
| 360 | 185 | .514 |
| 384 | 215 | .560 |
| 408 | 250 | .613 |
| 432 | 293 | .678 |
| 456 | 329 | .721 |
| 480 | 383 | .798 |
| 504 | 435 | .863 |
| 528 | 516 | .977 |
| 552 | 603 | 1.092 |
| 576 | 693 | 1.203 |

TABLE 67
MODE SHAPE FOR PLATE NO. 304,
4 SIDES SUPPORTED, 10^{-4} in.

| | | |
|-----|-----|-----|
| 167 | 230 | 182 |
| 176 | 306 | 221 |
| 192 | 258 | 185 |

Note: See Figure 9.

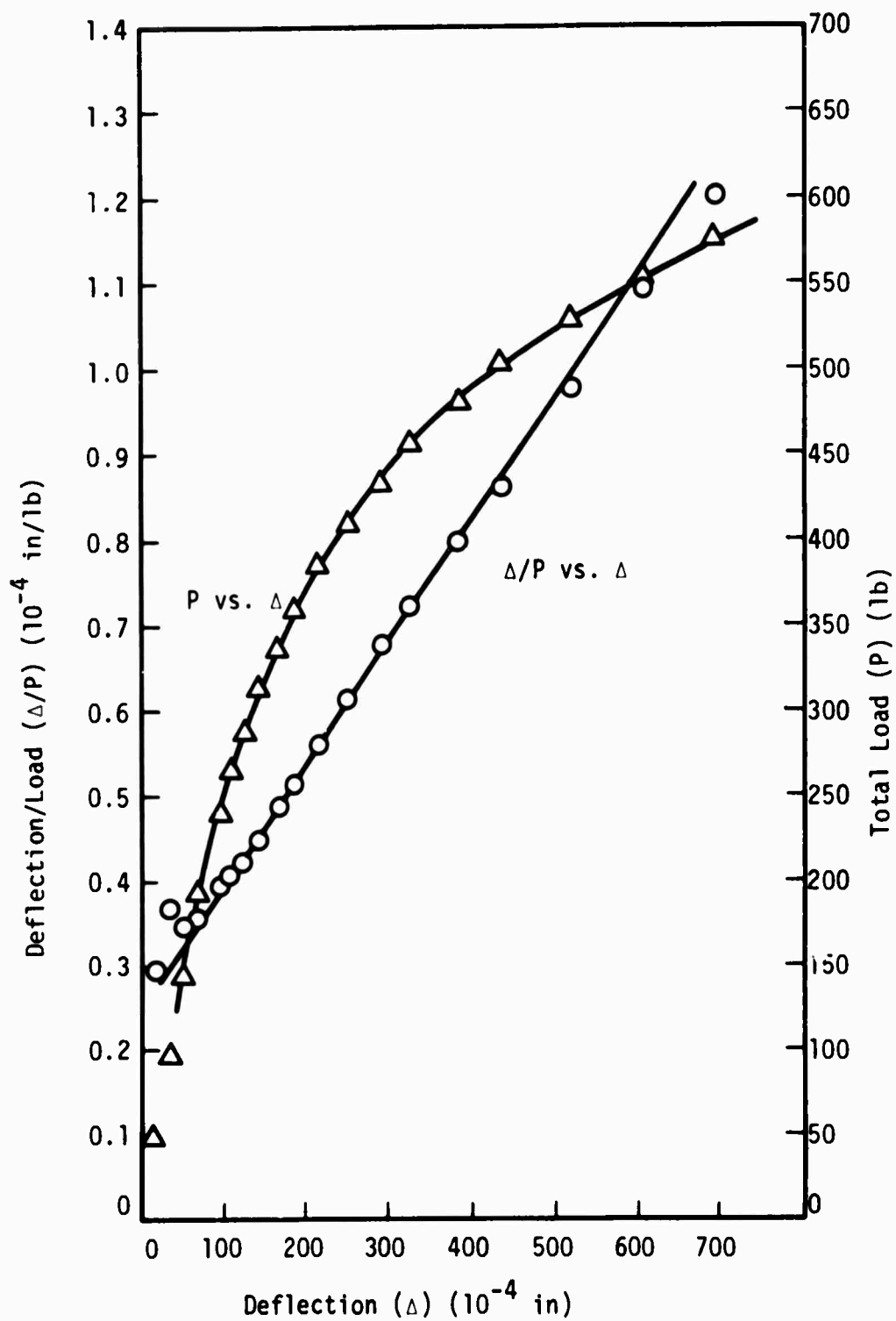


Figure 62. Southwell Plot and Load Deflection Curve
for Plate No. 304, 4 Sides Supported

TABLE 68
DATA AND CALCULATIONS FOR PLATE NO. 401,
2 SIDES SUPPORTED

| Total Load (P) (lb.) | Deflection (Δ) (10^{-4} in.) | Total Load/Deflection (Δ/P) (10^{-4} in./lb.) |
|-------------------------|---|--|
| 0 | 0 | 0 |
| 60 | 13 | .217 |
| 120 | 36 | .300 |
| 180 | 81 | .450 |
| 210 | 122 | .581 |
| 240 | 218 | .908 |
| 252 | 309 | 1.225 |

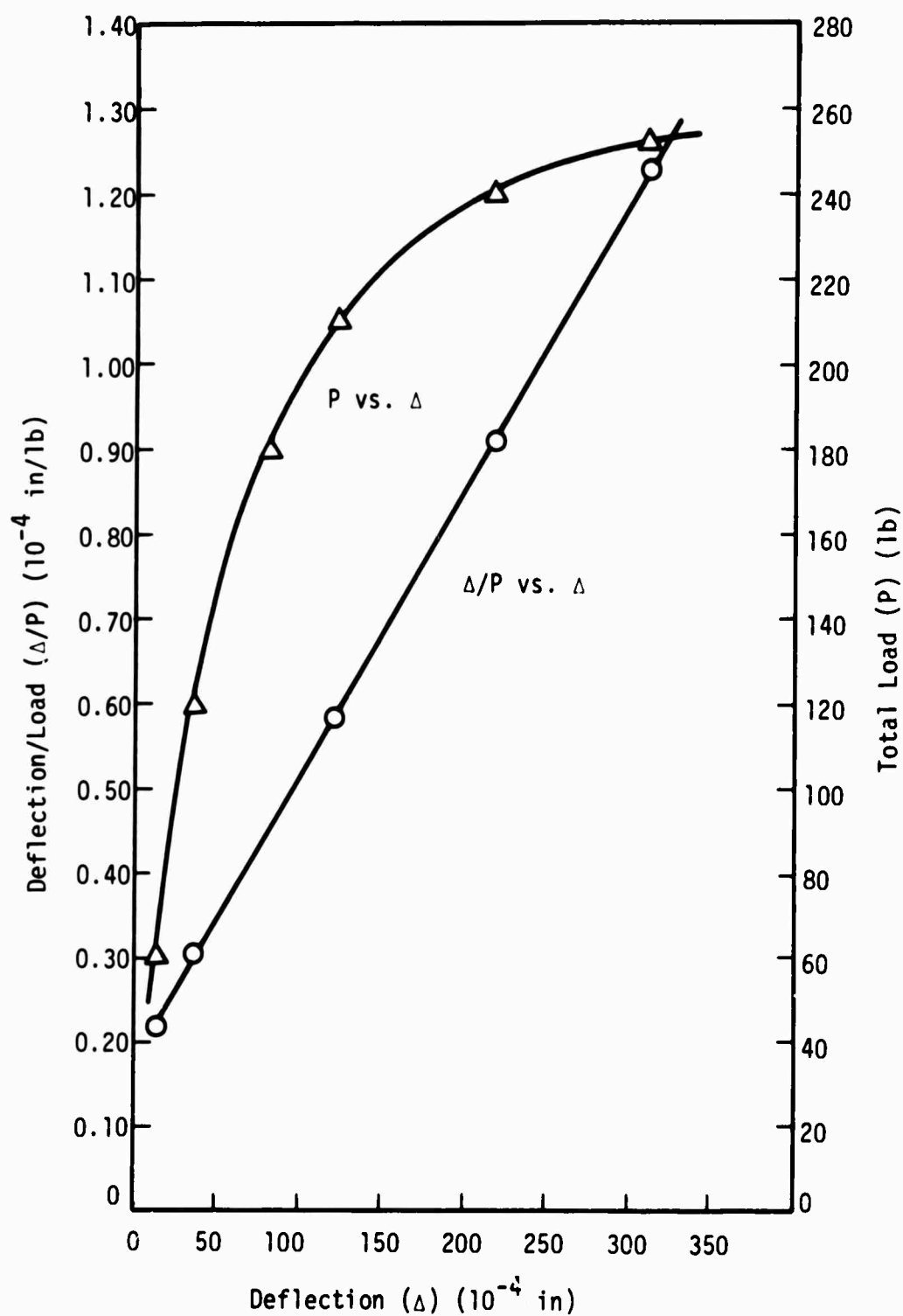


Figure 63. Southwell Plot and Load Deflection Curve for Plate No. 401, 2 Sides Supported

TABLE 69
DATA AND CALCULATIONS FOR PLATE NO. 401,
4 SIDES SUPPORTED

| Total Load (P) (lb.) | Deflection (Δ) (10^{-4} in.) | Total Load/Deflection (Δ/P) (10^{-4} in./lb.) |
|-------------------------|---|--|
| 0 | 0 | 0 |
| 1000 | 23 | .0230 |
| 2000 | 64 | .0320 |
| 2500 | 91 | .0364 |
| 3000 | 125 | .0417 |
| 3500 | 171 | .0488 |

TABLE 70
MODE SHAPE FOR PLATE NO. 401,
4 SIDES SUPPORTED, 10^{-4} in.

| | | |
|-----|------|---|
| | 135 | |
| -12 | -8 | 4 |
| | -100 | |

Note: See Figure 9.

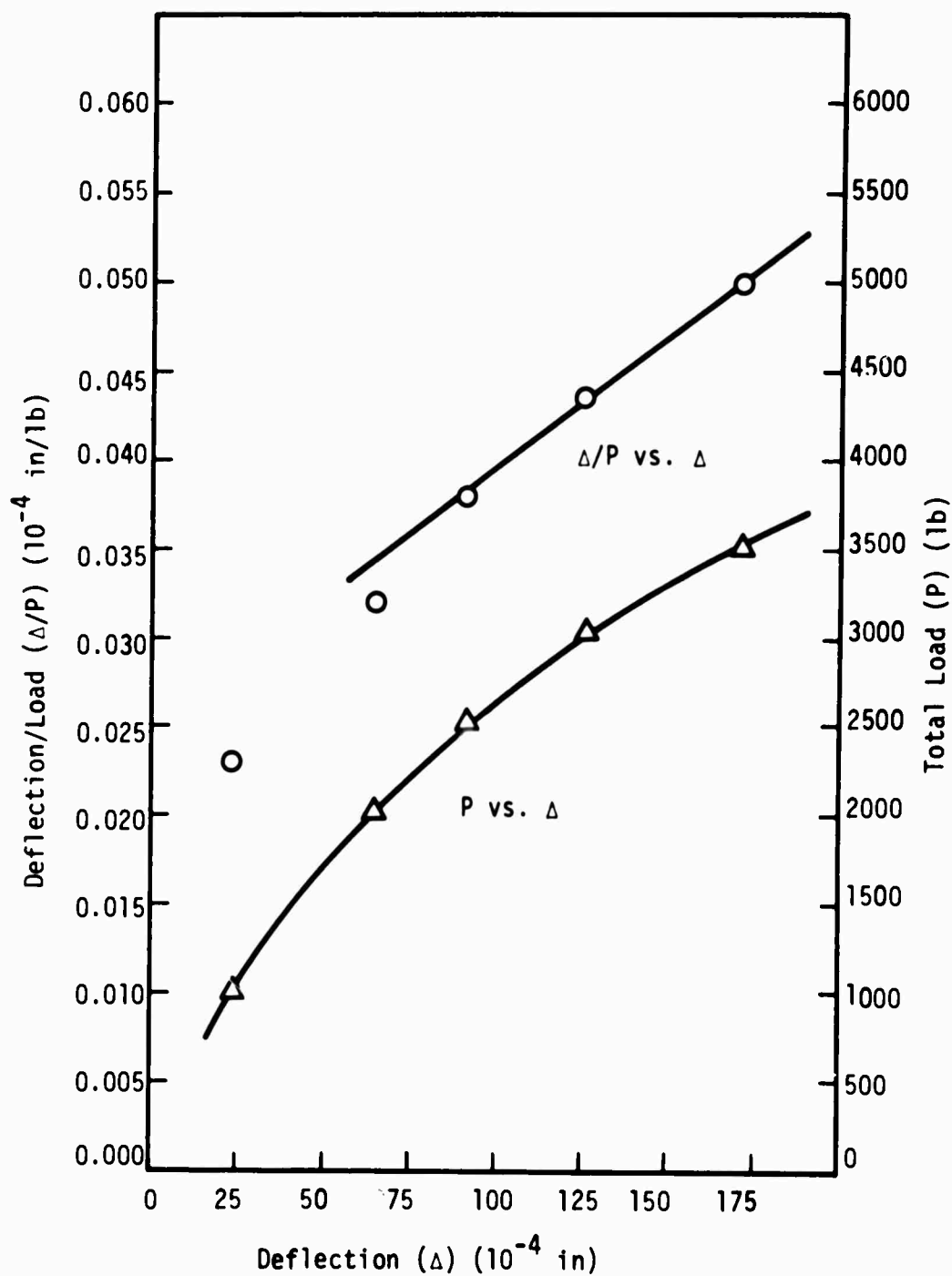


Figure 64. Southwell Plot and Load Deflection Curve
for Plate No. 401, 4 Sides Supported

TABLE 71
DATA AND CALCULATIONS FOR PLATE NO. 402,
2 SIDES SUPPORTED

| Total Load (P) (lb.) | Deflection (Δ) (10^{-4} in.) | Total Load/Deflection (Δ/P) (10^{-4} in./lb.) |
|-------------------------|---|--|
| 0 | 0 | 0 |
| 240 | 26 | .1083 |
| 480 | 34 | .0708 |
| 720 | 46 | .0639 |
| 960 | 76 | .0792 |
| 1080 | 109 | .1010 |
| 1200 | 265 | .2210 |
| 1230 | 335 | .2720 |
| 1260 | 485 | .3850 |

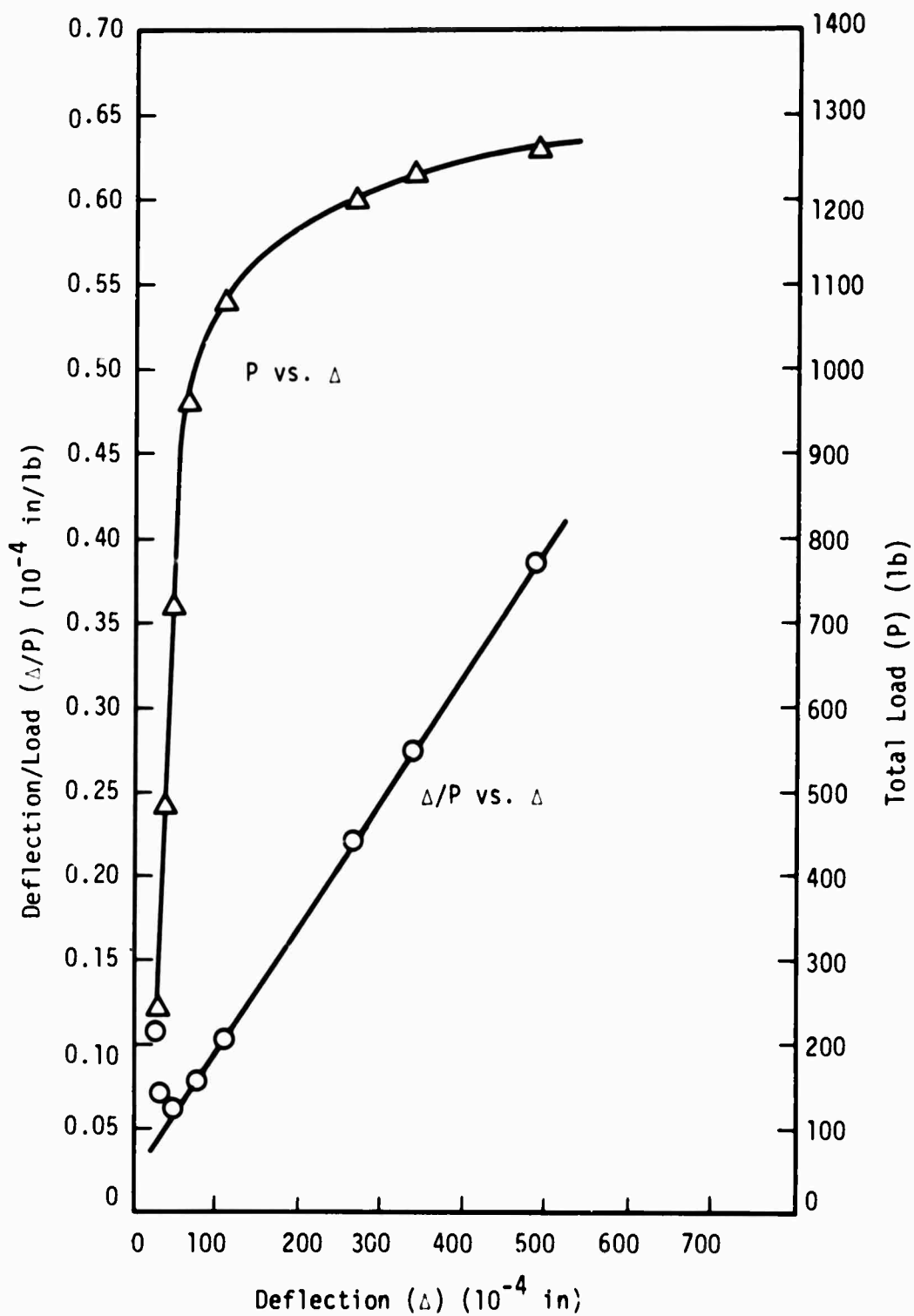


Figure 65. Southwell Plot and Load Deflection Curve for Plate No. 402, 2 Sides Supported

TABLE 72
DATA AND CALCULATIONS FOR PLATE NO. 402,
4 SIDES SUPPORTED

| Total Load (P) (lb.) | Deflection (Δ) (10^{-4} in.) | Total Load/Deflection (Δ/P) (10^{-4} in./lb.) |
|-------------------------|---|--|
| 0 | 0 | 0 |
| 1000 | --- | --- |
| 2000 | 8 | .00400 |
| 3000 | 35 | .01166 |
| 3500 | 50 | .01430 |
| 4000 | 76 | .01900 |
| 4250 | 109 | .0256 |
| 4500 | 137 | .0304 |
| 4750 | 161 | .0339 |
| 4900 | 189 | .0385 |

TABLE 73
MODE SHAPE FOR PLATE NO. 402,
4 SIDES SUPPORTED, 10^{-4} in.

| | | |
|----|-----|----|
| | 104 | |
| 88 | 132 | 90 |
| | 105 | |

Note: See Figure 9.

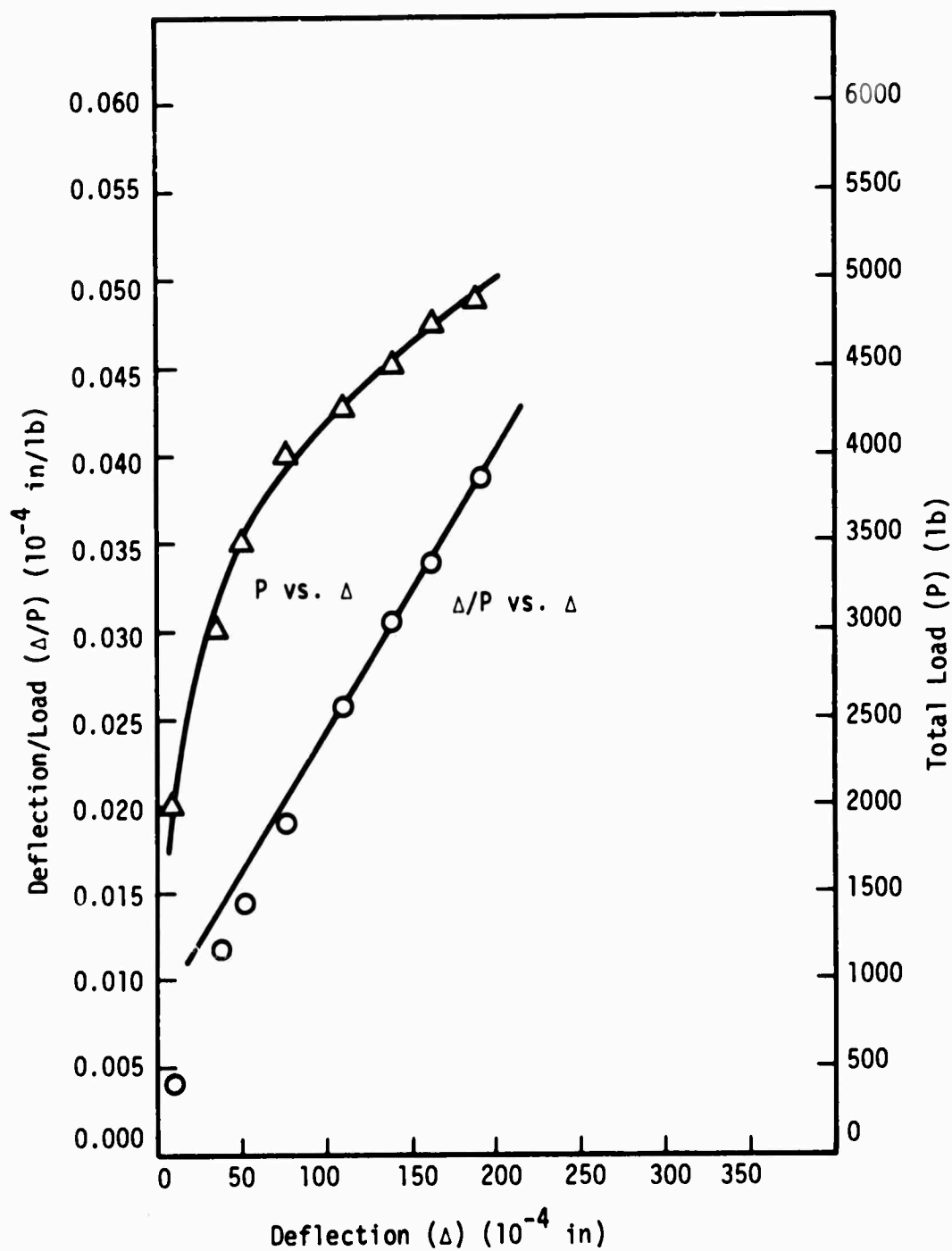


Figure 66. Southwell Plot and Load Deflection Curve
for Plate No. 402, 4 Sides Supported

TABLE 74
DATA AND CALCULATIONS FOR PLATE NO. 403a,
2 SIDES SUPPORTED

| Total Load (P) (lb.) | Deflection (Δ) (10^{-4} in.) | Total Load/Deflection (Δ/P) (10^{-4} in./lb.) |
|-------------------------|---|--|
| 0 | 0 | 0 |
| 24 | 8 | .333 |
| 48 | 20 | .417 |
| 72 | 35 | .487 |
| 96 | 50 | .521 |
| 120 | 75 | .625 |
| 144 | 99 | .688 |
| 168 | 125 | .743 |
| 192 | 155 | .807 |
| 216 | 186 | .860 |
| 240 | 219 | .913 |
| 264 | 263 | .996 |
| 288 | 322 | 1.118 |
| 312 | 399 | 1.280 |

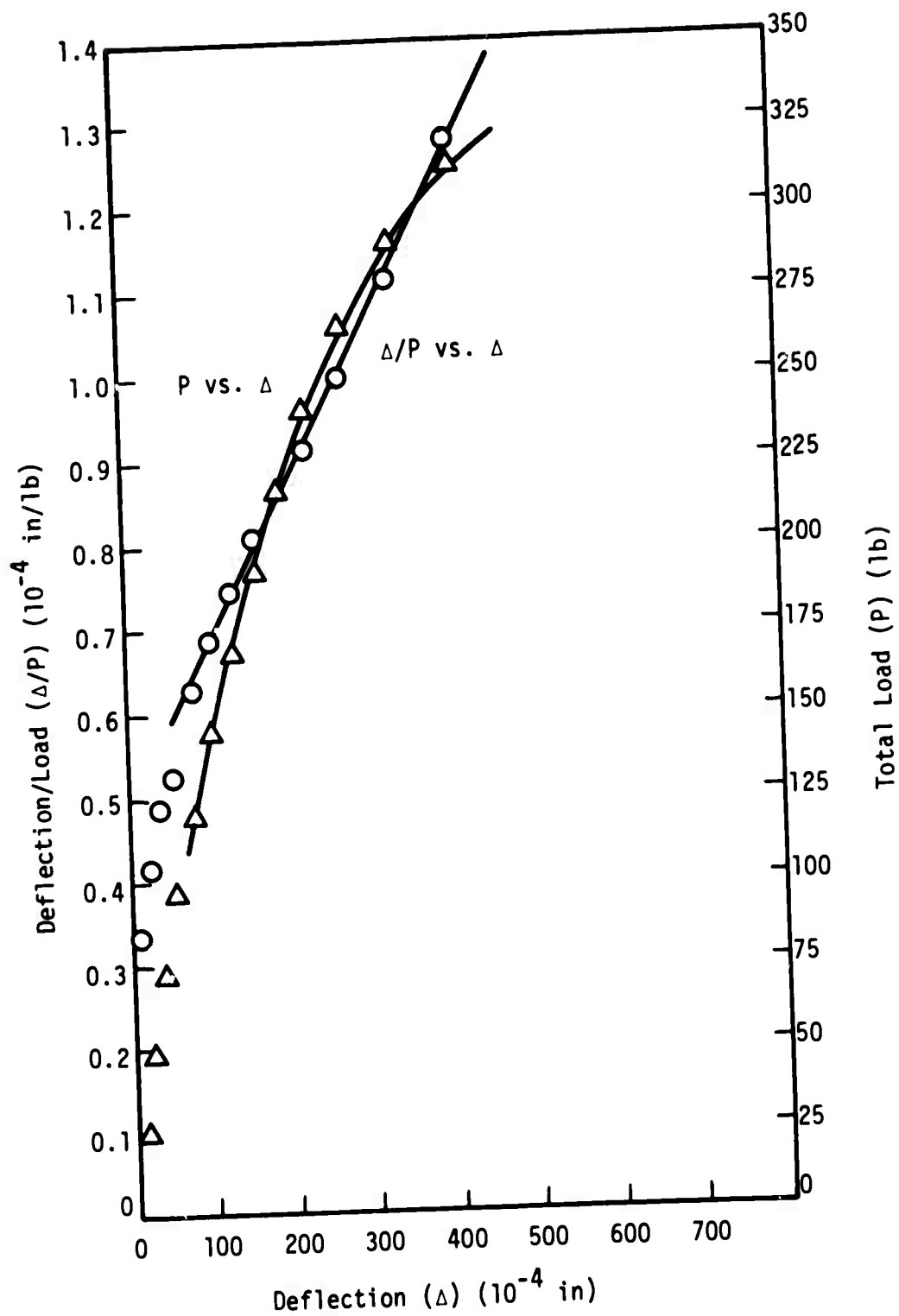


Figure 67. Southwell Plot and Load Deflection Curve for Plate No. 403a, 2 Sides Supported

TABLE 75
DATA AND CALCULATIONS FOR PLATE NO. 403b,
2 SIDES SUPPORTED

| Total Load (P) (lb.) | Deflection (Δ) (10 ⁻⁴ in.) | Total Load/Deflection (Δ/P) (10 ⁻⁴ in./lb.) |
|-------------------------|--|---|
| 0 | 0 | 0 |
| 24 | --- | --- |
| 48 | --- | --- |
| 72 | 5 | .0694 |
| 96 | 7 | .0729 |
| 120 | 12 | .1000 |
| 144 | 15 | .1042 |
| 168 | 20 | .1190 |
| 192 | 22 | .1047 |
| 216 | 27 | .1250 |
| 240 | 31 | .1292 |
| 264 | 37 | .1400 |
| 288 | 43 | .1493 |
| 312 | 59 | .1890 |
| 336 | 78 | .2320 |
| 360 | 113 | .3140 |
| 384 | 176 | .4580 |
| 396 | 218 | .5500 |
| 408 | 310 | .7600 |

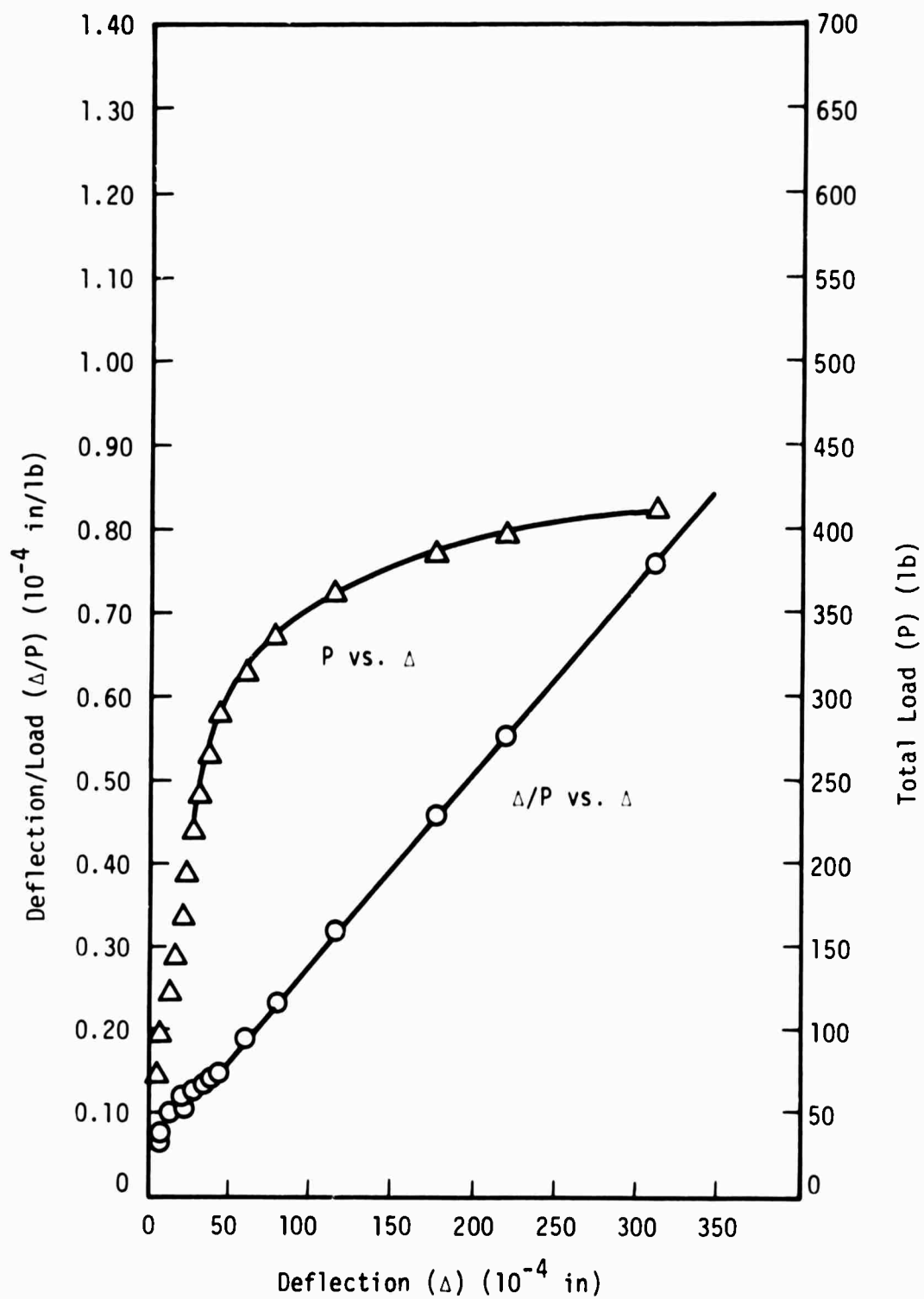


Figure 68. Southwell Plot and Load Deflection Curve for Plate No. 403b, 2 Sides Supported

TABLE 76
DATA AND CALCULATIONS FOR PLATE NO. 403a,
4 SIDES SUPPORTED, PERTURBED

| Total Load (P) (lb.) | Deflection (Δ) (10^{-4} in.) | Total Load/Deflection (Δ/P , (10^{-4} in./lb.) |
|-------------------------|---|--|
| 0 | 0 | 0 |
| 1000 | 20 | .0200 |
| 2000 | 69 | .0345 |
| 2500 | 92 | .0368 |
| 3000 | 130 | .0433 |
| 3500 | 181 | .0517 |
| 3750 | 216 | .0576 |
| 4000 | 267 | .0668 |
| 4250 | 345 | .0812 |
| 4500 | 441 | .0981 |

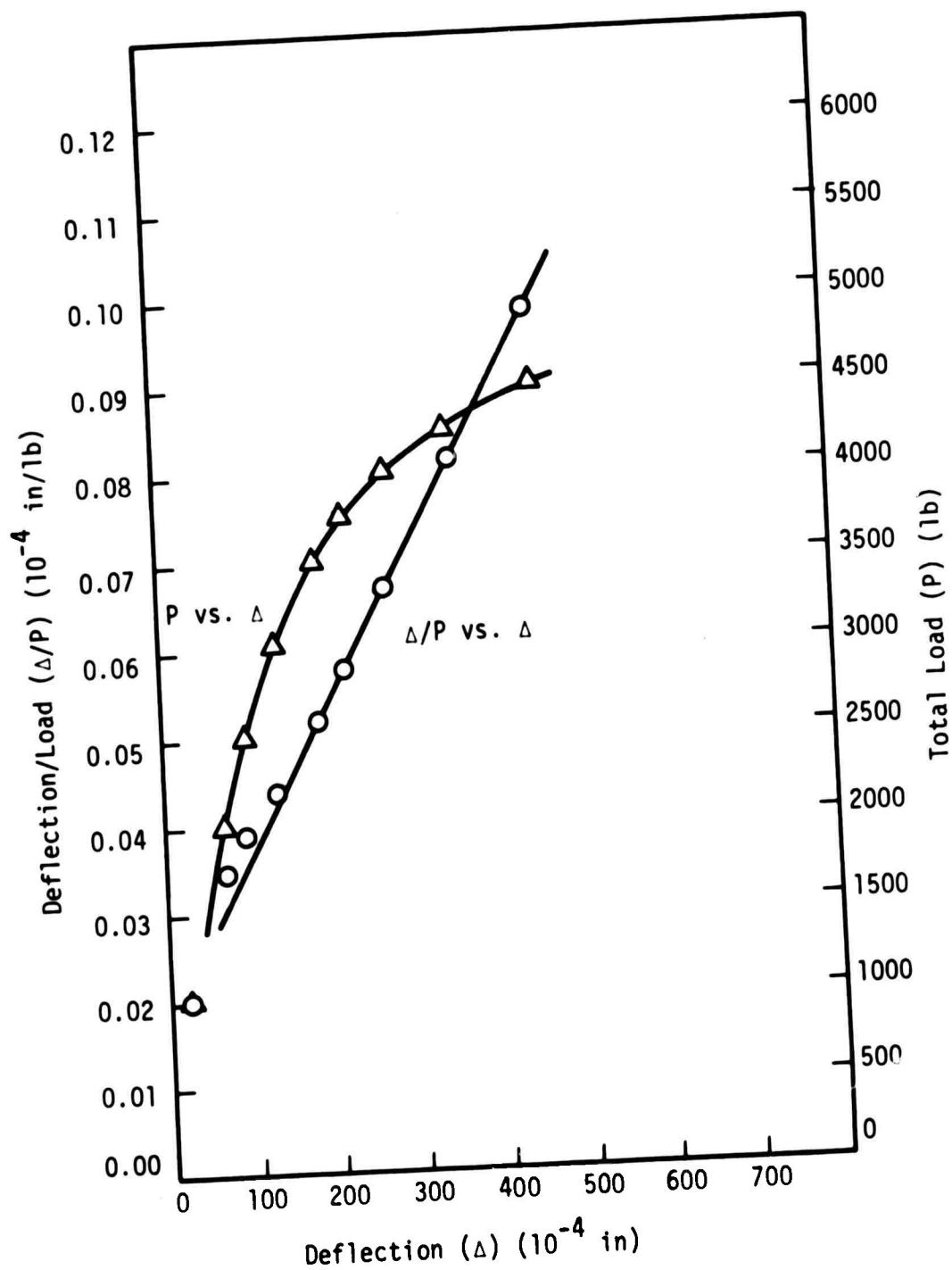


Figure 69. Southwell Plot and Load Deflection Curve
for Plate No. 403a, 4 Sides Supported

TABLE 77
DATA AND CALCULATIONS FOR PLATE NO. 403b,
4 SIDES SUPPORTED, PERTURBED

| Total Load (P) (lb.) | Deflection (Δ) (10^{-4} in./lb.) | Total Load/Deflection (Δ/P) (10^{-4} in./lb.) |
|-------------------------|---|--|
| 0 | 0 | 0 |
| 1000 | 2 | .002 |
| 2000 | 27 | .0135 |
| 3000 | 66 | .0220 |
| 3500 | 97 | .0277 |
| 4000 | 142 | .0355 |
| 4250 | 172 | .0404 |
| 4500 | 217 | .0483 |
| 4750 | 280 | .0589 |

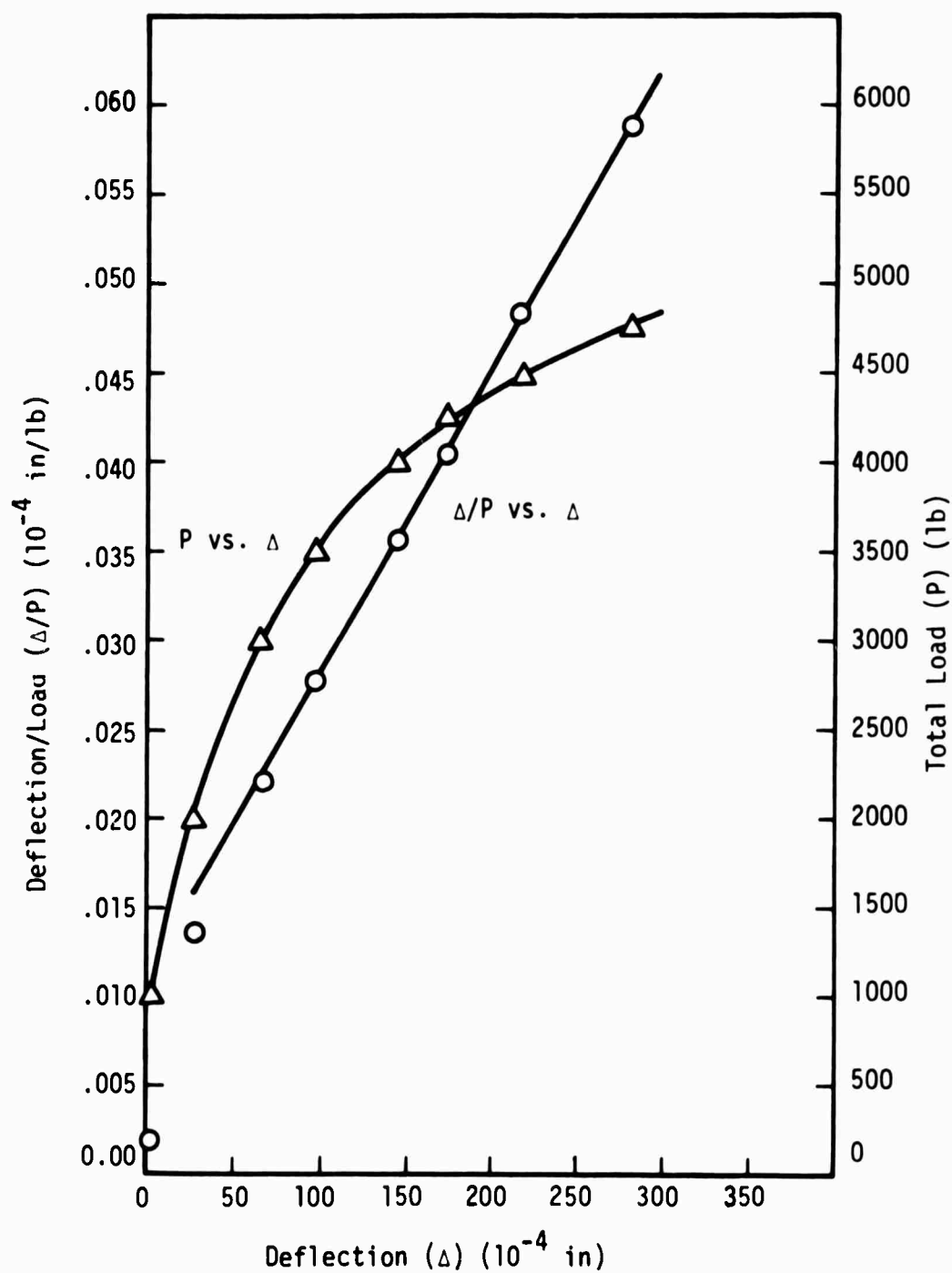


Figure 70. Southwell Plot and Load Deflection Curve
for Plate No. 403b, 4 Sides Supported

TABLE 78
DATA AND CALCULATIONS FOR PLATE NO. 404,
2 SIDES SUPPORTED

| Total Load (P) (lb.) | Deflection (Δ) (10^{-4} in.) | Total Load/Deflection (Δ/P) (10^{-4} in./lb.) |
|-------------------------|---|--|
| 0 | 0 | 0 |
| 480 | 1 | .0021 |
| 960 | 9 | .0094 |
| 1440 | 61 | .0423 |
| 1680 | 141 | .0838 |
| 1800 | 280 | .1555 |
| 1860 | 485 | .2610 |

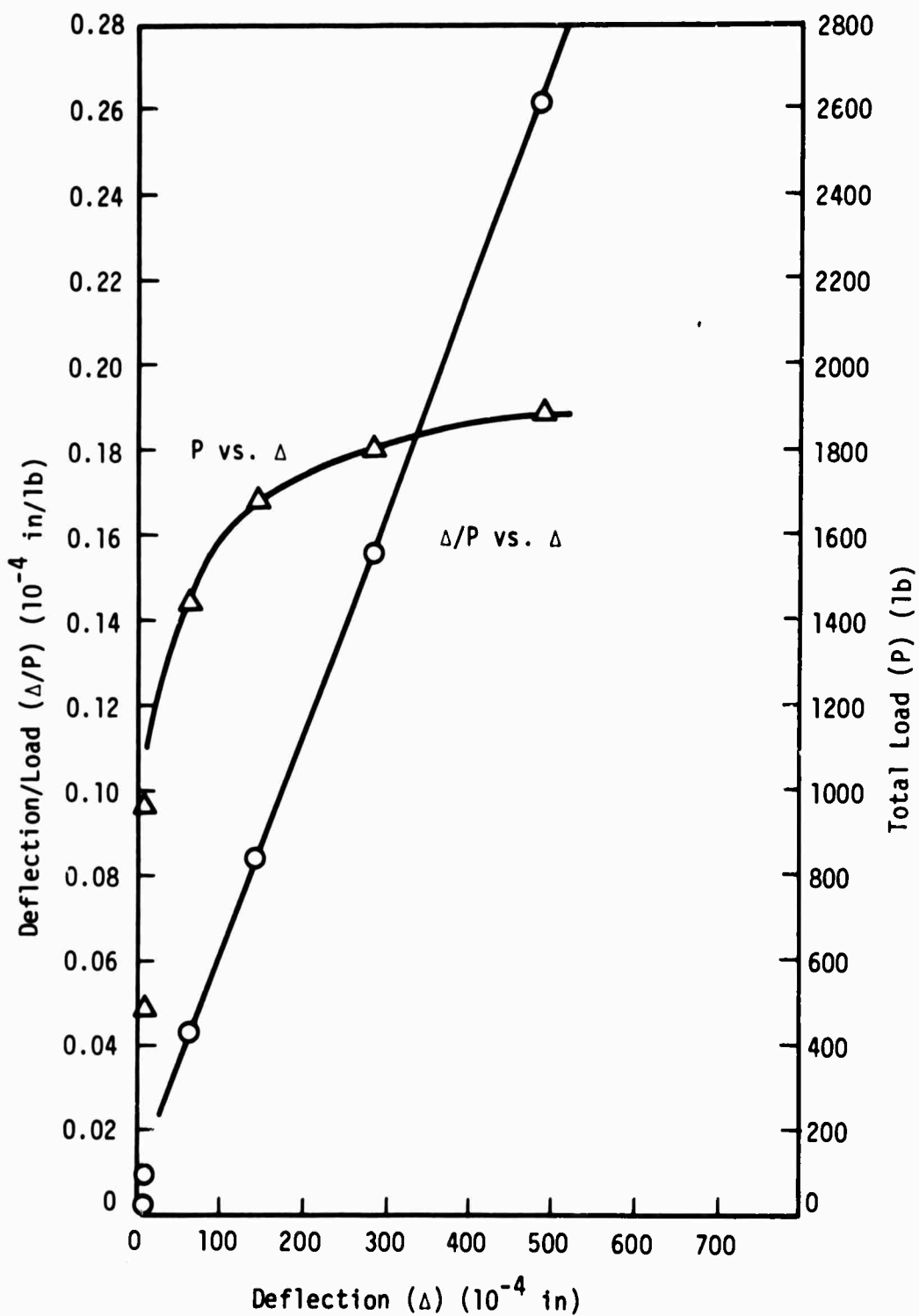


Figure 71. Southwell Plot and Load Deflection Curve
for Plate No. 404, 2 Sides Supported

TABLE 79
DATA AND CALCULATIONS FOR PLATE NO. 404,
4 SIDES SUPPORTED

| Total Load (P) (lb.) | Deflection (Δ) (10^{-4} in.) | Total Load/Deflection (Δ/P) (10^{-4} in./lb.) |
|-------------------------|---|--|
| 0 | 0 | 0 |
| 240 | 8 | .0333 |
| 480 | 18 | .0375 |
| 720 | 29 | .0403 |
| 960 | 47 | .0490 |
| 1200 | 65 | .0542 |
| 1440 | 113 | .0785 |
| 1680 | 175 | .1042 |
| 1800 | 223 | .1238 |
| 1920 | 281 | .1462 |
| 2040 | 352 | .1725 |
| 2160 | 451 | .209 |

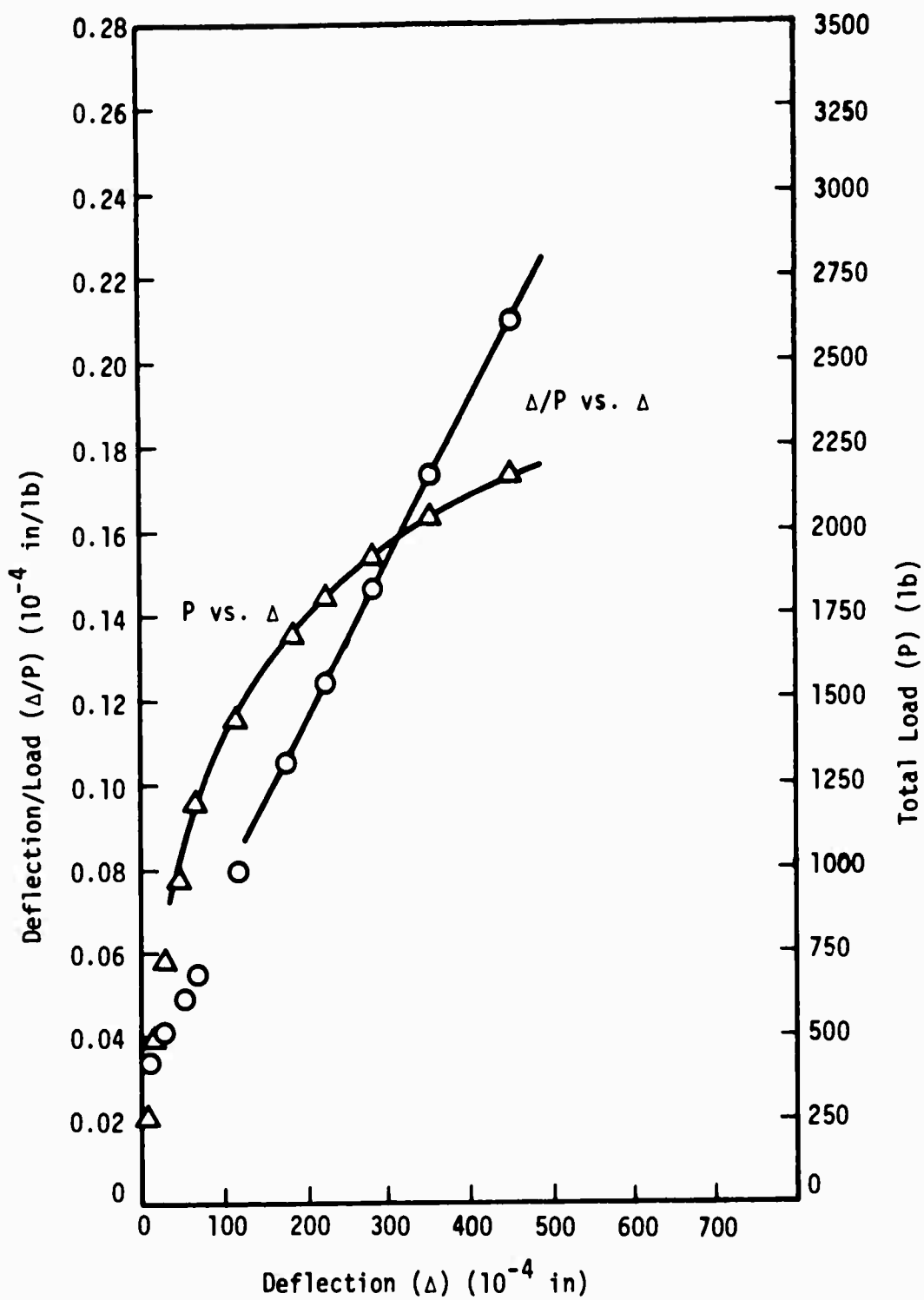


Figure 72. Southwell Plot and Load Deflection Curve
for Plate No. 404, 4 Sides Supported

TABLE 80
DATA AND CALCULATIONS FOR PLATE NO. 405,
2 SIDES SUPPORTED

| Total Load (P) (lb.) | Deflection (Δ) (10^{-4} in.) | Total Load/Deflection (Δ/P) (10^{-4} in./lb.) |
|-------------------------|---|--|
| 0 | 0 | 0 |
| 24 | 1 | .042 |
| 48 | 13 | .271 |
| 72 | 22 | .306 |
| 96 | 39 | .407 |
| 120 | 51 | .425 |
| 144 | 89 | .618 |
| 156 | 108 | .693 |
| 168 | 141 | .838 |
| 180 | 189 | 1.050 |
| 192 | 256 | 1.332 |
| 204 | 439 | 2.150 |

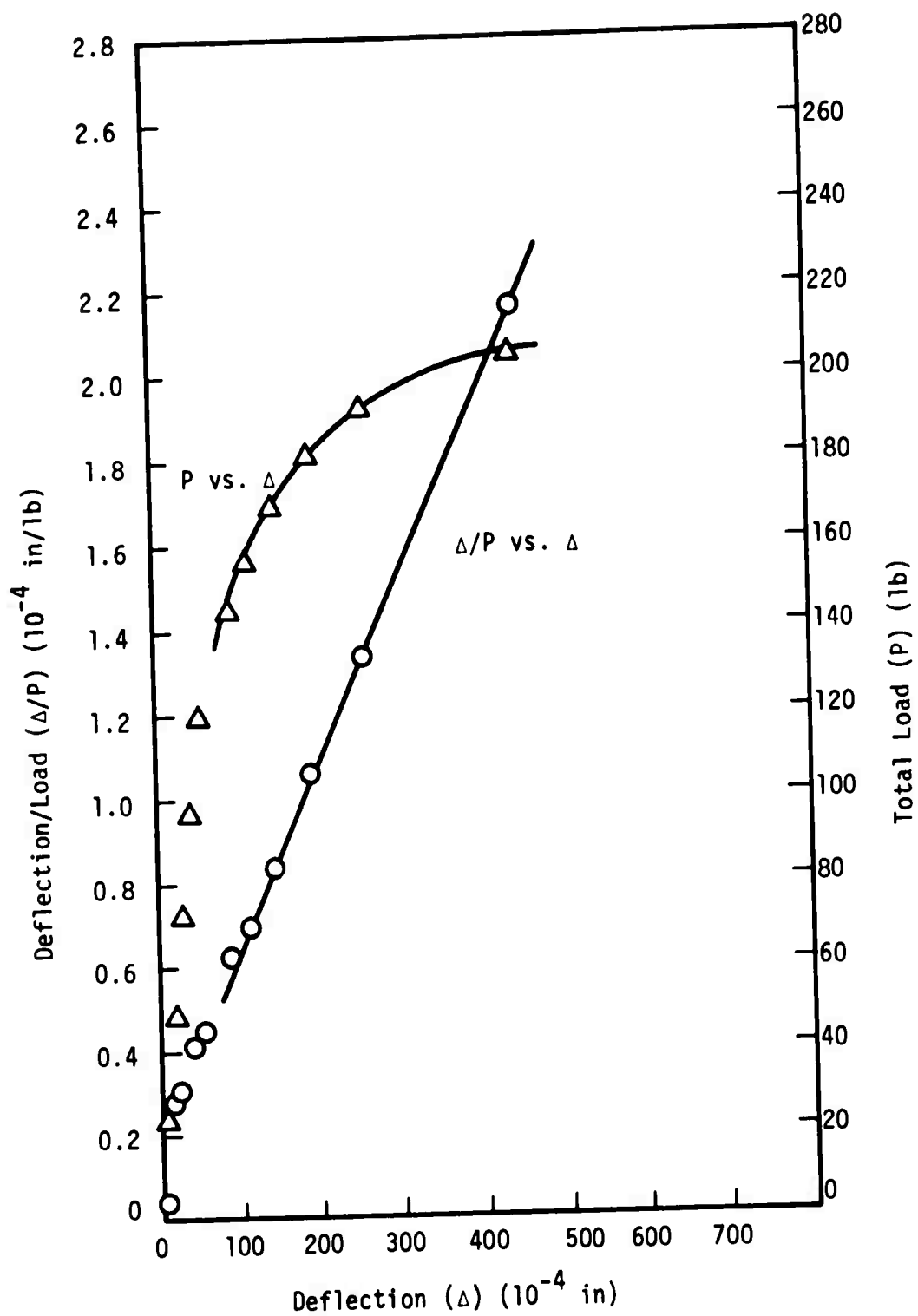


Figure 73. Southwell Plot and Load Deflection Curve
for Plate No. 405, 2 Sides Supported

TABLE 81
DATA AND CALCULATIONS FOR PLATE NO. 405,
4 SIDES SUPPORTED

| Total Load (P) (lb.) | Deflection (Δ) (10^{-4} in.) | Total Load/Deflection (Δ/P) (10^{-4} in./lb.) |
|-------------------------|---|--|
| 0 | 0 | 0 |
| 240 | 10 | .0417 |
| 480 | 27 | .0563 |
| 720 | 48 | .0668 |
| 960 | 75 | .0782 |
| 1200 | 106 | .0884 |
| 1440 | 142 | .0986 |
| 1560 | 166 | .1065 |
| 1680 | 197 | .1173 |
| 1800 | 251 | .1395 |
| 1920 | 340 | .1772 |
| 2040 | 442 | .2170 |

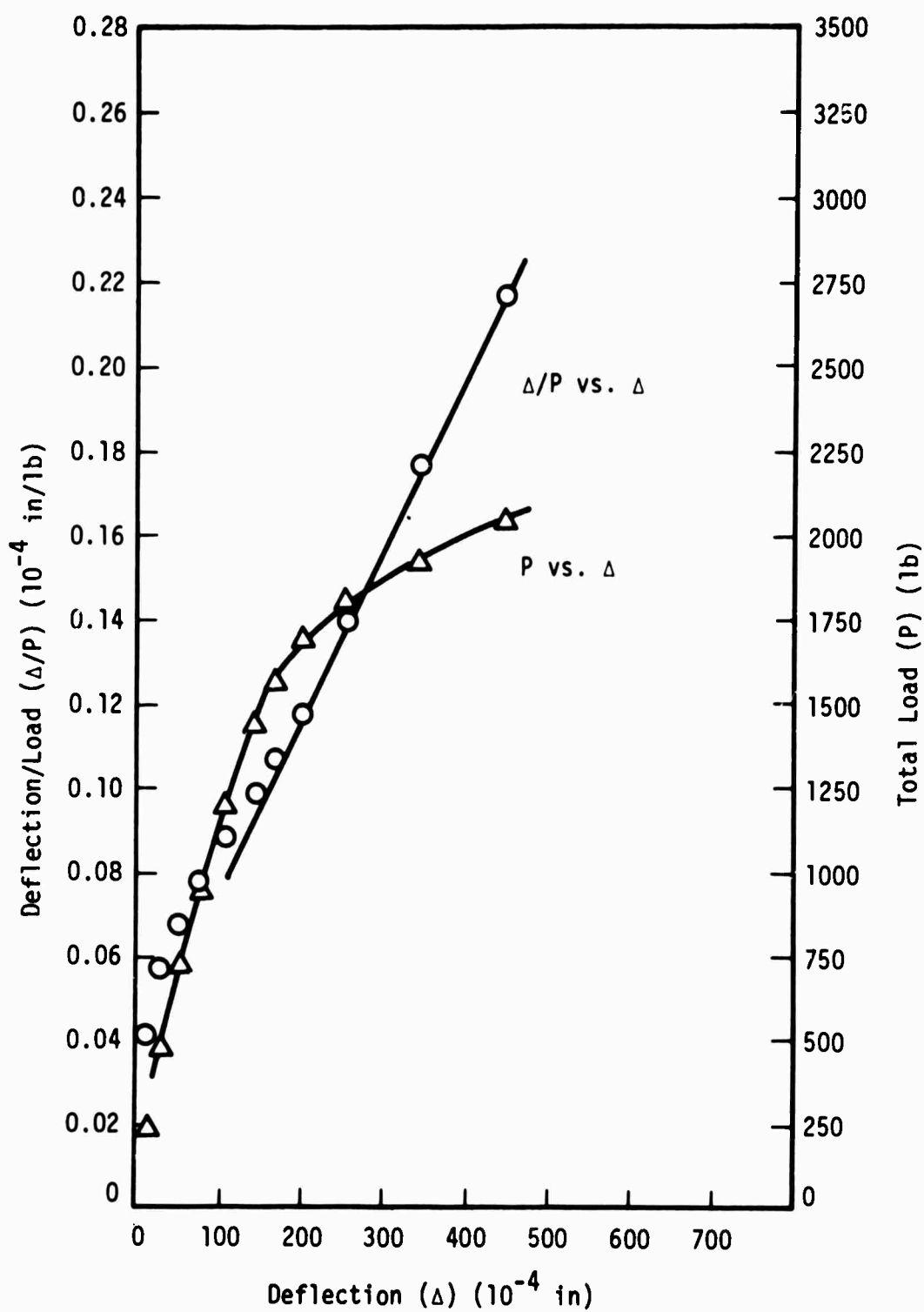


Figure 74. Southwell Plot and Load Deflection Curve
for Plate No. 405, 4 Sides Supported

TABLE 82
DATA AND CALCULATIONS FOR PLATE NO. 406,
2 SIDES SUPPORTED

| Total Load (P) (lb.) | Deflection (Δ) (10^{-4} in.) | Total Load/Deflection (Δ/P) (10^{-4} in./lb.) |
|-------------------------|---|--|
| 0 | 0 | 0 |
| 60 | 10 | .167 |
| 120 | 9 | .075 |
| 180 | 15 | .083 |
| 240 | 22 | .092 |
| 300 | 30 | .100 |
| 360 | 38 | .106 |
| 420 | 50 | .119 |
| 480 | 63 | .131 |
| 540 | 84 | .156 |
| 600 | 125 | .208 |
| 630 | 143 | .227 |
| 660 | 182 | .276 |
| 690 | 212 | .307 |
| 720 | 257 | .357 |
| 750 | 342 | .456 |
| 780 | 471 | .603 |

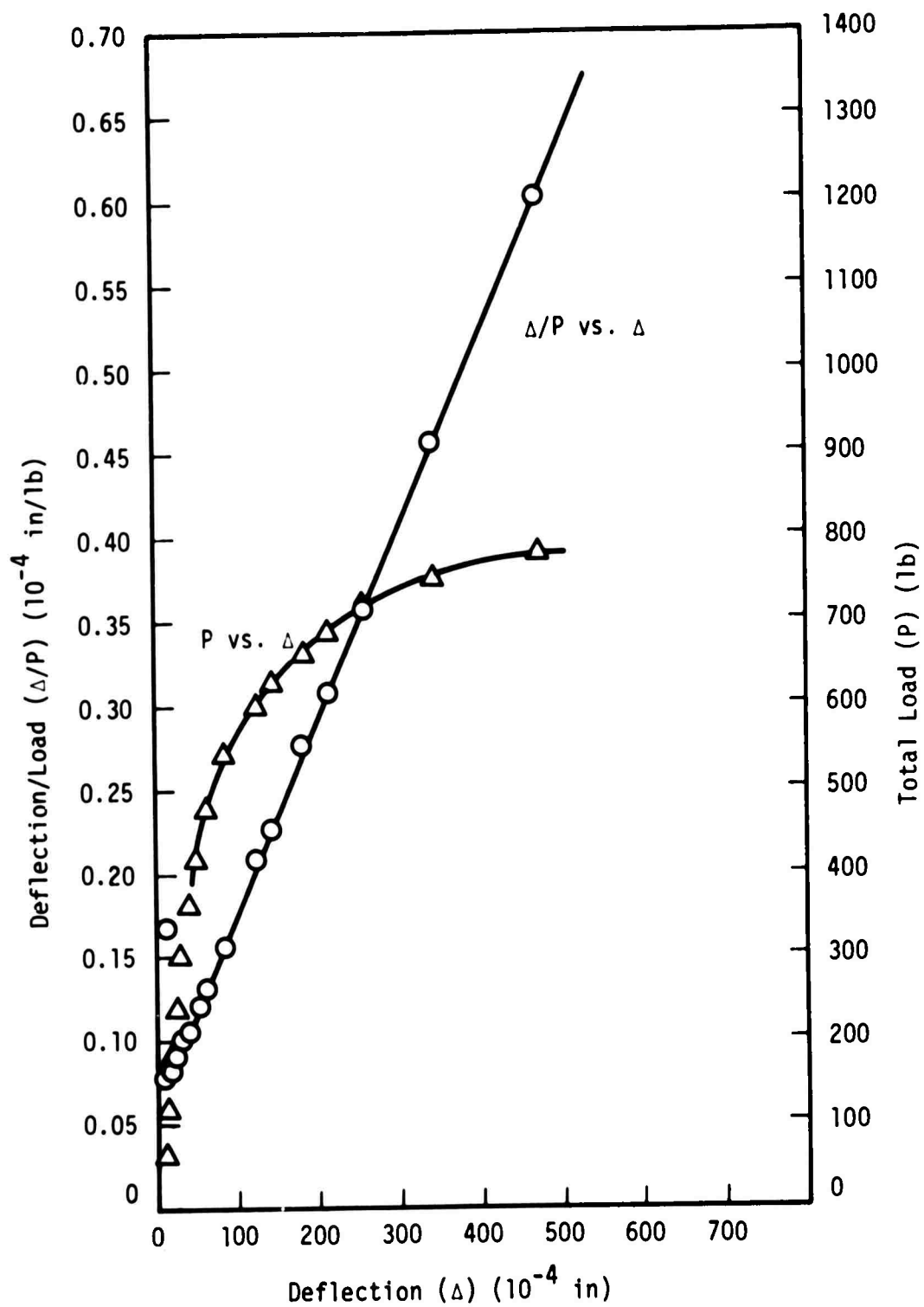


Figure 75. Southwell Plot and Load Deflection Curve
for Plate No. 406, 2 Sides Supported

TABLE 83
DATA AND CALCULATIONS FOR PLATE NO. 406,
4 SIDES SUPPORTED

| Total Load (P) (lb.) | Deflection (Δ) (10^{-4} in.) | Total Load/Deflection (Δ/P) (10^{-4} in./lb.) |
|-------------------------|---|--|
| 0 | 0 | 0 |
| 500 | 33 | .0660 |
| 1000 | 60 | .0600 |
| 1500 | 99 | .0660 |
| 1750 | 121 | .0692 |
| 2000 | 150 | .0750 |
| 2200 | 180 | .0818 |
| 2400 | 215 | .0895 |
| 2600 | 270 | .1036 |
| 2800 | 347 | .1240 |
| 3000 | 447 | .1490 |

TABLE 84
MODE SHAPE FOR PLATE NO. 406,
4 SIDES SUPPORTED, 10^{-4} in.

| | | | | | | |
|-----|-----|-----|-----|-----|-----|-----|
| 170 | 234 | 255 | 243 | 201 | 152 | 102 |
| 154 | 248 | 294 | 336 | 310 | 254 | 168 |
| 56 | 137 | 199 | 242 | 268 | 244 | 186 |

Note: See Figure 9.

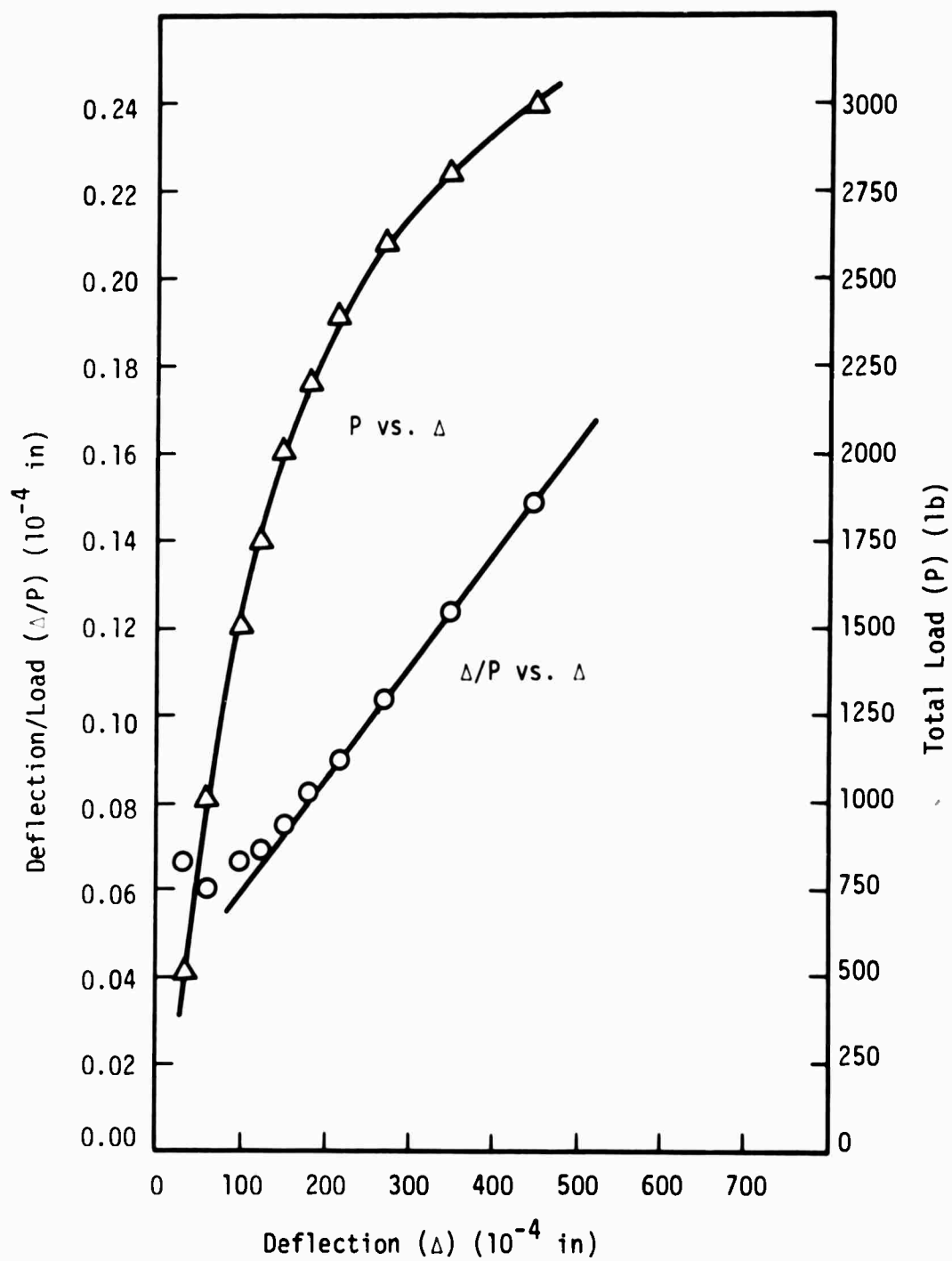


Figure 76. Southwell Plot and Load Deflection Curve
for Plate No. 406, 4 Sides Supported

TABLE 85
DATA AND CALCULATIONS FOR PLATE NO. 407,
2 SIDES SUPPORTED

| Total Load (P) (lb.) | Deflection (Δ) (10^{-4} in.) | Total Load/Deflection (Δ/P) (10^{-4} in./lb.) |
|-------------------------|---|--|
| 0 | 0 | 0 |
| 12 | 8 | .67 |
| 24 | 41 | 1.71 |
| 36 | 83 | 2.30 |
| 48 | 126 | 2.62 |
| 60 | 169 | 2.81 |
| 72 | 199 | 2.77 |
| 84 | 247 | 2.94 |
| 96 | 296 | 3.08 |
| 108 | 360 | 3.33 |
| 120 | 423 | 3.53 |

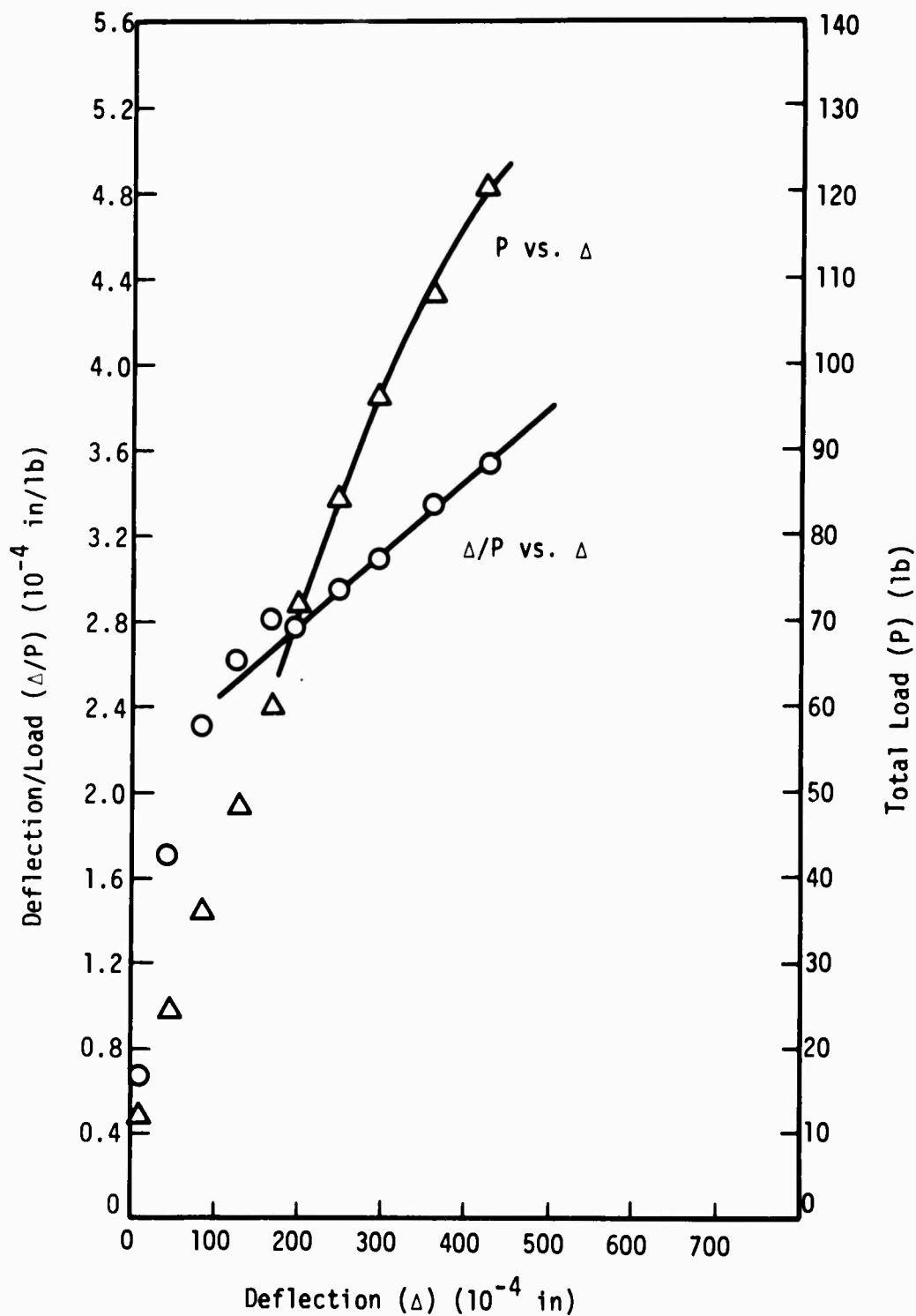


Figure 77. Southwell Plot and Load Deflection Curve
for Plate No. 407, 2 Sides Supported

TABLE 86
DATA AND CALCULATIONS FOR PLATE NO. 407,
4 SIDES SUPPORTED

| Total Load (P) (lb.) | Deflection (Δ) (10^{-4} in.) | Total Load/Deflection (Δ/P) (10^{-4} in./lb.) |
|-------------------------|---|--|
| 0 | 0 | 0 |
| 500 | 8 | .0160 |
| 1000 | 33 | .0330 |
| 1500 | 66 | .0440 |
| 2000 | 112 | .0560 |
| 2250 | 142 | .0631 |
| 2500 | 176 | .0703 |
| 2750 | 235 | .0853 |
| 3000 | 335 | .1116 |

TABLE 87
MODE SHAPE FOR PLATE NO. 407,
4 SIDES SUPPORTED, 10^{-4} in.

| | | | | | | |
|------|------|------|------|------|------|------|
| 159 | 229 | 272 | 262 | 228 | 160 | 74 |
| 56 | 27 | 10 | - 82 | -126 | -158 | -162 |
| -243 | -326 | -375 | -391 | -357 | -289 | -210 |

Note: See Figure 9.

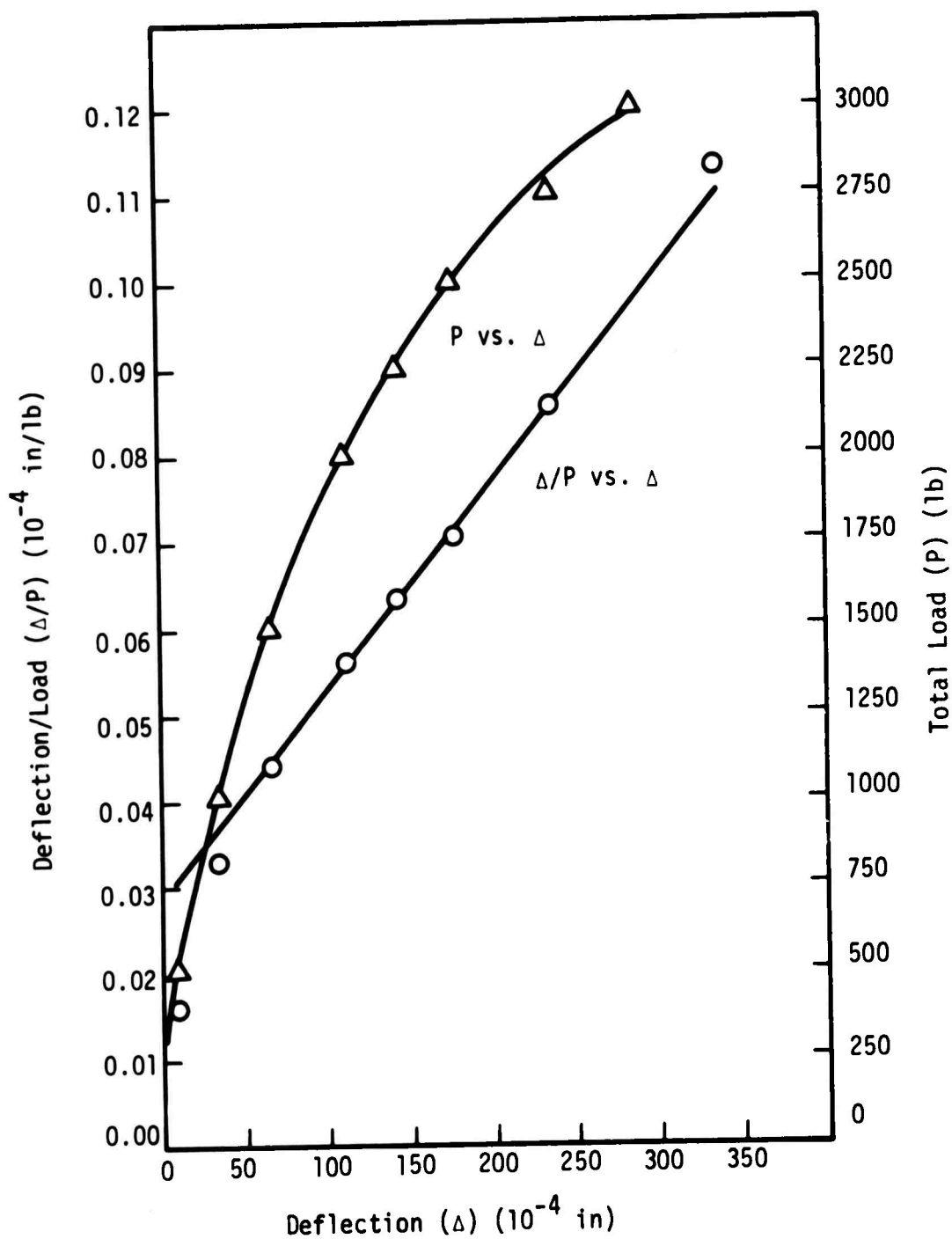


Figure 78. Southwell Plot and Load Deflection Curve
for Plate No. 407, 4 Sides Supported

TABLE 88
DATA AND CALCULATIONS FOR PLATE NO. 408a,
2 SIDES SUPPORTED

| Total Load (P) (lb.) | Deflection (Δ) (10^{-4} in.) | Total Load/Deflection (Δ/P) (10^{-4} in./lb.) |
|-------------------------|---|--|
| 0 | 0 | 0 |
| 24 | --- | --- |
| 48 | 3 | .063 |
| 72 | 16 | .222 |
| 96 | 37 | .385 |
| 120 | 72 | .600 |
| 144 | 112 | .778 |
| 168 | 168 | 1.000 |
| 180 | 199 | 1.105 |
| 192 | 237 | 1.234 |
| 204 | 273 | 1.338 |
| 216 | 315 | 1.458 |
| 228 | 376 | 1.650 |
| 240 | 441 | 1.835 |

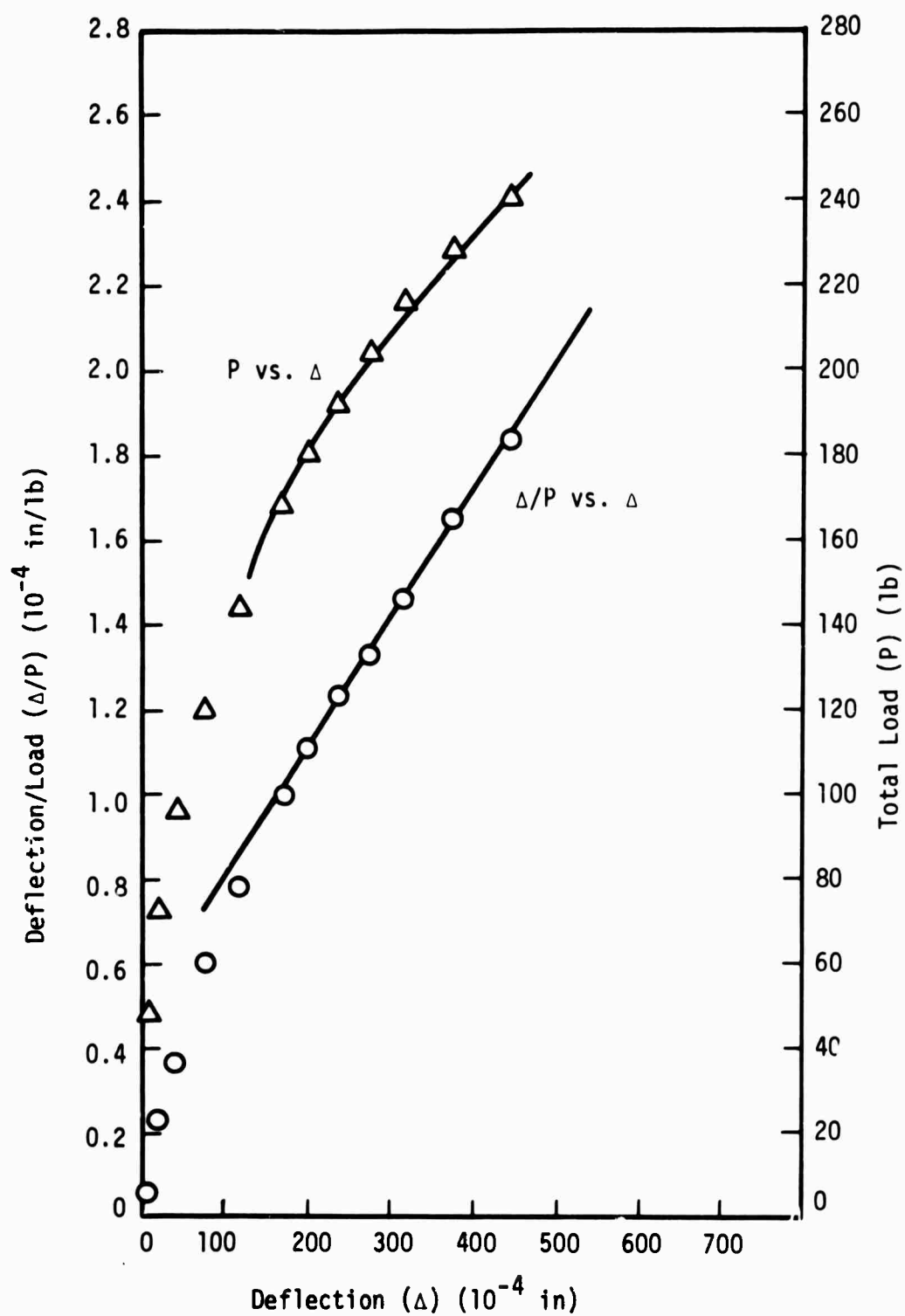


Figure 79. Southwell Plot and Load Deflection Curve for Plate No. 408a, 2 Sides Supported

TABLE 89
DATA AND CALCULATIONS FOR PLATE NO. 408b,
2 SIDES SUPPORTED

| Total Load (P) (lb.) | Deflection (Δ) (10^{-4} in.) | Total Load/Deflection (Δ/P) (10^{-4} in./lb.) |
|-------------------------|---|--|
| 0 | 0 | 0 |
| 60 | 33 | .550 |
| 120 | 58 | .483 |
| 180 | 103 | .572 |
| 204 | 133 | .652 |
| 228 | 168 | .737 |
| 252 | 215 | .853 |
| 264 | 253 | .958 |
| 276 | 288 | 1.042 |
| 288 | 333 | 1.156 |
| 300 | 372 | 1.239 |
| 312 | 425 | 1.361 |

TABLE 90
MODE SHAPE FOR PLATE NO. 408b,
2 SIDES SUPPORTED, 10^{-4} in.

| | | | | | | |
|-----|-----|-----|-----|-----|-----|-----|
| 166 | 165 | 154 | 166 | 173 | 188 | 205 |
| 179 | 185 | 194 | 203 | 215 | 227 | 250 |
| 130 | 126 | 142 | 149 | 155 | 170 | 185 |

Note: See Figure 9.

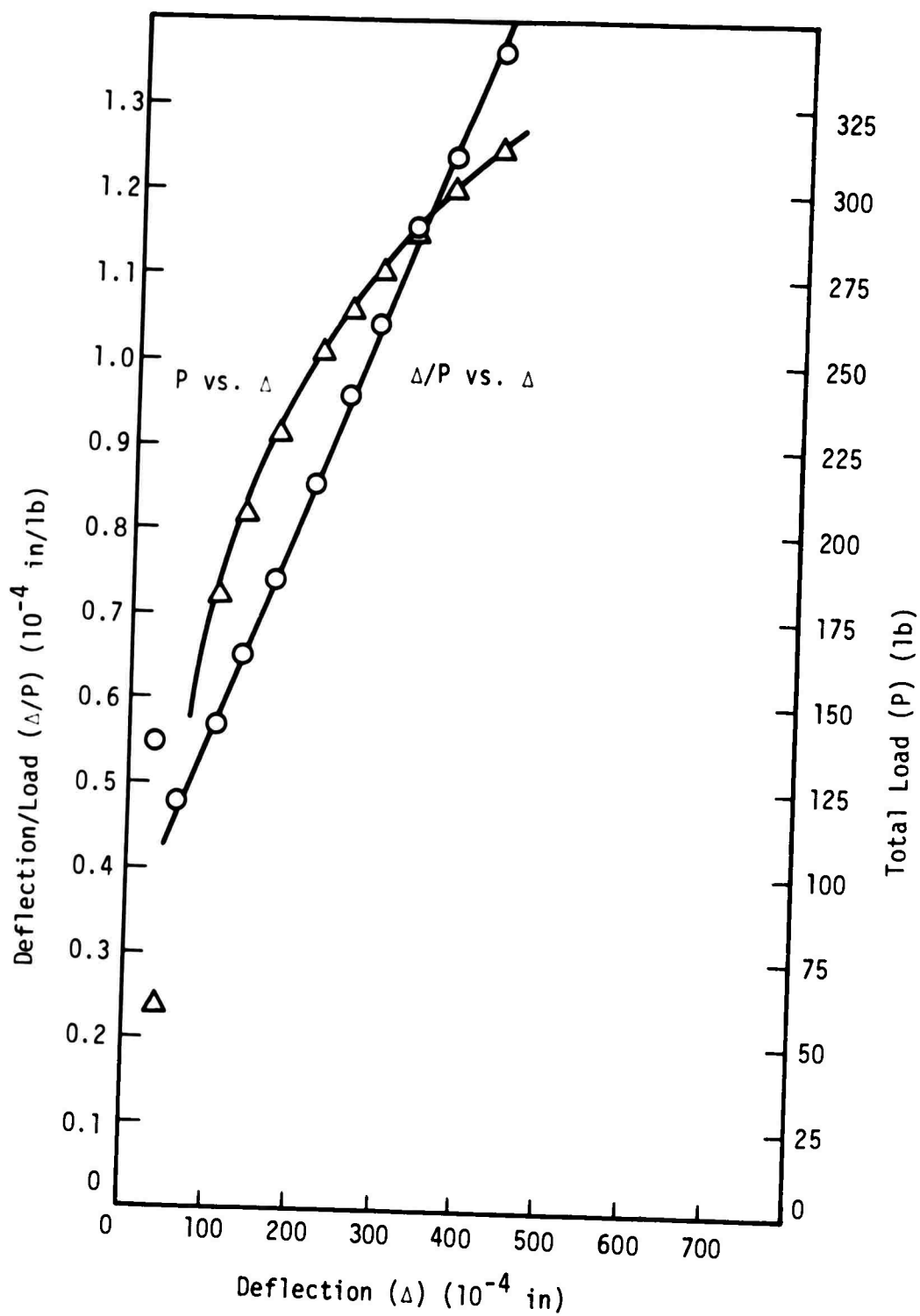


Figure 80. Southwell Plot and Load Deflection Curve
for Plate No. 408b, 2 Sides Supported

TABLE 91
DATA AND CALCULATIONS FOR PLATE NO. 408a,
4 SIDES SUPPORTED

| Total Load (P) (lb.) | Deflection (Δ) (10^{-4} in.) | Total Load/Deflection (Δ/P) (10^{-4} in./lb.) |
|-------------------------|---|--|
| 0 | 0 | 0 |
| 250 | 15 | .0600 |
| 500 | 31 | .06200 |
| 750 | 45 | .0643 |
| 1000 | 60 | .0600 |
| 1250 | 75 | .0600 |
| 1500 | 98 | .0653 |
| 1750 | 124 | .0708 |
| 2000 | 155 | .0776 |
| 2250 | 196 | .0871 |
| 2400 | 233 | .0970 |
| 2500 | 267 | .1068 |
| 2600 | 309 | .1187 |
| 2700 | 363 | .1345 |
| 2800 | 413 | .1475 |

TABLE 92
MODE SHAPE FOR PLATE NO. 408a,
4 SIDES SUPPORTED, 10^{-4} in.

| | | | | | | |
|-----|-----|-----|-----|-----|-----|-----|
| 37 | 68 | 104 | 116 | 142 | 141 | 131 |
| 95 | 164 | 232 | 249 | 254 | 227 | 175 |
| 168 | 243 | 272 | 280 | 251 | 204 | 129 |

Note: See Figure 9.

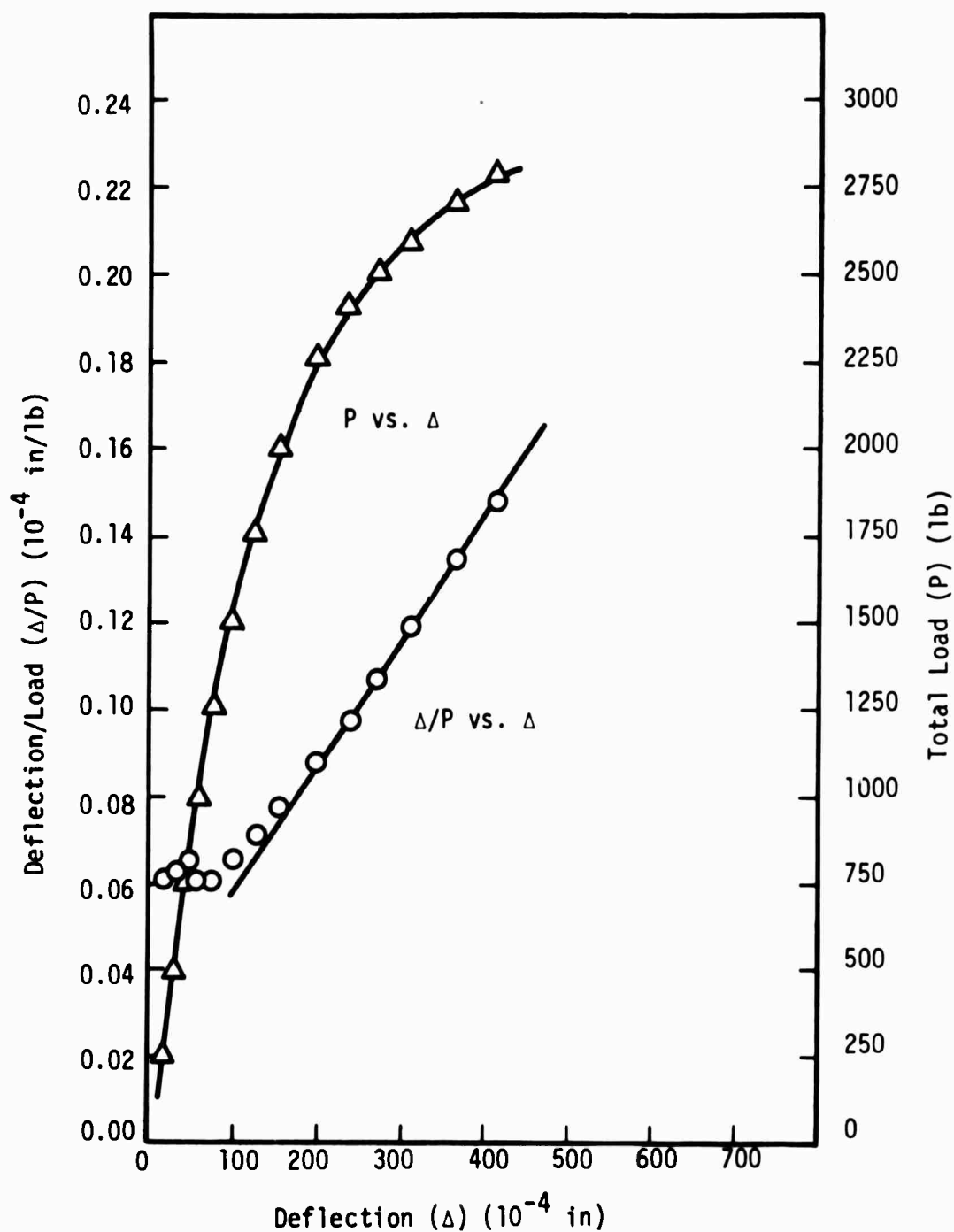


Figure 81. Southwell Plot and Load Deflection Curve
for Plate No. 408a, 4 Sides Supported

TABLE 93
DATA AND CALCULATIONS FOR PLATE NO. 408b,
4 SIDES SUPPORTED

| Total Load (P) (lb.) | Deflection (Δ) (10^{-4} in.) | Total Load/Deflection (Δ/P) (10^{-4} in./lb.) |
|-------------------------|---|--|
| 0 | 0 | 0 |
| 250 | 19 | .0760 |
| 500 | 34 | .0680 |
| 750 | 51 | .0680 |
| 1000 | 76 | .0760 |
| 1250 | 105 | .0840 |
| 1500 | 140 | .0933 |
| 1700 | 176 | .1035 |
| 1900 | 218 | .1147 |
| 2000 | 240 | .1200 |
| 2100 | 270 | .1285 |
| 2200 | 302 | .1375 |
| 2300 | 345 | .1500 |
| 2400 | 387 | .1614 |
| 2500 | 440 | .1760 |

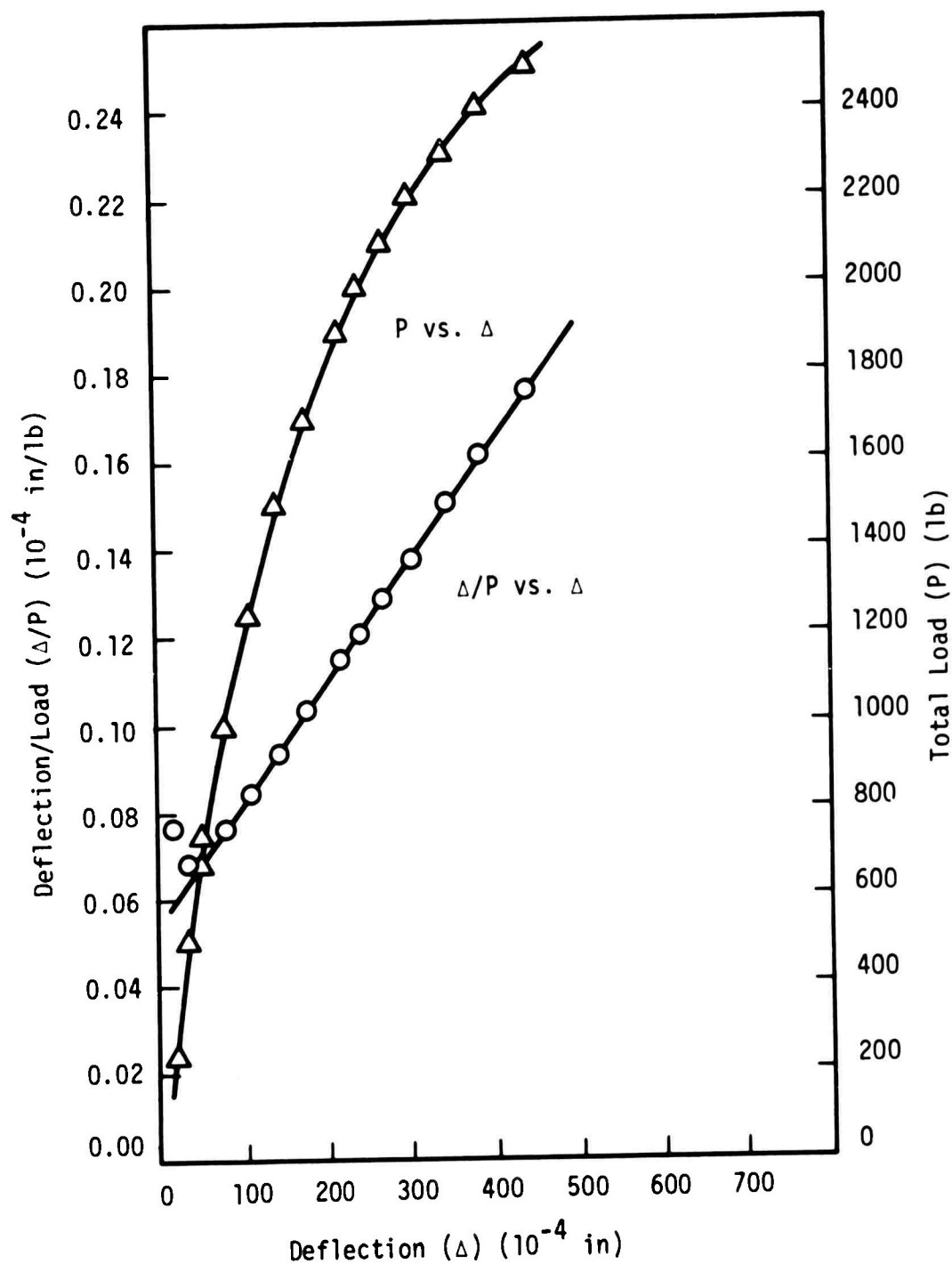


Figure 82. Southwell Plot and Load Deflection Curve
for Plate No. 408b, 4 Sides Supported

TABLE 94
DATA AND CALCULATIONS FOR PLATE NO. 409a,
2 SIDES SUPPORTED

| Total Load (P) (lb.) | Deflection (Δ) (10^{-4} in.) | Total Load/Deflection (Δ/P) (10^{-4} in./lb.) |
|-------------------------|---|--|
| 0 | 0 | 0 |
| 50 | 0 | 0 |
| 100 | 14 | .140 |
| 150 | 30 | .200 |
| 200 | 53 | .265 |
| 225 | 67 | .297 |
| 250 | 74 | .296 |
| 275 | 91 | .331 |
| 300 | 125 | .417 |
| 325 | 223 | .686 |
| 335 | 280 | .836 |
| 345 | 368 | 1.067 |
| 350 | 453 | 1.295 |

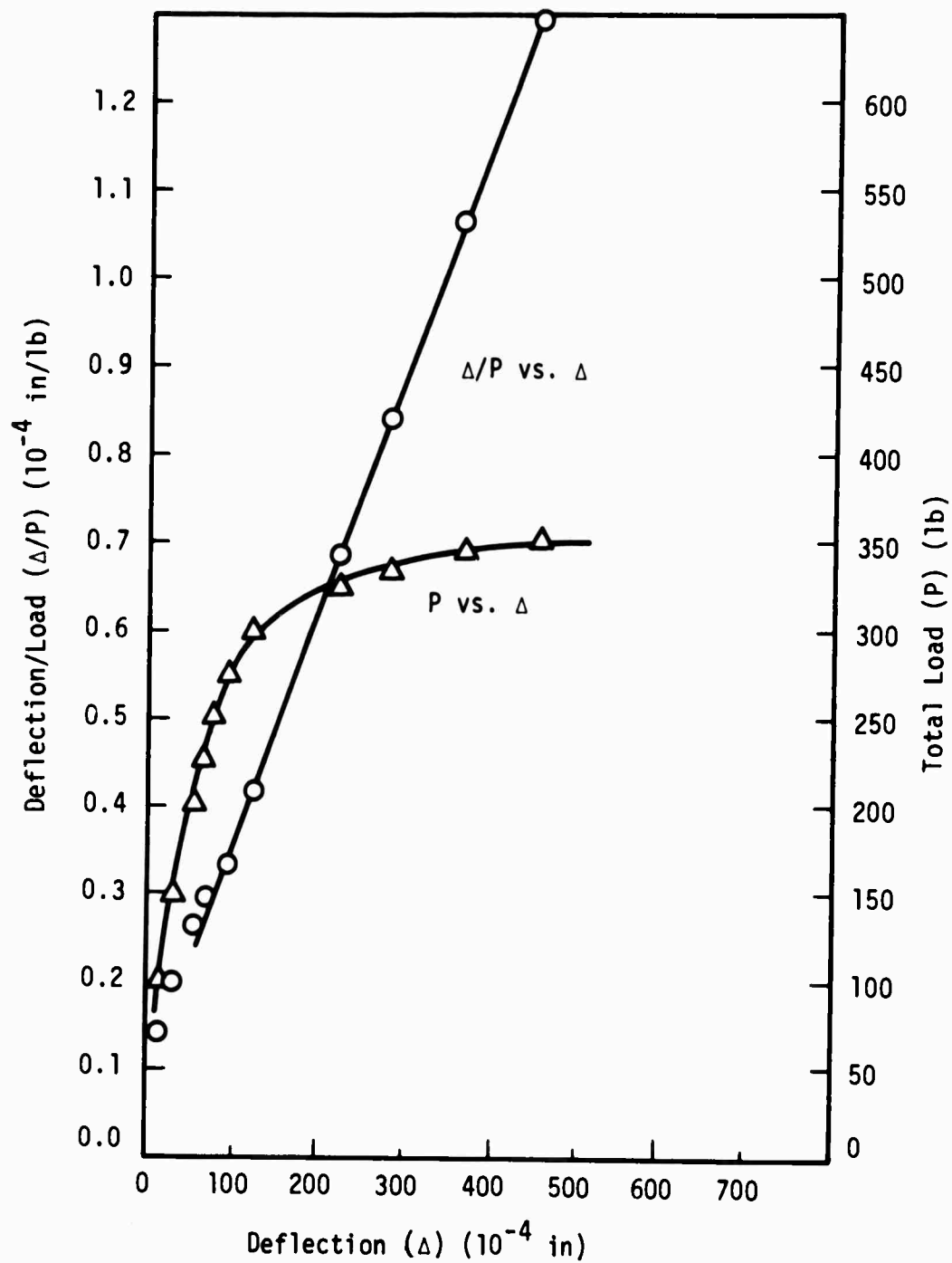


Figure 83. Southwell Plot and Load Deflection Curve
for Plate No. 409a, 2 Sides Supported

TABLE 95
DATA AND CALCULATIONS FOR PLATE NO. 409b,
2 SIDES SUPPORTED

| Total Load (P) (lb.) | Deflection (Δ) (10^{-4} in.) | Total Load/Deflection (Δ/P) (10^{-4} in./lb.) |
|-------------------------|---|--|
| 0 | 0 | 0 |
| 50 | 33 | .660 |
| 100 | 36 | .360 |
| 150 | 43 | .287 |
| 200 | 89 | .445 |
| 225 | 121 | .538 |
| 250 | 170 | .679 |
| 275 | 257 | .933 |
| 290 | 326 | 1.124 |
| 300 | 401 | 1.337 |
| 310 | 503 | 1.621 |

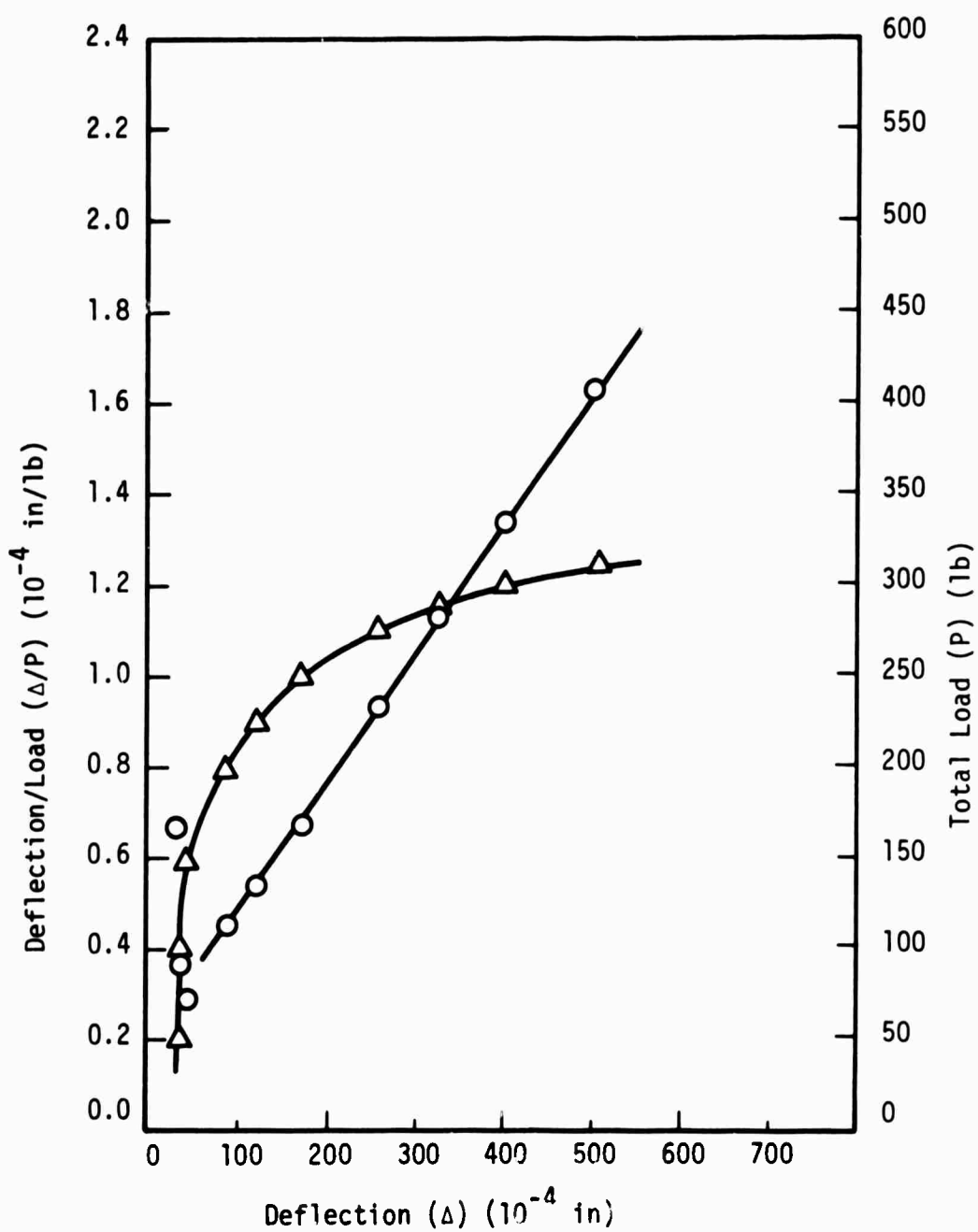


Figure 84. Southwell Plot and Load Deflection Curve
for Plate No. 409b, 2 Sides Supported

TABLE 96
DATA AND CALCULATIONS FOR PLATE NO. 409a,
4 SIDES SUPPORTED

| Total Load (P) (lb.) | Deflection (Δ) (10^{-4} in.) | Total Load/Deflection (Δ/P) (10^{-4} in./lb.) |
|-------------------------|---|--|
| 0 | 0 | 0 |
| 250 | 19 | .0761 |
| 500 | 34 | .0679 |
| 750 | 51 | .0679 |
| 1000 | 71 | .0710 |
| 1250 | 101 | .0808 |
| 1500 | 140 | .0933 |
| 1600 | 156 | .0975 |
| 1700 | 176 | .1035 |
| 1800 | 200 | .1112 |
| 1900 | 224 | .1180 |
| 2000 | 250 | .1250 |
| 2100 | 278 | .1325 |
| 2200 | 320 | .1456 |
| 2300 | 354 | .1539 |

TABLE 97
MODE SHAPE FOR PLATE NO. 409a,
4 SIDES SUPPORTED, 10^{-4} in.

| | | |
|-----|-----|-----|
| 96 | 152 | 103 |
| 142 | 213 | 152 |
| 137 | 199 | 145 |

Note: See Figure 9.

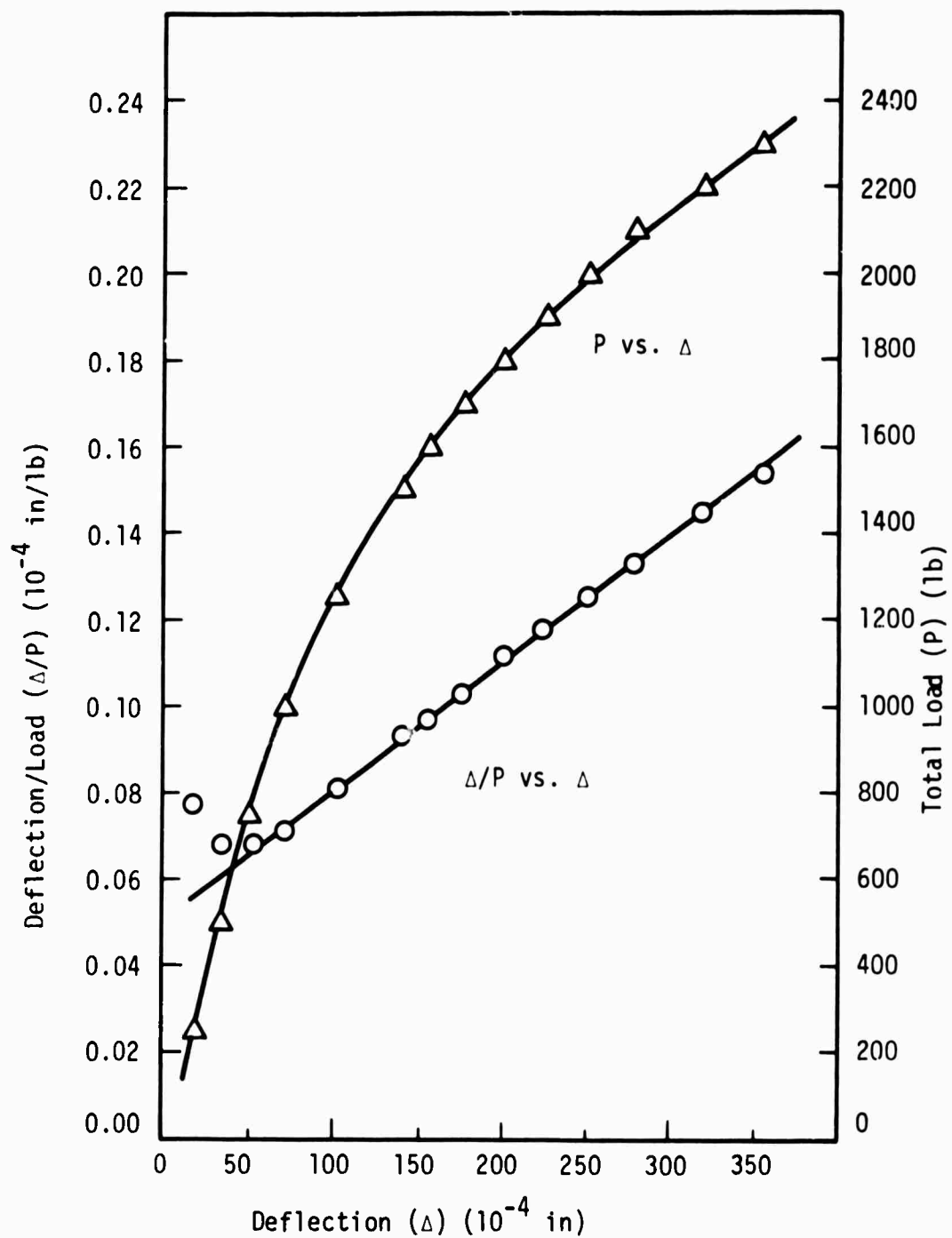


Figure 85. Southwell Plot and Load Deflection Curve
for Plate No. 409a, 4 Sides Supported

TABLE 98
DATA AND CALCULATIONS FOR PLATE NO. 409b,
4 SIDES SUPPORTED

| Total Load (P) (lb.) | Deflection (Δ) (10^{-4} in.) | Total Load/Deflection (Δ/P) (10^{-4} in./lb.) |
|-------------------------|---|--|
| 0 | 0 | 0 |
| 250 | 31 | .1240 |
| 500 | 46 | .0920 |
| 750 | 63 | .0840 |
| 1000 | 81 | .0810 |
| 1250 | 101 | .0808 |
| 1500 | 134 | .0893 |
| 1600 | 150 | .0938 |
| 1700 | 166 | .0977 |
| 1800 | 188 | .1044 |
| 1900 | 208 | .1095 |
| 2000 | 226 | .1130 |
| 2100 | 254 | .1208 |
| 2200 | 278 | .1263 |
| 2300 | 316 | .1374 |

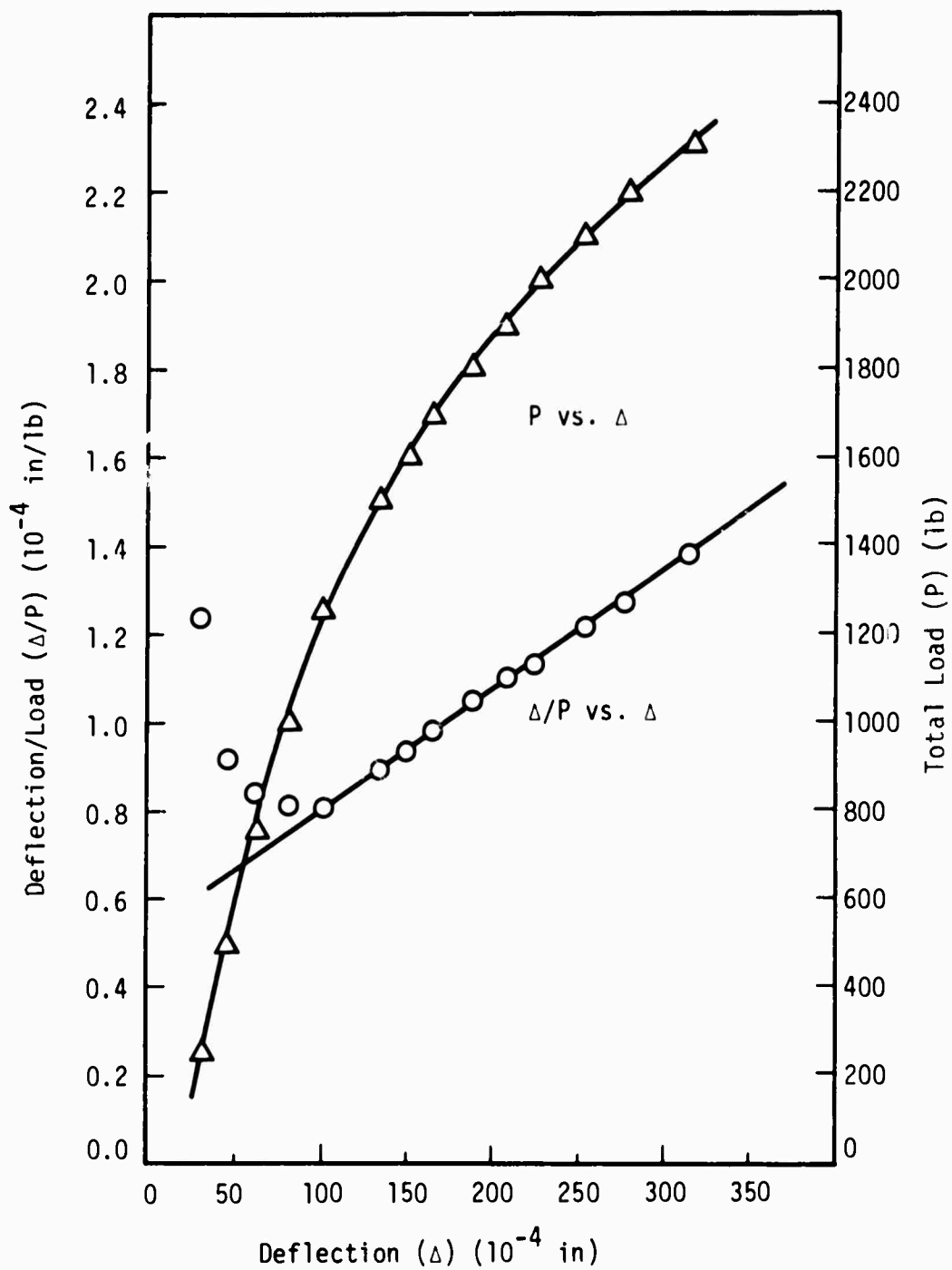


Figure 86. Southwell Plot and Load Deflection Curve
for Plate No. 409b, 4 Sides Supported

TABLE 99
DATA AND CALCULATIONS FOR PLATE NO. 501,
2 SIDES SUPPORTED

| Total Load (P) (lb.) | Deflection (Δ) (10 ⁻⁴ in.) | Total Load/Deflection (Δ/P) (10 ⁻⁴ in./lb.) |
|-------------------------|--|---|
| 6.4 | 0 | 0 |
| 20 | 1 | .050 |
| 30 | 8 | .267 |
| 40 | 17 | .425 |
| 50 | 25 | .500 |
| 60 | 35 | .583 |
| 70 | 44 | .628 |
| 80 | 61 | .763 |
| 90 | 92 | 1.020 |
| 100 | 127 | 1.270 |
| 110 | 196 | 1.780 |
| 115 | 257 | 2.23 |
| 120 | 390 | 3.25 |
| 125 | 675 | 5.40 |

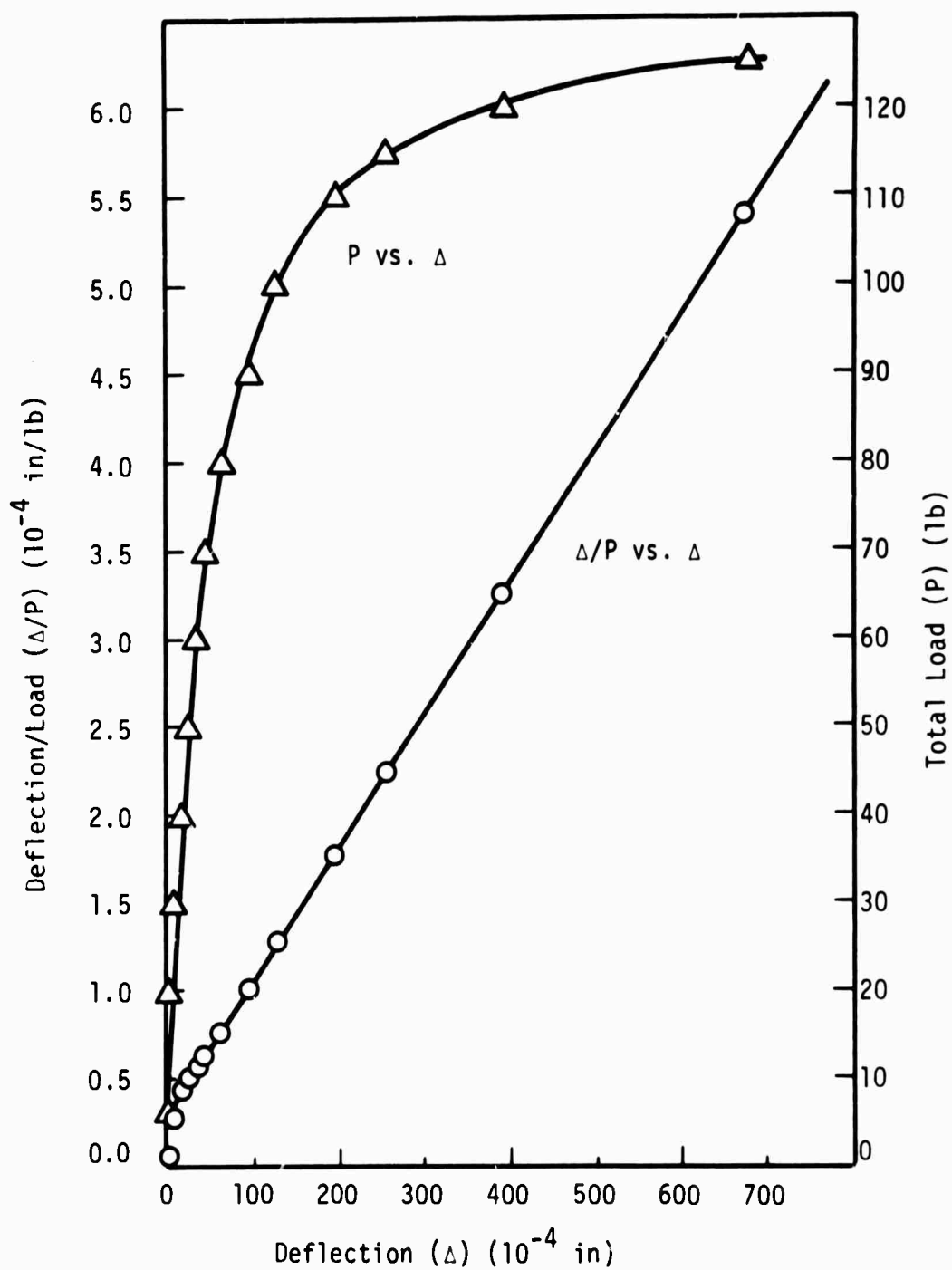


Figure 87. Southwell Plot and Load Deflection Curve
for Plate No. 501, 2 Sides Supported

TABLE 100
DATA AND CALCULATIONS FOR PLATE NO. 501,
4 SIDES SUPPORTED

| Total Load (P) (lb.) | Deflection (Δ) (10^{-4} in.) | Total Load/Deflection (Δ/P) (10^{-4} in./lb.) |
|-------------------------|---|--|
| 0 | 0 | 0 |
| 200 | 17 | .0850 |
| 400 | 41 | .1025 |
| 600 | 89 | .1485 |
| 700 | 122 | .1740 |
| 800 | 175 | .218 |
| 850 | 226 | .266 |
| 900 | 267 | .297 |
| 950 | 337 | .355 |
| 1000 | 430 | .430 |
| 1050 | 608 | .578 |

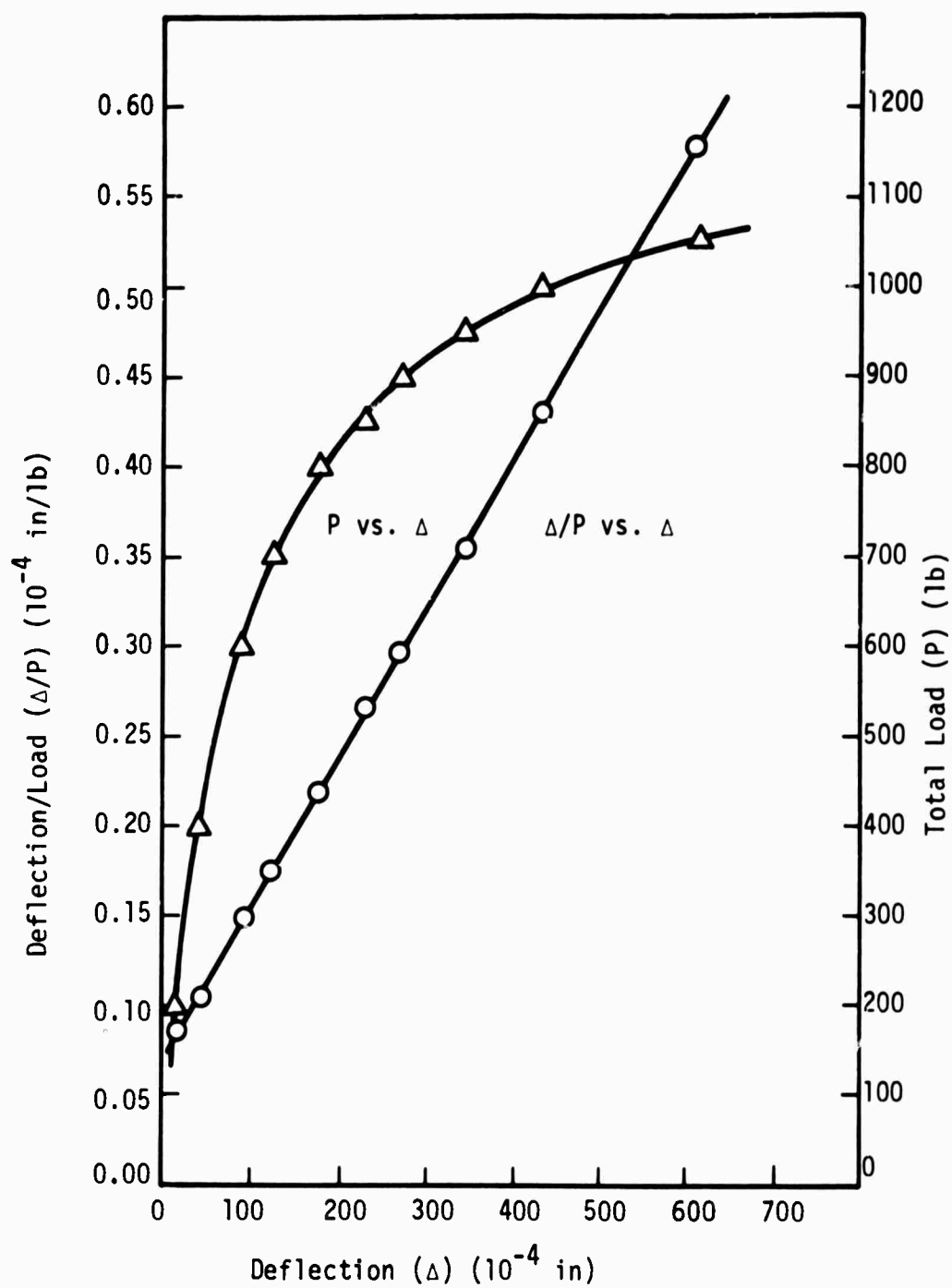


Figure 88. Southwell Plot and Load Deflection Curve
for Plate No. 501, 4 Sides Supported

TABLE 101
DATA AND CALCULATIONS FOR PLATE NO. 502,
2 SIDES SUPPORTED

| Total Load (P) (lb.) | Deflection (Δ) (10^{-4} in.) | Total Load/Deflection (Δ/P) (10^{-4} in./lb.) |
|-------------------------|---|--|
| 0 | 0 | 0 |
| 50 | --- | --- |
| 100 | 10 | .100 |
| 150 | 27 | .180 |
| 200 | 53 | .265 |
| 225 | 74 | .329 |
| 250 | 102 | .408 |
| 275 | 143 | .520 |
| 300 | 208 | .693 |
| 310 | 258 | .833 |
| 320 | 336 | 1.050 |
| 330 | 422 | 1.280 |
| 340 | 605 | 1.780 |

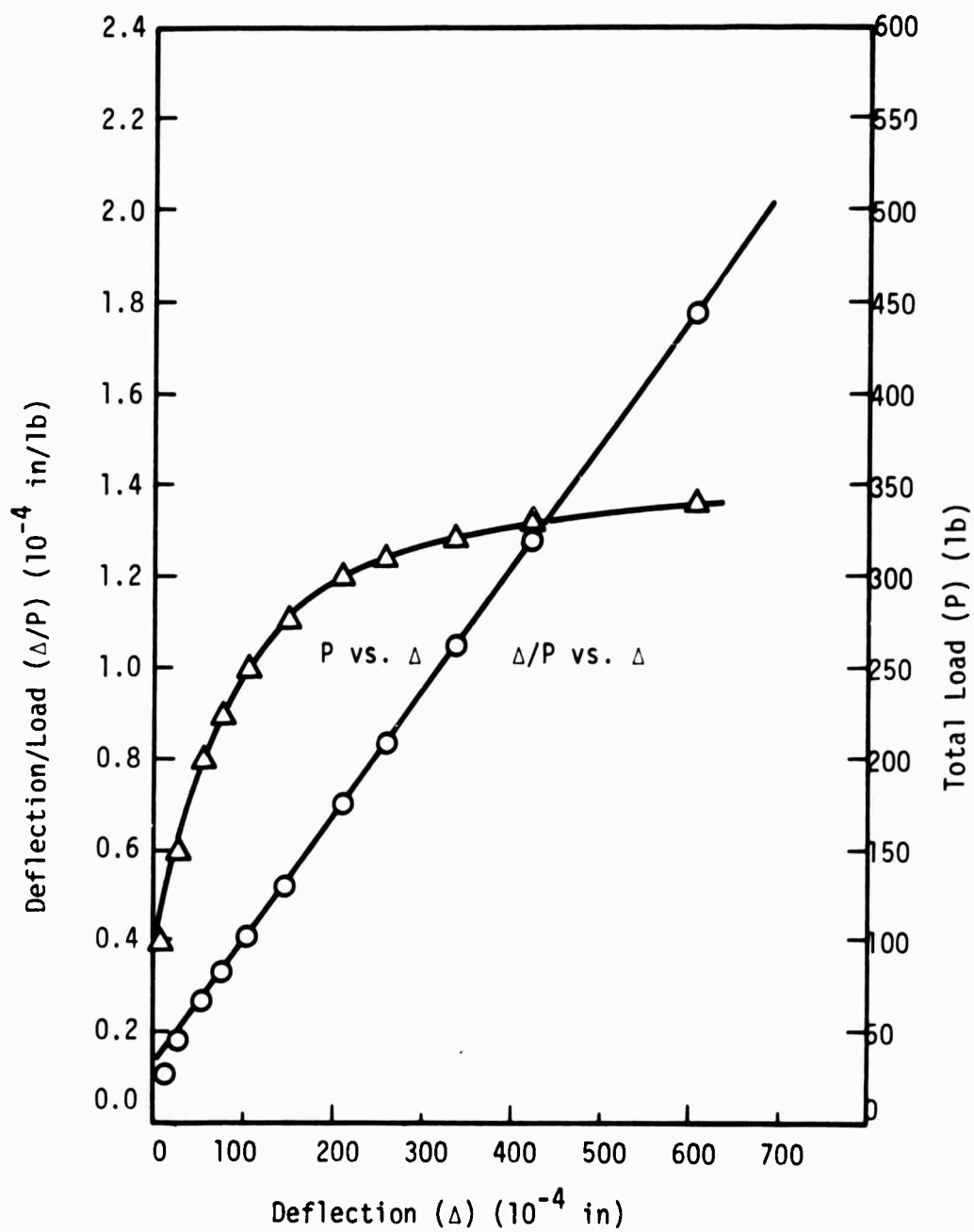


Figure 89. Southwell Plot and Load Deflection Curve
for Plate No. 502, 2 Sides Supported

TABLE 102
DATA AND CALCULATIONS FOR PLATE NO. 502,
4 SIDES SUPPORTED

| Total Load (P) (lb.) | Deflection (Δ) (10^{-4} in.) | Total Load/Deflection (Δ/P) (10^{-4} in./lb.) |
|-------------------------|---|--|
| 0 | 0 | 0 |
| 200 | 33 | .1650 |
| 400 | 75 | .1875 |
| 500 | 109 | .218 |
| 600 | 166 | .277 |
| 650 | 206 | .317 |
| 700 | 260 | .371 |
| 750 | 330 | .439 |
| 800 | 421 | .527 |
| 850 | 518 | .610 |
| 900 | 675 | .750 |

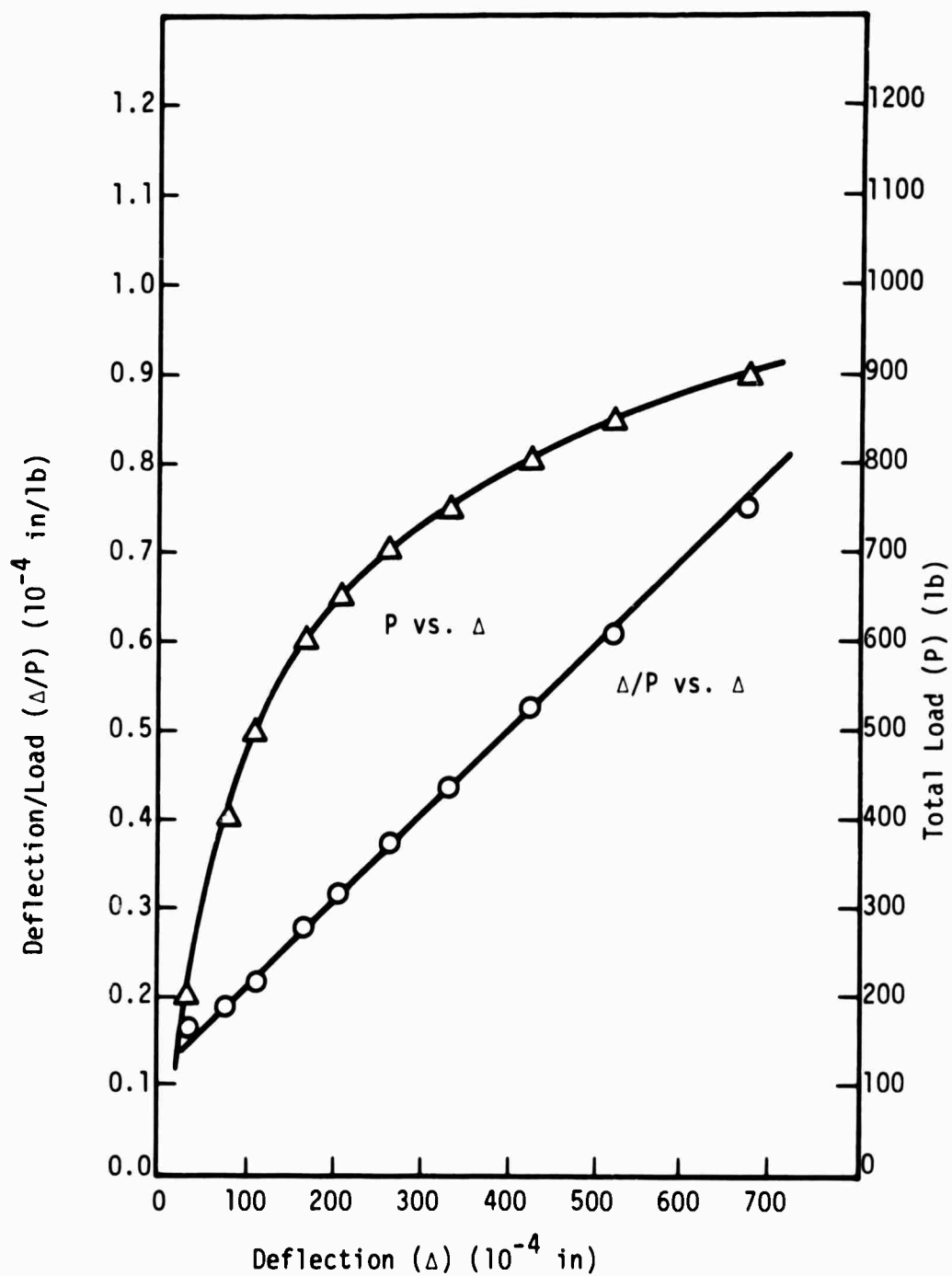


Figure 90. Southwell Plot and Load Deflection Curve
for Plate No. 502, 4 Sides Supported

TABLE 103
DATA AND CALCULATIONS FOR PLATE NO. 503,
2 SIDES SUPPORTED

| Total Load (P) (lb.) | Deflection (Δ) (10^{-4} in.) | Total Load/Deflection (Δ/P) (10^{-4} in./lb.) |
|-------------------------|---|--|
| 6.4 | 0 | 0 |
| 20 | 16 | .800 |
| 30 | 32 | 1.066 |
| 40 | 51 | 1.275 |
| 50 | 78 | 1.560 |
| 60 | 104 | 1.734 |
| 70 | 134 | 1.915 |
| 80 | 174 | 2.17 |
| 90 | 221 | 2.46 |
| 100 | 279 | 2.79 |
| 110 | 344 | 3.13 |
| 120 | 435 | 3.63 |
| 130 | 558 | 4.29 |
| 140 | 737 | 5.26 |

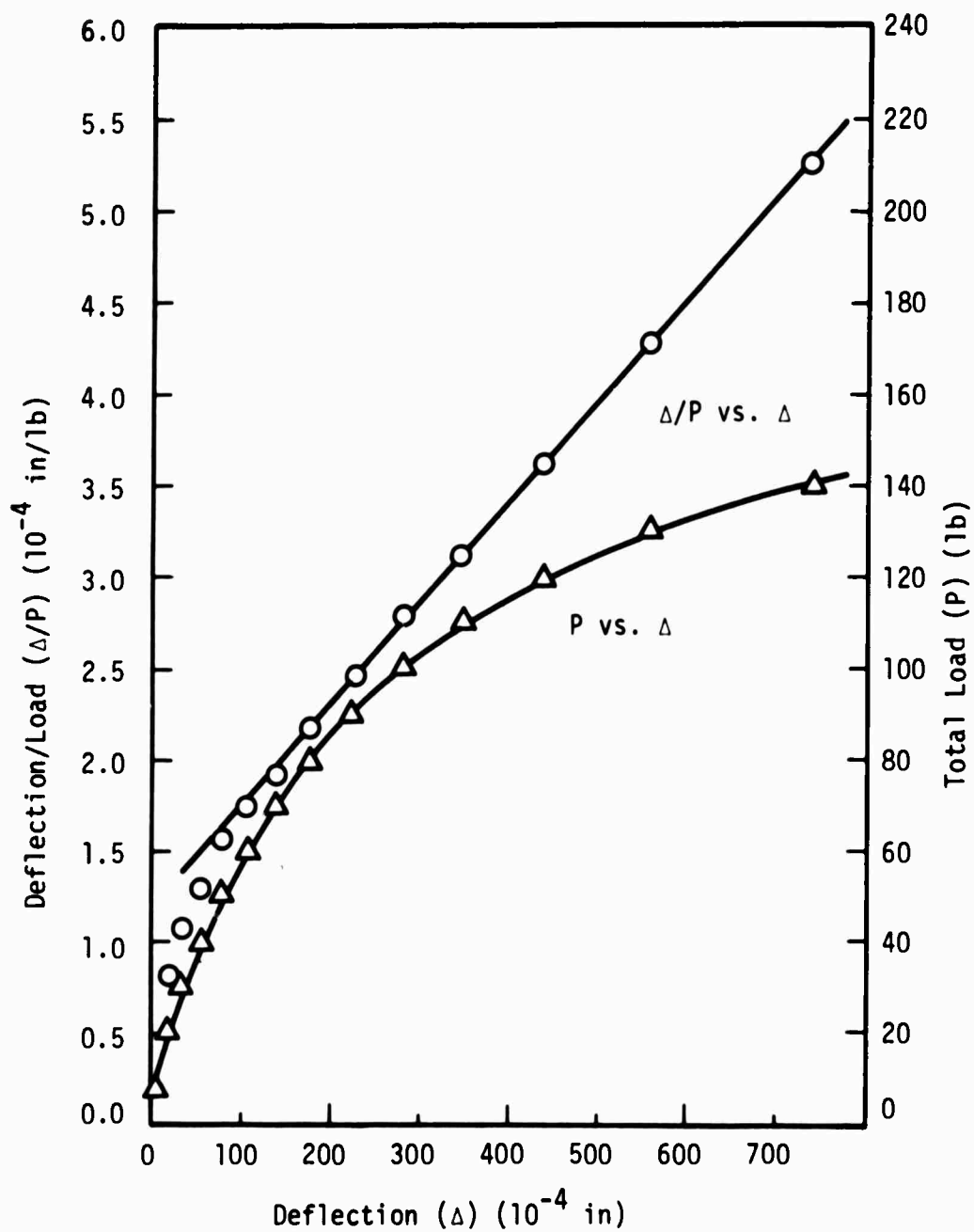


Figure 91. Southwell Plot and Load Deflection Curve
for Plate No. 503, 2 Sides Supported

TABLE 104
DATA AND CALCULATIONS FOR PLATE NO. 503,
4 SIDES SUPPORTED

| Total Load (P) (lb.) | Deflection (Δ) (10^{-4} in.) | Total Load/Deflection (Δ/P) (10^{-4} in./lb.) |
|-------------------------|---|--|
| 0 | 0 | 0 |
| 200 | 33 | .165 |
| 400 | 87 | .218 |
| 500 | 129 | .258 |
| 550 | 161 | .293 |
| 600 | 197 | .328 |
| 650 | 234 | .360 |
| 700 | 294 | .420 |
| 750 | 358 | .477 |
| 800 | 443 | .553 |
| 850 | 548 | .636 |
| 900 | 681 | .758 |

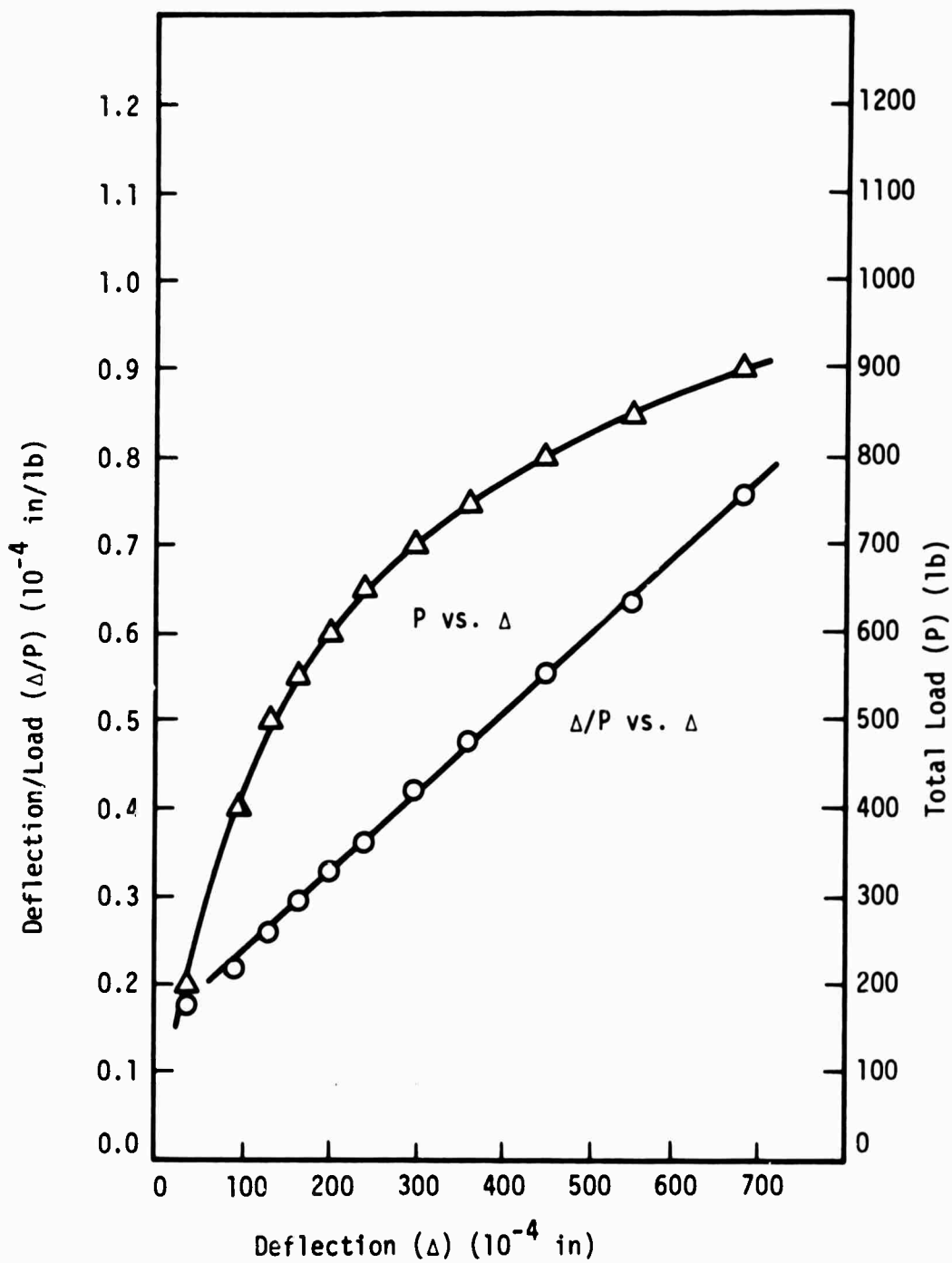


Figure 92. Southwell Plot and Load Deflection Curve
for Plate No. 503, 4 Sides Supported

TABLE 105
DATA AND CALCULATIONS FOR PLATE NO. 504,
2 SIDES SUPPORTED

| Total Load (P) (lb.) | Deflection (Δ) (10^{-4} in.) | Total Load/Deflection (Δ/P) (10^{-4} in./lb.) |
|-------------------------|---|--|
| 0 | 0 | 0 |
| 25 | --- | --- |
| 50 | 4 | .0800 |
| 75 | 7 | .0933 |
| 100 | 17 | .170 |
| 125 | 27 | .216 |
| 150 | 42 | .280 |
| 175 | 61 | .349 |
| 200 | 117 | .586 |
| 210 | 195 | .930 |
| 215 | 325 | 1.510 |

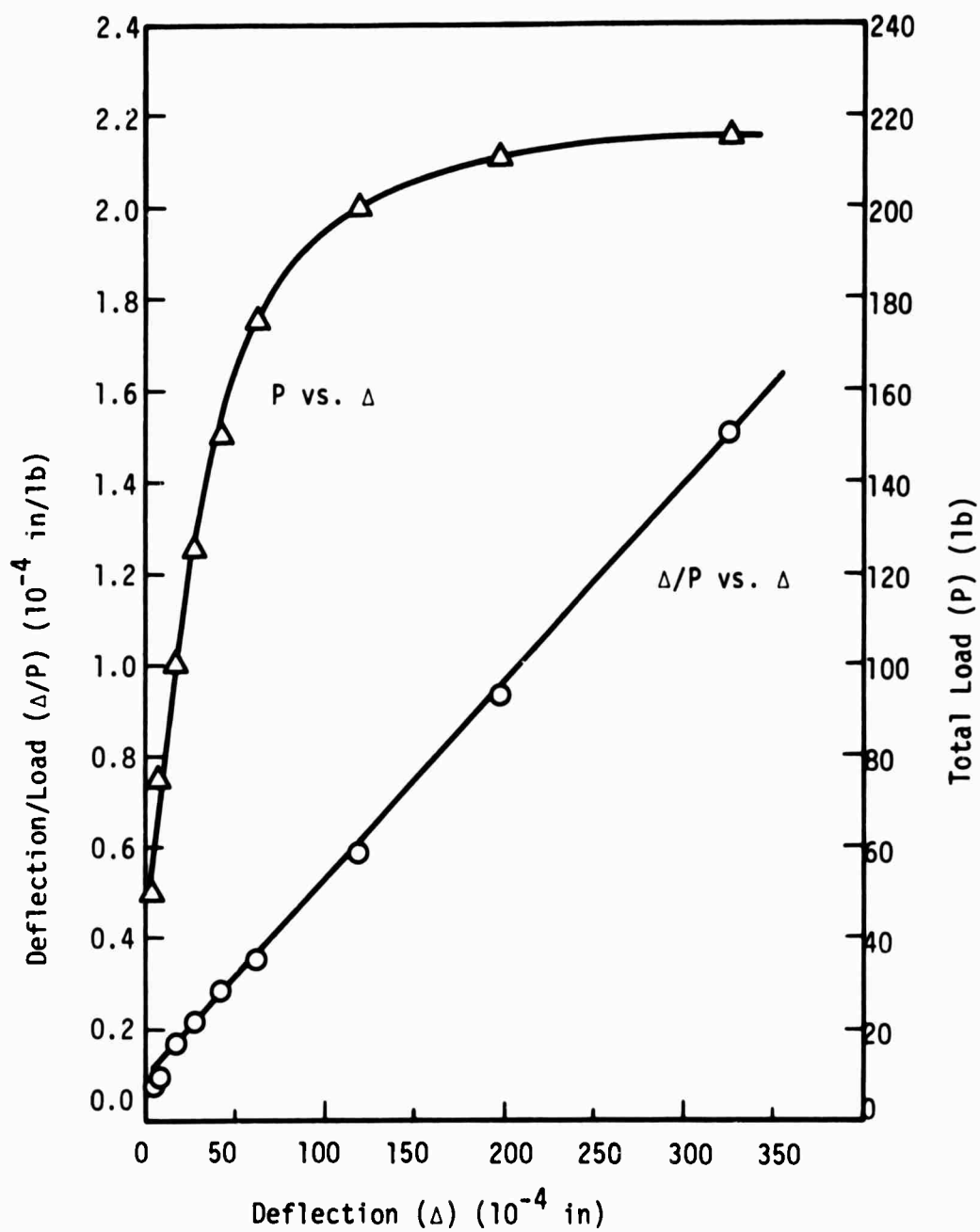


Figure 93. Southwell Plot and Load Deflection Curve
for Plate No. 504, 2 Sides Supported

TABLE 106
DATA AND CALCULATIONS FOR PLATE NO. 504,
4 SIDES SUPPORTED

| Total Load (P) (lb.) | Deflection (Δ) (10^{-4} in.) | Total Load/Deflection (Δ/P) (10^{-4} in./lb.) |
|-------------------------|---|--|
| 0 | 0 | 0 |
| 200 | 53 | .265 |
| 400 | 94 | .235 |
| 600 | 188 | .313 |
| 700 | 288 | .412 |
| 750 | 367 | .489 |
| 800 | 444 | .555 |
| 850 | 529 | .623 |
| 900 | 639 | .710 |
| 950 | 773 | .815 |

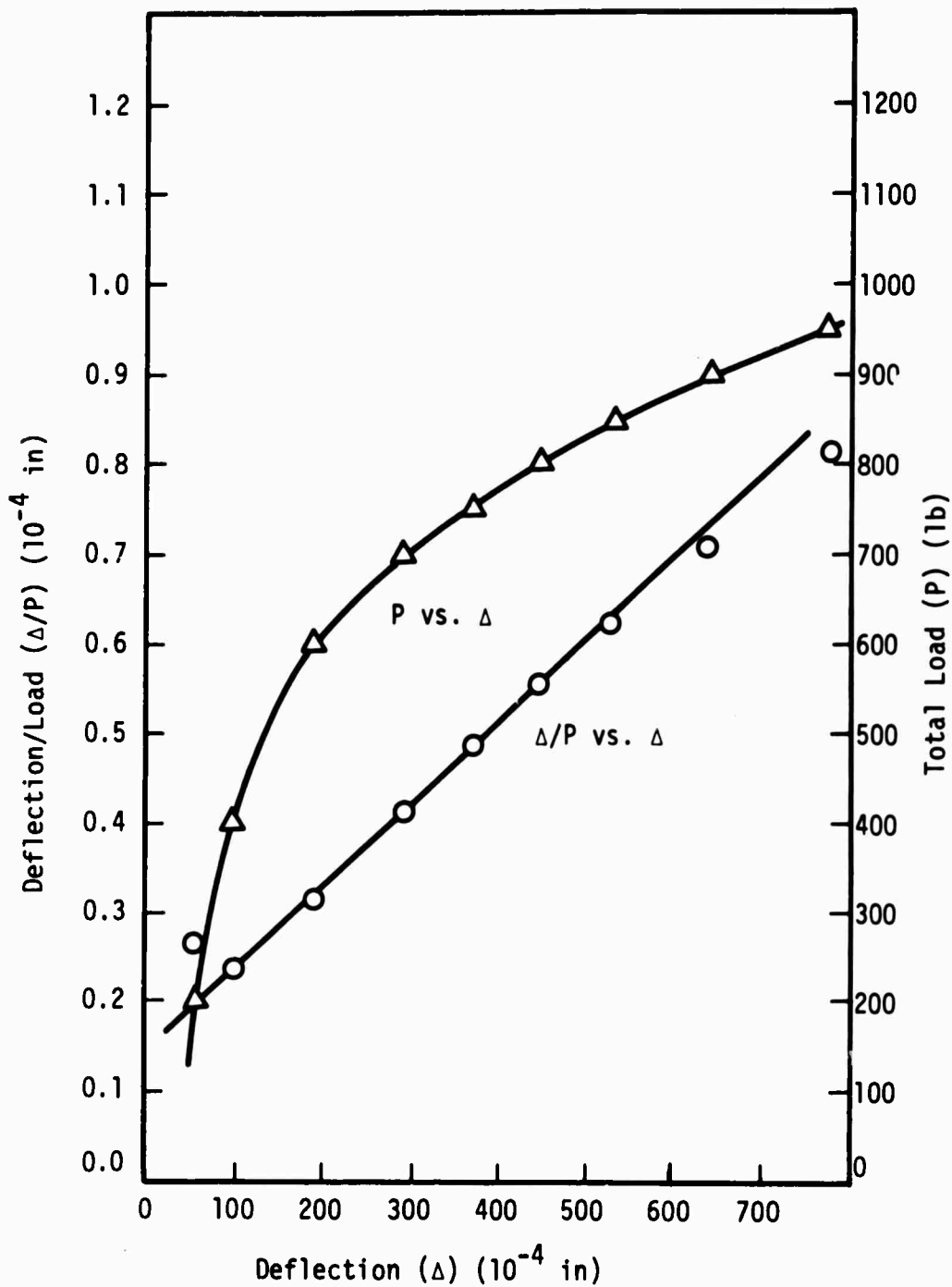


Figure 94. Southwell Plot and Load Deflection Curve
for Plate No. 504, 4 Sides Supported

TABLE 107
DATA AND CALCULATIONS FOR PLATE NO. 505,
2 SIDES SUPPORTED

| Total Load (P) (lb.) | Deflection (Δ) (10^{-4} in.) | Total Load/Deflection (Δ/P) (10^{-4} in./lb.) |
|-------------------------|---|--|
| 6.4 | 0 | 0 |
| 20 | 22 | 1.100 |
| 30 | 35 | 1.167 |
| 40 | 56 | 1.400 |
| 50 | 71 | 1.420 |
| 60 | 92 | 1.532 |
| 70 | 123 | 1.758 |
| 80 | 161 | 2.02 |
| 90 | 230 | 2.56 |
| 100 | 352 | 3.52 |
| 110 | 690 | 6.27 |

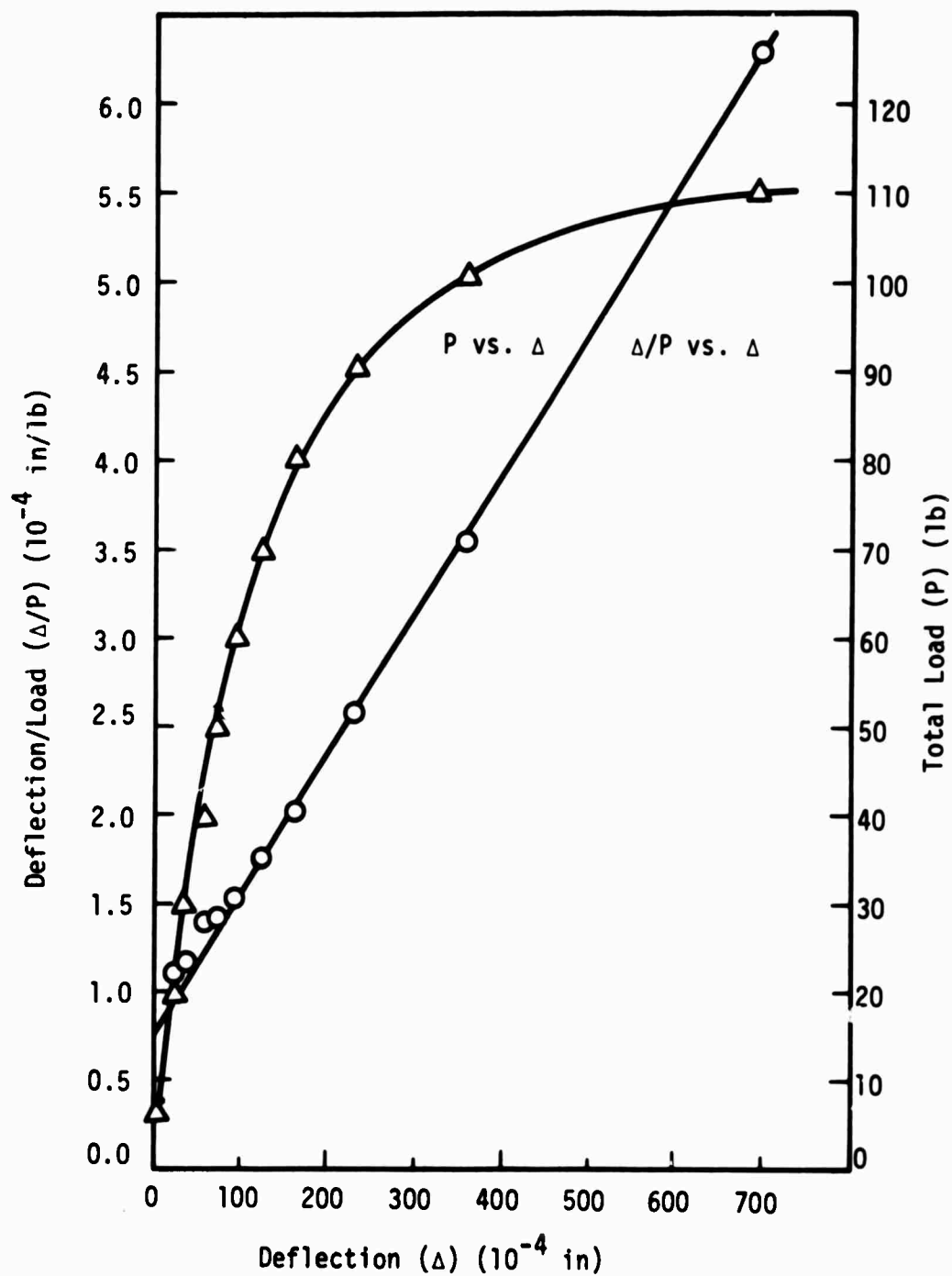


Figure 95. Southwell Plot and Load Deflection Curve
for Plate No. 505, 2 Sides Supported

TABLE 108
DATA AND CALCULATIONS FOR PLATE NO. 505,
4 SIDES SUPPORTED

| Total Load (P) (lb.) | Deflection (Δ) (10^{-4} in.) | Total Load/Deflection (Δ/P) (10^{-4} in./lb.) |
|-------------------------|---|--|
| 0 | 0 | 0 |
| 100 | 6 | .0600 |
| 200 | 11 | .0550 |
| 300 | 18 | .0600 |
| 400 | 28 | .0700 |
| 500 | 43 | .0860 |
| 600 | 69 | .1150 |
| 700 | 123 | .1755 |
| 750 | 147 | .1960 |
| 800 | 206 | .257 |
| 850 | 301 | .354 |
| 875 | 368 | .420 |
| 900 | 462 | .513 |
| 925 | 564 | .609 |
| 950 | 692 | .728 |

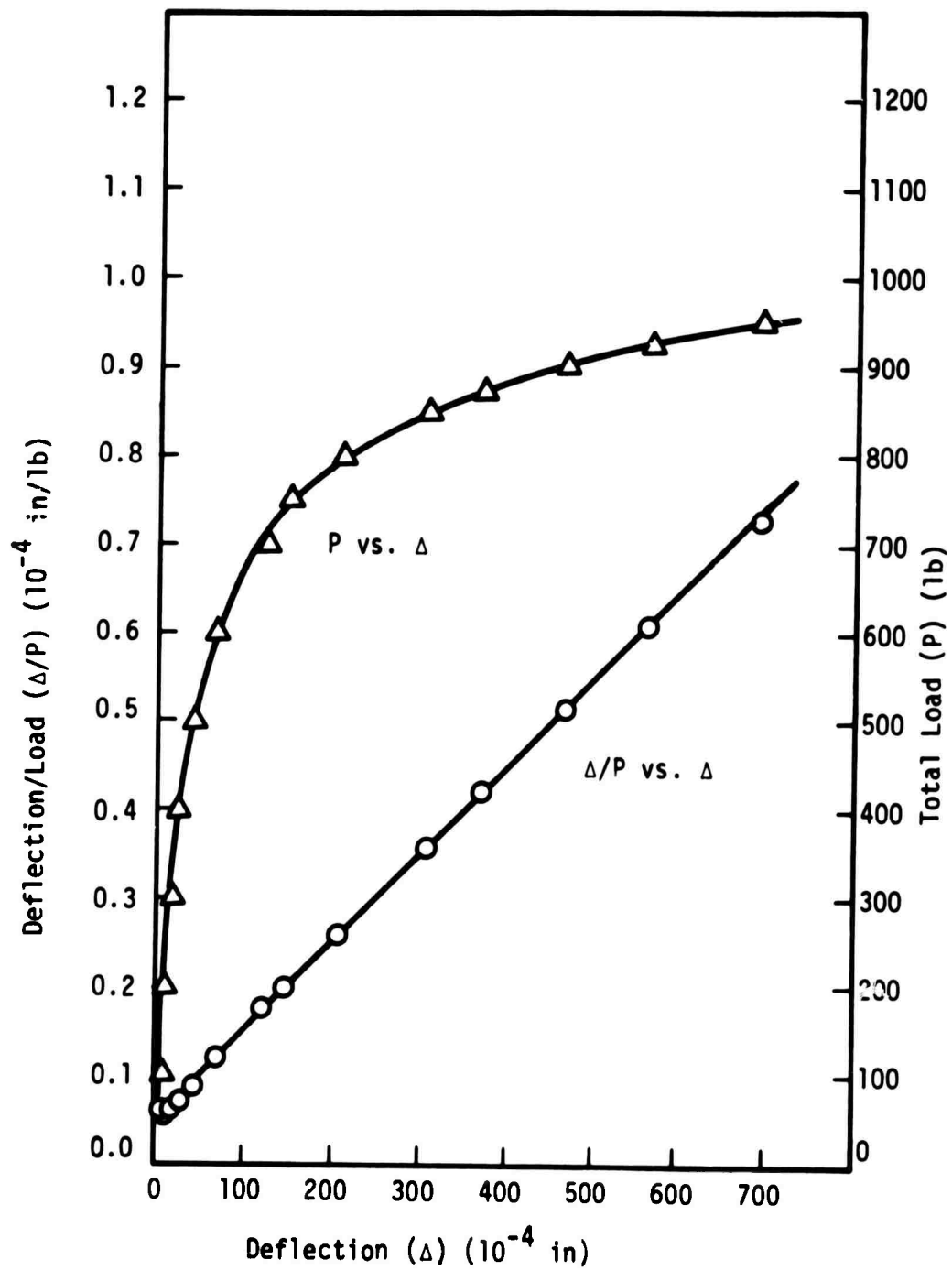


Figure 96. Southwell Plot and Load Deflection Curve
for Plate No. 505, 4 Sides Supported

TABLE 109
DATA AND CALCULATIONS FOR PLATE NO. 506,
2 SIDES SUPPORTED

| Total Load (P) (lb.) | Deflection (Δ) (10^{-4} in.) | Total Load/Deflection (Δ/P) (10^{-4} in./lb.) |
|-------------------------|---|--|
| 0 | 0 | 0 |
| 50 | --- | --- |
| 100 | 2 | .0200 |
| 150 | 11 | .0733 |
| 200 | 29 | .1450 |
| 250 | 34 | .1360 |
| 275 | 48 | .1745 |
| 300 | 69 | .230 |
| 325 | 104 | .320 |
| 340 | 140 | .412 |
| 350 | 179 | .512 |
| 360 | 239 | .664 |
| 370 | 354 | .958 |

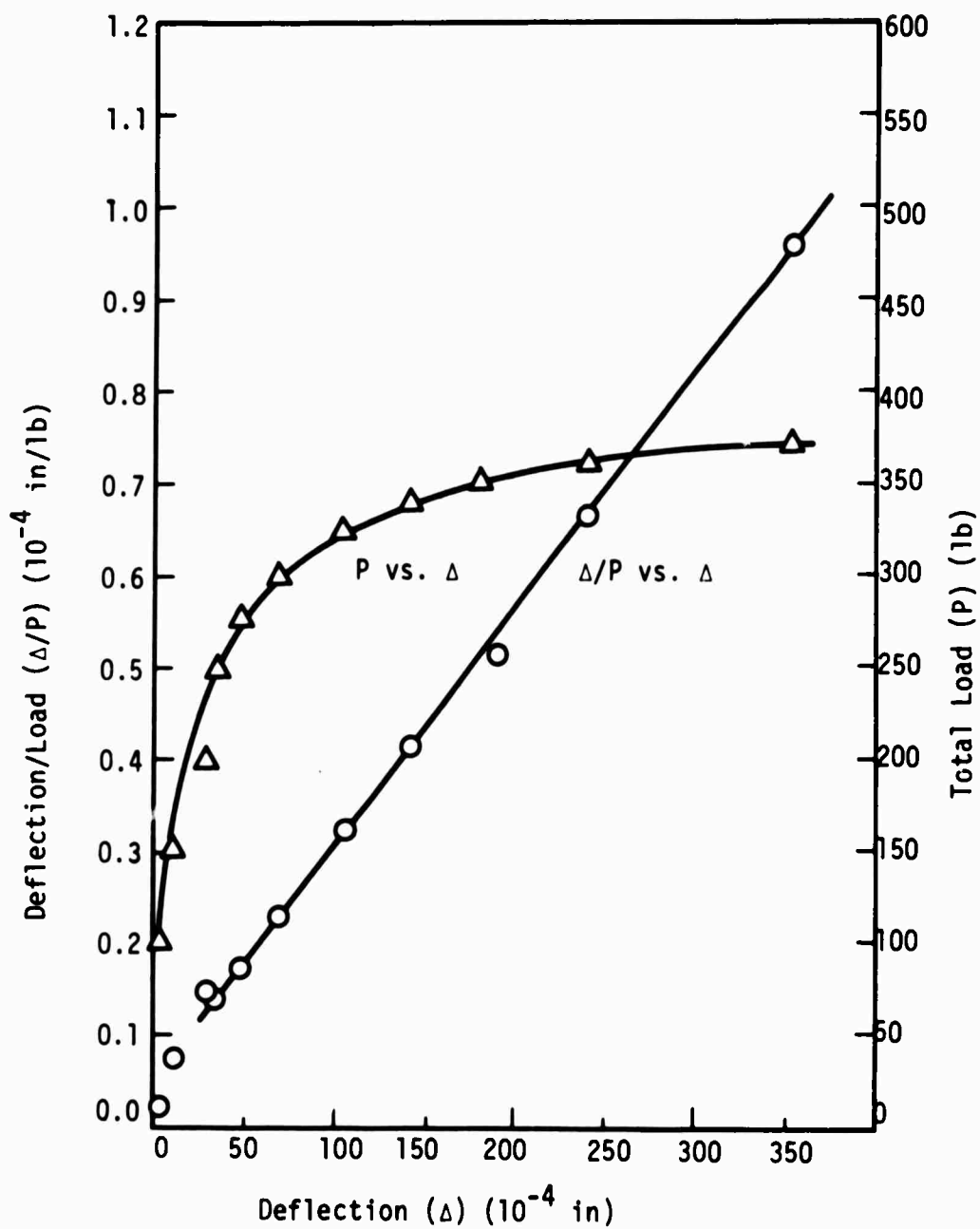


Figure 97. Southwell Plot and Load Deflection Curve
for Plate No. 506, 2 Sides Supported

TABLE 110
DATA AND CALCULATIONS FOR PLATE NO. 506,
4 SIDES SUPPORTED

| Total Load (P) (lb.) | Deflection (Δ) (10^{-4} in.) | Total Load/Deflection (Δ/P) (10^{-4} in./lb.) |
|-------------------------|---|--|
| 0 | 0 | 0 |
| 100 | --- | --- |
| 200 | --- | --- |
| 300 | --- | --- |
| 400 | 3 | .0075 |
| 500 | 17 | .0340 |
| 600 | 48 | .0800 |
| 700 | 101 | .1440 |
| 750 | 161 | .215 |
| 775 | 228 | .294 |
| 800 | 338 | .423 |
| 825 | 490 | .594 |
| 850 | 720 | .847 |

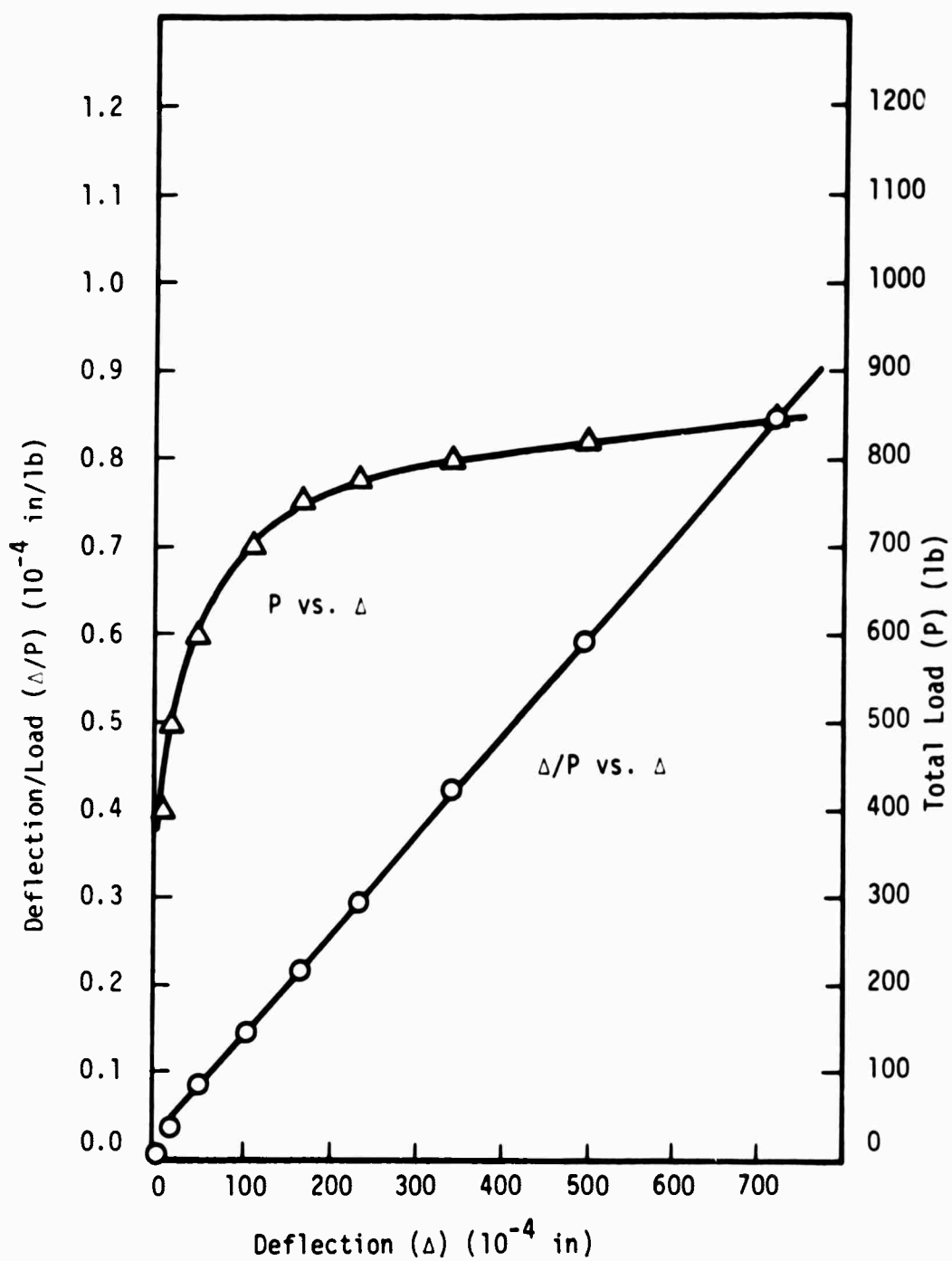


Figure 98. Southwell Plot and Load Deflection Curve
for Plate No. 506, 4 Sides Supported

TABLE 111
DATA AND CALCULATIONS FOR PLATE NO. 507,
2 SIDES SUPPORTED

| Total Load (P) (lb.) | Deflection (Δ) (10^{-4} in.) | Total Load/Deflection (Δ/P) (10^{-4} in./lb.) |
|-------------------------|---|--|
| 6.4 | 0 | 0 |
| 20 | 12 | .600 |
| 30 | 26 | .868 |
| 40 | 44 | 1.100 |
| 50 | 69 | 1.380 |
| 60 | 104 | 1.735 |
| 70 | 146 | 2.09 |
| 80 | 206 | 2.57 |
| 90 | 299 | 3.32 |
| 100 | 433 | 4.33 |
| 110 | 696 | 6.33 |

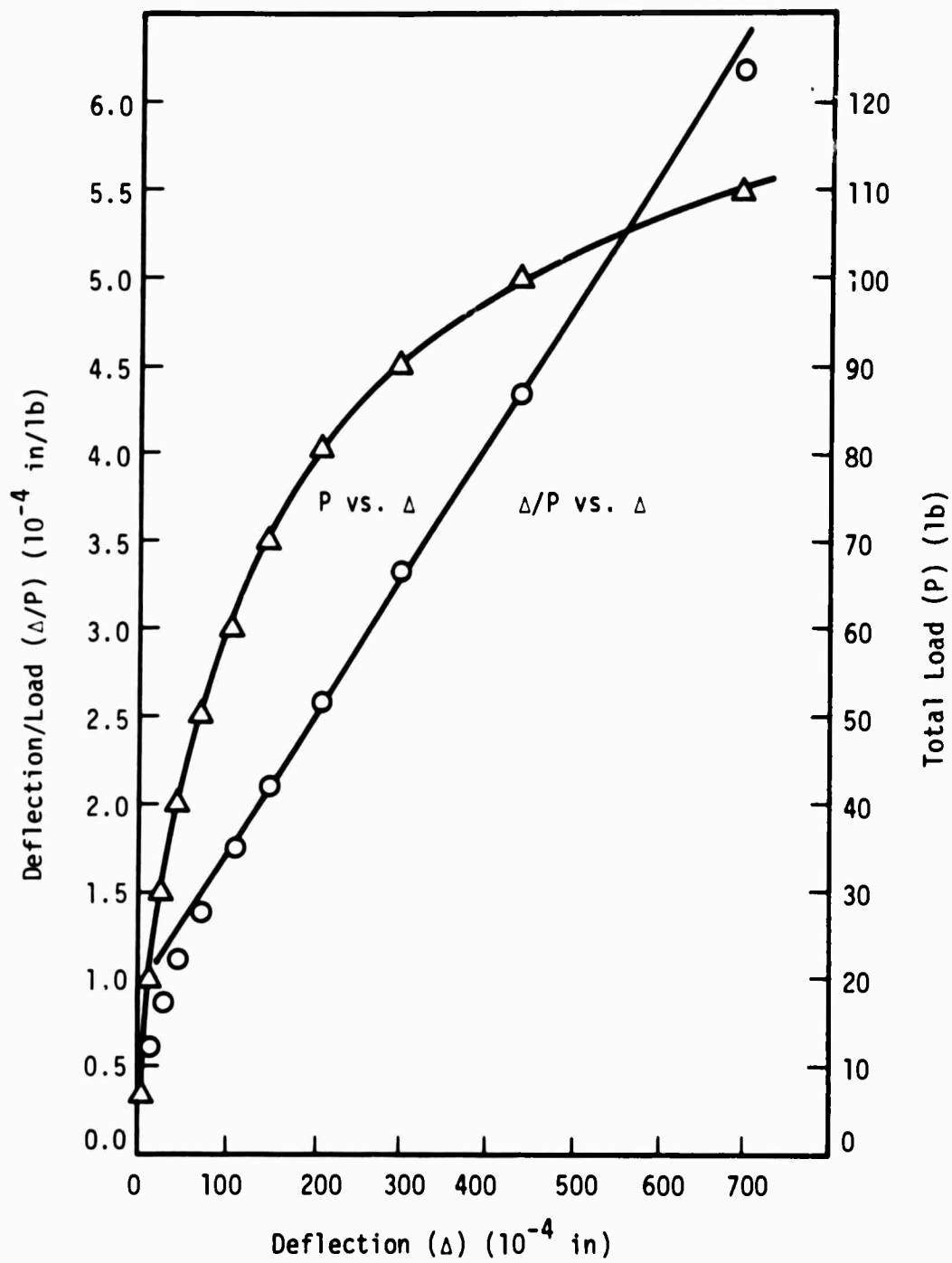


Figure 99. Southwell Plot and Load Deflection Curve
for Plate No. 507, 2 Sides Supported

TABLE 112
DATA AND CALCULATIONS FOR PLATE NO. 507,
4 SIDES SUPPORTED

| Total Load (P) (lb.) | Deflection (Δ) (10^{-4} in.) | Total Load/Deflection (Δ/P) (10^{-4} in./lb.) |
|-------------------------|---|--|
| 0 | 0 | 0 |
| 50 | 8 | .160 |
| 100 | 24 | .240 |
| 150 | 49 | .327 |
| 200 | 80 | .400 |
| 250 | 117 | .468 |
| 300 | 164 | .546 |
| 350 | 235 | .671 |
| 375 | 279 | .743 |
| 400 | 339 | .847 |
| 425 | 411 | .968 |
| 450 | 480 | 1.065 |
| 475 | 576 | 1.211 |
| 500 | 678 | 1.355 |

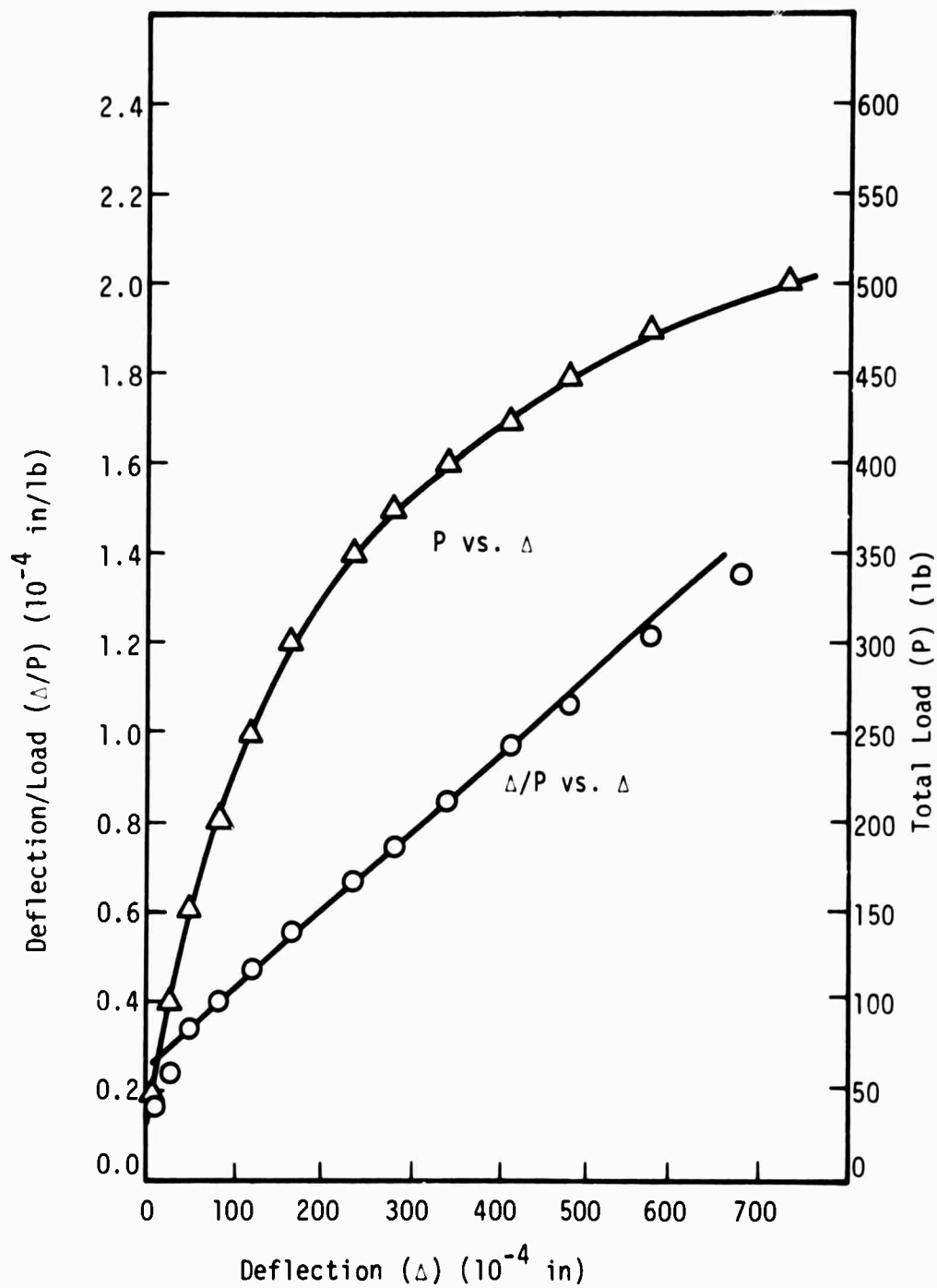


Figure 100. Southwell Plot and Load Deflection Curve
for Plate No. 507, 4 Sides Supported

TABLE 113
DATA AND CALCULATIONS FOR PLATE NO. 508,
2 SIDES SUPPORTED

| Total Load (P) (lb.) | Deflection (Δ) (10^{-4} in.) | Total Load/Deflection (Δ/P) (10^{-4} in./lb.) |
|-------------------------|---|--|
| 6.4 | 0 | 0 |
| 20 | 9 | .450 |
| 30 | 20 | .668 |
| 40 | 41 | 1.025 |
| 50 | 68 | 1.360 |
| 60 | 111 | 1.850 |
| 70 | 219 | 3.13 |
| 75 | 253 | 3.37 |
| 80 | 360 | 4.50 |
| 85 | 571 | 6.73 |

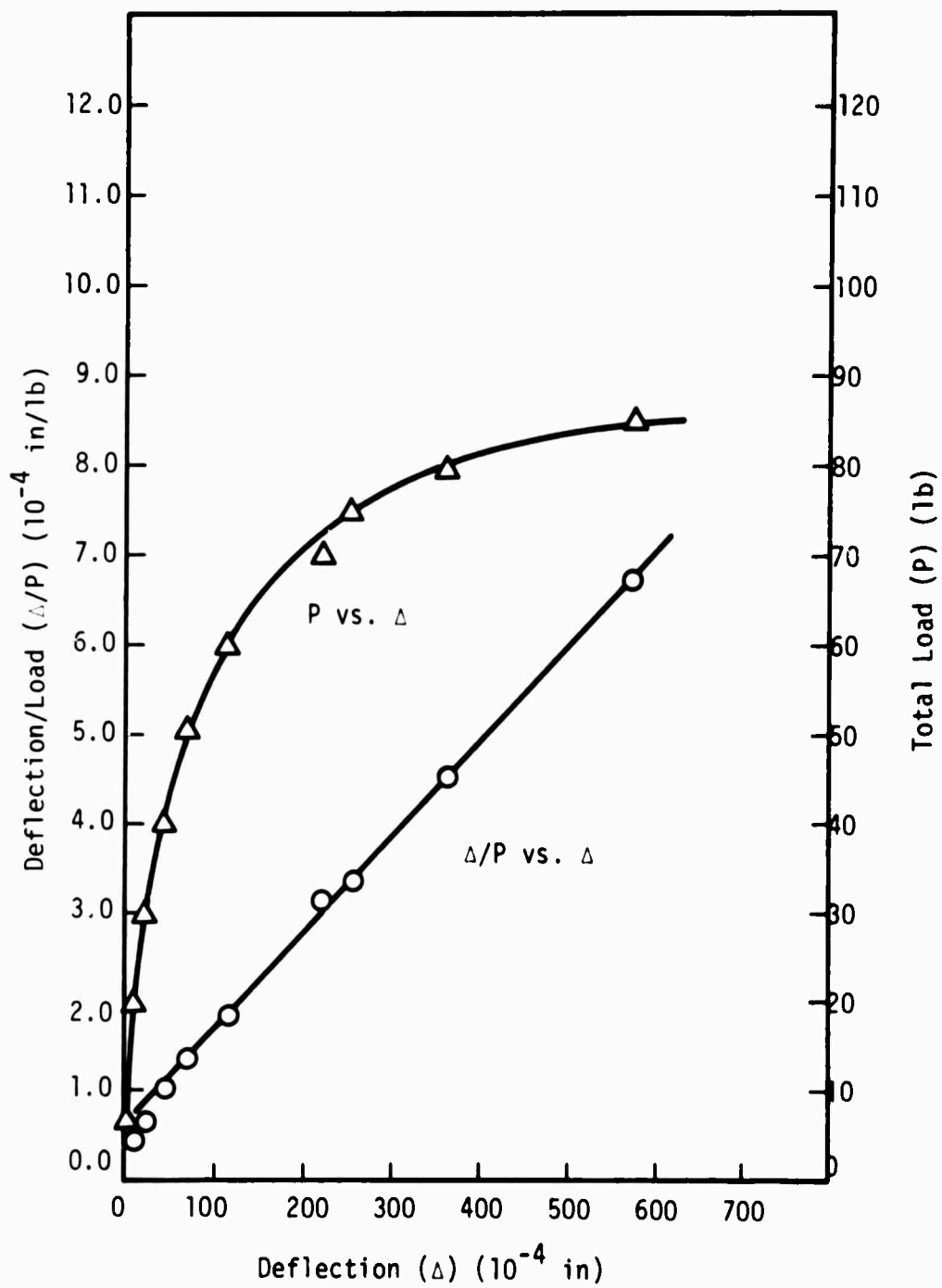


Figure 101. Southwell Plot and Load Deflection Curve for Plate No. 508, 2 Sides Supported

TABLE 114
DATA AND CALCULATIONS FOR PLATE NO. 508,
4 SIDES SUPPORTED

| Total Load (P) (lb.) | Deflection (Δ) (10^{-4} in.) | Total Load/Deflection (Δ/P) (10^{-4} in./lb.) |
|-------------------------|---|--|
| 0 | 0 | 0 |
| 50 | 8 | .160 |
| 100 | 28 | .280 |
| 150 | 56 | .373 |
| 200 | 84 | .420 |
| 250 | 126 | .504 |
| 300 | 161 | .537 |
| 350 | 224 | .640 |
| 400 | 309 | .773 |
| 450 | 426 | .933 |
| 500 | 562 | 1.125 |

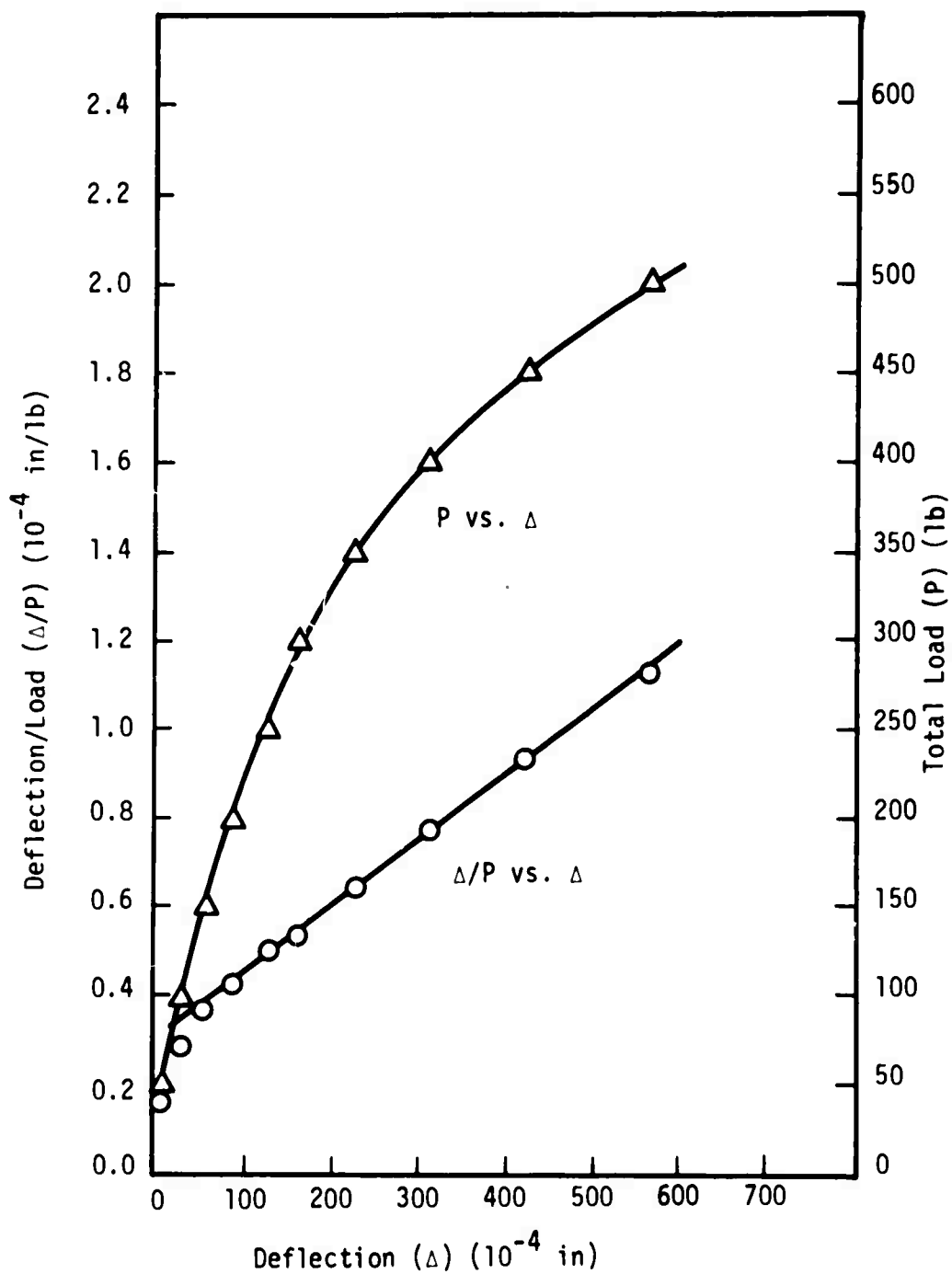


Figure 102. Southwell Plot and Load Deflection Curve
for Plate No. 508, 4 Sides Supported

TABLE 115
DATA AND CALCULATIONS FOR PLATE NO. 509a,
2 SIDES SUPPORTED

| Total Load (P) (lb.) | Deflection (Δ) (10^{-4} in.) | Total Load/Deflection (Δ/P) (10^{-4} in./lb.) |
|-------------------------|---|--|
| 6.4 | 0 | 0 |
| 20 | 29 | 1.45 |
| 30 | 55 | 1.83 |
| 40 | 91 | 2.27 |
| 50 | 130 | 2.60 |
| 60 | 177 | 2.95 |
| 70 | 234 | 3.34 |
| 80 | 300 | 3.75 |
| 90 | 399 | 4.43 |
| 100 | 517 | 5.17 |
| 110 | 695 | 6.32 |

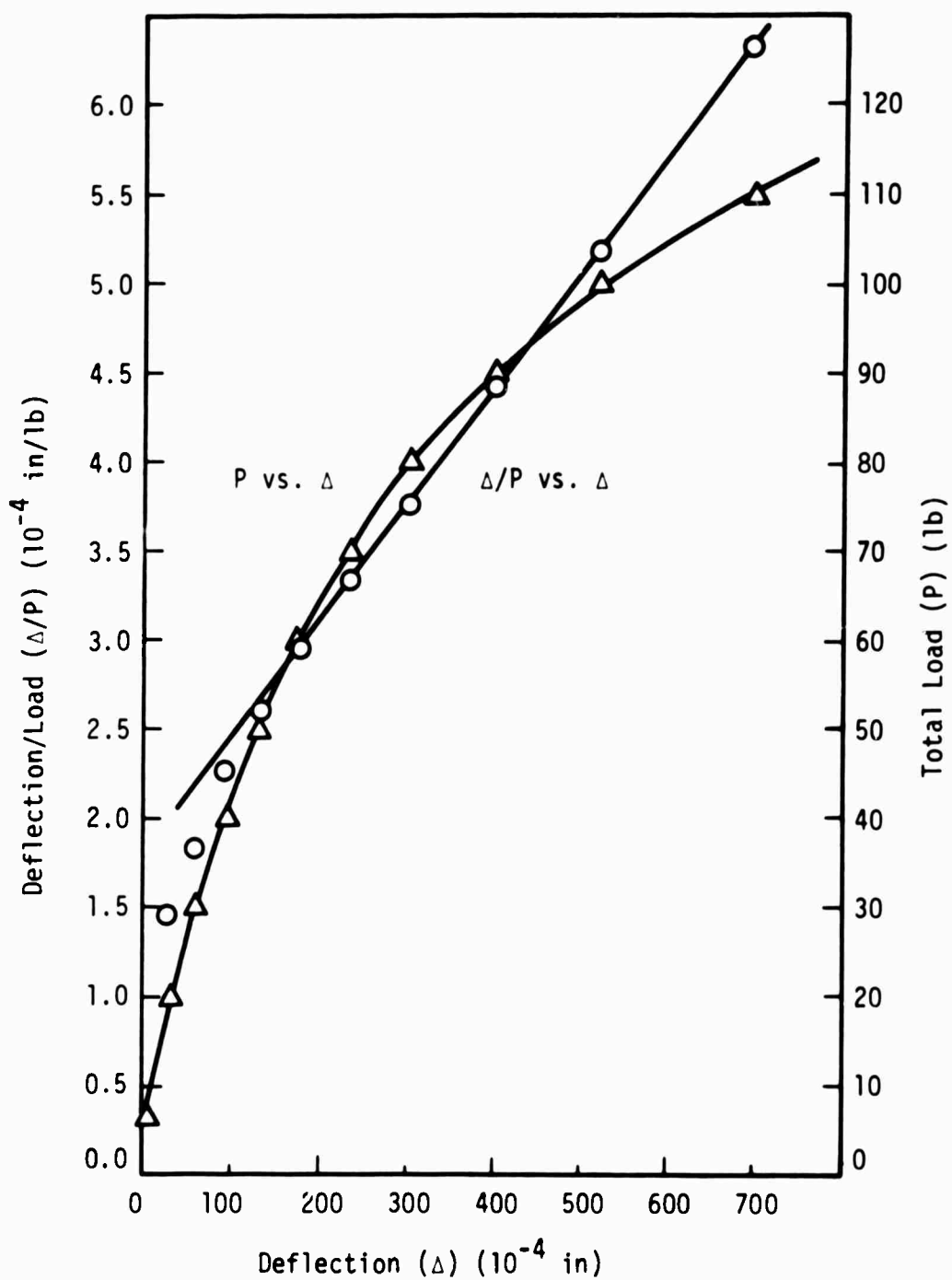


Figure 103. Southwell Plot and Load Deflection Curve
for Plate No. 509a, 2 Sides Supported

TABLE 116
DATA AND CALCULATIONS FOR PLATE NO. 509b,
2 SIDES SUPPORTED

| Total Load (P) (lb.) | Deflection (Δ) (10^{-4} in.) | Total Load/Deflection (Δ/P) (10^{-4} in./lb.) |
|-------------------------|---|--|
| 6.4 | 0 | 0 |
| 20 | 21 | 1.050 |
| 30 | 49 | 1.635 |
| 40 | 80 | 2.00 |
| 50 | 119 | 2.38 |
| 60 | 159 | 2.65 |
| 70 | 220 | 3.14 |
| 80 | 275 | 3.44 |
| 90 | 357 | 3.97 |
| 100 | 469 | 4.69 |
| 110 | 637 | 5.79 |

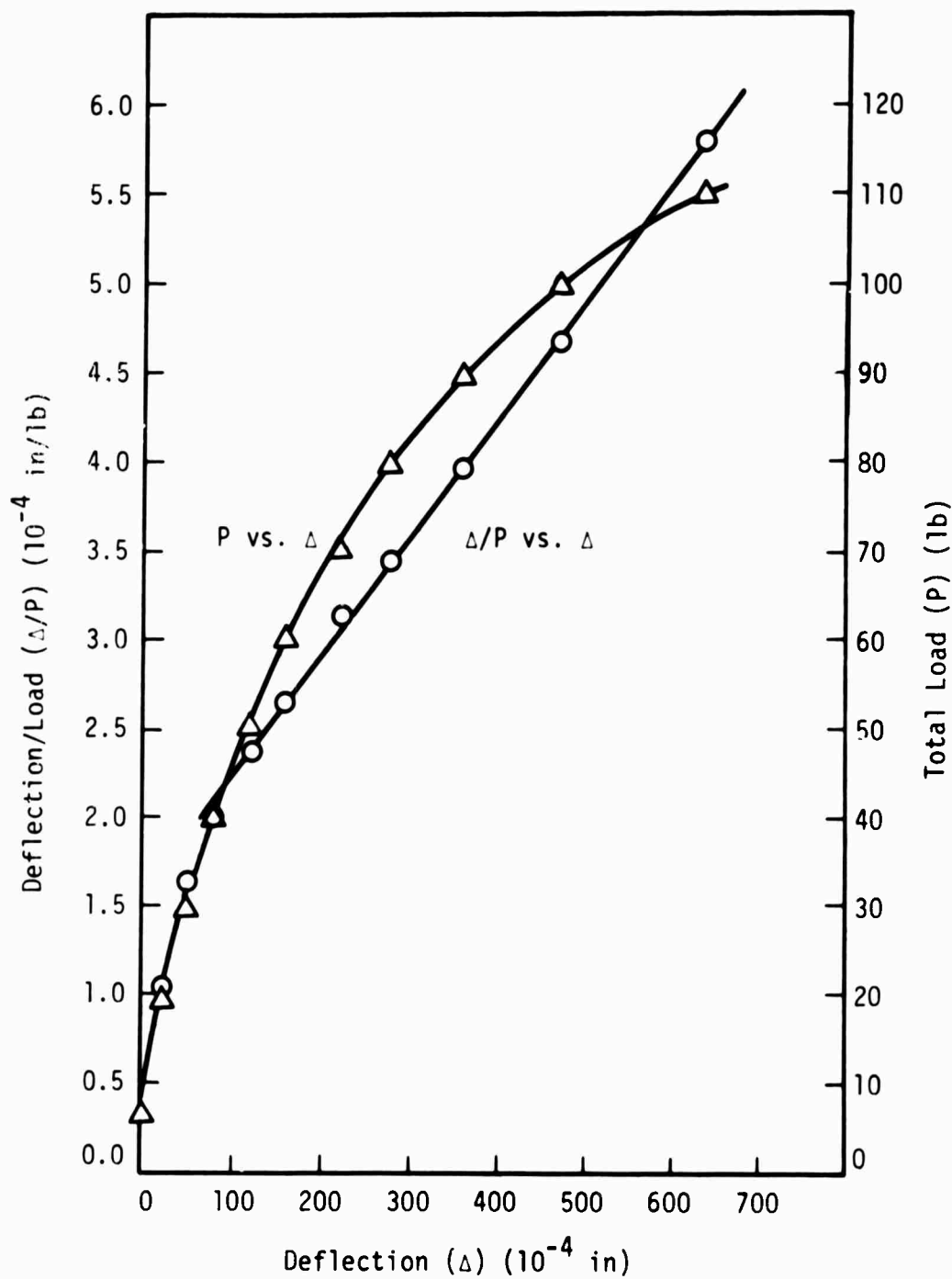


Figure 104. Southwell Plot and Load Deflection Curve
for Plate No. 509b, 2 Sides Supported

TABLE 117
DATA AND CALCULATIONS FOR PLATE NO. 509a,
4 SIDES SUPPORTED

| Total Load (P) (lb.) | Deflection (Δ) (10^{-4} in.) | Total Load/Deflection (Δ/P) (10^{-4} in./lb.) |
|-------------------------|---|--|
| 0 | 0 | 0 |
| 50 | 42 | .840 |
| 100 | 74 | .740 |
| 150 | 117 | .780 |
| 200 | 169 | .845 |
| 225 | 198 | .880 |
| 250 | 233 | .932 |
| 275 | 276 | 1.003 |
| 300 | 328 | 1.093 |
| 325 | 382 | 1.175 |
| 350 | 442 | 1.264 |
| 375 | 518 | 1.381 |
| 400 | 610 | 1.525 |
| 425 | 704 | 1.655 |

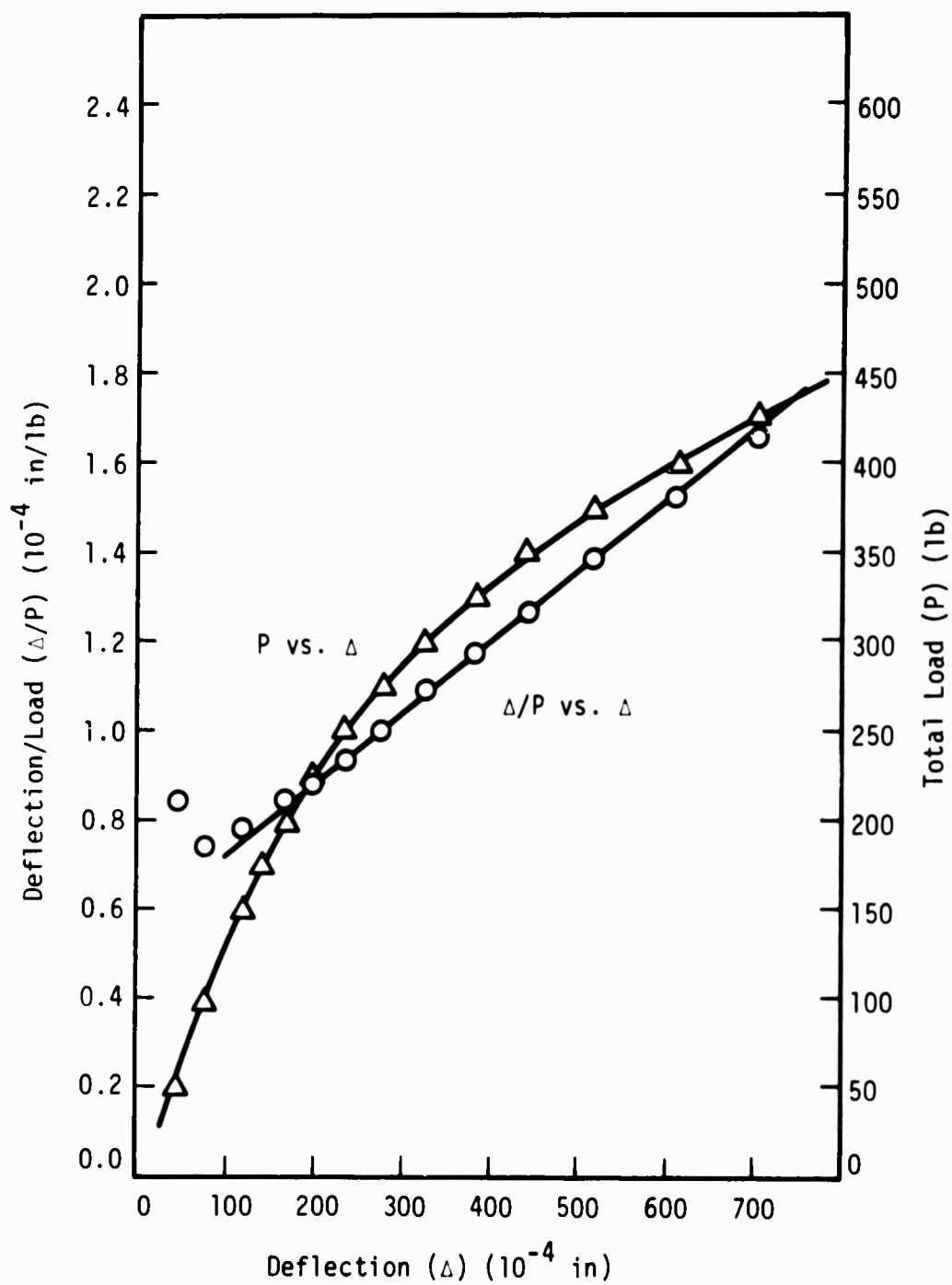


Figure 105. Southwell Plot and Load Deflection Curve
for Plate No. 509a, 4 Sides Supported

TABLE 118
DATA AND CALCULATIONS FOR PLATE NO. 509b,
4 SIDES SUPPORTED

| Total Load (P) (lb.) | Deflection (Δ) (10^{-4} in.) | Total Load/Deflection (Δ/P) (10^{-4} in./lb.) |
|-------------------------|---|--|
| 0 | 0 | 0 |
| 50 | 34 | .680 |
| 100 | 70 | .700 |
| 150 | 128 | .853 |
| 175 | 155 | .886 |
| 200 | 185 | .925 |
| 225 | 224 | .997 |
| 250 | 260 | 1.040 |
| 275 | 304 | 1.105 |
| 300 | 350 | 1.167 |
| 325 | 403 | 1.240 |
| 350 | 461 | 1.316 |
| 375 | 525 | 1.400 |
| 400 | 595 | 1.490 |
| 425 | 664 | 1.561 |
| 450 | 749 | 1.665 |

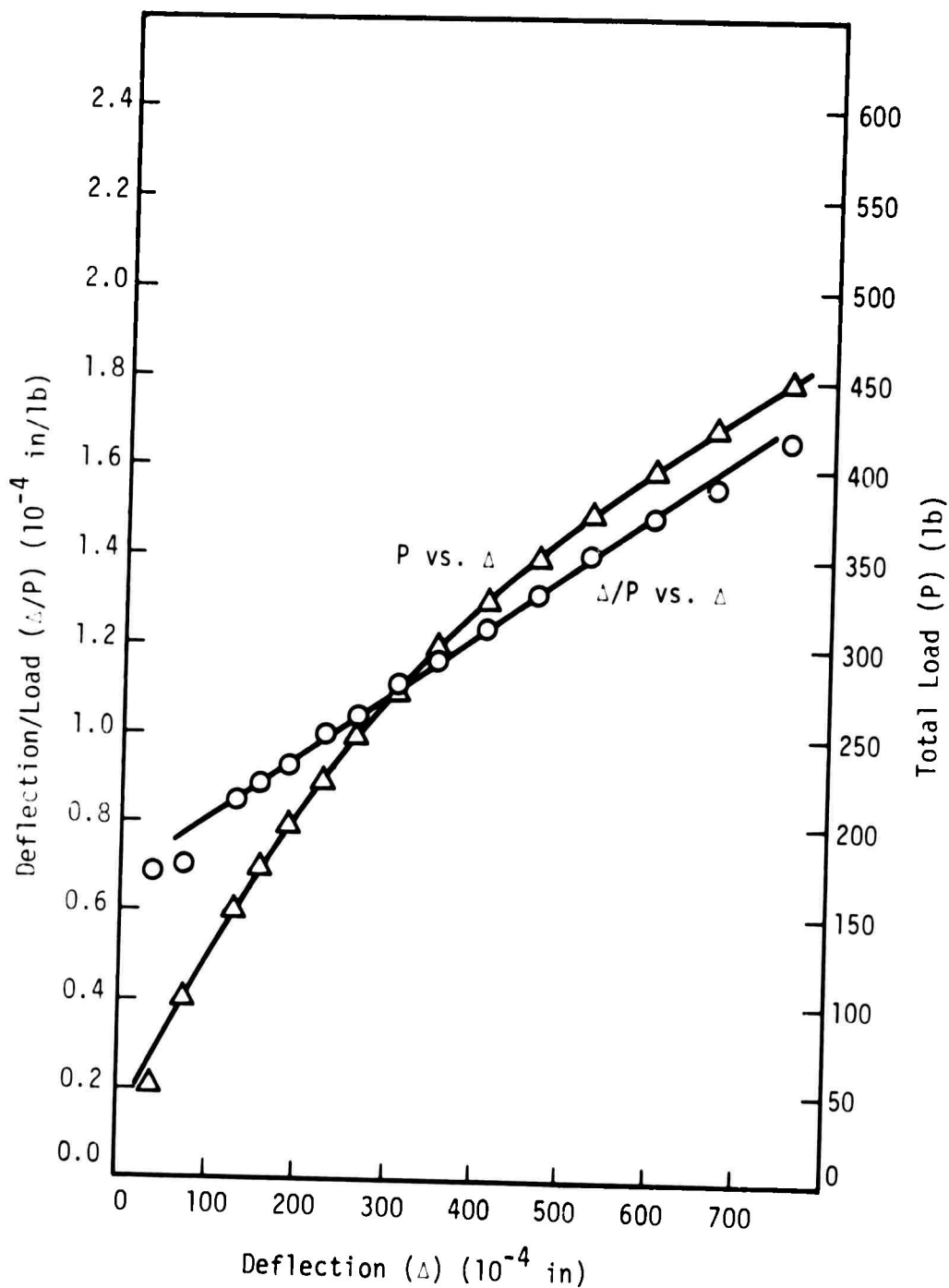


Figure 106. Southwell Plot and Load Deflection Curve
for Plate No. 509b, 4 Sides Supported

APPENDIX D

PLANS AND ASSEMBLY DRAWINGS FOR THE TEST FIXTURE

Appendix D gives the details for each individual part of the test fixture, as well as assembly drawings for the entire fixture. No scale factors have been included, but these can easily be determined from the dimensions. It is recommended that the following tolerances be observed:

| <u>Part No.</u> | <u>Tolerance</u> |
|---|-------------------|
| 1,2,5,8,22,24,31,38,39,40,51 | <u>+0.002 in.</u> |
| 4,6,7,9,17,25,26,32,33,34,37,67 | <u>+0.005 in.</u> |
| 3,10,11,12,13,14,15,16,17,20,21,27,35,36,62 | <u>+0.030 in.</u> |

In addition, Parts No. 3 and 5 should slide freely in the cylindrical holes of Parts No. 1 and 51. It is also highly recommended that any screw or bolt connections be jig drilled.

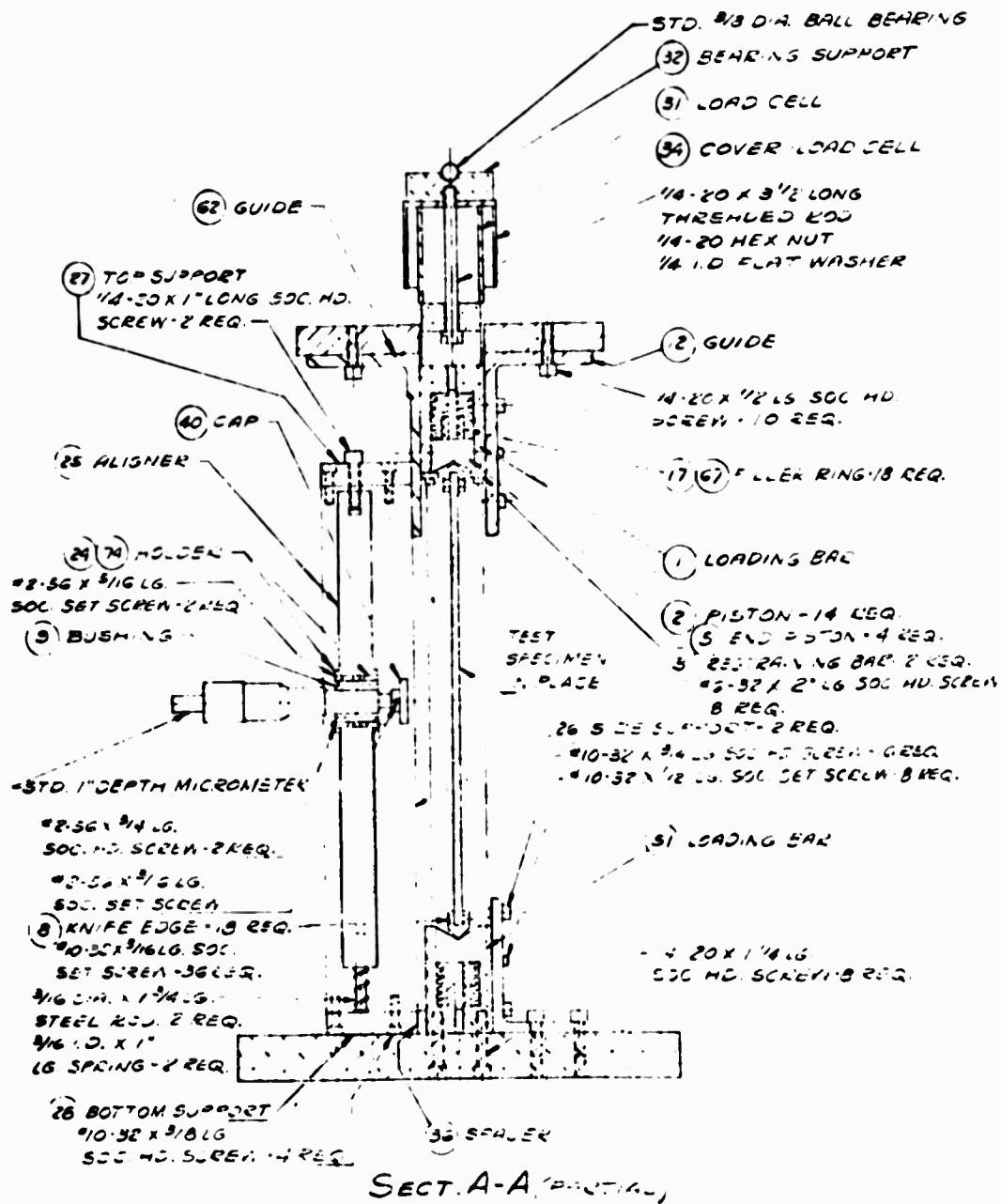
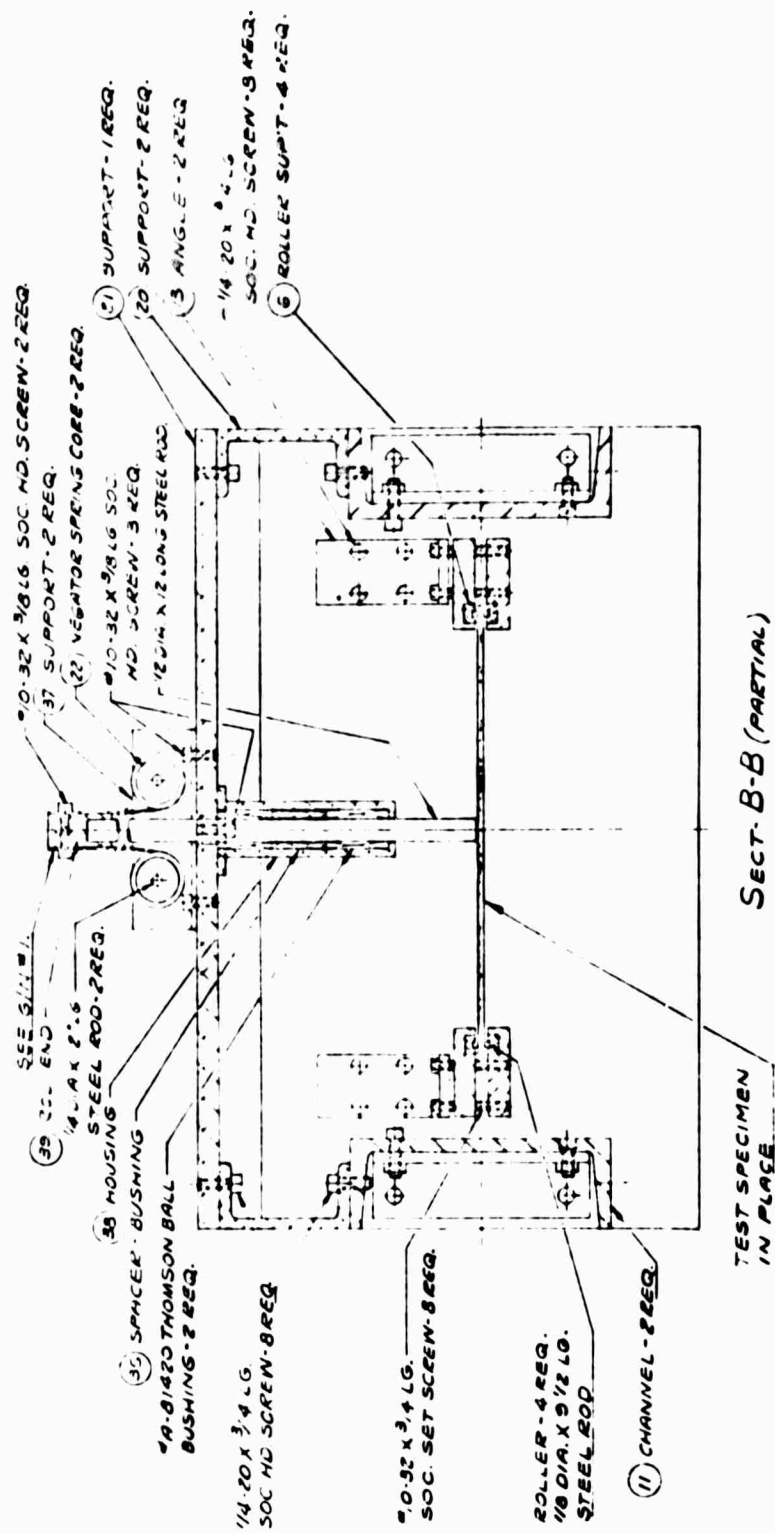


Figure 108. Horizontal Section Through Test Fixture



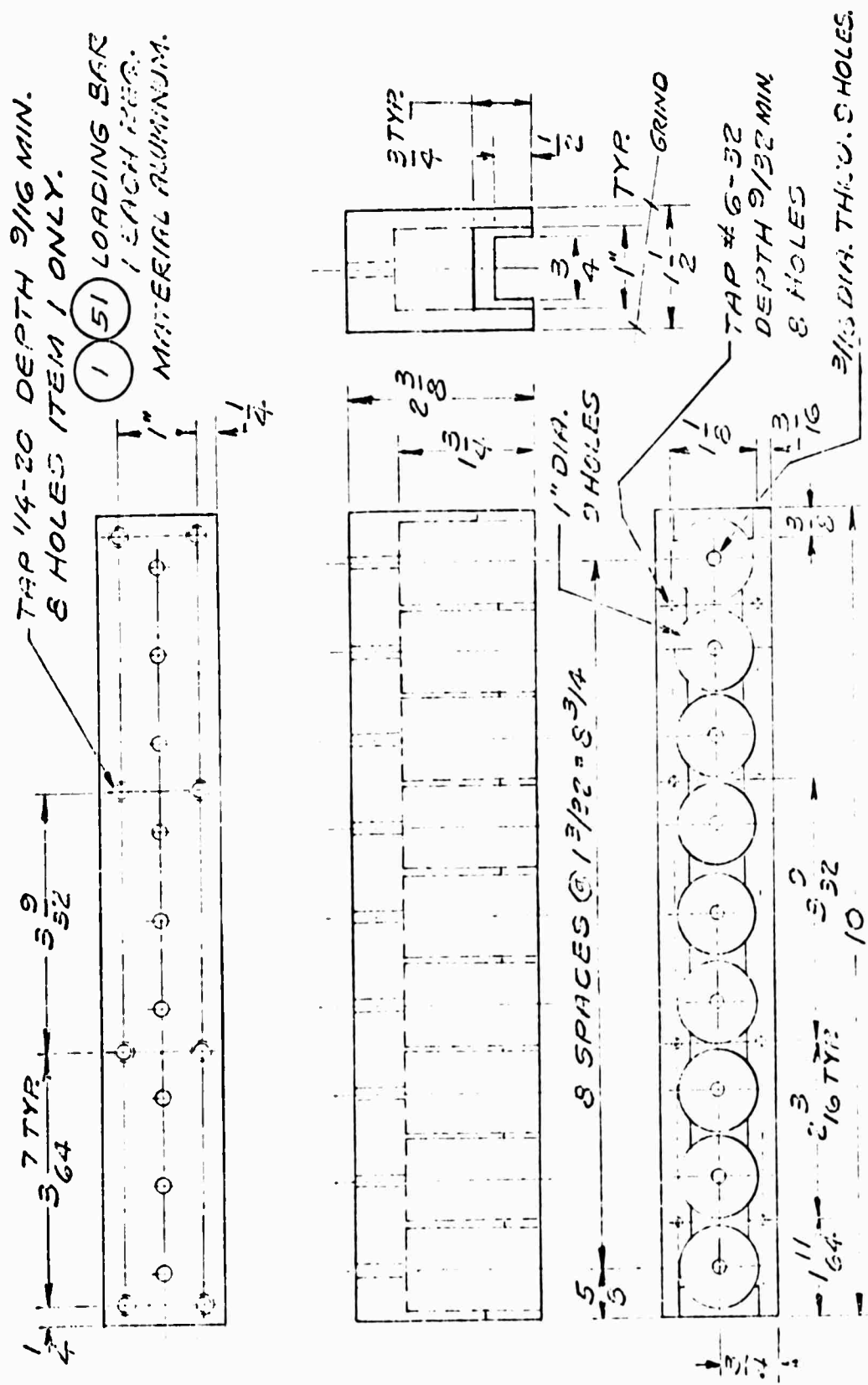
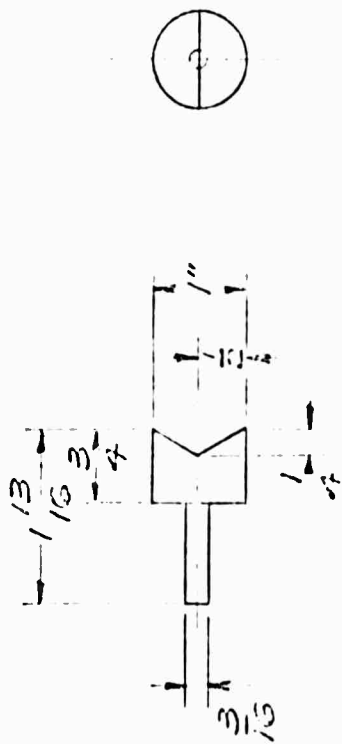
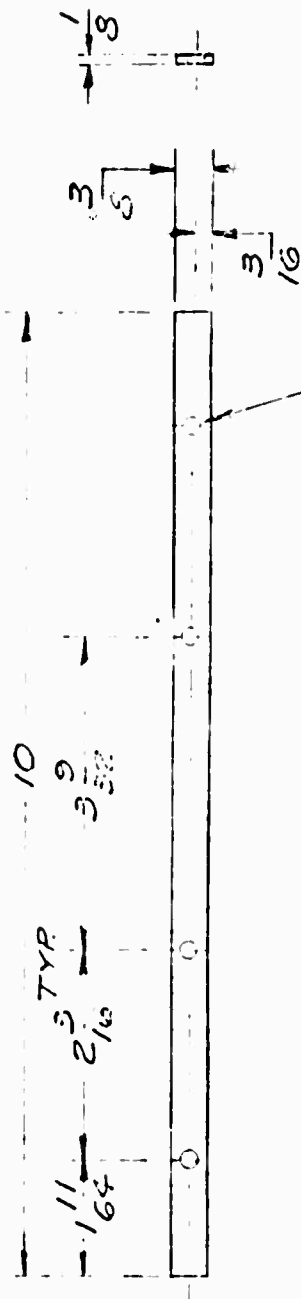


Figure 110. Loading Bar



2 PISTON - 14 REQ'D.
MAT'L. BRASS

Figure 111. Typical Middle Piston



3 RESTRAINING BAR - 2 REQ.
MAT'L. BRASS

DRILL #18 (.1695) THRU.
4 HOLES

Figure 112. Restraining Bar

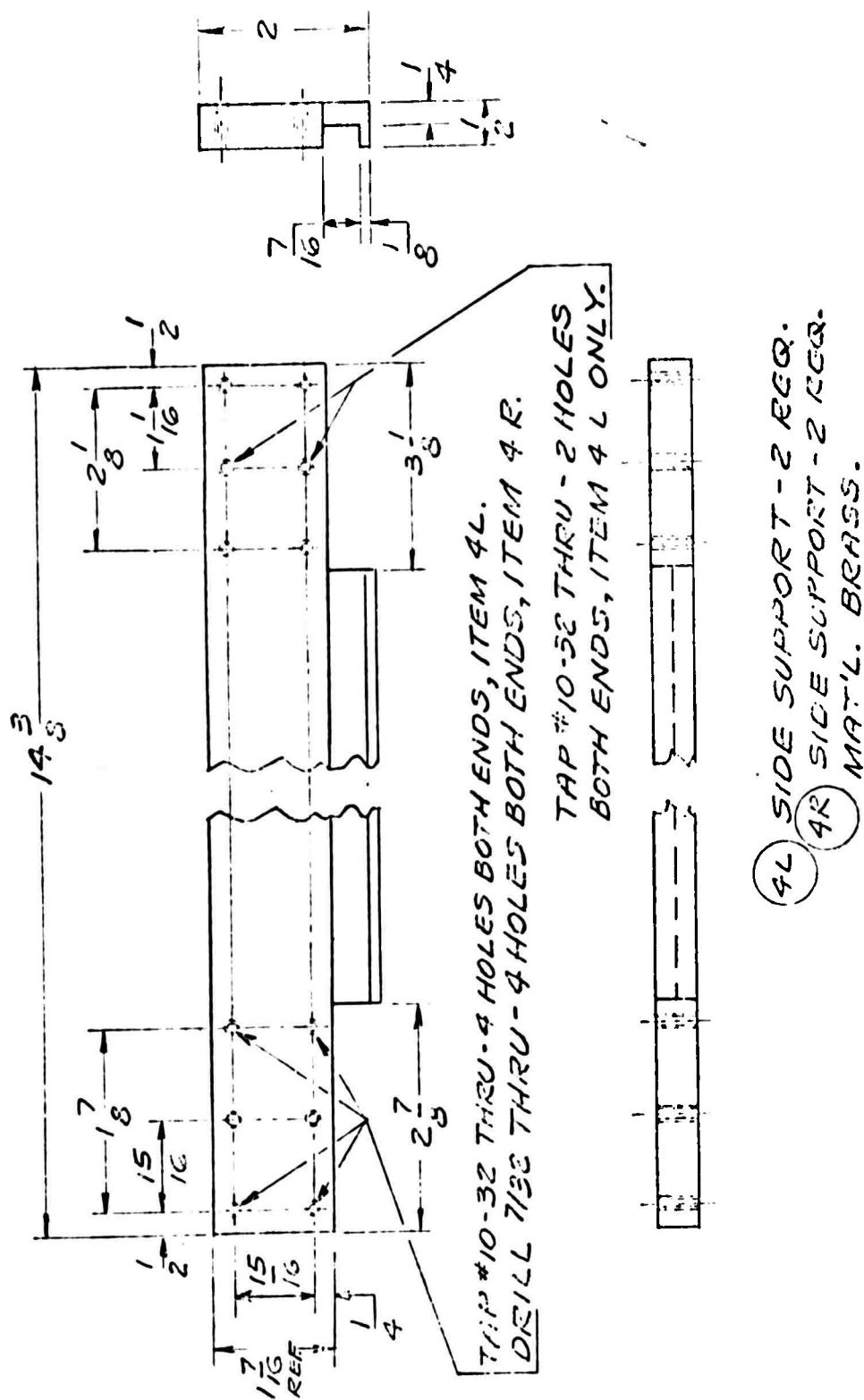
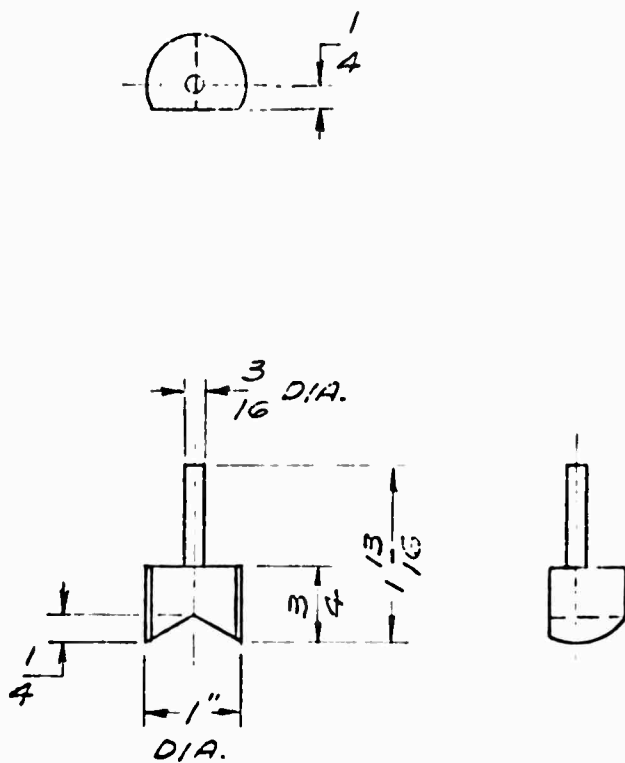


Figure 113. Side Supports



(5) END PISTON - 4 REQ.
MATERIAL BRASS

Figure 114. Typical End Piston

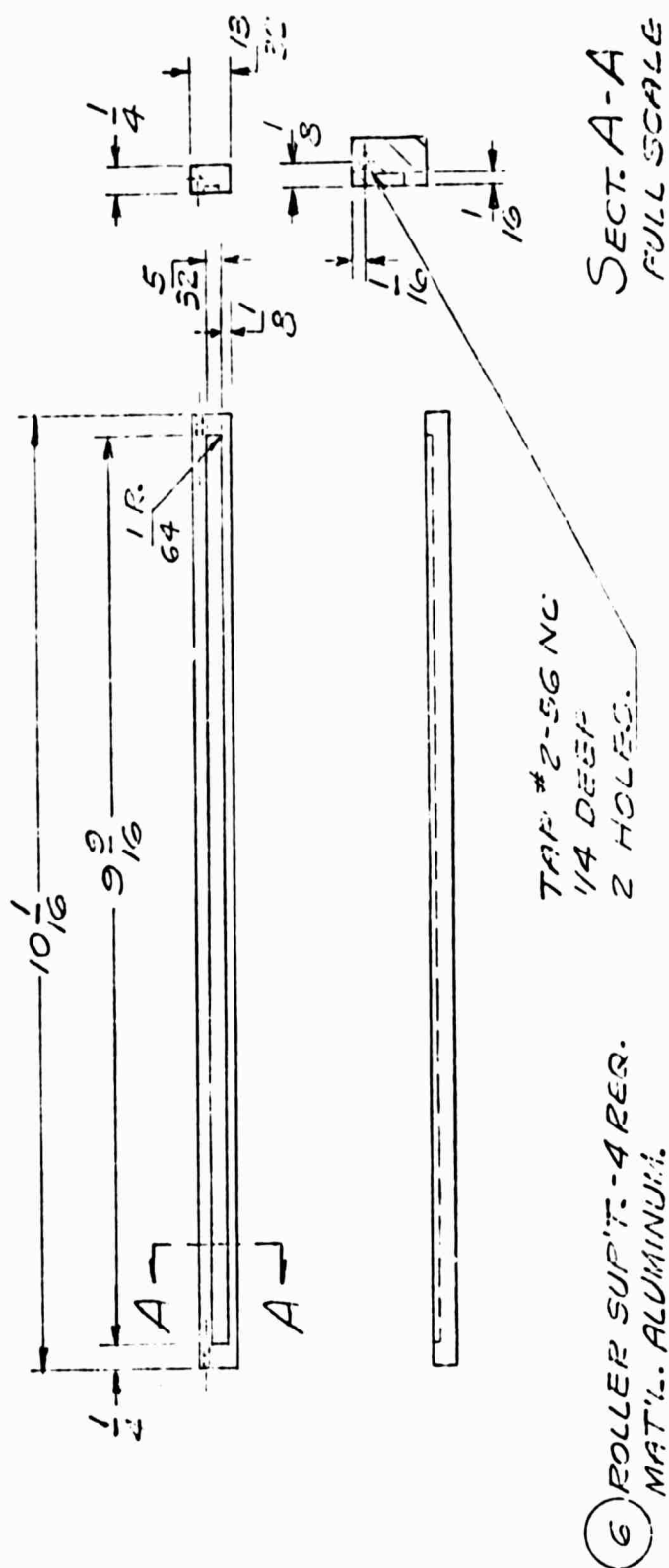


Figure 115. Slotted Bar Roller Support

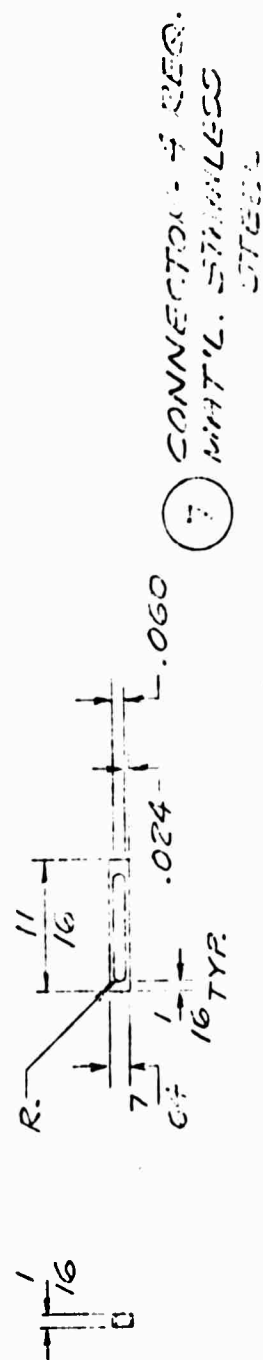
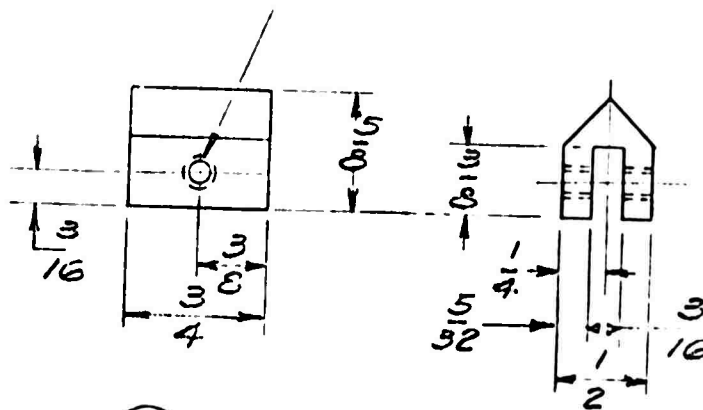


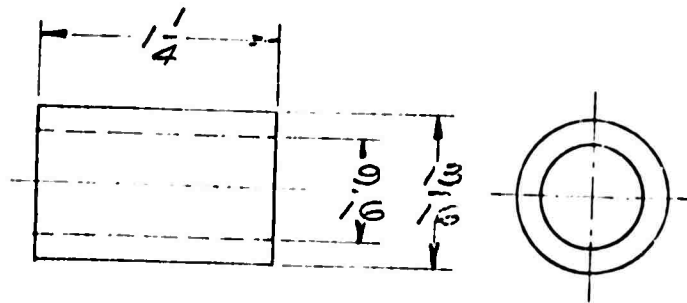
Figure 116. Slotted Bar Connector

-771.2 #10-32 THRU.



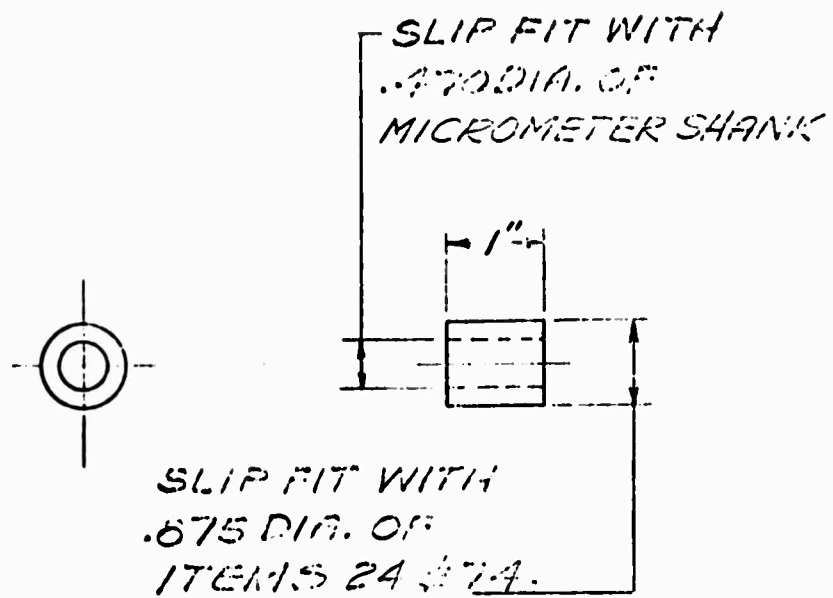
(8) KNIFE EDGE - 13 REQ.
MAT'L. ALUMINUM.

Figure 117. Typical Knife Edge



(35) SPACER - BALL BUSHING - 1 REQ.
MAT'L. ALUMINUM.

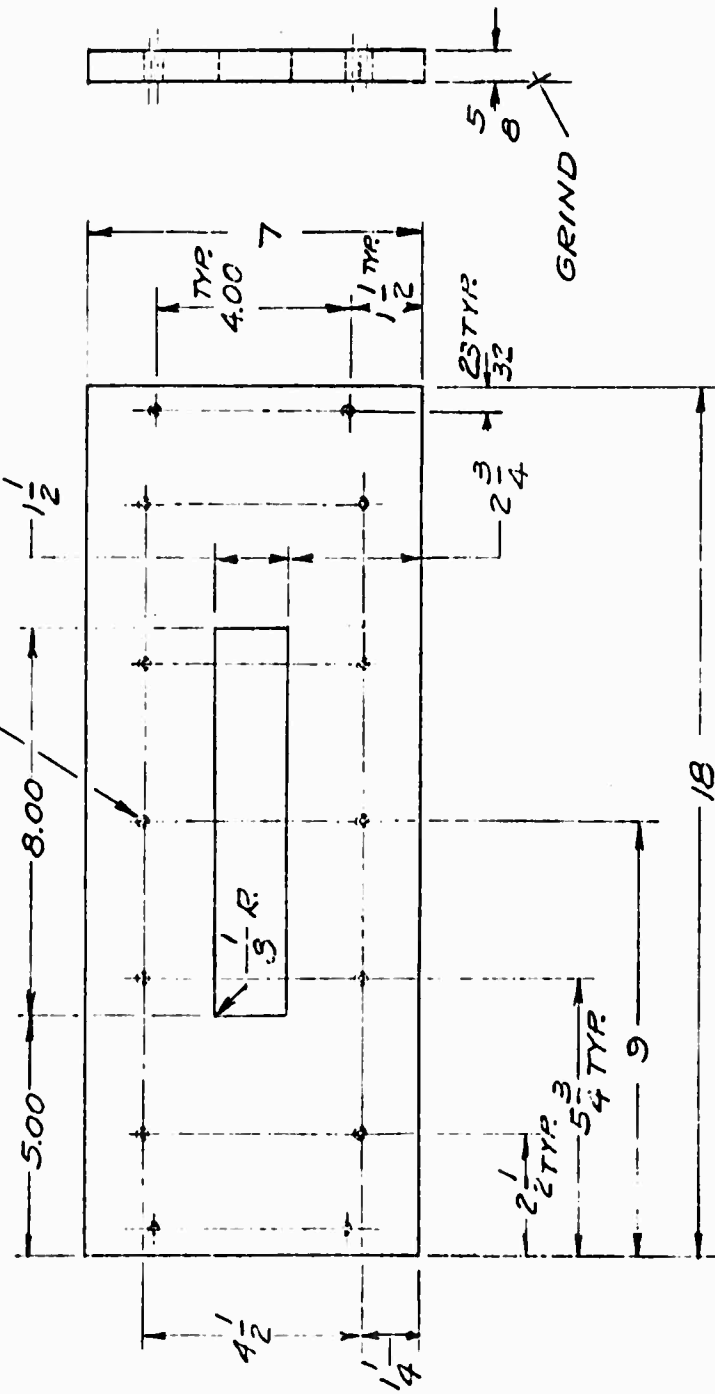
Figure 118. Ball Bushing Spacer



- ⑨ BUSHING-MICROMETER-REQ.
MAT'L. AL. ALLOY.

Figure 119. Micrometer Bushing

TAP 1/4-20 NC THRU.
14 HOLES.



10 TOP PLATE - 1 REQ.
MAT'L. STEEL.

Figure 120. Top Plate

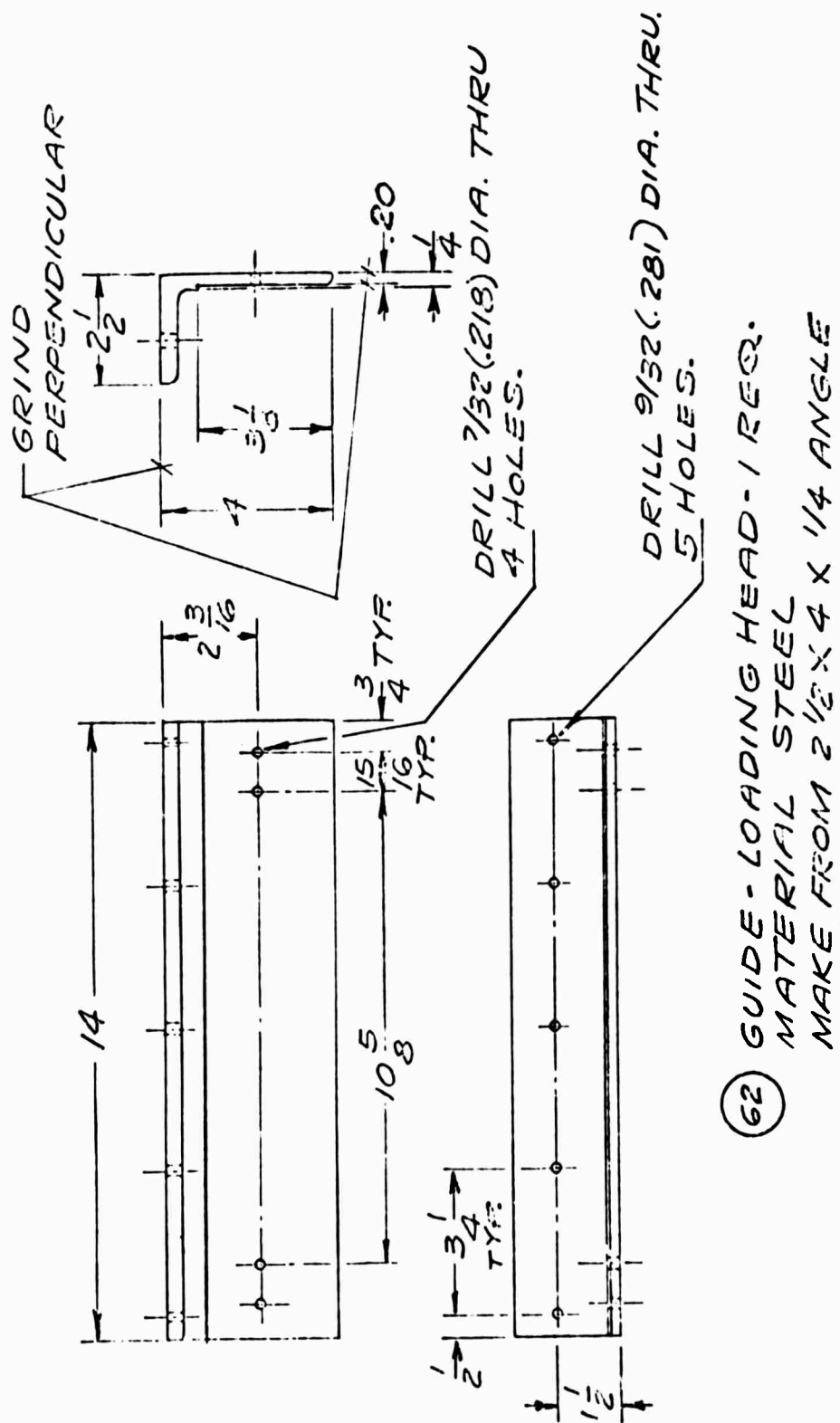
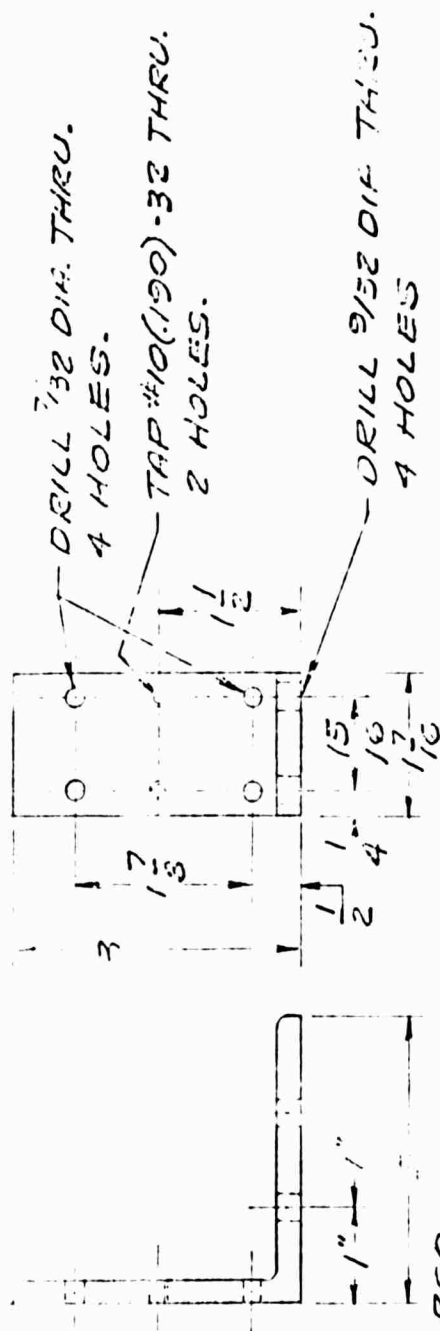


Figure 122. Front Angle Guide for Loading Bar



13 ANGLE - 2 REQ.
MAKE FROM STD. 3 X 3 X 1/4 ANGLE
MAT'L. STEEL
DRILL 9/32 DIA. THRU
4 HOLES.

Figure 124. Side Support Connector

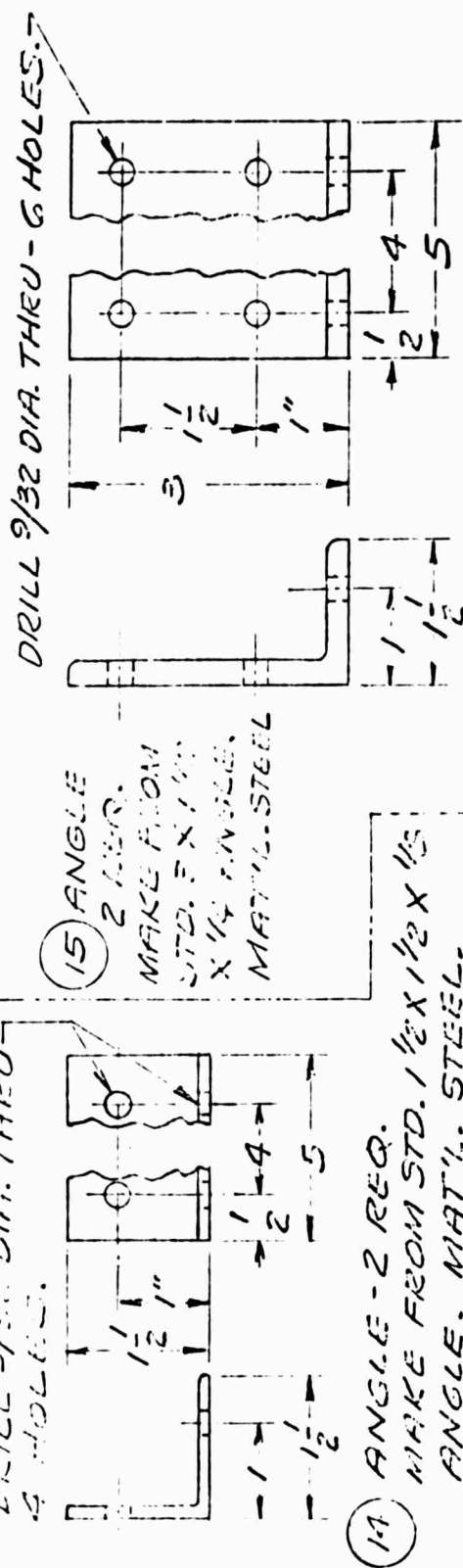


Figure 125. Top Channel Connector

Figure 126. Bottom Channel Connector

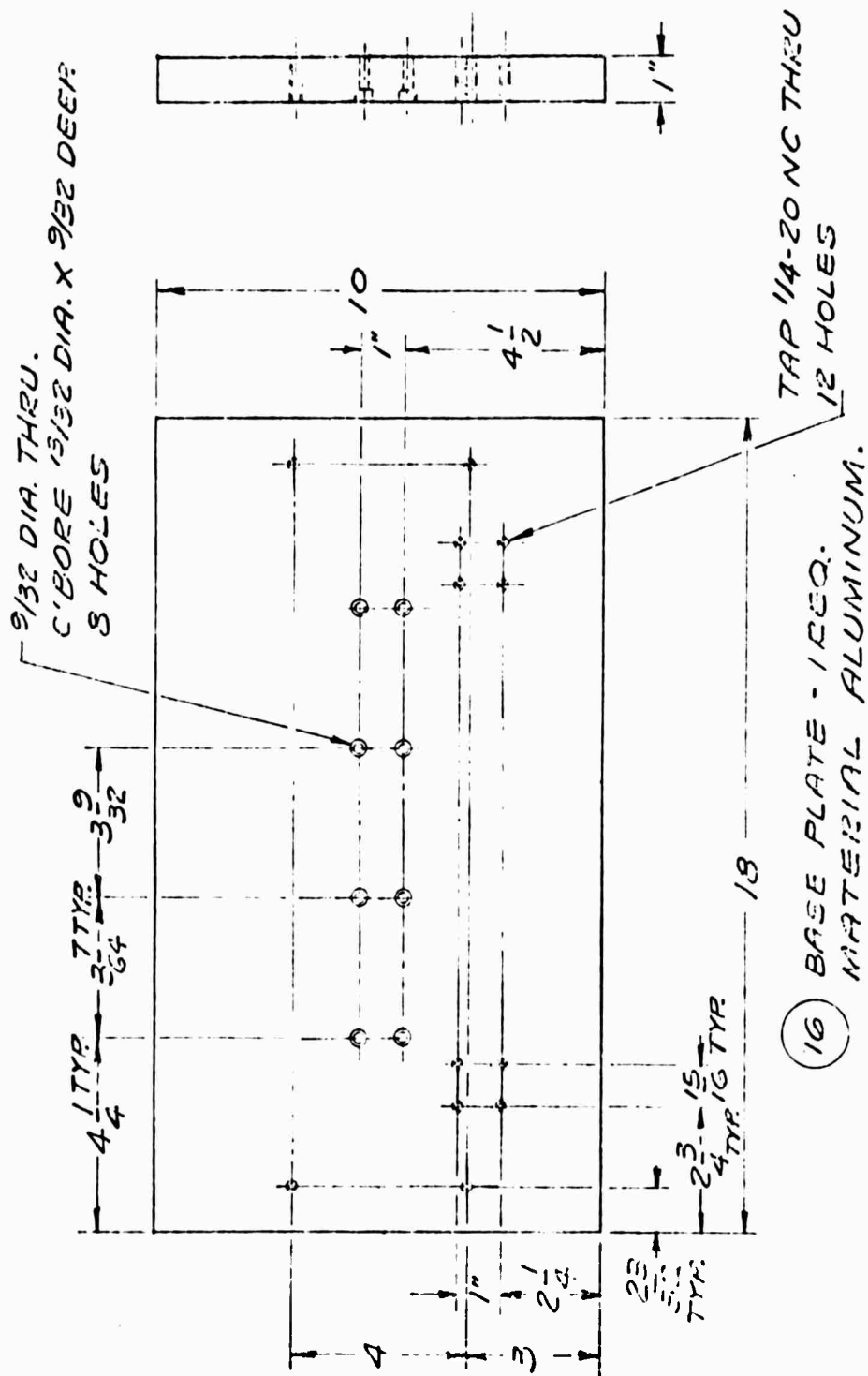


Figure 127. Base Plate

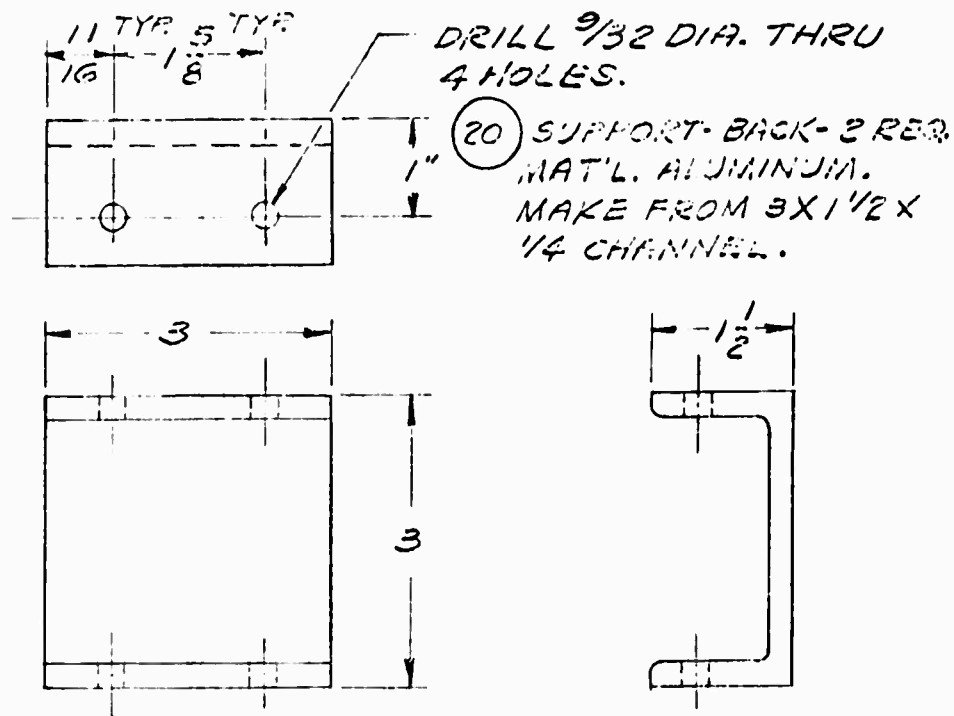


Figure 128. Perturbation Rod Support Bar Connector

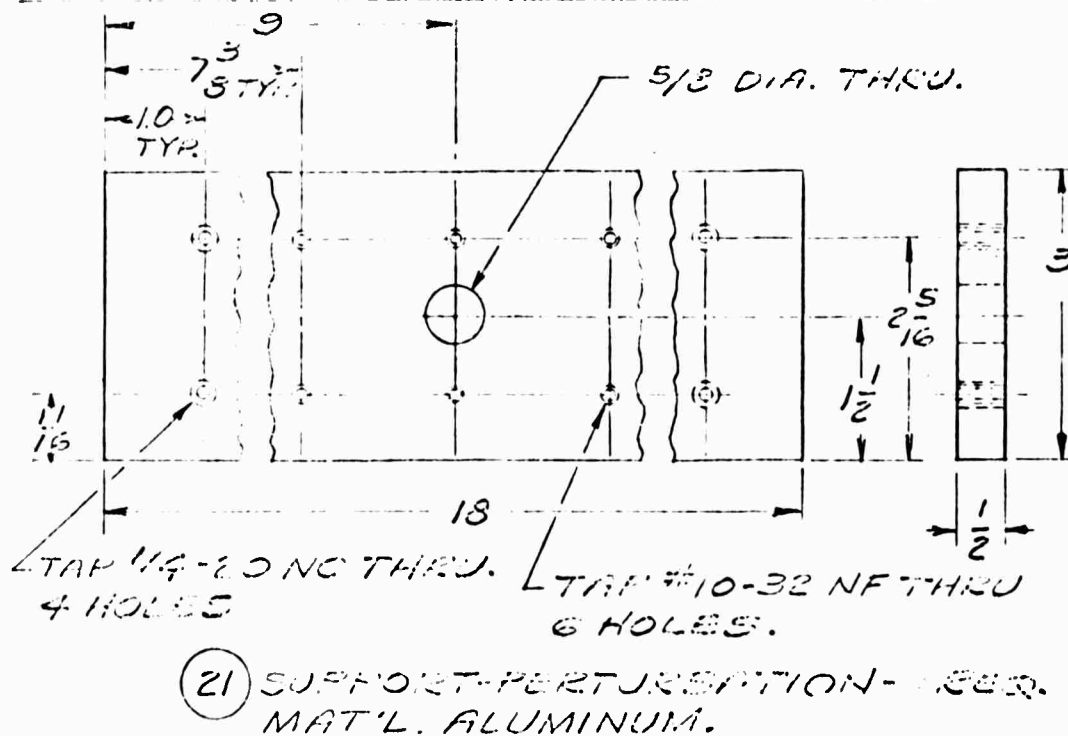
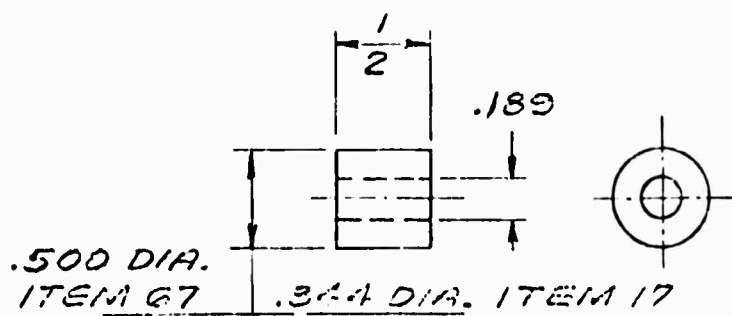
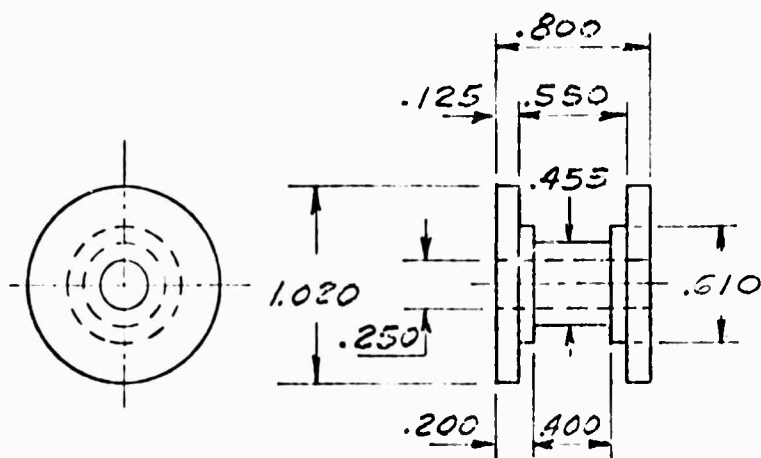


Figure 129. Perturbation Rod Support Bar



- (17) (67) FILLER RING - 18 EACH REQ.
MAT'L. ALUMINUM.

Figure 130. Piston Filler Ring



- (22) (23) NEGATOR SPRING CORE - 2 REQ.
MAT'L. ALUMINUM.

Figure 131. Negator Spring Core

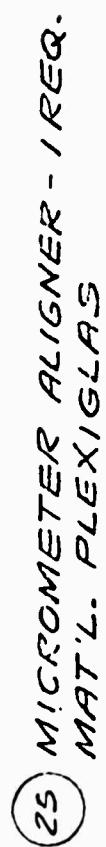
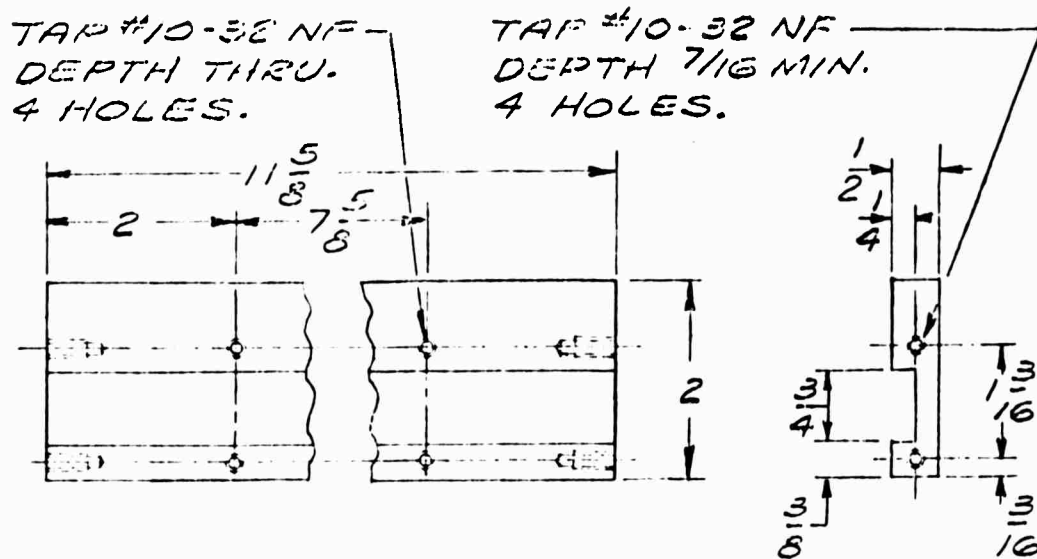


Figure 134. Micrometer Guide Plate



(26) SIDE SUPPORT-ALIGNER - 2 REQ.
MATERIAL - ALUMINUM.

Figure 135. Side Support for Guide Plate

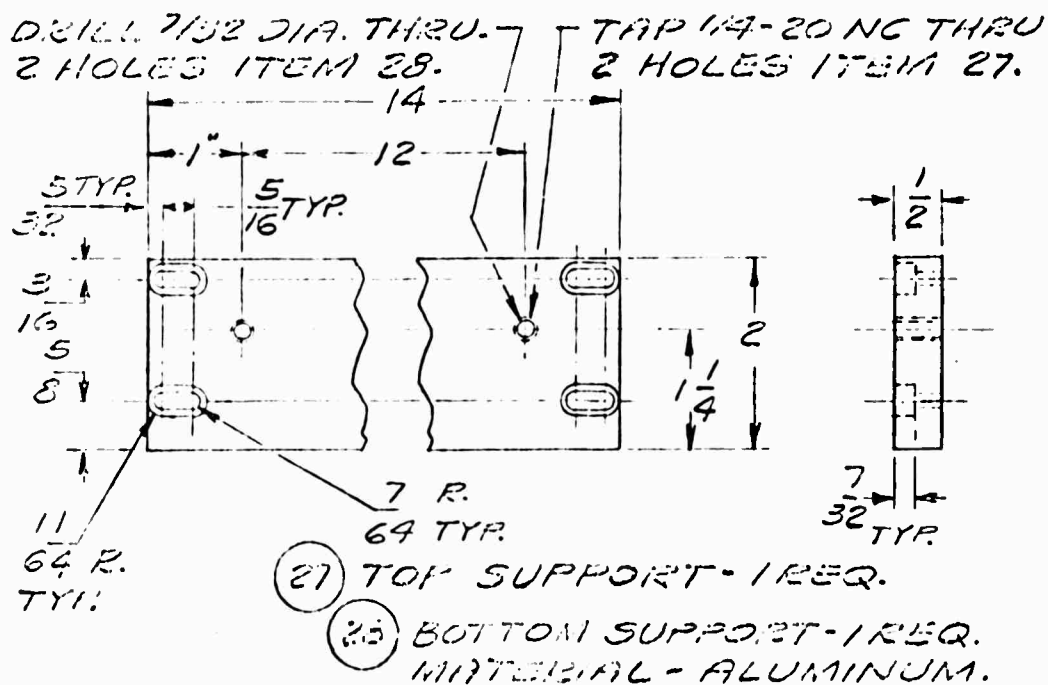
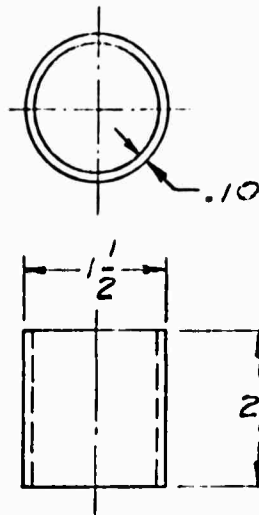
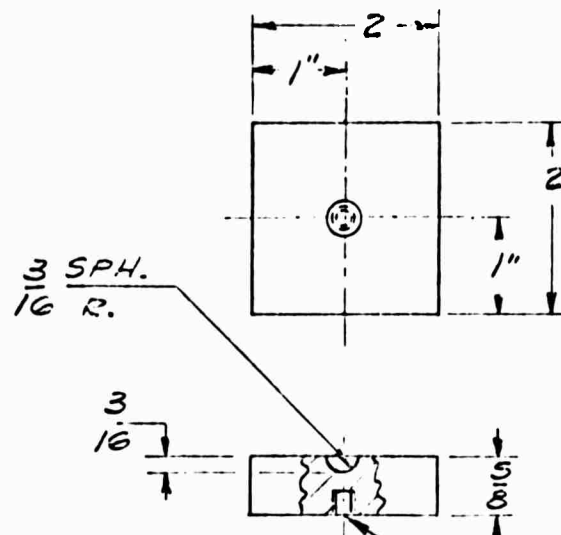


Figure 136. Top and Bottom Supports for Guide Plate



- (31) LOAD CELL - 1 REQ.
MATERIAL ALUMINUM.

Figure 137. Load Cell



TAP FLAT BOTTOM 1/4-20 NC
DEPTH 5/16 MAX.

- (32) SUPPORT-BEARINGS - 1 REQ.
MATERIAL ALUMINUM.

Figure 138. Bearing Support

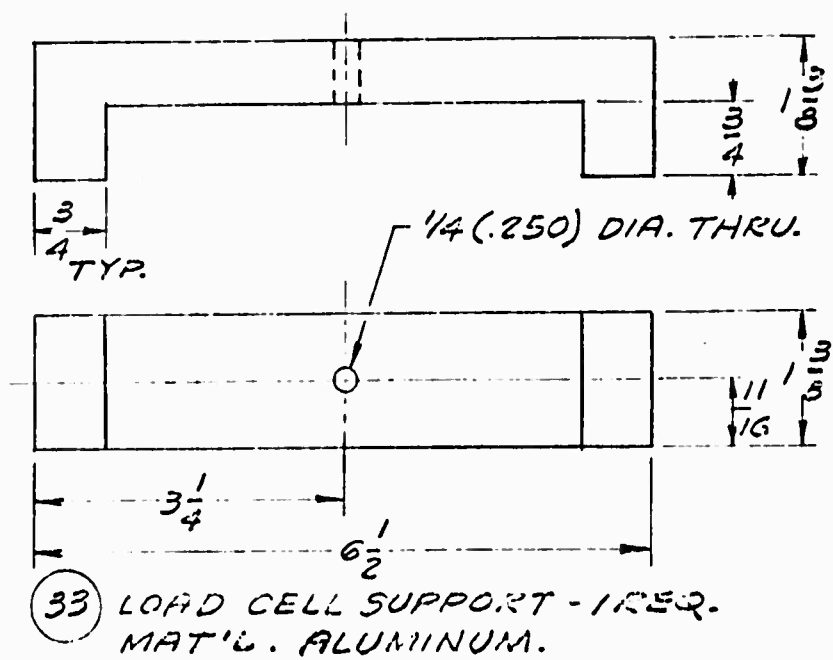


Figure 139. Load Cell Support

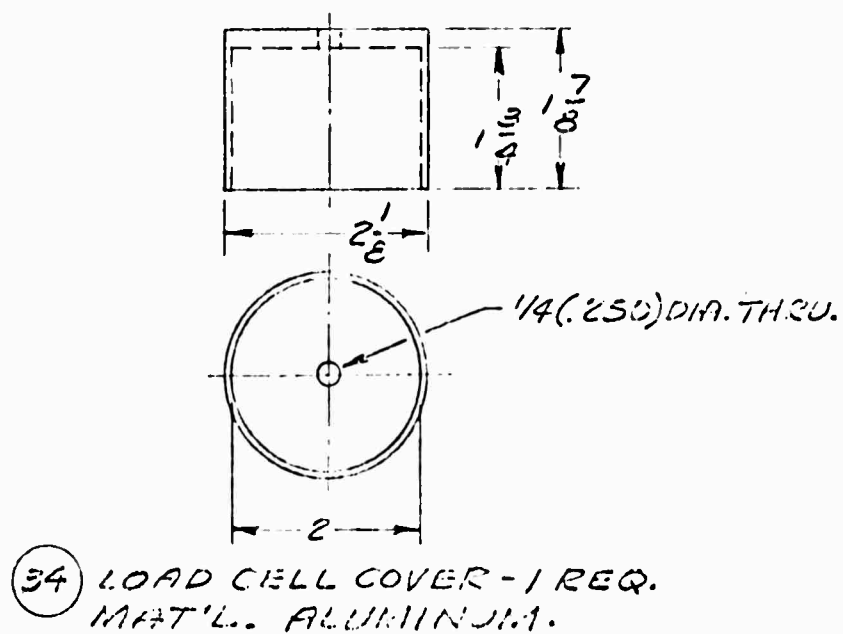


Figure 140. Load Cell Cover

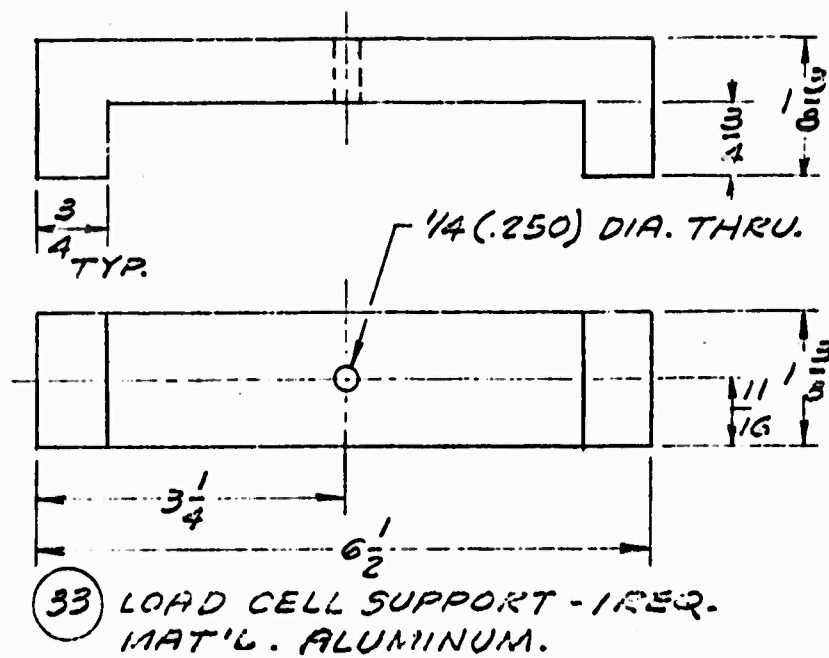


Figure 139. Load Cell Support

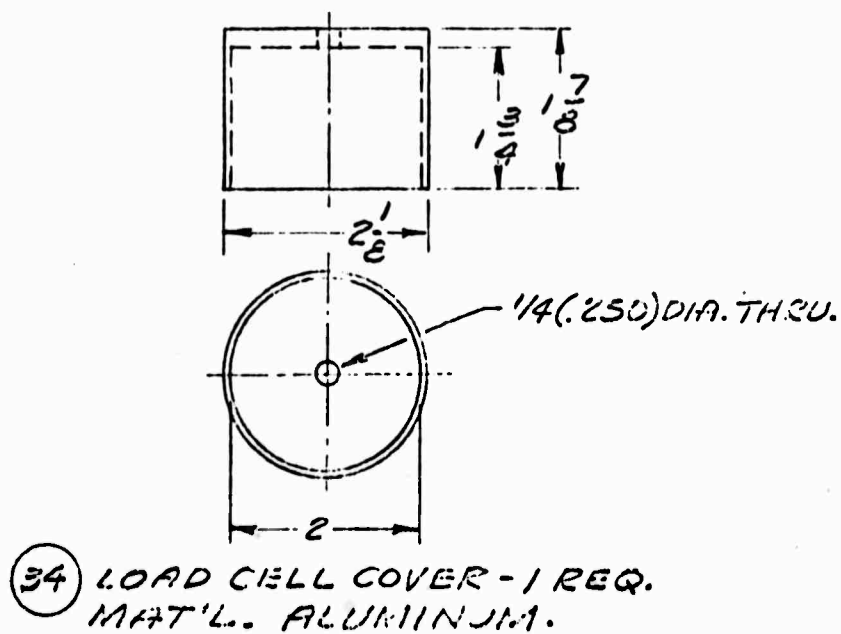
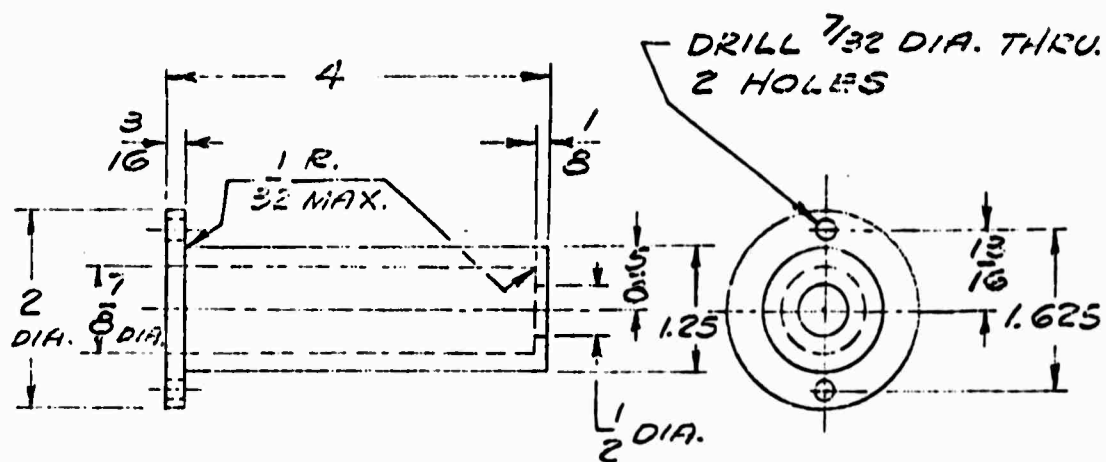
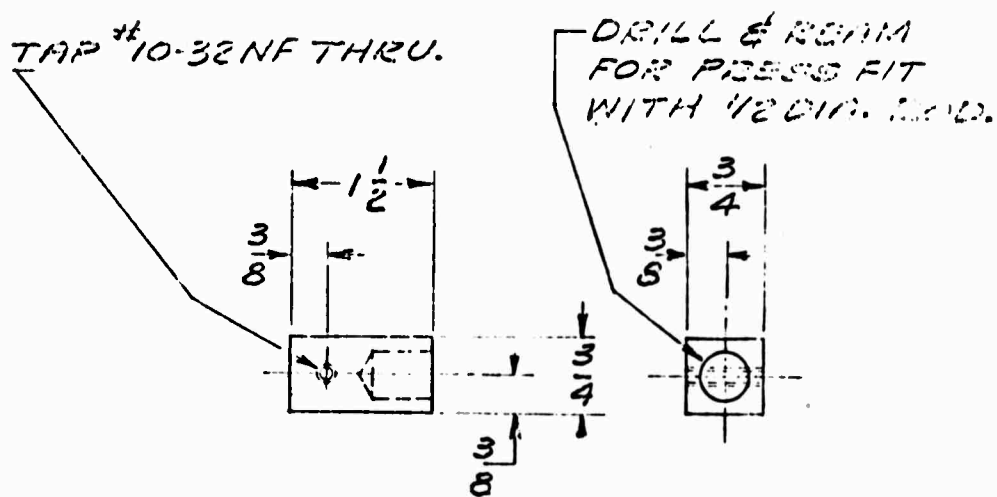


Figure 140. Load Cell Cover



(39) HOUSING-BALL BUSHING-1 REQ
MAT'L. ALUMINUM.

Figure 143. Ball Bushing Housing



(39) ROD END - 1 REQ.
MATERIAL - ALUMINUM

Figure 144. Perturbation Rod End Cover

DOCUMENT CONTROL DATA - R & D

(Security classification of title, body of abstract and indexing annotation must be entered when the overall report is classified)

| | | |
|--|---|--|
| 1. ORIGINATING ACTIVITY (Corporate author) Union Carbide Corporation, Case Western Reserve University, and Bell Aerosystems Company. | | 2a. REPORT SECURITY CLASSIFICATION Unclassified |
| | | 2b. GROUP |
| 3. REPORT TITLE An Experimental Investigation of the Buckling of Anisotropic Fiber Reinforced Plastic Plates. | | |
| 4. DESCRIPTIVE NOTES (Type of report and inclusive dates) Topical Report June 1966 to June 1968 | | |
| 5. AUTHOR(S) (First name, middle initial, last name) John F. Mandell | | |
| 6. REPORT DATE October 1968 | 7a. TOTAL NO. OF PAGES 315 | 7b. NO. OF REFS 16 |
| 8a. CONTRACT OR GRANT NO. AF 33(615)-3110 | 9a. ORIGINATOR'S REPORT NUMBER(S) SMSMD No. 23 | |
| b. PROJECT NO. ARPA Order No. 719 | | |
| c. Program Code No. 5D10 | 9b. OTHER REPORT NO(S) (Any other numbers that may be assigned this report) AFML-TR-68-281 | |
| 10. DISTRIBUTION STATEMENT This document has been approved for public release and sale; its distribution is unlimited. | | |
| 11. SUPPLEMENTARY NOTES | | 12. SPONSORING MILITARY ACTIVITY Air Force Materials Laboratory Air Force Systems Command Wright-Patterson Air Force Base, Ohio |
| 13. ABSTRACT Experimental buckling loads are determined for stiffened and unstiffened plates of the following materials: aluminum, steel, graphite fiber reinforced composite, glass fiber reinforced composite, and boron fiber reinforced composite. The plates are subjected to a uniformly distributed compressive edge load in one direction only. The boundary conditions are either simply supported on all four edges, or else simply supported on the loaded edges and free on the unloaded edges. The experimental buckling load is determined using the Southwell plot technique, and the results are compared to theoretical predictions obtained from a number of independent sources. Correlation between theoretical and experimental results is generally acceptable. It is believed that problems connected with material fabrication and evaluation resulted in some discrepancies between theoretical and experimental results, while problems associated with the test fixture and test procedure can be blamed for other discrepancies. The effects of bending-torsion and bending-membrane coupling is clearly shown in both the theoretical and experimental results. | | |

14.

KEY WORDS

LINK A

LINK B

LINK C

ROLE

WT

ROLE

WT

ROLE

WT

Plate Buckling
Experimental Data
Graphite Fibers
Anisotropic Plates
Composites